

ISOLATION AND STRUCTURE ELUCIDATION OF THE  
ANTIBACTERIAL CONSTITUENTS OF *SPHAERANTHUS INDICUS*,  
THE STEROIDAL ALKALOIDS OF *BUXUS HYRCANA*, AND  
BIOTRANSFORMATION STUDIES ON TERPENOIDS

By Jordan Betteridge

A Thesis submitted to the Faculty of Graduate Studies of  
The University of Manitoba  
in partial fulfillment of the requirements of the degree of

MASTER OF SCIENCE

Department of Chemistry

University of Manitoba

Winnipeg

Copyright © 2007 by Jordan Betteridge

**THE UNIVERSITY OF MANITOBA**  
**FACULTY OF GRADUATE STUDIES**  
\*\*\*\*\*  
**COPYRIGHT PERMISSION**

**ISOLATION AND STRUCTURE ELUCIDATION OF THE ANTIBACTERIAL  
CONSTITUENTS OF *SPHAERANTHUS INDICUS*, THE STEROIDAL ALKALOIDS OF  
*BUXUS HYRCANA*, AND BIOTRANSFORMATION STUDIES ON TERPENOIDS**

**BY**

**Jordan Betteridge**

**A Thesis/Practicum submitted to the Faculty of Graduate Studies of The University of  
Manitoba in partial fulfillment of the requirement of the degree**

**MASTER OF SCIENCE**

**Jordan Betteridge © 2007**

**Permission has been granted to the University of Manitoba Libraries to lend a copy of this  
thesis/practicum, to Library and Archives Canada (LAC) to lend a copy of this thesis/practicum,  
and to LAC's agent (UMI/ProQuest) to microfilm, sell copies and to publish an abstract of this  
thesis/practicum.**

**This reproduction or copy of this thesis has been made available by authority of the copyright  
owner solely for the purpose of private study and research, and may only be reproduced and copied  
as permitted by copyright laws or with express written authorization from the copyright owner.**

**Abstract:**

For this thesis, two ethnopharmacologically important plants, *Sphaeranthus indicus* and *Buxus hyrcana* were phytochemically investigated and their chemical constituents tested for antibacterial activity using the Minimum Inhibitory Concentration (MIC) procedure.

Biotransformation experiments on three natural products, sclareol (**110**), sclareolide (**111**), and colchicine (**112**), were also carried out.

A summary of the findings of this research work is described below:

- 1)  $7\alpha$ -hydroxyfrullanolide (**54**),  $7\alpha$ -hydroxyeudesmanolide (**56**), and dihydrocholesterol (**70**) were isolated from the *Sphaeranthus indicus* extract. Synthetic modification of **54** resulted in the semi-synthesis of 4,5-epoxy- $7\alpha$ -hydroxyfrullanolide (**71**), which was generated to examine the Structure Activity Relationship (SAR) of **54**. The MIC results indicated that **54** possess strong antibacterial activity (Gram-positive), while **56** and **71** had progressively decreasing activity. Compound **70** did not possess any activity.
- 2)  $N_b$ -dimethylcyclohexoviricine (**85**) and Buxamine B (**99**) were isolated from the *Buxus hyrcana* extract. The MIC results indicated that both compounds possess no antibacterial activity.
- 3) The sclareolide – *Penicillium crustosum* (ATCC#90147) biotransformation resulted in the isolation of 3-ketosclareolide (**131**) and 3 $\beta$ -

hydroxysclareolide (**132**). Tyrosol (**151**), a fungal natural product from *Candida albicans* (ATCC#90028), was isolated during the sclareolide – *Candida albicans* biotransformation experiment. MIC testing indicated that **151** possessed intermediate antibacterial activity (Gram-positive), whereas **131** and **132** did not.

## **Acknowledgements:**

I would like to thank Dr. Athar Ata for accepting me as his graduate student. I decided to pursue my Master of Science degree to learn new techniques and improve on existing ones and I believe I have succeeded in this goal.

Next, I would like to extend my gratitude towards Anu Arora, Chiyomi Sasaki, and Emmanuel Schaub; three very fine scientists that I had the distinct pleasure to work with and who helped me get through what was an extremely difficult time during my studies.

I would also like to thank Peter Balagus, Theresa Baran, and Ramin Vakili for their help for a wide variety of methodology. Thanks also to the Brandy Usick in the Student Advocacy Office at University of Manitoba. Thanks also to Devin Latimer.

Thanks also to Dr. Paul Holloway and Brenda van Dekerkhove in the University of Winnipeg Biology department for their assistance with microbiological work. I am also grateful for working with Robin Doyle and Tara Volkart in the Biology department.

My current employers, Dr. Carla Taylor and Dr. Peter Zahradka, also deserve thanks as without them I would not have the financial ability to complete this degree.

## Table of Contents:

	<b>Page</b>
Abstract	i
Acknowledgments	iii
List of Tables	vii
List of Figures	viii
List of Copyrighted Material for which Permission was Obtained	x
<b>Chapter 1.0 Introduction</b>	<b>1</b>
1.1 The Origin of Natural Products	1
1.2 Investigating Natural Products	3
1.3 The Importance of Natural Products	4
1.4 The Rise and Fall and Rise Again of Natural Products	5
1.5 Antibiotics and Antibiotic Resistance: An Escalating Problem	12
1.6 Phytochemical Sources of Biologically Active Natural Products	15
<b>Chapter 2.0 <i>Sphaeranthus indicus</i></b>	<b>17</b>
2.1 Previously Reported Compounds from <i>Sphaeranthus indicus</i>	20
2.1.1 Essential Oil Components	20
2.1.2 Sterols, Flavone Glycosides, and Alkaloids from <i>Sphaeranthus indicus</i>	22
2.1.3 Biosynthesis of Eudesmane Structure	25

## Table of Contents (continued):

	<b>Page</b>
2.1.4 Hydroxyeudesmanes, eudesmane acids, and eudesmanolides from <i>Sphaeranthus indicus</i>	26
2.2 <i>Sphaeranthus indicus</i> Experimental	31
2.3 <i>Sphaeranthus indicus</i> Results and Discussion	42
<b>Chapter 3.0 <i>Buxus hyrcana</i></b>	<b>56</b>
3.1 The <i>Buxus</i> genus and <i>Buxus hyrcana</i>	56
3.2 Previously Reported Steroidal Alkaloids from <i>Buxus hyrcana</i>	57
3.3 <i>Buxus hyrcana</i> Experimental	61
3.4 <i>Buxus hyrcana</i> Results and Discussion	63
<b>Chapter 4.0 Biotransformations of Natural Products</b>	<b>72</b>
4.1 Biotransformations and their Role in Microbial Metabolite Modeling	77
4.2 Sclareol and its Reported Biotransformations	81
4.3 Sclareolide and its Reported Biotransformations	84
4.4 Colchicine and its Reported Biotransformations	86
4.5 Biotransformation Experimental	89
4.6 Biotransformation Results and Discussion	97

**Table of Contents (continued):**

	<b>Page</b>
<b>Chapter 5.0:</b> Conclusions	106
<b>Chapter 6.0:</b> References	108
<b>Appendix A:</b> IR Spectra	
<b>Appendix B:</b> NMR spectra of <i>Sphaeranthus indicus</i> compounds	
<b>Appendix C:</b> NMR spectra of <i>Buxus hyrcana</i> compounds	
<b>Appendix D:</b> NMR spectra of Biotransformation compounds	



### List of Tables:

Table 1: Extraction solvent, yield, and plant mass data of previous investigations of eudesmanolides isolated from *Sphaeranthus indicus* (54 – 67)

Table 1: Extraction solvent and yield (relative and absolute) of eudesmanolides isolated from *Sphaeranthus indicus* (54 – 67)

Table 2:  $^{13}\text{C}$  NMR Chemical Shift Assignments and  $^1\text{H}/^{13}\text{C}$  One-Bond Shift Correlations of **70** as Determined from its HSQC Spectra

Table 3:  $^{13}\text{C}$  NMR Chemical Shift Assignments and  $^1\text{H}/^{13}\text{C}$  One-Bond Shift Correlations of **54** as Determined from its HSQC Spectra

Table 4:  $^{13}\text{C}$  NMR Chemical Shift Assignments and  $^1\text{H}/^{13}\text{C}$  One-Bond Shift Correlations of **56** as Determined from its HSQC Spectra

Table 5: MIC Assay for Compounds **70**, **54**, **71**, and **56**

Table 6:  $^{13}\text{C}$  NMR Chemical Shift Assignments and  $^1\text{H}/^{13}\text{C}$  One-Bond Shift Correlations of **85** as Determined from its HSQC Spectra

Table 7:  $^{13}\text{C}$  NMR Chemical Shift Assignments and  $^1\text{H}/^{13}\text{C}$  One-Bond Shift Correlations of **99** as Determined from its HSQC Spectra

Table 8: MIC Assay for Compounds **85** and **99**

Table 9:  $^1\text{H}$  and  $^{13}\text{C}$  NMR Chemical Shift Assignments of **131**

Table 10:  $^{13}\text{C}$  NMR Chemical Shift Assignments and  $^1\text{H}/^{13}\text{C}$  One-Bond Shift Correlations of **132** as Determined from its HSQC Spectra

Table 11:  $^1\text{H}$  and  $^{13}\text{C}$  NMR Chemical Shift Assignments of **151**

Table 12: MIC Assay for Compounds **131**, **132**, and **151**

## List of Figures:

Figure 1: Structures of morphine (1), aspirin (2), atropine (3), and cocaine (4)

Figure 2: Structures of penicillin G (5), 6-aminopenicillanic acid (6-APA) (6), methicillin (7), ampicillin (8) and amoxicillin (9)

Figure 3: A comparative Statistic analysis of Combinatorial Compounds (a), Natural Products (b) and Drugs in the Market (c) and their occupancy in statistically defined chemical space

Figure 4: *Sphaeranthus indicus*

Figure 5: Reported major chemical constituents of the essential oil of *Sphaeranthus indicus* (10 – 31)

Figure 6: Reported sterols (32 – 34), flavone glycosides (36 – 37), and alkaloids (38 – 40) from *Sphaeranthus indicus*

Figure 7: Biosynthesis of the eudesmane structure (47) from *E,E*-FPP (41)

Figure 8: Hydroxyeudesmanes (48 – 51) and eudesmane acids (52 – 53) isolated from *Sphaeranthus indicus*

Figure 9: Structures of eudesmanolides from *Sphaeranthus indicus* (54 – 67)

Figure 10: Michael-type addition of a thiol group onto parthenolide (68), an  $\alpha$ ,  $\beta$ -unsaturated lactone and the resulting irreversibly-bonded species (69)

Figure 11: HPLC Chromatogram of Column Chromatography Sub-fraction 32-33 of the methanolic *Sphaeranthus indicus* extract (with peak of interest selected)

Figure 12: The structures of penicillin G (5) and chloramphenicol (72)

Figure 13: Illustration of MIC Procedure

Figure 14: Important HMBC Interactions Observed in 70

Figure 15: Important HMBC Interactions Observed in 54

Figure 16: Important HMBC Interactions Observed in 56

**List of Figures (continued):**

Figure 17: *Buxus hyrcana*

Figure 18: Steroidal alkaloids from *Buxus hyrcana* (**73 – 85**)

Figure 19: Steroidal alkaloids from *Buxus hyrcana* (**86 – 98**)

Figure 20: Important HMBC Interactions Observed in Compounds **85**

Figure 21: Important HMBC Interactions Observed in Compounds **99**

Figure 22: The first reported biotransformation: transformation of progesterone (**100**) into 11 $\alpha$ -hydroxyprogesterone (**101**), 6 $\beta$ , 11 $\alpha$ -dihydroxyprogesterone (**102**), and 11 $\alpha$ -hydroxyallopregnane-3,20-dione (**103**) using *Rhizopus arrhizus*

Figure 23: An Overview of biotransformation reactions on examples of different natural product classes and their corresponding biotransformed derivatives

Figure 24: Cytochrome P<sub>450</sub> monooxygenase mechanism on drugs

Figure 25: Structures of the natural products for biotransformation: sclareol (**110**), sclareolide (**111**), and colchicine (**112**)

Figure 26 Reported biotransformations of sclareol (**110**)

Figure 27: Reported biotransformations of sclareolide (**111**)

Figure 28: Reported biotransformations of colchicine (**112**)

Figure 29: HPLC Chromatogram of Collection Run for Column Chromatography Fraction #18 of Sclareolide – *Candida albicans* Scale Up extract (with peak of interest selected)

Figure 30: Important HMBC Interactions Observed in **132**

Figure 31: Important HMBC Interactions Observed in **151**

### List of Copyrighted Material for which Permission was Obtained

Figure 3: A comparative Statistic analysis of Combinatorial Compounds (a), Natural Products (b) and Drugs in the Market (c) and their occupancy in statistically defined chemical space

Reprinted with permission from:

Feher, M.; Schmidt, J. M. Property distributions: differences between drugs, natural products, and molecules from combinatorial chemistry. *Journal of Chemical Information and Computer Sciences*. 43 [1] (2003): 218 -227

Copyright 2003 American Chemical Society

Figure 4: *Sphaeranthus indicus*

Reprinted with permission from:

*Sphaeranthus indicus*. Fleurs du Vietnam -2. Retrieved Dec. 21, 2007 from <[http:// www.mythofleurs.com/images/Fleurs du Vietnam/fleurs du Vietnam 2/Sphaeranthus indicus.jpg](http://www.mythofleurs.com/images/Fleurs_du_Vietnam/fleurs_du_Vietnam_2/Sphaeranthus_indicus.jpg)>.

Copyright 2007 Mr. Bernard Loison

## Chapter 1.0 Introduction

### 1.1 The Origin of Natural Products

Natural products can be defined as secondary metabolites, that is to say metabolites that are not the result of primary metabolism, such as amino acids, saccharides, and fats, which are essential for functioning and are found in all organisms. Instead, these metabolites are produced through alternative biochemical pathways (polyketide, shikimic, etc.) and can be genus- or species-specific. Although the presence of these compounds is not vital to the functioning of the organism (as evidenced by the production of non-expressing mutants), these products can greatly aid in the ecological survival of the relevant species. This can be accomplished in several ways, such as providing various toxic defenses against predators, attraction of mates, luring prey, mutualistic attraction (eg. pollination), and so on.

The reason why natural products exist at all can be explained when evolution, or rather coevolution, is examined.<sup>1</sup> One organism's genotype produces variations on proteins as a result of mutation, and eventually this may result in a new "gene product" (possibly an enzyme or receptor). If this imparts an advantage to this organism which competes with other populations, it would seem logical that from these other populations a compound that binds to, and acts against, this protein (possibly an enzyme or receptor) may be produced, i.e. self-defense.<sup>1</sup>

If the natural product functions in successfully sabotaging this protein, it will result in more expressing organisms when the organism reproduces. In this case, genetic changes for expression of the relevant gene(s) or increasing an enzyme's efficiency are selected for over time. The former choice is more common.<sup>1</sup> However,

convergent evolution has been proven to occur also.<sup>1</sup> This line of reasoning can also explain the specificity of a natural product (often to the genus or species) since every species encounters different environmental factors.

Thus it can be said that the natural products that survive are inherently able to penetrate biological barriers, bind to their biological target, and exert their effect with remarkable specificity. This has been described as “existing biological validation” or chemical relevance.<sup>2</sup>

This scenario involving natural selection can be referred to as “microbial warfare”.<sup>2</sup> It provides a splendid example of why treatment involving natural product administration is tremendously effective against infectious diseases.

There is a bit of controversy concerning natural products as to the effectiveness of secondary metabolites when the issue of therapeutic use against other diseases arises. This is a matter of practicality. This is particularly relevant in cases when the biological activities being sought are against ailments with which the host organism would not be susceptible. An example of this would be investigating phytochemicals for compounds treating schizophrenia, Diabetes mellitus, or Alzheimer’s disease. This is a logical question to ask. Why would such a natural product be useful for a molecular target of a human disease? After all, why should it? The organism did not encounter such an obstacle during its evolution.

Although this may be the case, it is important to take into consideration that there is great conservatism in nature regarding proteins, especially the structures of their domains. Many of the same enzymes that exist in humans exist in other animals

(particularly mammals), hence the rationale for the use of animal models (and more recently animal cell lines) for the study of disease. Even fungi, possess the same (or slightly altered) enzymes such as P<sub>450</sub> oxidases.

Thus, it is quite probable that some natural product, through coevolution, has been produced to act against a protein that is remarkably similar to the one relevant to a human disease.

## **1.2 Investigating Natural Products**

The question, then, is which organisms should be investigated? A random or systematic selection would likely result in the same compounds being isolated multiple times. It would not yield the novel structures that are a characteristic of this type of research.

Often, interesting natural products can be discovered by examining the chemistry of organisms that are the last remaining of their kind (“living fossils”).<sup>2</sup> Perhaps a chemical compound is responsible for facilitating the survival of these species, while their non-expressing relatives have become extinct. An example relating to this hypothesis is *Ginkgo biloba*.<sup>3</sup>

Another valuable starting point for choosing an organism (especially plants) to investigate chemically is to consider if there are any ethnopharmacological (“folklore medicine”) data concerning its use. Within some cultures, particularly those of Southeast Asia (China and India being major contributors), these systems of therapeutic medicine are vastly complex and may involve a multitude of different agents, of which the great majority are plants, but which may also include insects, and

even medicinal agents from higher animals, such as Cod liver oil, etc. Interpreting these data can result in more efficient screening of initial samples; testing for antibacterial activity in plants that have reported use in tonics for aiding wound healing, testing anti-inflammatory activity in plants that are used for this purpose, etc.

### **1.3 The Importance of Natural Products**

The doubling of the average human's life span that occurred during the twentieth century is mainly due to the use of secondary metabolites. They have been used to reduce pain and suffering, and revolutionized medicine by allowing for the transplantation of organs. Almost half of the best selling pharmaceutical agents are secondary metabolites produced by microbial or plant products, or are closely related to them.<sup>4</sup> Despite the pharmaceutical industry today being a multi-billion dollar industry, there is no doubt that we have only begun to scratch the surface of the potential for natural products. Slightly less than 50 000 natural products have been identified, but the total number has been estimated at hundreds of thousands.<sup>1</sup>

In the case of antibiotics, there are three basic approaches used in isolating new metabolites: 1) direct isolation from marine and soil microorganisms; 2) production of higher-yield mutants by genetic modification; and 3) use of metabolic pathway inhibitors to prevent downstream metabolite formation. The direct detection from natural sources (1) has proven to be much more successful for the discovery of novel, lead therapeutic compounds.<sup>5</sup>

Natural product chemistry focuses on the isolation of secondary metabolites, the characterization of their structures, analysis of their biological activities, and the



semi-synthesis (derivatization) or total synthesis of these compounds, often for potential medicinal impact.

#### 1.4 The Rise and Fall and Rise Again of Natural Products

A suitable place to begin an abridged history of natural products (with special emphasis on antibiotics) would be the mid-19<sup>th</sup> century. It was during this time that many potent natural products including morphine (1804) **(1)**, aspirin (1828) **(2)**, atropine (1831) **(3)**, cocaine (1855) **(4)** and others were discovered. However, this period of research rose and fell.

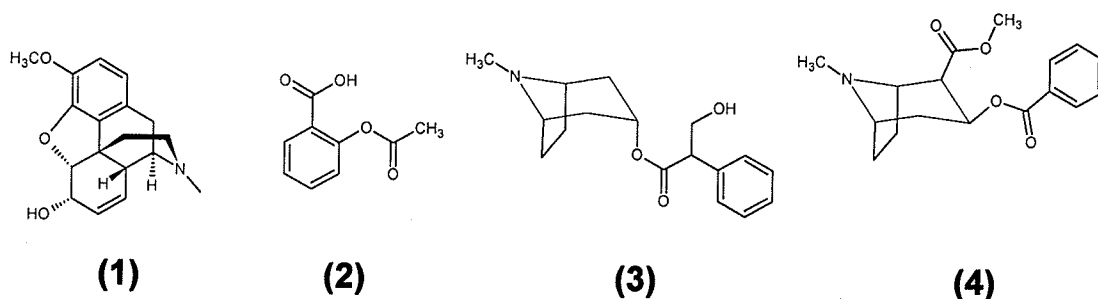


**Figure 1: Structures of morphine (1), aspirin (2), atropine (3), and cocaine (4)**

It was not until 1929 that Alexander Fleming published an unheard of observation, a yellow colony of unidentified *Penicillium* resulted in inhibition and lysis of a bacterial culture of *Staphylococcus aureus*.<sup>4, 6, 7</sup> Its active agent was isolated from the later identified *Penicillium notatum* and named penicillin, penicillin G **(5)** to be precise. This was the first successful antibiotic, a chemotherapeutic agent produced by a microbe. The term “antibiotic” was coined by Waksman, another extremely important scientist responsible for the discovery of streptomycin.<sup>8</sup> It was not until much later, in 1940, that isolation of stable penicillin<sup>9</sup>, and subsequent

production was successful.<sup>4</sup> This was the beginning of the “Antibiotic era”. Today, these compounds are ubiquitous and it is difficult to imagine a world without them.

Despite its tremendous therapeutic ability (which led to it and other penicillins being called “wonder drugs”), penicillin G has several properties which limited its use. Penicillin G has excellent activity against Gram-positive bacteria, but is ineffective against Gram-negative bacteria. Additionally, it is acid-labile; i.e. it was administered by injection as it cannot tolerate the hydrochloric acid in the stomach.

In 1957, the active nucleus of penicillin G (including the active pharmacophore: the 4-membered heteroatomic  $\beta$ -lactam ring), 6-aminopenicillanic acid (6-APA) **(6)** was isolated.<sup>10</sup> Synthetic derivatization of this intermediate produced a wide number of new antibiotics such as methicillin **(7)**, ampicillin **(8)**, and amoxicillin **(9)**, among many others. These derivatives are notable for their improvement in activity. Ampicillin (developed in 1961) was the first penicillin effective against Gram-negative bacteria.<sup>7, 10</sup> Methicillin (developed in 1960) was the first penicillinase-resistant penicillin. Amoxicillin (developed in 1972) is currently the most commonly prescribed antibiotic in United States.

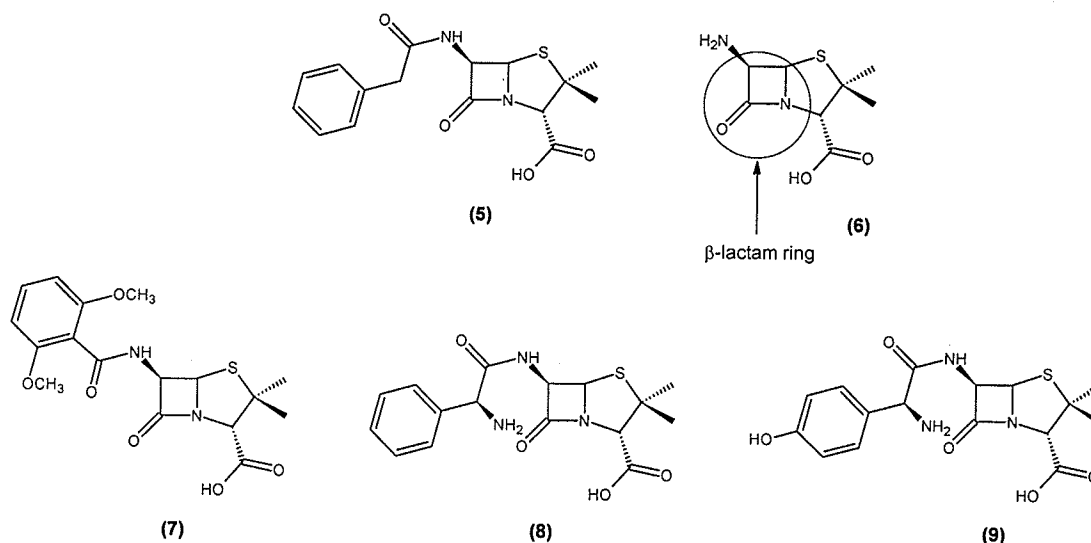


**Figure 2: Structures of penicillin G (5), 6-aminopenicillanic acid (6-APA) (6), methicillin (7), ampicillin (8) and amoxicillin (9)**

Since then, many antibiotic natural products classes have been discovered and developed into effective medicines: penicillins, cephalosporins, tetracyclins, aminoglycosides, macrolides, statins, etc.

In addition, a multitude of natural products have been isolated for numerous other therapeutic areas besides combating microbial pathogens, such as (1) immunosuppression, eg.) mycophenolic acid; (2) antiparasitic agents, eg.) artemisinin [qinghaosu]; (3) antitumor agents, eg.) taxol [paclitaxel]; (4) biopesticides, etc.

Discoveries in natural product chemistry have certainly given no indication that all the major discoveries worth noting have already occurred, despite this being a common misconception.<sup>3</sup> Greater than 95% of all soil microorganisms are still unculturable,<sup>3</sup> thus tremendous developments in natural product chemistry are still coming. This is not the end, but the beginning.

The results of a scholarly survey indicate that during the period of 1981 – 2002, 877 small molecule compounds were introduced as drugs, of which 61% were

in some way derived from natural products (including natural products themselves, derivatives, and synthetic mimics). The success rate of antibacterial drug and anticancer drug subgroups of this total are even higher [than 61%], corresponding to 78% and 74%, respectively.<sup>11</sup>

However, in the early 1990's, there was a trend in big pharmaceutical companies that drug discovery programs moved their resources away from – or eliminated completely – natural products as a source<sup>3</sup> (exceptions being Bayer, Merck, and Wyeth) and embraced a new system: combinatorial chemistry.<sup>2</sup>

Combinatorial chemistry as a method for drug development involves the creation of enormous groups of similar compounds called “libraries”. These libraries are produced by reacting precursors in differing orders. A greatly simplified analogy would be creating a library using three reagents. In this analogy, one reaction would involve compound “A” with “B”, and then subsequently with “C”. If the synthetic reaction order is changed (“A” with “C”, then “B”) it results in two distinct, yet similar compounds. Screening is then done for detectable biological activity. In actuality, libraries are generated by using a combination of thousands of precursors.

The trend of shifting away from natural products was due to practical reasons. In the early 1990's, molecular biology experienced an explosion with its breakneck pace in identifying biological targets. At this time, natural product chemistry was unable to fill the need for a multitude of compounds to screen against these newly available targets.<sup>2,3</sup>

A short summary of drug development and approval should be included at this point. After the initial point of discovering a new therapeutic compound, its structure

is determined and its bioactivity and mechanism of action are determined using *in vitro* methods. Next, its structure-activity relationship [SAR] is examined by making structural modifications to hopefully improve its properties, which can include its biological activity, toxicity, and *in vivo* stability. Next, animal models are used to determine initial *in vivo* efficacy and safety of the proposed agent and comparing to similar approved drugs. This step is necessary as *in vitro* activity does not always, or even frequently, correspond to *in vivo* activity.<sup>10</sup> Quite often the problem with the proposed drug is it inactivates important liver enzymes. Next are the three clinical trials, performed in humans. Phase I clinical trials test the safety of the proposed agent in healthy subjects, Phase II clinical trials test the safety of the agent in afflicted subjects, and Phase III clinical trials test the efficacy of the agent for each intended use; eg. different bacteria, different cancers.<sup>10</sup>

How does the modern drug discovery procedure relate to the findings of combinatorial chemistry? What was observed was that combinatorial chemistry's productivity from initial screening "hits" until the isolation of "lead" compounds was faster, more cost effective, and had a higher rate of success than with natural products. However, if productivity is measured from hit to lead to approved drug, combinatorial chemistry has been monumentally unsuccessful to date. Thus, the screening results of the combinatorial products were more successful in the initial steps of development, but unsuccessful in the later stages.

During the period of 1981 – 2002, no approved drugs have been developed using combinatorial chemistry. It would seem that a multitude of new compounds have been produced, but none which successfully – and safely – binds to a molecular

target (usually a protein).<sup>11</sup> In other words, their selectivity for the target over host is insufficient. It would seem that there are certain intricacies for how a compound interacts with its *in vivo* environment to reach its target that have not been grasped with combinatorial chemistry.

This hugely dissimilar output between the two methods is due to a number of differences. On average, natural products have higher formula weights; incorporate fewer nitrogen, halogen, and sulphur atoms; incorporate more oxygen atoms; possess more rings (both fused and bridged) and chiral centers (steric complexity); and have larger dissimilarity between themselves.<sup>12</sup>

The last reason is an important one as the screening process for testing activity (whatever that activity may be) relies on a diverse group of analytes to detect the infrequent occurrence of binding to a molecular target. A comparative study was done in 2003 comparing natural products, combinatorial compounds, and drugs in the market using statistically defined chemical space, i.e. molecules are points in a statistical plot defined by their descriptors. These statistical plots reveal that there exists a greater similarity between compounds using combinatorial chemistry than which exists with natural products or drugs in the market. Combinatorial Chemistry, it would seem, evidently has not "cast a wide-enough net" to date. Also, with regard to distributions of chemical space there is a greater correlation between natural products and drugs than with combinatorial compounds and drugs (see Figure 3).<sup>12</sup>

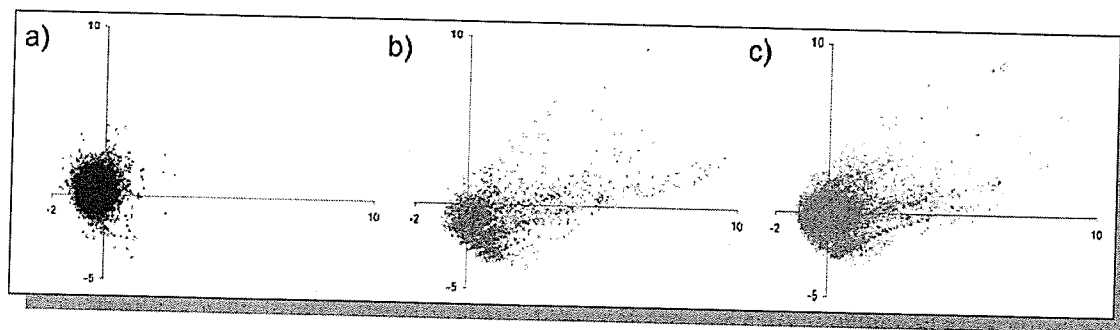


**Figure 3: A comparative Statistical analysis of Combinatorial Compounds (a), Natural Products (b) and Drugs in the Market (c) and their occupancy in statistically defined chemical space**

With the lack of success to date of combinatorial chemistry, it has been suggested that it may serve a better role as a way of producing natural product derivatives or analogues (that retain or augment their activity) than as a method to discover new drugs.<sup>11</sup> In this approach, combinatorial synthesis is performed on biologically active pharmacophores, i.e. modification around a core structure, such as the macrolide core of erythromycin. Given that numerous compounds with the core structure are successful in binding to receptors and enzymes, this results in the desirable traits of the natural product being incorporated while facilitating the specificity and potency for cellular targets.<sup>13</sup>

There are indications that interest in natural product research for drug development is increasing again.<sup>2</sup> The three main reasons for this are (as mentioned above) combinatorial chemistry's performance being (to date) below expectation, tremendous improvements in natural product chemistry's isolation methodologies due to technology, and the argument that natural products may be intrinsically better-suited for drug leads (as explained above).

## 1.5 Antibiotics and Antibiotic Resistance: An Escalating Problem

As hypothesized by Alexander Fleming, evolution on the part of microorganisms would allow them to develop adaptations to resist antibiotics. Indeed, by 1948, 50% of *Staphylococci* strains in hospitals were resistant.<sup>14</sup>

The origin of antibiotic-resistance is unclear. One theory is that the genes responsible for resistance were fluke mutations which propagated due to the natural advantage it bestowed to the organisms<sup>15</sup> involved when coevolving with natural antibiotic-producing soil bacteria.<sup>16</sup> Regardless of its origin, the ability and speed that bacteria gain resistance to antibiotics is most disconcerting. Resistance can be gained by chance mutation, inheritance from previous generations, or exchange of genetic material, especially plasmids.<sup>15, 17</sup> Resistance mechanisms can be due to (1) impermeability of the drug, the most common method; (2) alteration of the cellular target, eg. penicillin-binding proteins; (3) alteration of the drug structure, eg. hydrolysis of the lactam amide bond by  $\beta$ -lactamase; and (4) disabling efflux pumps that discharge drugs before binding to their intercellular targets occurs.<sup>15, 16</sup>

Antibiotics are effective because they inhibit bacterial growth, thus allowing the host's immune system to overwhelm and annihilate the remaining pathogens. This has an unfortunate side-effect of stressing microbial ecology, since the most resistant cells will inevitably out-complete all others. This in turn significantly alters the kinds and proportions of bacteria, resulting in antibiotics promoting the survival and proliferation of resistant strains.

This phenomenon is more important than may be initially suspected because the benign, non-pathogenic bacteria that exist as natural flora in / on our bodies (and



in our environment) compete with and limit the growth of pathogenic bacteria. The antibiotic-resistant pathogens are not more virulent, but it is their cellular defenses which make them more dangerous. Normally, antibiotic susceptible strains are more likely to survive due to their metabolism not having to divert resources to producing /maintaining resistance mechanisms, such as an the four listed on page 12. <sup>15</sup>

The two main factors which determine whether bacteria in a location gain resistance to an antibiotic are: 1) the presence of resistance genes (which result in modified bacterial phenotype) and 2) the extent of antibiotic use. As antibiotic (and antimicrobial) agents are self-limiting due to microbial evolution,<sup>15</sup> they are in fact “the architects of their own destruction”.

During the 1980's, major pharmaceutical companies severely reduced novel antibacterial research. This is for the reason that during this period, resistant bacteria that did not respond to a certain antibiotic treatment were easily annihilated by a readily available alterative. <sup>16</sup>

However, in the past 30 years, an alarming increase in resistance to antibiotics and other antimicrobial agents has started occurring. <sup>18, 19, 20</sup> Some experts state that it is not antibiotic use but its misuse that is responsible for the expeditious spread of antibiotic resistance. <sup>15, 16</sup> Some prominent factors include (1) lack of education / regulation, particularly a concern in developing nations; (2) hospital-acquired infections, (3) agricultural overuse, where low doses are given for growth promotion, and (4) superfluous use of antibacterial compounds in household products, eg.) triclosan. <sup>15, 16</sup>

Increasing antibiotic resistance has become a dire situation indeed due to the emergence of vancomycin-resistant bacteria in the last decade. This is notable as certain strains are already resistant to all other antibiotics except vancomycin.<sup>16</sup> It is for this reason that vancomycin is often called “the last line of defense”.<sup>8</sup>

One solution to the problem of bacterial resistance to antibiotics has been structural modification to improve potency, such as the semi-synthesis around 6-APA (2). Another solution has been to develop inhibitors of resistance mechanisms, such as  $\beta$ -lactamase inhibitors and efflux pump inhibitors. However, these methods are alike to a “patch” solution, they are temporary measures that will eventually be exhausted. Combating antibiotic resistance cannot be viewed as a battle of attrition. The future of antimicrobial compounds relies on discovering novel compounds and natural products is likely the most promising source.

Despite the enormous progress that has been accomplished in the war against pathogenic microorganisms, antimicrobial technology will need to continue to evolve. In the future, 1) resistance mechanisms will undoubtedly multiply and intensify; 2) new diseases are continuing to emerge at a distressing rate, such as AIDS, Ebola virus, Hanta virus, etc. and 3) drugs with improved activity will be in continual demand.<sup>10</sup> For reasons such as those listed above, the isolation and development of new antimicrobial agents will be absolutely necessary for a long time to come. One last note on this topic is that antimicrobial compounds cannot be the sole solution to a permanent end to this ever-present dilemma. Other changes in society will be necessary.<sup>4</sup>

## 1.6 Phytochemical Sources of Biologically Active Natural Products

The use of plant-based medicines for therapeutic use is as ancient and ubiquitous as the practice of medicine itself. Until the beginning of the 20<sup>th</sup> century, natural products have served as the mainstay of all medicines worldwide. According to the World Health Organization, over 70% of the world's population is still reliant on herbal remedies for their healthcare needs.<sup>21</sup>

Thus in the modern era, secondary metabolites produced by plants are a vast, largely untapped source of bioactive substances. Recently, scientific interest in this source has increased due to the search for new drugs of plant origin.<sup>22</sup> There are a multitude of plants that show therapeutic, medicinal application. Some examples are St. John's Wort, aloes, cinnamon, garlic, etc.<sup>23</sup>

Plants are an important source to discover new compounds with novel skeletons as well as a discovering new antibacterial compounds that can lead to a better understanding of antibacterial activity. Currently, a multitude of plants worldwide are being investigated to discover new biologically active compounds, which includes compounds having antibacterial activity, as well as numerous other types of activity. Often, compounds are isolated without any biological activity testing being executed or no work is done concerning the active pharmacophore of the isolated compound.

The next two chapters of this thesis describe the phytochemical examination of two ethnopharmacologically-important plants, *Sphaeranthus indicus* and *Buxus hyrcana*. The objectives of the study of each plant includes isolating natural products,

determine their structure using spectroscopic methods, and assess their antibacterial activity (if present) in the isolated compounds. Such information concerning the compounds of the two plants mentioned above is sporadic at best and is well deserving of a more in-depth investigation.

## Chapter 2.0 *Sphaeranthus indicus*

*Sphaeranthus indicus* Linn., in the Order *Compositae*, is a widely branching annual<sup>24</sup> herbal plant<sup>25</sup>, growing 30 – 60 cm tall,<sup>26</sup> with sessile leaves and rounded purple coloured flowers.<sup>25, 27</sup> It is quite fragrant,<sup>26</sup> but is bitter and sharp in taste.<sup>27</sup>

*S. indicus* is widely distributed, growing in tropical Asia, Africa, and Australia.<sup>23</sup> It is known to grow quite commonly in China, Sri Lanka, and especially India.<sup>27</sup> In India (particularly southern<sup>28</sup> and northern India<sup>26, 29, 30</sup> although it can be found throughout all of India<sup>25, 31, 32, 33</sup>), where its growth is most abundant in the plains, it prefers damp environments<sup>26</sup> such as in rice fields (where it is considered a weed)<sup>34, 35, 36, 37</sup> and other marshy areas.<sup>38</sup> The plant is also known as Gorakmundi in Hindi.<sup>26, 31, 33, 39, 40</sup>



**Figure 4:** *Sphaeranthus indicus*

Particularly in India, due to the therapeutic properties of *Sphaeranthus indicus* the plant have found their way into several indigenous systems of medicine including Ayurveda, Unani, and Siddha.<sup>21, 26, 41 - 46</sup>

Within these systems herbal medicines have been the basis of treatment and cure for various diseases and physiological conditions.<sup>47</sup>

An interesting note about *S. indicus* is that all parts of the plant have medicinal uses in ethnopharmacology or “folklore medicine”. The roots and seeds are anthelmintic and stomachic,<sup>25, 27, 39</sup> and are useful for treatment of bronchitis, jaundice, nervous depression, and glandular swellings.<sup>48</sup> The flowers are highly alterative, depurative, cooling, and tonic. It is also useful as a blood purifier in skin diseases.<sup>47, 49</sup> The leaves (prepared as dried and powdered, or the fresh juice) are useful for treatment of chronic skin diseases, urethral discharges, jaundice,<sup>53</sup> and for alleviating cough.<sup>27</sup> The juice (whole plant) is styptic and diuretic, and is useful in treating liver and gastric disorders.<sup>50</sup>

Additionally, the plant (unspecified portion) or its aqueous extract<sup>27</sup> has also been reported to possess antiseptic, antitussive, tonic effects,<sup>51</sup> laxative, anthelmintic, diuretic, analgesic, antimicrobial, antifungal,<sup>27</sup> anti-inflammatory, and antiallergic activity.<sup>52, 53</sup> *Sphaeranthus indicus* is also reported to be therapeutic in treatment of asthma, leucoderma, scabies,<sup>27</sup> dysentery,<sup>39</sup> rheumatic arthritis, and diabetes mellitus.<sup>52, 53</sup>

Concerning more modern research, the crude extract of *S. indicus* has been investigated for antimicrobial activity and it has been reported that it contains remarkable activity against a number of Gram-positive and Gram-negative bacteria<sup>23,</sup>

<sup>54</sup> including *Escherichia coli* and *Pseudomonas aeruginosa*, two important Gram-negative bacteria.<sup>47</sup> However, Narasimha Rao and Nigam investigated the antibacterial activity of the essential oil of *S. indicus* using the agar cup plate diffusion technique and found that it is highly effective agent (1:1000 dilution) against *Staphylococcus aureus* (a Gram positive bacteria), while totally ineffective against *Escherichia coli*.<sup>55</sup>

On a similar note Dubey et al. have investigated the antifungal activity of aqueous and ethanolic extracts of *S. indicus* by including it as an ingredient in the agar and then testing the inhibition against *Alternaria solani* (leaf pathogen), *Fusarium oxysporum* [Agent Green] (causative agent of Fusarium Wilt disease), and *Penicillium pinophilum* species and reported that it is extremely effective not only in concentrate but in 1000x dilution at inhibiting the growth of these pathogenic fungi.<sup>27</sup>

*S. indicus* (diluted ethanolic extract) has also been investigated for antioxidant activity (free radical scavenging potential) by testing against 4 compounds: 2,2-azinobis-(3-ethylbenzothiazoline-6-sulphonate) [ABTS], 1,1-diphenyl, 2-picrylhydrazyl (DPPH), superoxide dismutase, and nitric oxide radical. The extract possessed strong antioxidant activity.<sup>56</sup> This is of therapeutic interest because free radicals are implicated in degenerative diseases.<sup>57</sup>

Additionally, Sadaf et al. have investigated the wound-healing activity of the ethanolic extract of the aerial portion of *S. indicus* by preparing a cream and testing on Guinea pigs and discovered that it significantly accelerated both wound contraction and falling of eschar (scab). This activity is comparable to neomycin, an

approved drug,<sup>23</sup> which favourably indicates a possible use as an antiseptic, if not an antimicrobial agent.

Furthermore, a methanolic extract of *S. indicus* has been investigated for *in vitro* macrofilaricidal activity on adult *Setaria digitata*, the bovine filarial worm [nematode], by using the Worm Motility Test. It promises to be most useful (complete inhibition of motility and subsequent mortality) in this area as there are few chemotherapeutic agents to act against adult filarial nematodes.<sup>22</sup>

Also, a fraction of methanolic *S. indicus* extract has been shown to stimulate cell-mediated and humoral immunity, thus offering protection against cyclophosphamide (CP), an immunosuppressant in mice.<sup>28</sup>

Furthermore, the leaves of *S. indicus* have been investigated for sugar and amino acid composition.<sup>39</sup>

In view of the fact that a great deal of ethnopharmacological data exists about this plant and its importance for its multiple uses, it is not surprising then that it has been researched extensively for these uses. Additionally, due to its fragrant nature, it has been investigated for its fragrant compounds.

## **2.1 Previously Reported Compounds from *Sphaeranthus indicus***

### **2.1.1 Essential Oil Components**

To date, four research groups have investigated the essential oil of *Sphaeranthus indicus*, and have been successful in identifying the chemical compounds in highest yield therein. Analysis was carried out using GC/MS<sup>26, 30, 58, 59</sup> and in one case professional olfactory analysis.<sup>59</sup>



The analysis by Kaul et al. indicates that 38 compounds (84.0% of total) have been identified from the oil. The compounds that were major contributors to the oil include 2,5-dimethoxy-p-cymene (**10**) (18.2%),  $\alpha$ -agarofuran (**11**) (11.8%), 10-epi- $\gamma$ -eudesmol (**12**) (7.9%), and selin-11-en-4 $\alpha$ -ol (**13**) (12.7%).<sup>58</sup>

The analysis by Lodha states that 15 compounds in the capitula (69.9% of total) were identified including cadinene (**14**) (15.7%),  $\alpha$ -terpinene (**15**) (2.8%), ocimene (**16**) (6.5%), geraniol (**17**) (8.0%), eugenol (**18**) (7.9%), sphaeranthol (**19**) (13.0%), 1-ionone (**20**), citral (**21**) (6.0%), p-methoxy cinnamaldehyde (**22**) (7.8%), and geranyl acetate (**23**) (2.2%).<sup>26</sup>

Jirovetz et al. analyzed *S. indicus* and found over 95 components from the three selected parts studied (flowers, roots, and herb; stems with leaves). Major components (and their location of highest yield) include 2,5-dimethoxy-p-cymene (**18**) (28.3%; root),  $\beta$ -caryophyllene (**24**) (7.8%; flower), caryophyllene oxide (**25**) (6.9%; flower),  $\tau$ -cadinol (**26**) (7.2%; flower),  $\beta$ -eudesmol (**27**) (21.4%; flower), and  $\alpha$ -eudesmol (**28**) (7.0%; herb).<sup>59</sup>

The article by Baslas mirrors these findings with cadinene (**14**) (12.5%), ionone (**20**) (16.25%), p-methoxycinnamaldehyde (**22**) (11.88%), and estragole [methylchavicol] (**29**) (16.25%), as major components and terpinene (**15**) (4.38%), ocimene (**16**) (5%), geraniol (**17**) (4.38%), sphaeranthol (**19**) (3.75%),  $\alpha$ -citral (**21**) (5.63%), geranyl acetate (**23**) (6.25%), sphaeranthene (**30**) (4.38%), indicusene (**31**) (3.75%), and as minor components.<sup>30</sup>

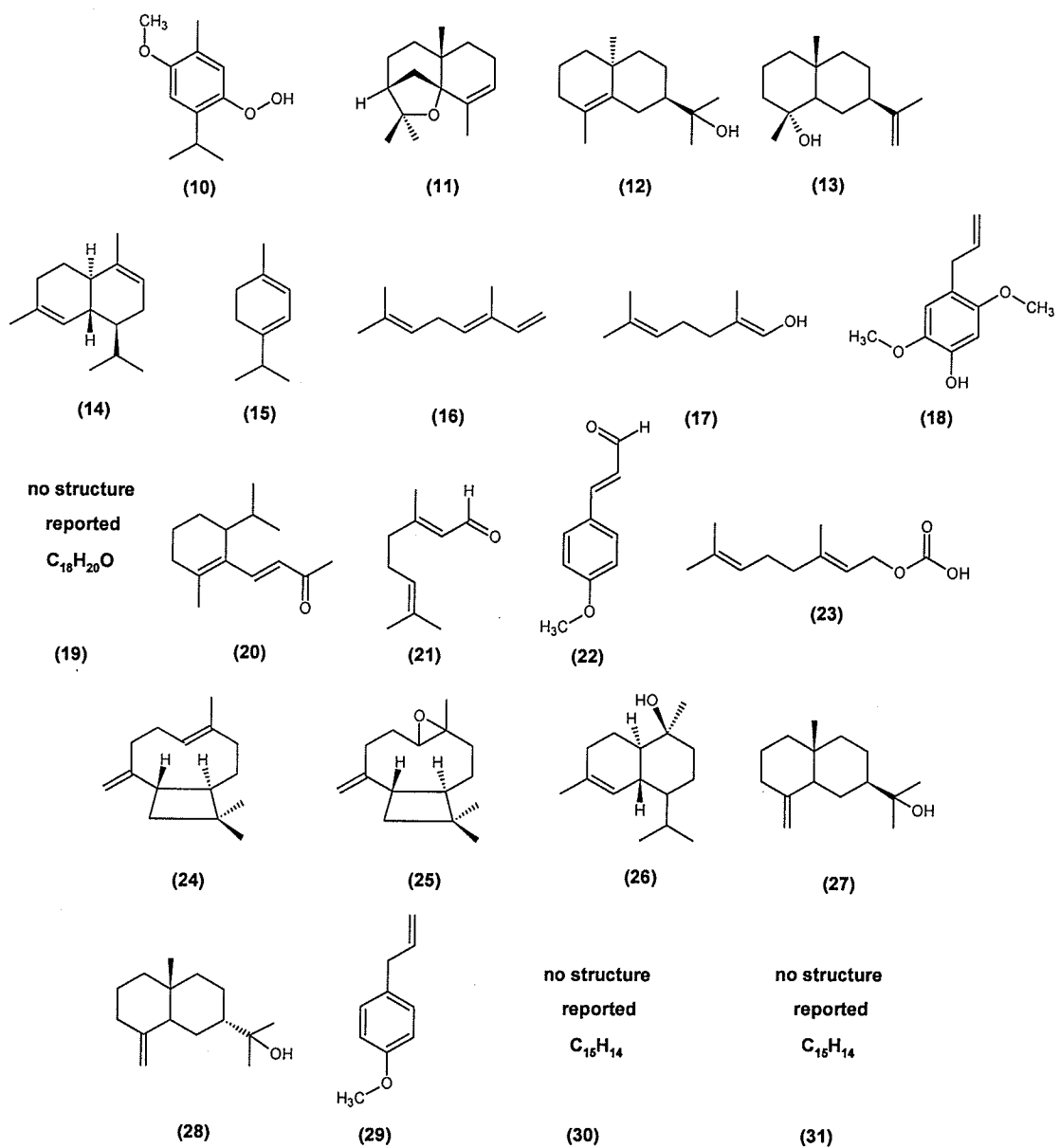


**Figure 5: Reported major chemical constituents of the essential oil of *Sphaeranthus indicus* (10 – 31)**

### 2.1.2 Sterols, Flavone glycosides, and Alkaloids from *Sphaeranthus indicus*

*S. indicus* has also been investigated to a moderate degree for the presence of sterols, flavone glycosides, and alkaloids in the search for novel structures.

For sterols, stigmasterol (**32**),<sup>24,25</sup>  $\beta$ -sitosterol (**33**), and  $\beta$ -sitosterol-*O*- $\beta$ -D-glycoside (**34**). Additionally, though not a sterol, hentriacontane (**35**) has also been isolated.<sup>24</sup>

For flavone glycosides, two compounds have been isolated: 5,4'-dimethoxy-3'-prenylbiochanin-7-*O*- $\beta$ -D-galactoside (**36**)<sup>31</sup> and 7-hydroxy-3',4',5,6-tetramethoxy-flavone 7-*O*- $\beta$ -D-(1 $\rightarrow$ 4)-diglucoside (**37**)<sup>39</sup>.

There are three isolated alkaloids from this plant: two unnamed alkaloids (**38**, **39**)<sup>60</sup> and sphaeranthinine (**40**).<sup>38</sup>

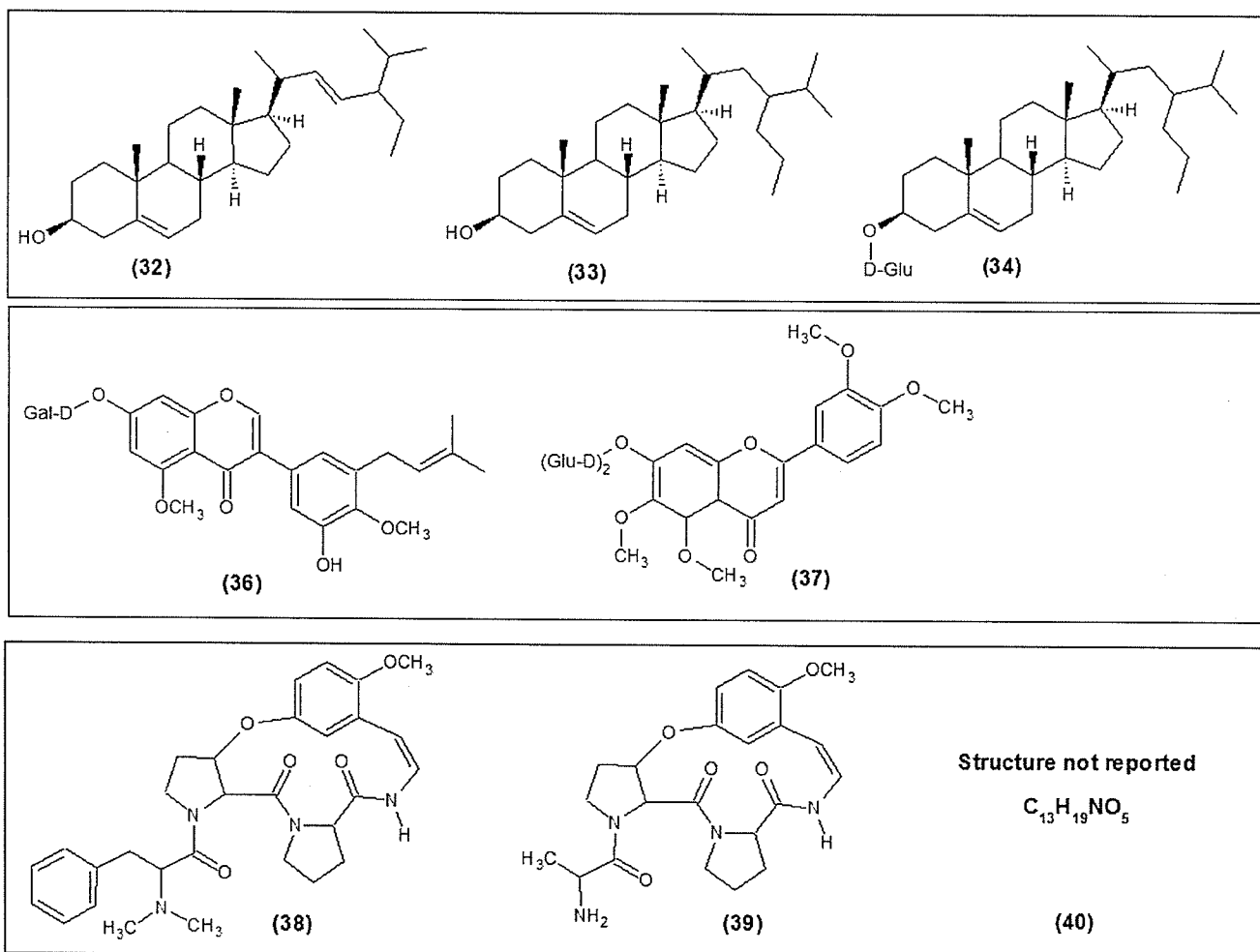


**Figure 6: Reported sterols (32 - 34), flavone glycosides (36 - 37), and alkaloids (38 - 40) from *Sphaeranthus indicus***

### 2.1.3 Biosynthesis of Eudesmane Structure

The compounds that have received the most research interest from *Sphaeranthus indicus* are the ones possessing the eudesmane structure. The eudesmane structure is biosynthesized starting from *E,E*-farnesyl diphosphate (or pyrophosphate) [*E,E*-FPP] (**41**), which loses its OPP leaving group to become a cation (or ion-pair) and then rearranges to the *E,Z*-farnesyl cation (**42**), which then folds and rearranges into the nerolidyl cation (**43**), rearranging again to form the *E,E*-farnesyl cation [*E,E*-FPP] (**44**). Cyclization occurs next due to electrophilic attack of the cation (or ion-pair) onto a double bond, forming the germacryl cation (**45**), followed by another cyclization resulting in the eudesmyl cation (**46**), and finally an elimination reaction to form the tetrasubstituted 4,5-double bond structure, eudesmane (**47**).<sup>61</sup>

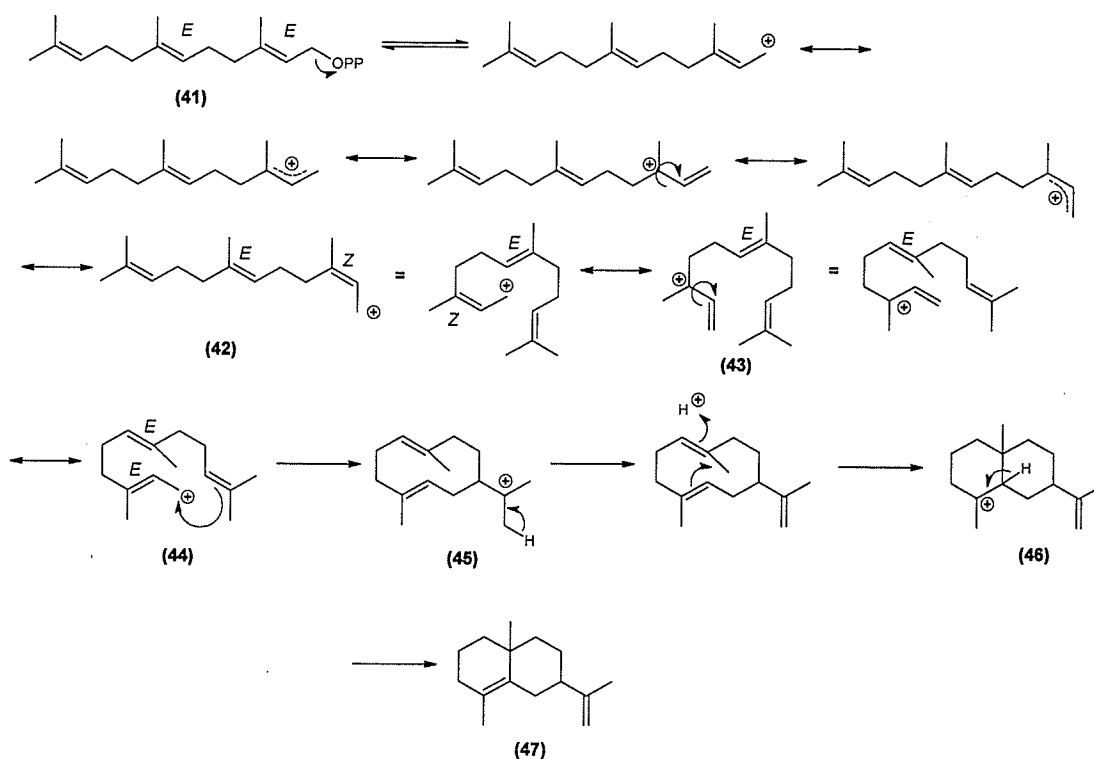
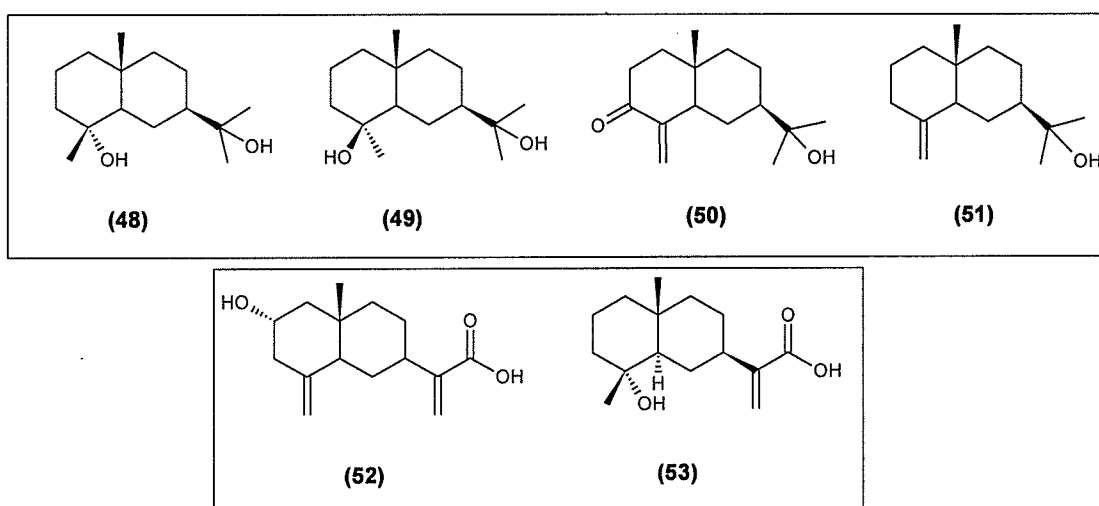


Figure 7: Biosynthesis of the eudesmane structure (47) from *E,E*-FPP (41)

## 2.1.4 Hydroxyeudesmanes, eudesmane acids, and eudesmanolides from *Sphaeranthus indicus*

There are quite a variety of compounds with the basic eudesmane structure present but with varying degrees of oxidation present in *Sphaeranthus indicus*. The hydroxyeudesmanolides isolated so far include cryptomeridiol (**48**) epicryptomeridiol (**49**),<sup>34</sup> 3-keto- $\beta$ -eudesmol (**50**), and  $\beta$ -eudesmol (**51**).<sup>51</sup> 2 $\alpha$ -hydroxycostic acid (**52**) and illicic acid (**53**) are reported eudesmane acids.



**Figure 8: Hydroxyeudesmanes (48 – 51) and eudesmane acids (52 – 53) isolated from *Sphaeranthus indicus***

However, the eudesmanolides (*-olide* being the standard suffix for lactones) are the most significant chemical findings in *S. indicus*. Most of the eudesmanolides that have been isolated have novel skeletons. In total, there are 14 such sesquiterpenes isolated thus far from this plant.

7 $\alpha$ -hydroxyfrullanolide (**54**) was the first to be isolated. There is some discrepancy about the original isolation of this compound, which occurred in either 1985 by Gogtet and co-workers,<sup>42</sup> in 1988 by Sohoni and co-workers,<sup>32</sup> or by Atta-ur-Rahman and co-workers in 1989.<sup>62</sup> 7 $\beta$ -hydroxyfrullanolide (**55**) and 7 $\alpha$ -

hydroxyeudesmanolide (**56**) were also reported in 1985.<sup>42</sup> Sphaerantholcide (**57**),<sup>63</sup> 11 $\alpha$ ,13-dihydro-3 $\alpha$ ,7 $\alpha$ -dihydroxyfrullanolide<sup>64</sup> (**58**), 11 $\alpha$ ,13-dihydro-7 $\alpha$ ,13-dihydroxyfrullanolide (**59**), and 11 $\alpha$ , 13-dihydro-7 $\alpha$ -hydroxy-13-methoxyfrullanolide (**60**)<sup>48</sup> were discovered during 1990 – 1991 by the Shekhani<sup>48, 63</sup> and Ruangrunsi<sup>64</sup> groups, respectively. Rojatkar and co-workers isolated 3-keto-7 $\alpha$ -hydroxyeudesmanolide (**61**), and 4,5-dehydro-5 $\alpha$ ,7 $\alpha$ -dihydroxyfrullanolide (**62**) in 1992.<sup>34</sup> In 1999, Pujar and co-workers reported 11 $\alpha$ ,13-dihydro-7 $\alpha$ -acetoxy-3 $\beta$ -hydroxy-6 $\beta$ -7-eudesm-4-enolide (**63**) and 11 $\alpha$ ,13-dihydro-3 $\alpha$ ,7 $\alpha$ -dihydroxy-4,5-epoxy-6 $\beta$ ,7-eudesmanolide (**64**).<sup>51</sup> Most recently, 2 $\alpha$ -7 $\alpha$ -dihydroxy-4-en-11,13-dihydroeudesmen-6-12-olide (**65**),<sup>65</sup> 11 $\alpha$ ,13-dihydro-3 $\alpha$ ,7 $\alpha$ -dihydroxyeudesm-4-en-6 $\alpha$ ,12-olide (**66**), and 4-en-6 $\beta$ ,7 $\alpha$ -eudesmanolide (**67**) were reported in 2007.<sup>66</sup>

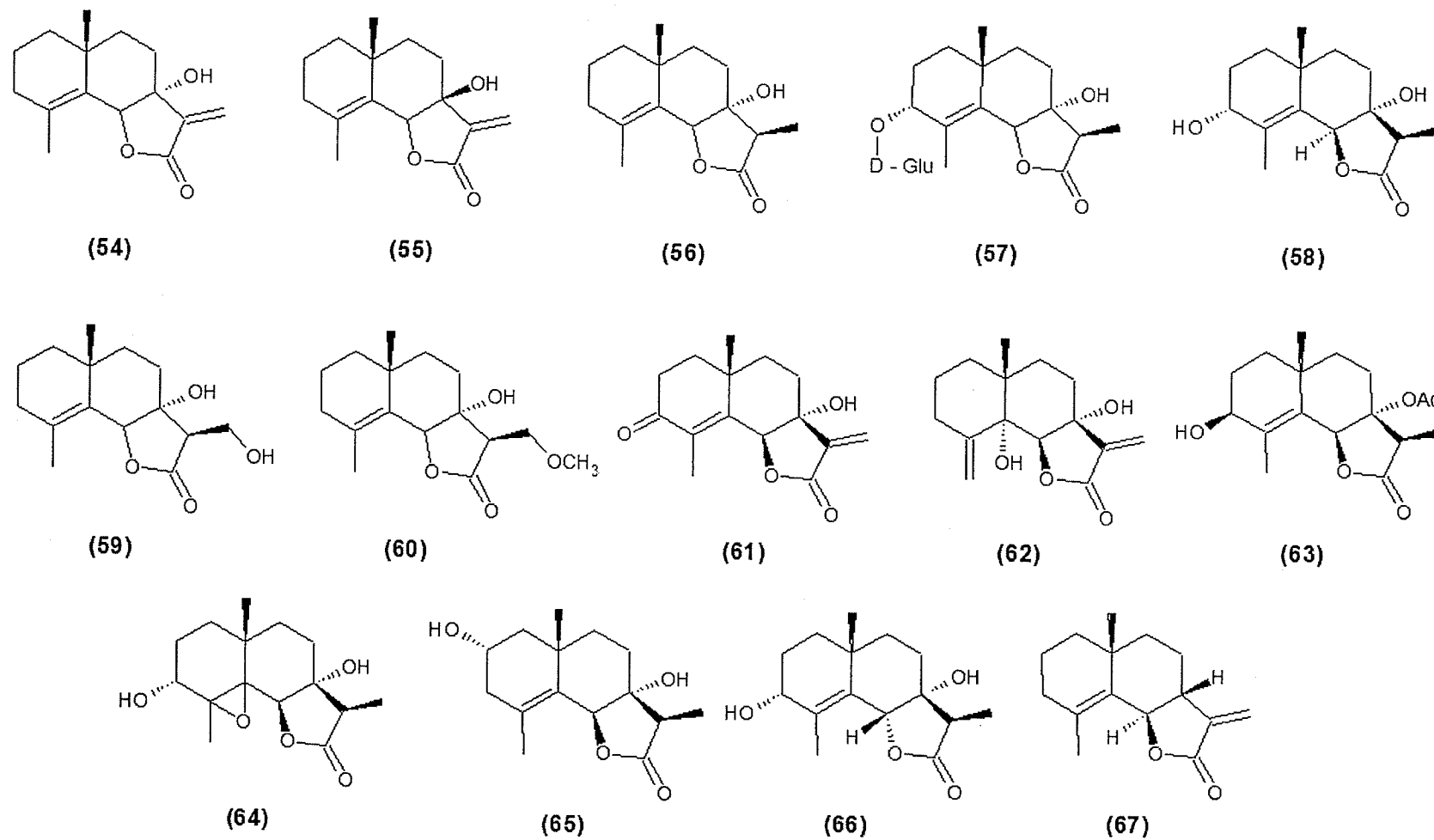


**Figure 9: Structures of eudesmanolides isolated from *Sphaeranthus indicus* (54 - 67)**



Table 1 describes the extraction solvent, yield, and starting plant mass, where possible, of previous examinations of these eudesmanolides that have been isolated from *Sphaeranthus indicus*. This was done as a way to better compare the current examination with the previous examinations.

**Table 1: extraction solvent, yield, and plant mass data of previous investigations of eudesmanolides isolated from *Sphaeranthus indicus* (54 – 67)**

Number	Extraction Solvent	Yield	Plant Mass	Reference
<b>54</b>	chloroform	2.9 g	20 Kg	42
	acetone	8.5 g	3 Kg	32
	ethanol	-	-	62
<b>55</b>	chloroform	8.1 g	20 Kg	42
<b>56</b>	chloroform	1.7 g	20 Kg	42
	acetone	18 mg	2 Kg	34
<b>57</b>	methanol	95 mg	40 Kg	63
<b>58</b>	ethanol	35 mg	2 Kg	64
<b>59</b>	ethanol	80 mg	40 Kg	48
<b>60</b>	ethanol	10 mg	40 Kg	48
<b>61</b>	acetone	10 mg	2 Kg	34
<b>62</b>	acetone	12 mg	2 Kg	34
<b>63</b>	acetone	12 mg	1 Kg	51
<b>64</b>	acetone	13 mg	1 Kg	51
<b>65</b>	acetone	27 mg	850 g	65
<b>66</b>	-	-	-	66
<b>67</b>	-	-	-	66

These structures are significant findings because sesquiterpene lactones containing the unusual 7-hydroxy substituent are very rare in nature. Lactones such as 7-hydroxyfrullanolide (**54**)<sup>67</sup> that possess an  $\alpha$ ,  $\beta$ -unsaturated group are known to be biologically active, such as with parthenolide (**68**), but often this activity is cytotoxicity; i.e. non-selective toxicity. This is due to this functional group acting as a powerful alkylating agent in a Michael-type addition of an appropriate nucleophile –

such as a thiol group on a protein – onto the  $\alpha$ ,  $\beta$ -unsaturated lactone, binding irreversibly (69).<sup>68</sup>

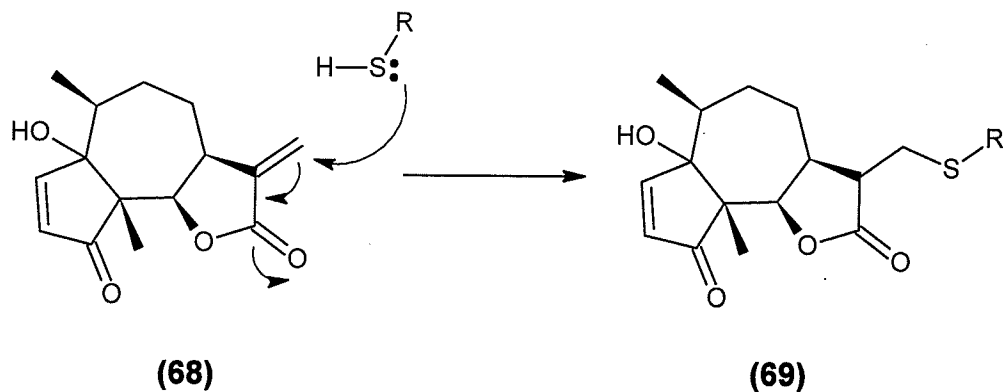


**Figure 10: Michael-type addition of a thiol group onto parthenolide (68), an  $\alpha$ ,  $\beta$ -unsaturated lactone and the resulting irreversibly-bonded species (69)**

As was mentioned in the introduction (Section 1.6), there is scarce data available on the antibacterial constituents of *S. indicus*. Previous examinations (mostly of crude extracts) are indicative of constituent compounds with strong antibacterial activity. Thus, this warrants a new investigation with the means to measure the antibacterial activity of these pure, isolated compounds, relative to each another. Such an investigation has not been done in any comprehensive fashion to date.

## 2.2 *Sphaeranthus indicus* Experimental

### General

Analytical thin layer chromatography was conducted on Merck pre-coated, aluminum-backed, 250  $\mu\text{m}$  layer, 20 cm x 20 cm silica gel G F<sub>254</sub> plates. Column chromatography was performed on Aldrich silica gel, 200 – 400 mesh. Preparative thin layer chromatography was conducted on Merck pre-coated, glass-backed, 1000  $\mu\text{m}$  layer, 20 cm x 20 cm UV<sub>254</sub> silica gel plates. TLC UV-visualization was done by using a Entela multiband (UV-256/366 nm) Model UVGL-58 Mineralight® Lamp. 95% ethanol was supplied by Les Alcools de Commerce Inc. All other solvents (non-deuterated) were ACS reagent grade and purchased from Anachemia. CDCl<sub>3</sub> was supplied by CDN Isotopes.

Mueller – Hinton broth (powder) was purchased from EM Science.

### Bacteria

The following bacterial strains were obtained from the University of Winnipeg Department of Biology: *Escherichia coli* (ATCC #25922), *Staphylococcus aureus* (ATCC #25923), *Streptococcus agalactiae* (ATCC #13813), and *Pseudomonas aeruginosa* (ATCC #27853). The *E. coli*, *S. aureus*, and *P. aeruginosa* cultures were periodically replated onto tryptic soy agar, whereas the *S. agalactiae* was replated onto blood agar to facilitate its slow growth. Replating of the stock cultures was executed once a week and cultures were maintained at 4°C.

### Spectroscopy

All <sup>13</sup>C NMR spectra were obtained using a Varian Gemini 200 MHz nuclear magnetic resonance (NMR) spectrometer at the University of Winnipeg, operating at

50.28 MHz using CDCl<sub>3</sub> as solvent. All <sup>1</sup>H NMR and 2D NMR spectra (COSY, HSQC, HMBC, and NOESY) of the purified products were obtained using a Bruker Avance 300 MHz NMR spectrometer at the University of Manitoba, operating at 300.13 MHz for <sup>1</sup>H and 75.47 MHz for <sup>13</sup>C, using CDCl<sub>3</sub> as solvent. In all cases for NMR spectra, referencing was done to the residual peak of CHCl<sub>3</sub> at δ 7.26 and 77.0 for <sup>1</sup>H and <sup>13</sup>C, respectively.

IR spectra were obtained using a Bomem Hartmann & Braun MB Series spectrophotometer as a CCl<sub>4</sub> film. UV spectra were obtained using a Shimadzu UV-2501 PC UV/ Vis spectrophotometer or an Agilent Technologies 8453 E Dual-Array UV spectrometer in methanol.

### **High Performance Liquid Chromatography (HPLC)**

A Waters HPLC system was used, equipped with the following: a Model 1525 Binary Pump, a Waters In-Line Degasser AF, a Model 2996 photodiode array detector, and a Waters Nova-Pak 4µm 3.9 x 150 mm C18 stainless steel cartridge column. The separation was isocratic at ambient temperature and the mobile phase used was either a mixture of acetonitrile / 80% water, 20% methanol or methanol / 80% water, 20% methanol.

### **Plant Collection and Extraction**

The roots and leaves of a *Sphaeranthus indicus* plant were collected by Dr. Radhika Samersekera, Natural Products Institute, Sri Lanka. The plant was extracted with methanol and the solvent was evaporated under reduced pressure to prepare a dark green gum. This gum (20.6 g) was then shipped to the University of Winnipeg.

## Isolation of Natural Products

The gum-like crude plant extract was dissolved in ethyl acetate and was adhered onto silica gel by evaporating the solvent under reduced pressure until the texture was a crumbly solid. This silica gel/extract solid was then loaded (dry) onto a silica gel chromatography column.

Column chromatography was then performed on the extract, following a stepwise gradient elution using hexanes / ethyl acetate, followed by ethyl acetate / methanol. The volume for each mobile phase was 150 mL and the gradient for subsequent mobile phases was 5%; i.e. 100 % hexanes → 95% hexanes / 5% ethyl acetate, etc. The 42 fractions were then examined using analytical TLC with the mobile phase, 50% hexanes / 50% ethyl acetate, which was determined to be the optimum for this analysis. Fractions that exhibited similar chromatographic profiles on analytical TLC were combined to reduce the total number of [pooled] fractions. <sup>1</sup>H NMR spectroscopy was then used to inspect the fractions for relative purity and quantity of the analytes contained within, thus further reducing the number of fractions for further analysis. Results were generated from two of these pooled fractions: fraction 33 – 36 and fraction 52 – 56.

Pooled fraction 33 - 36 displayed evidence of containing significant quantity of UV-inactive compounds on analytical TLC. This fraction was subjected to preparative TLC using 70% hexanes / 30% ethyl acetate and aluminum-backed TLC plates that enabled the ends to be removed and subjected to charring treatment (spraying the TLC plate with 10% sulphuric acid (1.8 M), then charring with a heat gun) until the “end-bands” became visible. In total, five plates were used. One of the

bands ( $R_f = 0.86$ ) was observed to be darkened more than the other five. This band's silica gel was scratched off the pTLC plates, and extracted (DCM, 5 x 30 mL) to yield dihydrocholesterol (**70**) (33.0 mg).

Pooled fraction 52 – 56 was subjected to secondary column chromatography using 30.0 g silica. Again, a stepwise gradient was used using hexanes / ethyl acetate, and followed by ethyl acetate / methanol mixtures. The volume of each mobile phase was 100 mL and the gradient for subsequent mobile phase was 5% increments from hexanes to ethyl acetate, then 25% increments from ethyl acetate to 50% ethyl acetate / 50% methanol, and finally 50% increments from 50% ethyl acetate / 50% methanol to 100% methanol. There were 115 sub-fractions from this pooled fraction. Analytical TLC analysis of these fractions and subsequent  $^1\text{H}$  NMR spectroscopy were used to screen for pure compounds (in sufficient yield), as had been done previously with the primary column chromatography. Sub-fractions 27 - 29 afforded 7 $\alpha$ -hydroxyfrullanolide (**54**) (78.6 mg), while sub-fractions 32 – 33 yielded a slightly impure compound. It was decided to attempt to purify this analyte by HPLC.

HPLC separation of sub-sample 32 - 33 (from pooled fraction 52 – 56) was executed by using the following operating parameters: 50% methanol / 50% acetonitrile isocratic mobile phase, 15 min run time, 50  $\mu\text{L}$  injection volume, 1 mL/min flow rate, and 254 nm detection (scan 210 – 380 nm). The principal compound was isolated by collecting the eluent from  $R_T$  2.40 – 3.40 min in 20 collection runs, resulting in a white powder, identified as 7 $\alpha$ -hydroxyeudesmanolide (**56**) (2.6 mg). The other major constituent of this fraction, detected from  $R_T$  1.50 – 2.00 though isolated, had insufficient quantity for structure determination.

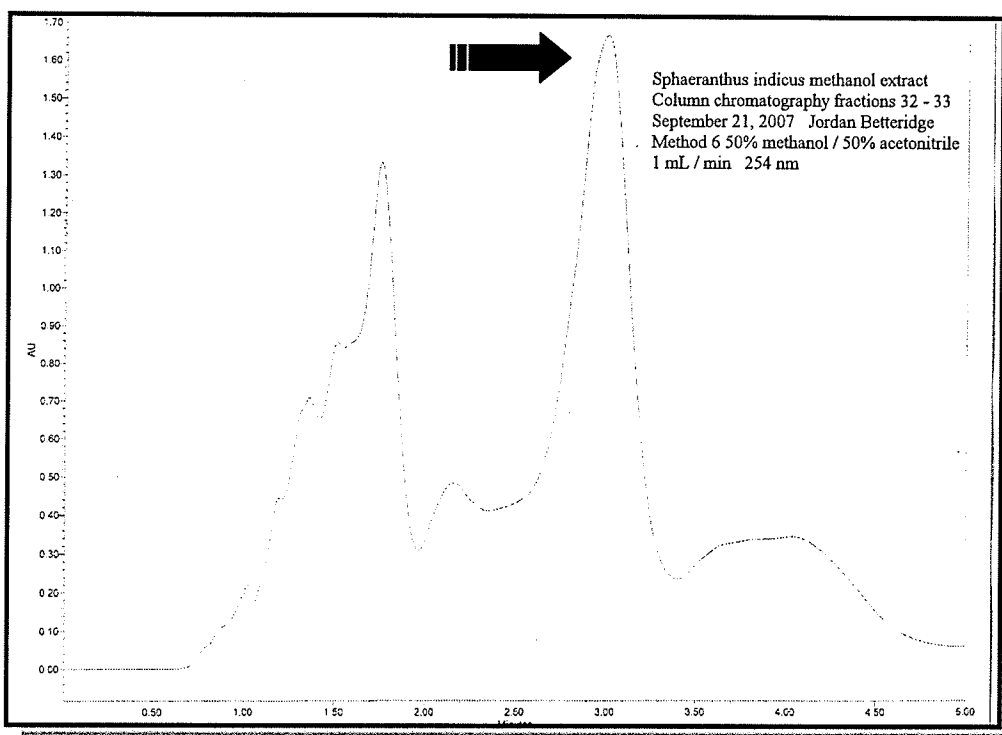


**Figure 11: HPLC Chromatogram of column chromatography sub-fraction 32-33 of the methanolic *Sphaeranthus indicus* extract (with peak of interest selected)**

Dihydrocholesterol **70**; white powdery solid; 33.0 mg; fraction 33-36; UV  $\lambda_{\max}$  (MeOH) = terminal; IR (CCl<sub>4</sub>) = 3354, 2933, 1075 cm<sup>-1</sup>; <sup>1</sup>H NMR (CDCl<sub>3</sub>, 300.13 MHz) = see Table 2; <sup>13</sup>C NMR (CDCl<sub>3</sub>, 75.47 MHz) = see Table 2; EI-MS = m/z 388 (M<sup>+</sup>).

7 $\alpha$ -hydroxyfrullanolide **54**; white powdery solid, 78.6 mg; fraction 52 – 56; UV  $\lambda_{\max}$  (MeOH) = 241 nm; IR (CCl<sub>4</sub>) = 3453, 2932, 1771, 1750, 1683, 1144 cm<sup>-1</sup>; <sup>1</sup>H NMR (CDCl<sub>3</sub>, 300.13 MHz) = see Table 3; <sup>13</sup>C NMR (CDCl<sub>3</sub>, 75.47 MHz) = see Table 3, EI-MS = m/z 248, 233, 215, 187, 178, 109, 81, 55, 41.

7 $\alpha$ -hydroxyeudesmanolide **56**; white powdery solid, 2.6 mg, fraction 52 – 56; UV  $\lambda_{\text{max}}$  (MeOH) = terminal; IR (CCl<sub>4</sub>) = 3494, 2930, 1785, 1650, 1219 cm<sup>-1</sup>; <sup>1</sup>H NMR (CDCl<sub>3</sub>, 300.13 MHz) = see Table 4; <sup>13</sup>C NMR (CDCl<sub>3</sub>, 75.47 MHz) = see Table 4, EI-MS = m/z 250, 235, 189, 161, 60.

### Structure Activity Relationship Analysis (SAR)

In order to study the structure-activity relationship of compound **54**, chemical modification using semi-synthetic techniques was done to investigate what effect alteration of certain functional groups would have on its biological activity, if any. Due to the low quantity of **54**, SAR studies were limited to the effect of the C-4/C-5 bond on antibacterial activity, though other modifications were attempted. To achieve this objective, **54** was epoxidized using *m*-chloroperbenzoic acid. Compound **56** was isolated in sufficient quantity for MIC testing, but not SAR studies.

#### 1) Epoxidation of 7 $\alpha$ -hydroxyfrullanolide (**54**)

10 mg of 7 $\alpha$ -hydroxyfrullanolide (**54**) was added to 4 mL of dry, distilled DCM containing 4.5 mg of *m*-chloroperbenzoic acid [mcpBA] (accounted for 77% purity) in a 25 mL roundbottom flask, and stirred for 4 hours at room temperature. Reaction progress was checked by analytical TLC (50% ethyl acetate/50% hexanes for mobile phase). At the end of the reaction time, 4 mL of saturated sodium hydrogen carbonate solution was added to neutralize the side-product, meta-chlorobenzoic acid. The organic layer was separated, pooled, and dried under reduced pressure to yield 8.6 mg (86% yield) of 4, 5-epoxy-7 $\alpha$ -hydroxyfrullanolide (**71**) as a



white solid.  $^1\text{H}$  and  $^{13}\text{C}$  NMR analysis confirmed that a diastereomeric structure of epoxides was the result of the reaction.

## 2) Acetylation of 7 $\alpha$ -hydroxyfrullanolide (**54**)

3.1 mg of 7 $\alpha$ -hydroxyfrullanolide (**54**) was added to 5 mL of acetic anhydride in pyridine (4 mL) in a 10 mL roundbottom flask, and stirred for 16 h at room temperature. After the reaction time, 2 mL of water was added to allow extraction using DCM (4x, 10 mL). The organic layer was separated, pooled, and dried under reduced pressure.  $^1\text{H}$  and  $^{13}\text{C}$  NMR analysis was done to inspect the structure, initially.

The reaction was ultimately unsuccessful as evidenced by the absence of an additional downfield acetyl methyl proton signal ( $\sim \delta 2.0$ ) in the  $^1\text{H}$  NMR spectrum, and downfield acetyl carbonyl carbon signal ( $\sim \delta 170$ ) and acetyl methyl carbon signal ( $\sim \delta 24$ ). This is most likely due to the tertiary ( $3^\circ$ ) nature of the C-7 hydroxyl functionality, being less reactive than  $1^\circ$  or  $2^\circ$  hydroxyl groups.

---

4, 5-epoxy-7 $\alpha$ -hydroxyfrullanolide **71**; white powdery solid, 8.6 mg; UV  $\lambda_{\text{max}}$  (MeOH) = 275 nm; IR ( $\text{CCl}_4$ ) = 3366, 2934, 1773  $\text{cm}^{-1}$ , 1121  $\text{cm}^{-1}$ ;  $^1\text{H}$  NMR ( $\text{CDCl}_3$ , 300.13 MHz) =  $\delta$  6.24 (s), 5.82 (s), 4.79 (s), 3.90 (d), 1.40 (s), 1.05 (s);  $^{13}\text{C}$  NMR ( $\text{CDCl}_3$ , 75.47 MHz) =  $\delta$  167.9, 143.4, 121.2, 83.4, 75.7, 63.6, 62.7, 62.1, 60.4, 33.7, 32.2, 31.9, 30.9, 29.7, 27.7, 21.1, 19.8

## Minimum Inhibitory Concentration (MIC) Testing

The following procedure was developed for executing the Minimum Inhibitory Concentration (MIC) testing with consultation with Dr. Holloway and the guidelines from the NCCLS document M7-A3<sup>69</sup>. This was performed on the purified natural products. Each pure compound was tested against the four bacteria available.

Along with the pure natural products two known antibacterial compounds, penicillin G (**5**) and chloramphenicol (**72**) (as standards), were tested against the four bacteria. These standards were selected due to their different activities: penicillin G (**5**) is only antibacterial against Gram-positive bacteria and has an extremely low reported MIC value [ $\leq 1 \mu\text{g/mL}$ ], whereas chloramphenicol (**72**) is antibacterial against both Gram-positive and Gram-negative bacteria and has a higher reported MIC value. These were obtained from Dr. Holloway, University of Winnipeg, Department of Biology.

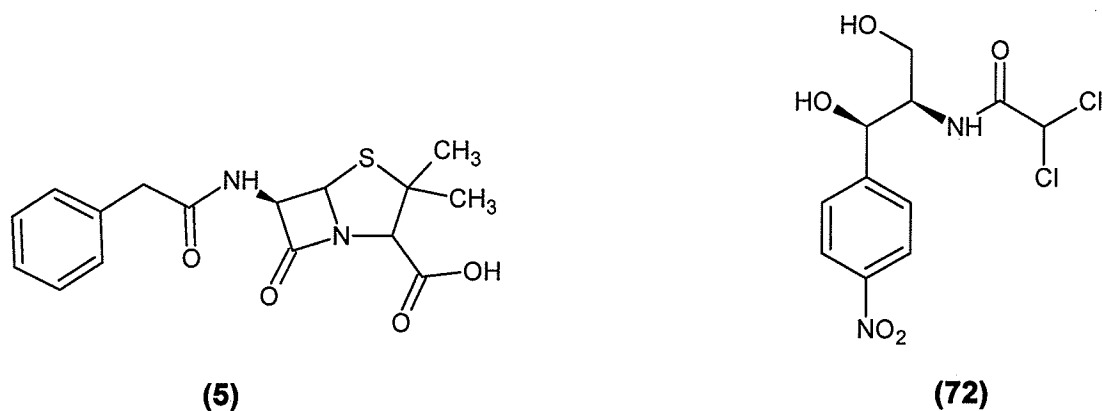


**Figure 12: The structures of penicillin G (5) and chloramphenicol (72)**

An overnight culture (16 – 18 h) of each bacteria using Mueller – Hinton broth (pH adjusted to 7.3 using NaOH) was diluted to optically match the turbidity of a McFarland 0.5 standard, equivalent to  $1.5 \times 10^8$  CFU/mL. These diluted solutions

were further diluted 150x ( $1 \times 10^6$  CFU/mL) into sterile broth, from which a 1 mL aliquot of this bacterial solution was transferred to nine sterile 13 mm test tubes.

A stock solution of the “potential” antimicrobial compound to be tested was prepared (2.56 mg/mL) by using a minimum amount of 95% ethanol to dissolve the compound and then diluting with sterile distilled water. This stock solution was then diluted 10x (254  $\mu$ g/mL) with sterile water to produce a working solution.

A serial dilution of the “potential” antimicrobial compound was performed to produce a concentration testing range of 128  $\mu$ g/mL – 1  $\mu$ g/mL. This was performed in the following manner: to the first test tube (for each bacteria) in the serial dilution, 1 mL of this working solution (256  $\mu$ g/mL) of compound was added, thus diluting the bacteria to  $5 \times 10^5$  CFU/mL and diluting the compound to a concentration of 128  $\mu$ g/mL. A 1 mL aliquot of this solution was then transferred to the next tube (64  $\mu$ g/mL), and this was continued until the concentration of “potential” antimicrobial compound was 1  $\mu$ g/mL.

Additionally, a positive “growth” control and a negative “sterile” control were prepared for each bacterium tested against a natural product (4 of each control per compound) to determine whether the bacteria grew properly and if sterility was maintained, respectively. The positive “growth” control was prepared by adding the appropriate concentration of bacteria, but using sterile water instead of “potential” antimicrobial agent, mixing, and then 1 mL was discarded, while the negative “sterile” control was prepared by adding a 1 mL aliquot of working solution [“potential” antimicrobial], but using sterile water instead of working bacterial solution, mixing, and 1 mL was discarded

After the serial dilution was completed, the tubes were incubated on a gyrorotary shaker at 37°C for 20 hours with 120 rpm. After incubation, the tubes were examined optically; the tube with the lowest concentration of compound that inhibits all growth of bacteria was determined to be the minimum inhibitory concentration (expressed as  $\leq \mu\text{g} / \text{mL}$ ). This analysis was performed in triplicate and the results were averaged.

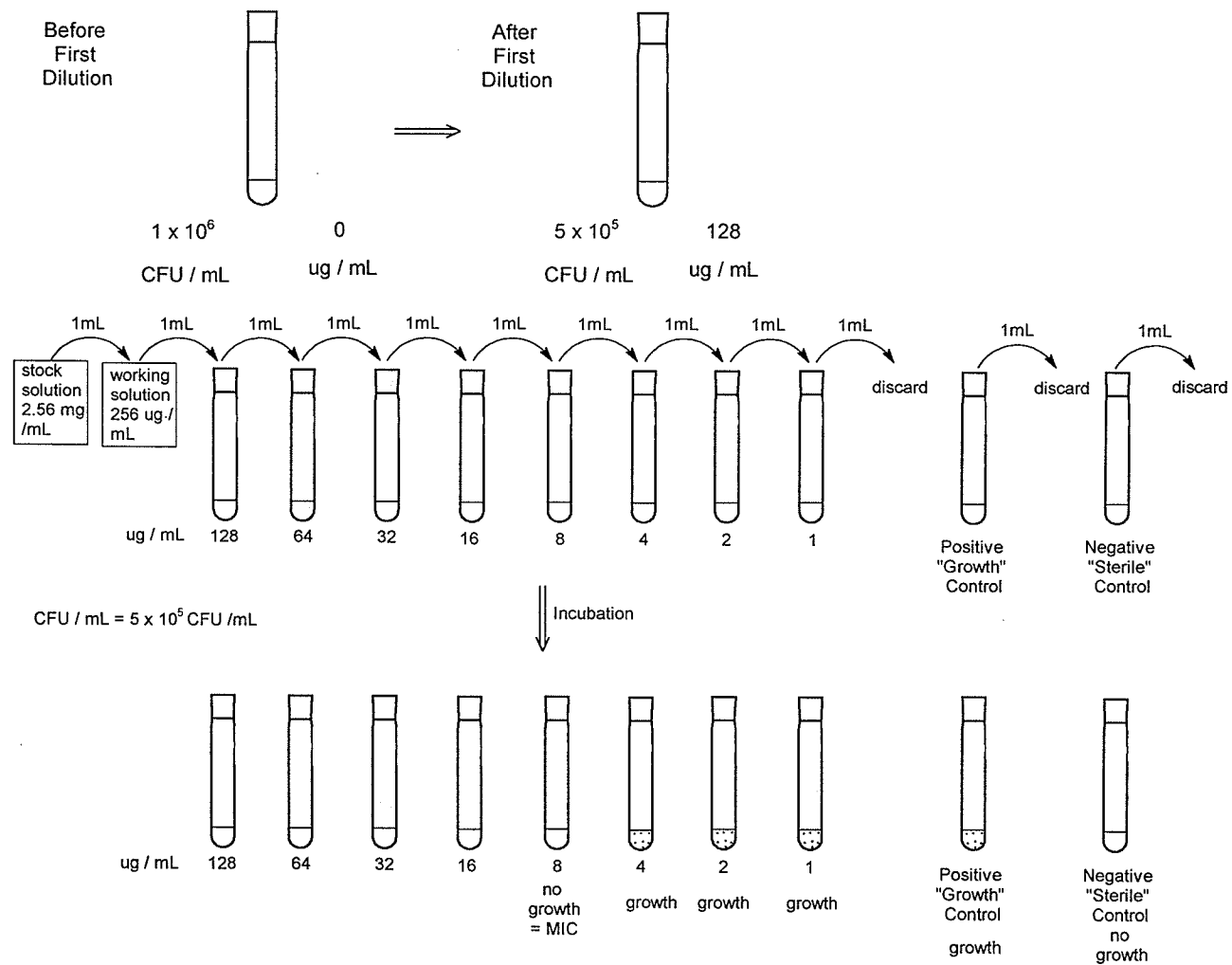
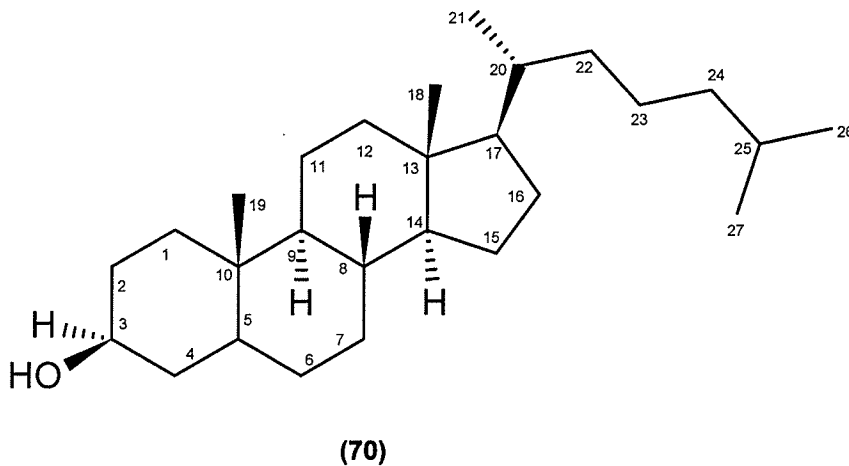


Figure 13: Illustration of MIC Procedure

## 2.3 *Sphaeranthus indicus* Results and Discussion

### Dihydrocholesterol (70)

The UV spectrum of compound **70** showed only terminal absorption indicating the lack of a conjugated system. It has been previously reported. The IR spectrum of **70** displayed strong peaks at 3354 (OH), 2933 (CH), and 1075 (CO)  $\text{cm}^{-1}$ .



The  $^1\text{H}$  NMR spectrum of compound **70** showed the presence of a downfield multiplet at  $\delta$  3.59, which was assigned to the methine geminal to the hydroxyl group. Two methyl groups resonated as singlets at  $\delta$  0.65 and 0.80, and were assigned to C-18 and C-19, respectively. There were additionally three methyl groups as doublets at  $\delta$  0.90, 0.87, and 0.85, which were assigned to the C-21, C-26, and C-27, respectively. Beyond this, there was no further evidence of any downfield peaks. The  $^1\text{H}$  NMR spectral data suggested a cholestane-type sterol structure.

The Attached Proton Test (APT) spectrum of **70** revealed the presence of all 27 carbon signals in **70** and was used to determine their multiplicity. The APT showed the presence of five  $\text{CH}_3$ , twelve  $\text{CH}_2$ , eight  $\text{CH}$ , and two quaternary ( $4^\circ$ )

carbons. The negative phase signal at  $\delta$  71.4 was assigned to the hydroxyl-bearing C-3. The negative phase signals at  $\delta$  12.1, 12.3, 18.6, 22.8, and 22.6 were assigned to the C-18, C-19, C-21, C-26, and C-27 methyl carbons, respectively. This spectrum was remarkably similar to the relevant spectrum of cholesterol, although missing its two  $sp^2$ -hybridized carbon peaks responsible for the endocyclic 4/5 double bond.

The Correlation Spectroscopy (COSY) spectrum of **70** displayed vicinal and geminal coupling between protons. Most importantly, the signal at  $\delta$  3.58 showed coupling with the signals at 1.56 and 1.29, assigned to the C-3 methine proton and the C-4 methylene protons.

The Heteronuclear Single Quantum Coherence (HSQC) spectrum of **70** displayed direct coupling between a carbon atom and its attached protons. The HSQC spectrum was used to find the  $^1\text{H}/^{13}\text{C}$  chemical shift assignments of **70** (see Table 2).

The Heteronuclear Multiple Bond Coherence (HMBC) spectrum of **70** displayed long-range coupling between protons and proximal (but not vicinal) carbons. This spectrum is used to confirm the  $^1\text{H}/^{13}\text{C}$  chemical shift assignments. It is especially useful for quaternary carbons. In this spectrum, the C-14 methine proton ( $\delta$  1.07) showed cross-peaks with C-12 (40.0), and C-13 (42.6). The C-17 methine proton ( $\delta$  0.65) showed coupling with C-12 (40.0). The C-1 methylene protons ( $\delta$  1.73, 1.69) had cross-peaks with the hydroxylated carbon, C-3 (71.4). The C-4 methylene protons ( $\delta$  1.56, 1.29) showed coupling with C-2 (31.5). The C-6 methylene protons ( $\delta$  1.30, 1.27) showed HMBC interaction with C-5 (44.8). C-7 methylene protons ( $\delta$  1.69, 1.64) showed long-range heteronuclear coupling with C-5 (44.8) and C-8 (35.4). The C-12 methylenes ( $\delta$  1.99, 1.95) had cross-peaks with C-9

(54.3), C-11 (21.2), and C-13 (42.6). The C-18 methyl protons ( $\delta$  0.65) showed coupling with C-12 (40.0), C-13 (42.6), and C-17 (56.2). The C-19 methyl protons ( $\delta$  0.80) showed HMBC interaction with C-5 (44.8) and C-9 (54.3). The C-21 methyl protons ( $\delta$  0.88) showed cross-peaks with C-17 (56.2) and C-20 (35.8). Lastly, both C-26 and C-27 methyl protons ( $\delta$  0.87 and 0.85, respectively) showed coupling with C-24 (39.5) and C-25 (28.0). Important HMBC interactions of **70** are displayed in Figure 14.

Additionally,  $^{13}\text{C}$  NMR and  $^1\text{H}/^{13}\text{C}$  HSQC data matched very closely with literature values, thus the structure is concluded to be dihydrocholesterol (**70**).<sup>70</sup>

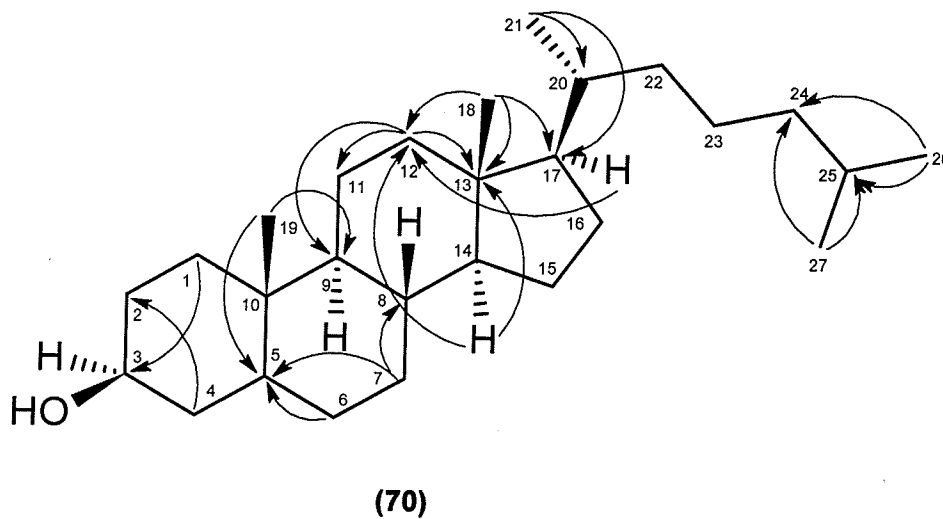


**Figure 14: Important HMBC Interactions Observed in 70**

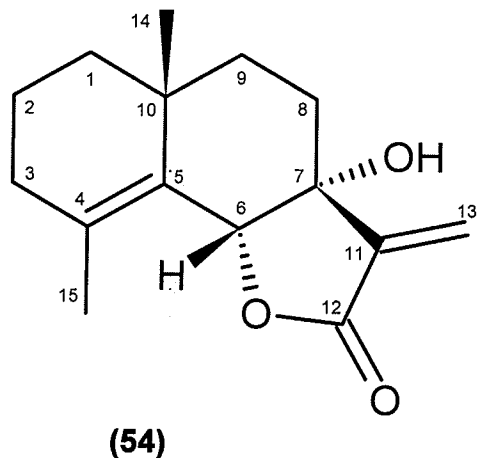


**Table 2:  $^{13}\text{C}$  NMR Chemical Shift Assignments and  $^1\text{H}/^{13}\text{C}$  One-Bond Shift Correlations of 70 as determined from its HSQC Spectra**

Carbon #	70		$^{13}\text{C}$ $\delta$
	$^1\text{H}$ $\delta$	$J$ (Hz)	
1	$\alpha$ 1.73 (m)		37.0
	$\beta$ 1.69 (m)		
2	$\beta$ 1.81 (m)		31.5
	$\alpha$ 1.40 (m)		
3	$\alpha$ 3.58 (m)		71.4
4	$\alpha$ 1.56 (m)		38.2
	$\beta$ 1.29 (m)		
5	1.13 (m)		44.8
6	$\beta$ 1.30 (m)		28.7
	$\alpha$ 1.27 (m)		
7	$\alpha$ 1.69 (m)		32.1
	$\beta$ 1.64 (m)		
8	$\beta$ 1.34 (m)		35.4
9	$\alpha$ 0.65 (m)		54.3
10	-		35.5
11	$\beta$ 1.49 (m)		21.2
	$\alpha$ 1.29 (m)		
12	$\alpha$ 1.99 (t)	3.1	40.0
	$\beta$ 1.95 (t)	3.2	
13	-		42.6
14	$\alpha$ 1.07 (m)		56.5
15	$\beta$ 1.57 (m)		24.2
	$\alpha$ 1.02 (m)		
16	$\alpha$ 1.84 (m)		28.2
	$\beta$ 1.82 (m)		
17	$\alpha$ 0.65 (m)		56.2
18	$\beta$ 0.65 (s)		12.1
19	$\beta$ 0.80 (s)		12.3
20	$\beta$ 0.88 (m)		35.8
21	$\alpha$ 0.90 (d)	6.5	18.6
22	$\alpha$ 1.02 (m)		36.1
	$\beta$ 0.97 (m)		
23	$\beta$ 1.34 (m)		23.8
	$\alpha$ 1.14 (m)		
24	$\alpha$ 1.15 (m)		39.5
	$\beta$ 1.12 (m)		
25	$\beta$ 1.53 (m)		28.0
26	0.87 (dd)	1.2	22.8
27	0.85 (dd)	1.2	22.6

### 7 $\alpha$ -hydroxyfrullanolide (**54**)

The UV spectrum of compound **54** displayed absorptions at 241 nm, indicating a conjugated system. It has been previously reported.<sup>32, 42, 62</sup> The IR spectrum of **54** displayed strong peaks at 3453 cm<sup>-1</sup> (OH), 2932 (CH), 1771 (ester C=O), 1750 (five-membered lactone), 1683 (C=C), and 1144 (CO) cm<sup>-1</sup>.



The <sup>1</sup>H NMR spectrum of **54** showed the presence of two 3H singlets at  $\delta$  1.10 and 1.80, assigned to the C-14 and C-15 methyl groups, respectively. The signal at  $\delta$  4.90 was assigned to the C-6 methine proton; its downfield value indicated the presence of a geminal oxygen functionality. The signals at  $\delta$  6.21 and 5.79 were due to the C-13 olefinic protons.

The <sup>13</sup>C NMR spectrum of **54** showed the resonances of all 15 carbon atoms. The signal at  $\delta$  168.0 was assigned to the C-12 carbonyl carbon. The assignment of the four sp<sup>2</sup>-hybridized carbons ( $\delta$  144.7, 140.5, 126.7, 121.1) were confirmed by the Heteronuclear Single Quantum Coherence (HSQC) spectrum, with C-4, C-5, and C-11 being assigned to the last three signals. These signals were determined to be quaternary, as they did not exhibit <sup>1</sup>H/<sup>13</sup>C one-bond correlations for these carbons.

The COSY spectrum of **54** showed cross-peaks between two olefinic proton signals at  $\delta$  5.80 and 6.30, due to geminal coupling between the exocyclic double bond of C-11, as indicated in the HSQC spectrum, which showed  $^1\text{H}/^{13}\text{C}$  one-bond shift correlation with C-13 ( $\delta$  121.1). Additionally, there was geminal coupling between the signals at  $\delta$  1.48 and 1.39, assigned to the C-1 methylene protons and vicinal coupling between both the aforementioned signals and the signals at 1.69 and 1.64, the C-2 methylene protons, which showed further coupling with the signals at 2.11 and 2.09, belonging to C-3. Also evident in the COSY spectrum was geminal coupling between the signals at  $\delta$  2.01 and 1.66, the C-8 methylene protons, and vicinal coupling between the aforementioned signals and the signals at  $\delta$  1.51 and 1.42, the C-9 methylene protons.

The HSQC spectrum of **54** was used to find the  $^1\text{H}/^{13}\text{C}$  chemical shift assignments of **54** (see Table 3).

In the HMBC spectrum of **54** both C-13 olefinic protons ( $\delta$  6.21 and 5.79) showed long-range heteroatomic coupling with C-11 (144.7) and C-8 (31.4), while there was also coupling between one of the C-13 methylene protons (6.21) with C-7 (75.9). The C-6 methine proton ( $\delta$  5.02) displayed coupling with C-7 (75.9) and C-11 (144.7). This led to the assignment of C-7 and C-11 and the suggested existence of a lactone. Finally the methyl protons of C-14 ( $\delta$  1.05) showed cross-peaks with C-1 (38.8). Important HMBC interactions of **54** are displayed in Figure 15.

The stereochemistry of the C-14 methyl group ( $\beta$ ), the C-6 methine proton ( $\beta$ ), and the C-7 hydroxyl group ( $\alpha$ ) was decided by comparing the  $^1\text{H}$  and  $^{13}\text{C}$  NMR

chemical shifts with the reported chemical shifts in the literature. This spectral data helped to characterize this compound as 7 $\alpha$ -hydroxyfrullanolide (**54**).<sup>63</sup>

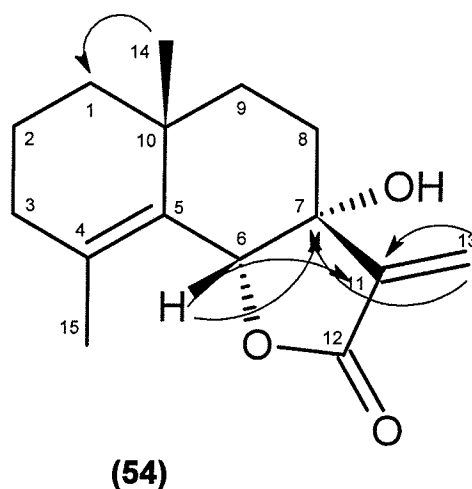


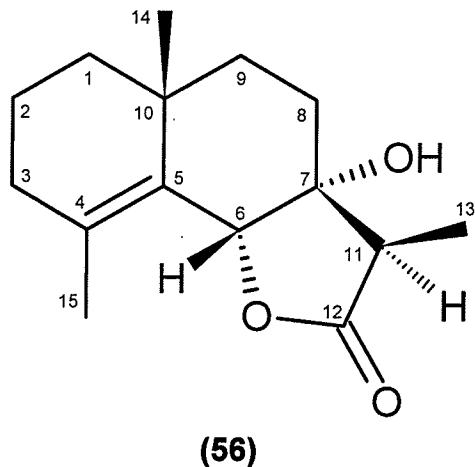
**Figure 15: Important HMBC Interactions Observed in 54**

**Table 3: <sup>13</sup>C NMR Chemical Shift Assignments and <sup>1</sup>H/<sup>13</sup>C One-Bond Shift Correlations of 54, as determined from its HSQC Spectra**

Carbon #	<b>54</b>	
	<sup>1</sup> H $\delta$	<sup>13</sup> C $\delta$
1	$\alpha$ 1.48 (m) $\beta$ 1.39 (m)	38.8
2	$\beta$ 1.69 (m) $\alpha$ 1.64 (m)	18.2
3	$\alpha$ 2.11 (m) $\beta$ 2.09 (m)	33.1
4	-	140.5
5	-	126.7
6	$\beta$ 5.02 (s)	81.4
7	-	75.9
8	$\beta$ 2.01 (m) $\alpha$ 1.66 (m)	31.4
9	$\alpha$ 1.51 (m) $\beta$ 1.42 (m)	34.9
10	-	32.7
11	-	144.7
12	-	169.0
13	6.21 (s) 5.79 (s)	121.1
14	$\beta$ 1.05 (s)	26.1
15	1.75 (s)	19.4

### 7 $\alpha$ -hydroxyeudesmanolide (**56**)

The UV spectrum of compound **56** showed only terminal absorption indicating the presence of an  $\alpha,\beta$ -unsaturated carbonyl group. It has been previously reported.<sup>34, 42</sup> The IR spectrum of **56** displayed strong peaks at 3494 (OH), 2930 (CH), 1785 (ester C=O), 1650 (C=C), and 1219 (CO)  $\text{cm}^{-1}$ .



The  $^1\text{H}$  NMR spectrum of **56** showed the presence of many of the same signals as the previous compound but unlike **54** there was no evidence of a  $\text{sp}^2$ -hybridized methylene carbon peak and also the resonance of a upfield doublet ( $\delta$  1.32), belonging to C-13 suggested the presence of a methyl group.

The  $^{13}\text{C}$  NMR spectrum of **56** had many similarities to the corresponding spectra of **54**, such as the signal at  $\delta$  178 being assigned to a C-12 carbonyl carbon. The  $\text{sp}^2$ -hybridized quaternary carbons at  $\delta$  140.6 and 126 were assigned to C-4 and C-5, in a similar manner as was done in the assignment of 7 $\alpha$ -hydroxyfrullanolide (**54**).

Most importantly, the COSY spectrum of **56** showed cross-peaks between the signal at  $\delta$  2.47 and the signal at  $\delta$  1.32, corresponding to the C-11 methine proton

and the C-13 methyl protons, respectively. Additionally, there was geminal coupling between the signals  $\delta$  1.46 and 1.37, assigned to the C-1 methylene protons and vicinal coupling between the aforementioned signals with 1.67 and 1.65, the C-2 methylene protons, respectively, which showed further coupling with the signals at  $\delta$  2.11 and 2.09, the C-3 methylene protons. Also evident in the COSY spectrum was geminal coupling between the signals at  $\delta$  1.99 and 1.66, belonging to the C-8 methylene protons and vicinal coupling between the aforementioned signals with 1.49 and 1.43, the C-9 methylenes.

The HSQC spectrum of **56** was used to find the  $^1\text{H}/^{13}\text{C}$  chemical shift assignments of **56** (see Table 4).

In the HMBC spectrum of **56**, the C-6 methine proton ( $\delta$  5.07) displayed cross-peaks with C-4 (140.6), C-7 (75.3) and C-10 (33.2), conversely the C-11 methine proton (2.47) showed coupling with C-6 (78.9) and C-12 (178.0). The methylene protons of C-9 ( $\delta$  1.48, and 1.43) displayed cross-peaks with C-5 (126.0) and C-7 (75.3). The methylene protons of C-3 ( $\delta$  2.11,  $\delta$  2.09) showed coupling with C-1 (39.5) and C-4 (140.6). The methyl protons of C-13 ( $\delta$  1.32) showed heteroatomic coupling with C-7 (75.3), C-13 (47.5), and C-12 (178.0). Additionally, the methyl protons of C-14 ( $\delta$  1.08) showed coupling with C-1 (39.5) and C-5 (126.0). Lastly, the methyl protons of C-15 ( $\delta$  1.79) had cross-peaks with C-3 (33.5), C-4 (140.6), and C-5 (126.0). Important HMBC interactions of **56** are displayed in Figure 16.

The NOESY spectrum of **56** was used to establish the stereochemistry for **56**. The signal at  $\delta$  5.07 showed NOE with another signal at (1.32), corresponding to the

C-6 $\beta$  methine proton and the C-13 methyl protons, which led to the assignment of  $\beta$ -stereochemistry for the C-13 methyl group. Furthermore, it has been reported in the literature that H-6 has  $\beta$ -orientation in this class of compounds.<sup>32, 34, 35, 42, 48, 51, 62, 65, 66</sup>

The stereochemistry of the C-14 methyl group ( $\beta$ ), and the C-7 hydroxyl group ( $\alpha$ ) were decided based on very close matching with the literature values of the  $^1\text{H}$  and  $^{13}\text{C}$  NMR chemical shifts ( $\leq \delta 0.1$ ) of the reported compound. This spectral data helped to characterize this compound as 7 $\alpha$ -hydroxyeudesmanolide (**56**).<sup>42</sup>

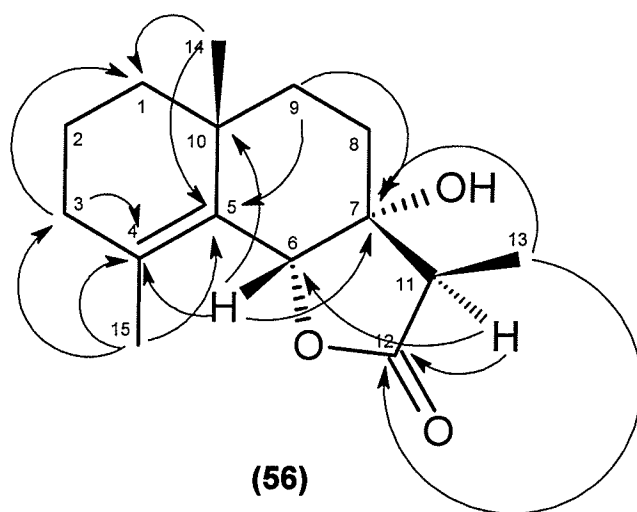
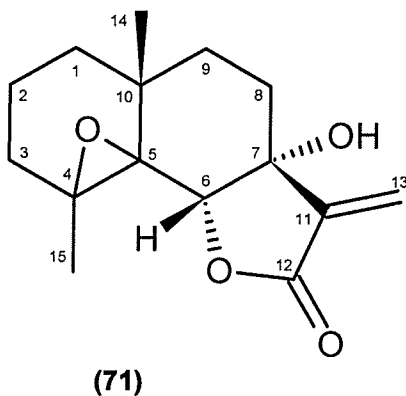


**Figure 16: Important HMBC Interactions Observed in 56**

**Table 4:  $^{13}\text{C}$  NMR Chemical Shift Assignments and  $^1\text{H}/^{13}\text{C}$  One-Bond Shift Correlations **56** as Determined from its HSQC Spectra**

Carbon #	<b>56</b>	
	$^1\text{H}$ $\delta$	$J$ (Hz)
1	$\alpha$ 1.46 (m)	
	$\beta$ 1.37 (m)	
2	$\beta$ 1.67 (m)	
	$\alpha$ 1.65 (m)	
3	$\alpha$ 2.11 (m)	
	$\beta$ 2.09 (m)	
4	-	140.6
5	-	126.0
6	$\beta$ 5.07 (s)	78.9
7	-	75.3
8	$\beta$ 1.99 (m)	
	$\alpha$ 1.66 (m)	
9	$\alpha$ 1.48 (m)	
	$\beta$ 1.43 (m)	
10	-	33.2
11	$\alpha$ 2.47 (q)	7.7
12	-	178.0
13	$\beta$ 1.32 (d)	7.7
14	$\beta$ 1.08 (s)	25.5
15	1.79 (s)	19.5

**4, 5-epoxy-7 $\alpha$ - hydroxyfrullanolide (71)**



The UV spectrum of compound **71** showed an absorbance maximum at 226 nm, indicating a conjugated system. The IR spectrum of **71** displayed strong peaks at 3366 (OH), 2934 (CH), 1773 (ester C=O), and 1121 (CO)  $\text{cm}^{-1}$ .



The  $^1\text{H}$  NMR spectrum of **71** displayed additional signals at  $\delta$  3.9 (m) and 2.8 (t, 1.2 Hz), due to the C-4 and C-5 methine protons, that resulted from the epoxidation reaction.

The  $^{13}\text{C}$  NMR spectrum of **71** also showed an upfield shift for C-4 and C-5 at  $\delta$  64 – 60 suggested the presence of an epoxides at C-4/C-5. The presence of four peaks in the aforementioned range indicated that two diastereomeric epoxides were formed from **54**: the  $4\alpha$ ,  $5\alpha$ -epoxy- $7\alpha$ - hydroxyfrullanolide and the  $4\beta$ ,  $5\beta$ -epoxy- $7\alpha$ -hydroxyfrullanolide. The endocyclic olefinic group (C-4/C-5) is more reactive than the exocyclic olefinic group (C-11/C-13) due to the latter being  $\alpha$ ,  $\beta$ -unsaturated with the carbonyl carbon, C-12, while the former has more electron-donating groups on C=C.

Numerous attempts (preparative TLC and RP-HPLC) to isolate the mixture of **71** were made, but were unsuccessful. It was therefore decided to evaluate this mixture of epoxides for antibacterial activity.

### **Minimum Inhibitory Concentration (MIC) Assay**

All positive (growth) controls and negative (sterile) controls were satisfactory (not shown). The MIC values for the standards, penicillin G (**5**) and chloramphenicol (**72**) were in agreement with the published values for those agents.<sup>69</sup>

The MIC results indicated that dihydrocholesterol (**70**) possesses very weak to no antimicrobial activity as there was no activity detected in the concentration range tested. Regarding the eudesmanolides and eudesmanolide derivative,  $7\alpha$ -hydroxyfrullanolide (**54**),  $4, 5$ -epoxy- $7\alpha$ - hydroxyfrullanolide (**71**), and  $7\alpha$ -

hydroxyeudesmanolide (**56**), there was potent (**54**) to intermediate (**56**) antibacterial activity for the Gram-positive bacteria, *Staphylococcus aureus* and *Streptococcus agalactiae*, whereas there was no Gram-negative antibacterial activity (in the concentration range tested). (see Table 5)

This result was in agreement with the results of the crude extract by Narasimha Rao and Nigam<sup>55</sup>, but contrary to the findings by Sadaf<sup>23</sup> and Naqvi<sup>54</sup> which state that *both* Gram-positive and Gram-negative antimicrobial activity were evident in the crude extract.

A probable explanation of this discrepancy is that other compounds in the crude extract possess the Gram-negative antibacterial activity.

Additionally, regarding the eudesmanolides and eudesmanolides derivative, 7 $\alpha$ -hydroxyfrullanolide (**54**), 7 $\alpha$ -hydroxyeudesmanolide (**56**), and 4, 5-epoxy-7 $\alpha$ -hydroxyfrullanolide (**71**) there was evidenced a 2-fold increase in MIC (i.e. less activity) for the Gram-positive bacteria. Comparative SAR analysis of utilizing the MICs of the three compounds indicated that the excellent antibacterial activity (in the range of clinically-used antimicrobial agents, including antibiotics) of **54** was due in large part to its exocyclic (C-11/C-13) *and* endocyclic (C-4/C-5) double bonds, with the endocyclic C-4/C-5 tetra-substituted double bond having perhaps more importance. The further reduced compounds (**56** and **71**) exhibited less activity.

The activity of **54** may be due to its exocyclic C-11/C-13 double bond binding irreversibly to a bacterial protein in a Michael addition, disabling it. The endocyclic

C-4/C-5 double bond may be crucial for an optimal arrangement in the active site of the protein.

**Table 5: MIC Assay for Compounds 70, 54, 71, and 56**

Bacteria	Compounds				Standards	
	<b>70</b>	<b>54</b>	<b>71</b>	<b>56</b>	<b>5</b>	<b>72</b>
<i>S. aureus</i>	>128	≤32	≤128	≤64	≤1	≤8
<i>S. agalactiae</i>	>128	≤32	≤128	≤64	≤1	≤2
<i>E. coli</i>	>128	>128	>128	>128	≤32	≤4
<i>P. aeruginosa</i>	>128	>128	>128	>128	>128	≤64

**\*Values are expressed as concentration of analyte (µg/mL)**

## Chapter 3.0 *Buxus hyrcana*

### 3.1 The *Buxus* genus and *Buxus hyrcana*

*Buxus hyrcana* Pojark (Buxaceae) is a tree-like shrub<sup>71, 72</sup> that is abundant and widely distributed in Iran.<sup>71, 73</sup> The plants of the genus *Buxus* (and their extracts) are found extensively in the indigenous system of medicine, used for treatment of a number of disorders and diseases including malaria, rheumatism, and skin infections.<sup>74</sup>



**Figure 17:** *Buxus hyrcana*

*B. hyrcana* has been investigated for the presence of certain chemical classes and tested positive for saponins, alkaloids, and flavonoids, but not tannins.<sup>75</sup> The *Buxus* steroidal alkaloids have received the most research interest as screening has identified them as being accountable for the bioactivities listed above and others such as antibacterial (including antimycobacterial), antiviral (HIV), anticholinesterase activity,<sup>71</sup> and other enzyme inhibitory activities.<sup>72</sup> Interesting to note is that *Buxus* alkaloids were isolated as early as the first half of the 18<sup>th</sup> century, but structure determination has only been pursued in the last half of the 20<sup>th</sup> century,<sup>76</sup> due to advances in structure determination brought about by NMR spectroscopy.

*Buxus* alkaloids have a unique triterpenoid-steroidal-pregnane-type skeleton with C-4 methyl groups, a 9 $\beta$ ,10 $\beta$ -cycloartenol system, and a degraded side-chain. Over 200 compounds of this class has been reported from this genus<sup>77</sup> and 26 have been isolated from *Buxus hyrcana* to date.

The genus *Buxus* is well-known to be a rich source of steroidal/triterpenoidal compounds, many including novel structures, with over 200 such compounds isolated from the genus and 26 such compounds isolated from *Buxus hyrcana* to date.

### **3.2 Previously Reported Steroidal Alkaloids from *Buxus hyrcana***

The first reported isolation of *B. hyrcana* steroidal alkaloids occurred with Kurakina's group in 1974 with cyclomicrobuxine (**73**), cyclobuxine D (**74**), and *N*-3-benzoylcyclooxobuxidine (**75**).<sup>78</sup> Cycloprotobuxine C (**76**) was also reported that year by Aliev.<sup>79</sup> There was renewed interest in this area in the last decade with (-)-hyrcanine (**77**)<sup>80</sup>, and homomoenjodaramine (**78**), and moenjodaramine (**79**)<sup>81</sup> being

isolated in 1998 – 1999. Next, (+)-*N*-benzoylbuxahyrcanine (**80**), (+)-*N*-tigloylbuxahyrcanine (**81**), (+)-*N*-isobutyrylbuxahyrcanine (**82**) were isolated in 2003.<sup>82</sup> The majority of steroidal alkaloids being isolated from *B. hyrcana* occurred in 2006 with hyrcanone (**83**), hyrcanol (**84**), *N*<sub>b</sub>-dimethylcyclobuxoviricine (**85**), hyrcatrienine (**86**), buxabenzacinine (**87**), hyrcamine (**88**), buxidine (**89**), buxandrine (**90**), E-buxenone (**91**), buxippine-K (**92**) being isolated by Choudhary and co-workers,<sup>71</sup> while Ata and co-workers were successful in isolating (+)-*O*<sup>6</sup>-buxafurandiene (**93**), (+)-7-deoxy-*O*<sup>6</sup>-buxafurandiene (**94**), (+)-buxapapilline (**95**), (+)-benzoylbuxidienine (**96**), (+)-buxaquamarine (**97**), and (+)-irehine (**98**).<sup>73</sup>

As was mentioned in the introduction (Section 1.6), there is almost no data available on the antibacterial constituents of *B. hyrcana*. Previous examinations (mostly of crude extracts) are indicative of constituent compounds with some antibacterial activity, but which compounds possess this activity has not been determined. Thus, this warrants a new investigation with the means to measure the antibacterial activity of these pure, isolated compounds, relative to each another. Such an investigation has not been done in any comprehensive fashion to date.

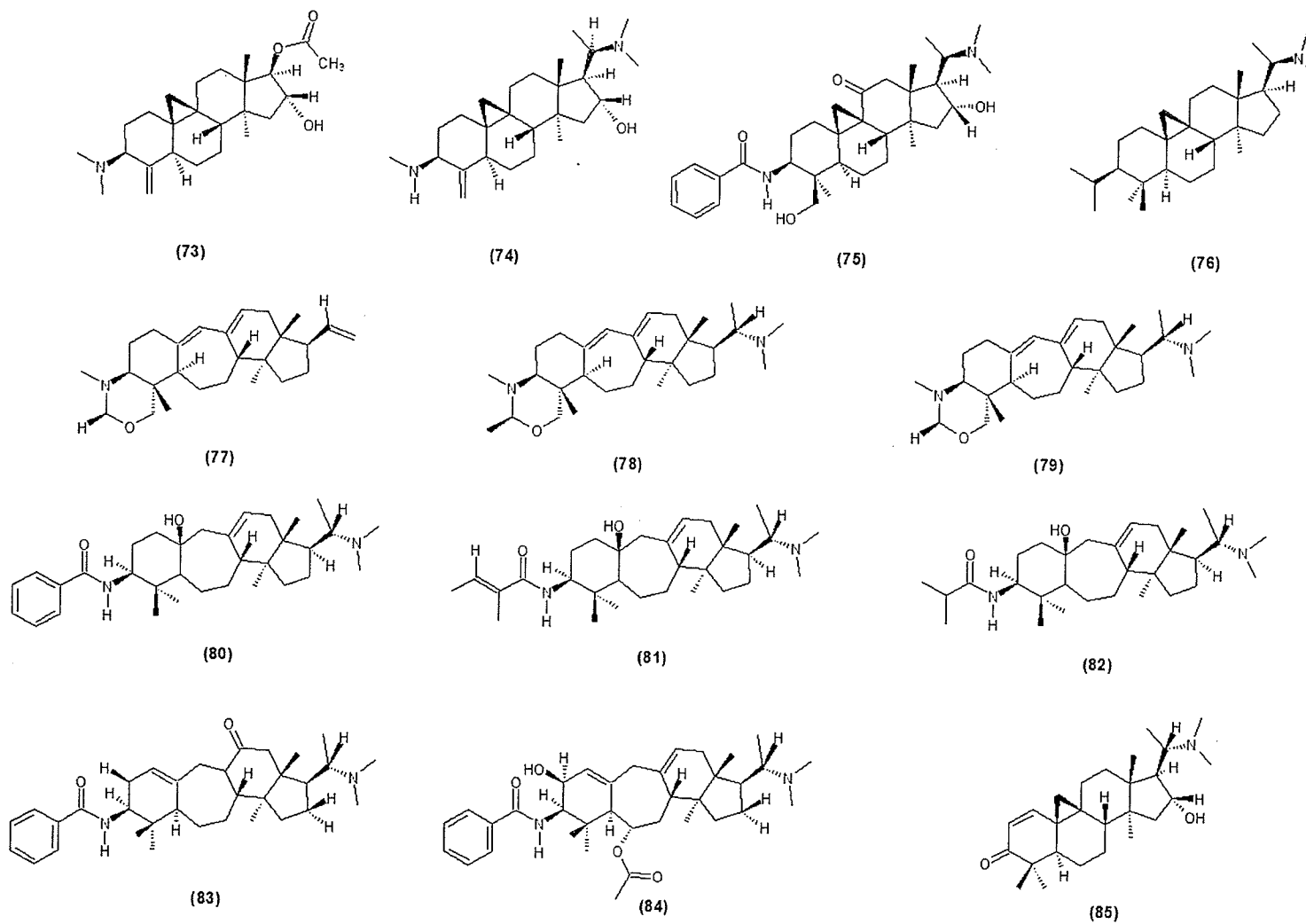


Figure 18: Structures of steroidal alkaloids isolated from *Buxus hyrcana* (73 - 85)

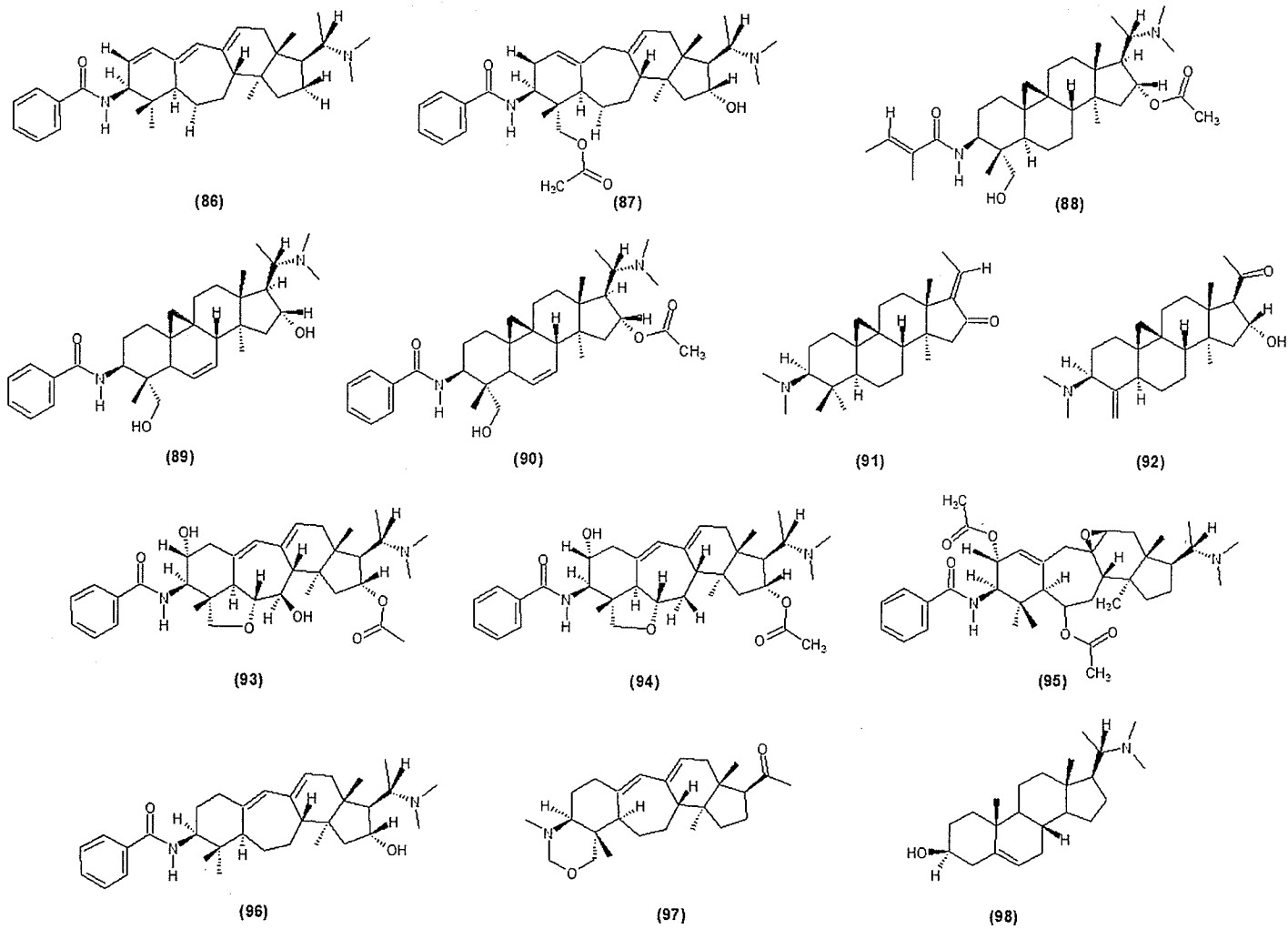


Figure 19: Structures of steroidal alkaloids isolated from *Buxus hyrcana* (86 - 98)



### 3.3 *Buxus hyrcana* Experimental

General experimental conditions used in this research were the same as those discussed in section 2.2

#### **Plant Collection**

The leaves of a *Buxus hyrcana* pojark plant were collected by Dr. Meshkata-Psadat, on August 14, 2004 in Iran. This plant was identified by Professor Jahad Sazandegi, Mazandaran State, Iran and a voucher specimen (#B530) was deposited in the herbarium of the Shaheed Beheshti University, Tehran, Iran.

#### **Extraction and Isolation**

The leaves of *B. hyrcana* were dried and extracted with methanol (5 L) at 25°C. The solvent was evaporated under reduced pressure, resulting in a gummy mixture (38.1g) This extract was then shipped to the University of Winnipeg.

The crude methanolic extract was loaded onto a silica gel column (200 g) and eluted using a stepwise gradient elution using hexanes / ethyl acetate (0 – 100%), followed by ethyl acetate / methanol (0 – 100%). This afforded several fractions which were pooled on the basis of similar  $R_f$  on analytical TLC, resulting in 10 pooled fractions.

One of the fractions, fraction 20 – 23 (45% hexanes/ 55% ethyl acetate) showed the presence of one major compound, along with several minor compounds on analytical TLC. Preparative TLC of this fraction using the mobile phase, 86.3% hexanes / 13.6% acetone / 0.1% diethylamine, afforded  $N_b$ -dimethylcyclohexoviricine (**85**) and six minor compounds. The minor compounds were not isolated in sufficient quantities for spectral analysis.

A second fraction 31 – 34 (35% hexanes / 65% ethyl acetate) also displayed the presence of one major compound, with small impurities. Preparative TLC of this fraction using the mobile phase, 49.9% hexanes / 49.9% diethyl ether / 0.2% diethylamine, afforded buxamine B (**99**).

---

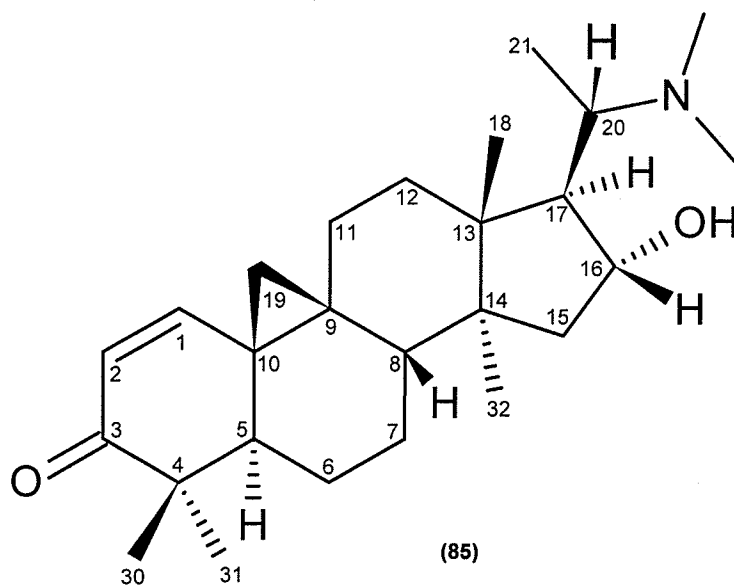
*N*<sub>b</sub>-dimethylcyclohexoviricine **85**; white powdery solid, 2.6 mg, fraction 31 – 34; UV  $\lambda_{\text{max}}$  (MeOH) = 256 nm; IR (CCl<sub>4</sub>) = 3453, 2933, 1673, 1552, 1098, and 1371 cm<sup>-1</sup>; <sup>1</sup>H NMR (CDCl<sub>3</sub>, 300.13 MHz) = see Table 7; <sup>13</sup>C NMR (CDCl<sub>3</sub>, 75.47 MHz) = see Table 7; EI-MS = m/z 399 (M<sup>+</sup>), 384, 831, 73, 72.

Buxamine B **99**; white powdery solid, 4.6 mg, fraction 20 – 23; UV  $\lambda_{\text{max}}$  (MeOH) = 246 nm; IR (CCl<sub>4</sub>) = 3453, 2933, 1552, 1098, and 1371 cm<sup>-1</sup>; <sup>1</sup>H NMR (CDCl<sub>3</sub>, 300.13 MHz) = see Table 6; <sup>13</sup>C NMR (CDCl<sub>3</sub>, 75.47 MHz) = see Table 6; EI-MS = m/z 398 (M<sup>+</sup>), 383, 368, 355, 353, 253, 84, 71, 58.

### 3.4 *Buxus hyrcana* Results and Discussion

#### ***N*<sub>β</sub>-dimethylcycloxbuxoviricine (85)**

*N*<sub>β</sub>-dimethylcycloxbuxoviricine (**85**) was isolated as a colourless, white solid. It has been previously reported.<sup>71</sup> The UV spectrum of **85** displayed maximum absorptions at 247 and 256 nm, indicating a conjugated system. The IR spectrum of **85** displayed strong peaks at 3453 (OH), 2933 (CH), 1673 (α,β-unsaturated C=O), 1552 (amine NH), 1098 (C-N<sup>2°</sup>), and 1371 (H-C=C) cm<sup>-1</sup>.



The <sup>1</sup>H NMR spectrum of compound **85** displayed three upfield 3H singlets at δ 0.96, 0.94, and 0.98, due to the protons of C-18, C-30, and C-32 methyl groups, respectively. Additionally, the downfield doublet at δ 1.84 and singlet at 1.10, were assigned to the C-21 and C-31 methyl groups, respectively. Two *AB* doublets at δ 1.31 and 0.75 were assigned to the C-19 methylene protons, which indicated the presence of a 9β,10β-cyclopropane group in the compound. The signal at δ 3.64 was assigned to the C-16 methine proton, geminal to the hydroxyl group. Also evident

was two doublets at  $\delta$  6.76 and 5.95, assigned to C-1 and C-2, respectively. The large singlet peak at  $\delta$  2.45 was assigned to the N<sub>b</sub>-dimethyl protons.

The <sup>13</sup>C NMR spectrum of **85** showed the resonance for all 26 carbon atoms. The carbon signal at  $\delta$  205.1 was assigned to the C-3 ketone. The sp<sup>2</sup>-hybridized carbon signal at  $\delta$  126.8 was assigned to the C-2, an olefinic carbon vicinal to the C-3 ketone group, while the sp<sup>2</sup>-hybridized carbon signal at 153.4 was assigned to C-1. The signal at  $\delta$  43.3 was assigned to the N<sub>b</sub>-dimethyl carbons.

The COSY spectrum of **85** showed cross-peaks between the signals at  $\delta$  6.76 and 5.95, corresponding to the olefinic protons of C-1 and C-2. Another important COSY interaction was the geminal coupling between the signals at  $\delta$  0.75 and 1.31 corresponding to the C-19 methylene protons.

The HSQC spectrum of **85** was used to find the <sup>1</sup>H/<sup>13</sup>C chemical shift assignments of **85** (see Table 7).

In the HMBC spectrum of **85**, there was long-range heteronuclear coupling between the C-1 methine proton ( $\delta$  6.76) with C-3 (205.1). There was also coupling between the C-30 methyl ( $\delta$ 0.96) and C-31 methyl (1.10) with C-3 (205.1), confirming the ketone peak at C-3 and along with the previous statement, the location of the double bond. Also, the C-31 methyl ( $\delta$  1.10) showed coupling with C-4 (46.7) and C-30 (19.4), while the C-30 methyl (0.94) showed coupling with C-4 (46.7), and C-5 (49.3). The C-17 methine ( $\delta$  1.84) showed long-range HMBC interaction with C-13 (44.2) and C-14 (46.0). The C-18 methyl (0.96) showed coupling with C-12 (32.2), C-13 (44.2), and C-14 (46.0). Important HMBC interactions of **85** are displayed in Figure 20.

The orientation of the C-16 hydroxyl group ( $\beta$ ) was done based on very close matching with literature values of similar compounds ( $\leq \delta 0.5$ ). Additionally, other  $^{13}\text{C}$  NMR and  $^1\text{H}/^{13}\text{C}$  one-bond shift correlations and literature spectra helped conclude the structure as *N*<sub>6</sub>-dimethylcyclohexoviricine (**85**).<sup>71</sup>

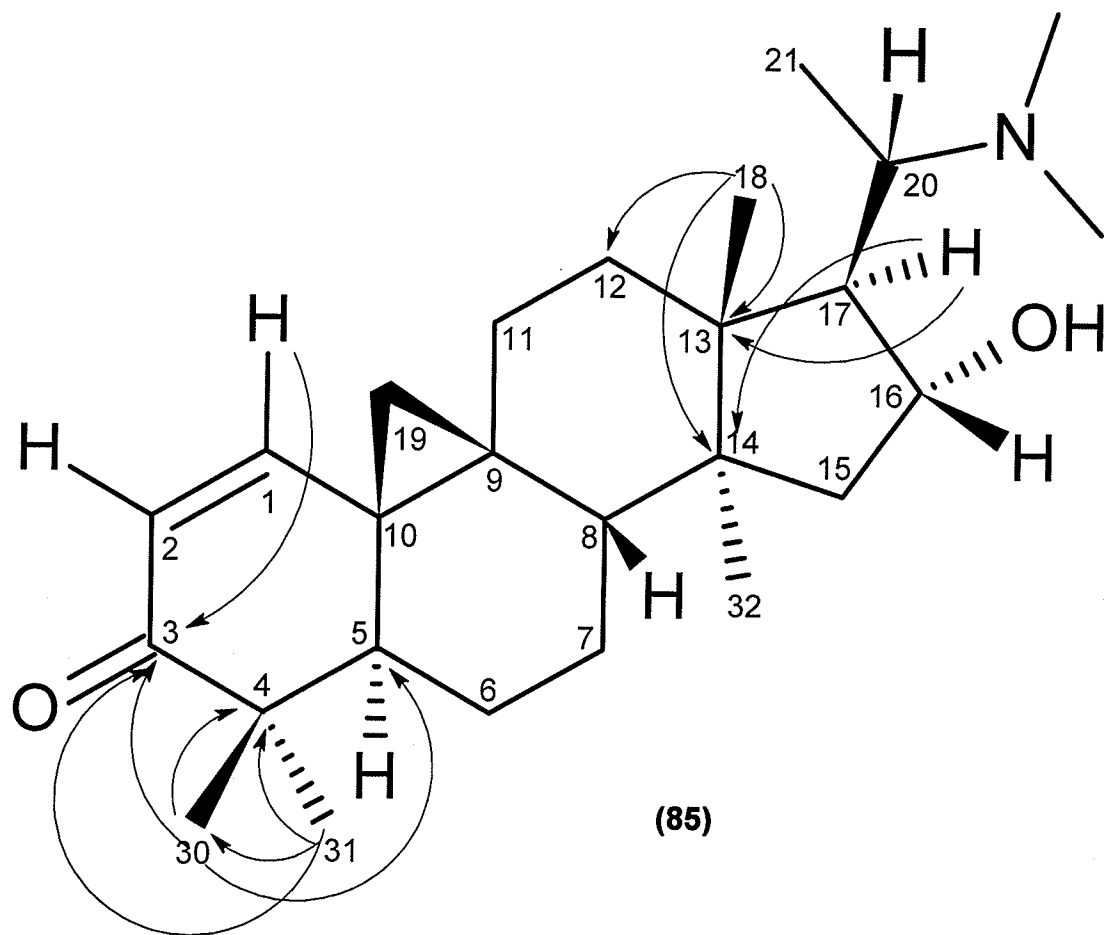


**Figure 20: Important HMBC Interactions Observed in Compound 85**

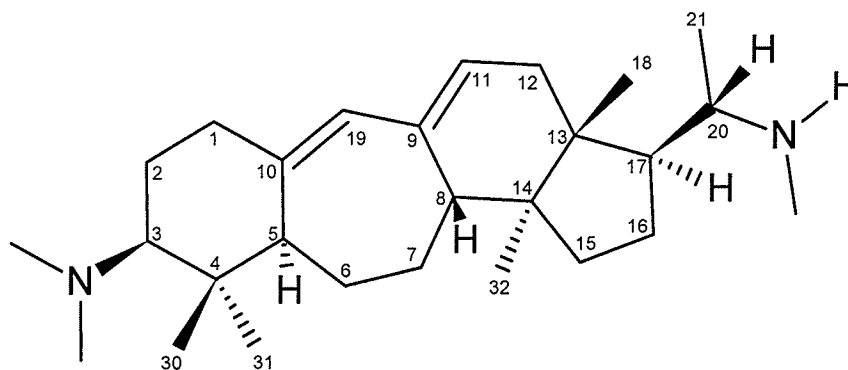
**Table 6:  $^{13}\text{C}$  NMR Chemical Shift Assignments and  $^1\text{H}/^{13}\text{C}$  One-Bond Shift Correlations of **85** as determined from its HSQC Spectra**

Carbon #	<b>85</b>		
	$^1\text{H}$ $\delta$	$J$ (Hz)	$^{13}\text{C}$ $\delta$
1	6.76 (d)	10.1	153.4
2	5.95 (d)	10.0	126.8
3	-		205.1
4	-		46.7
5	$\alpha$ 2.10		49.3
6	$\beta$ 1.60 (m)		27.6
	$\alpha$ 1.00 (m)		
7	$\alpha$ 1.55 (m)		28.9
	$\beta$ 1.25 (m)		
8	$\beta$ 1.80 (m)		39.0
9	-		23.2
10	-		29.8
11	1.45 (m)		27.0
12	1.27 (m)		32.2
	1.20 (m)		
13	-		44.2
14	-		46.0
15	1.37 (m)		34.4
	1.30 (m)		
16	$\beta$ 3.64 (m)		77.2
17	$\alpha$ 1.84 (d)	7.5	31.1
18	$\beta$ 0.96 (s)		19.1
19	(AB) 1.31	4.6	29.7
	(AB) 0.75	4.7	
20	2.59 (br.s)		74.1
21	1.84 (d)	7.5	13.0
30	$\beta$ 0.94 (s)		19.4
31	$\alpha$ 1.10 (s)		21.4
32	$\alpha$ 0.98 (s)		18.6
Me <sub>2</sub> N <sub>b</sub>	2.45 (s)		43.3

### Buxamine B (**99**)

Buxamine B (**99**) was isolated as a colourless, white solid. It has been previously reported,<sup>83</sup> though not from *Buxus hyrcana*. The UV spectrum of **99** displayed absorptions at 239, and 246 nm, indicating the presence of a 9(10→19)

*abeo*-diene system. The IR spectrum of **99** displayed strong peaks at 3453 (OH), 2933 (CH), 1552 (amine NH), 1098 (C-N<sup>2°</sup>) and 1371 (H-C=C) cm<sup>-1</sup>



(99)

The <sup>1</sup>H NMR spectrum of compound **99** indicated three upfield 3H singlets at  $\delta$  0.74, 0.72, and 0.71, assigned to the methyl groups at C-18, C-30, and C-32, respectively. Additionally, two downfield signals at  $\delta$  0.89 and 1.02 were assigned to the C-21 and C-31 methyl groups, respectively. The vinylic signals at  $\delta$  5.51 and 5.92, were assigned to the C-11 and C-19 methines of the 9(10 $\rightarrow$ 19) *abeo*-diene system, respectively. The 6H peak at  $\delta$  2.11 was assigned to the N<sub>a</sub>-dimethyl protons, while a broad singlet at 2.29 was due to the 3H N<sub>b</sub>-methylamino proton. Finally the signal at  $\delta$  5.30 was assigned to the exchangeable N-H of the N<sub>b</sub> group.

The <sup>13</sup>C NMR spectrum of **99** showed the resonance of all 27 carbon atoms. The two quaternary sp<sup>2</sup>-hybridized signals at  $\delta$  136.6 and 138.6 were indicative of C-9 and C-10, respectively of the 9(10 $\rightarrow$ 19) *abeo*-diene system. The two sp<sup>2</sup>-hybridized carbon signals at  $\delta$  128.8 and 128.4, were assigned to the C-11 and C-19 of the 9(10 $\rightarrow$ 19) *abeo*-diene system, respectively. The peaks at  $\delta$  39.9 and 44.5 were assigned to the N<sub>a</sub> methyl carbon and the N<sub>b</sub>-dimethyl carbons, respectively.

The COSY spectrum of **99** was used to trace the  $^1\text{H} - ^1\text{H}$  spin correlations. The COSY spectrum showed cross-peaks between the signal at  $\delta$  5.51 and the signals at 2.02 and 1.96, assigned to the C-11 olefinic proton and the C-12 methylene protons, respectively. There were also cross-peaks between the signals at  $\delta$  1.46 and 1.41 and the signals 2.31 and 2.10, assigned to the C-15 and the C-16 methylene protons, respectively, which showed further coupling with the signal at 1.88, the C-17 methine protons. The signals at  $\delta$  1.42 and 1.38 showed coupling with the signal at 2.13, assigned to the C-7 methylene protons and C-8 methine proton, respectively.

The HSQC spectrum of **99** was used to find the  $^1\text{H}/^{13}\text{C}$  chemical shift correlations of **99** (see Table 6).

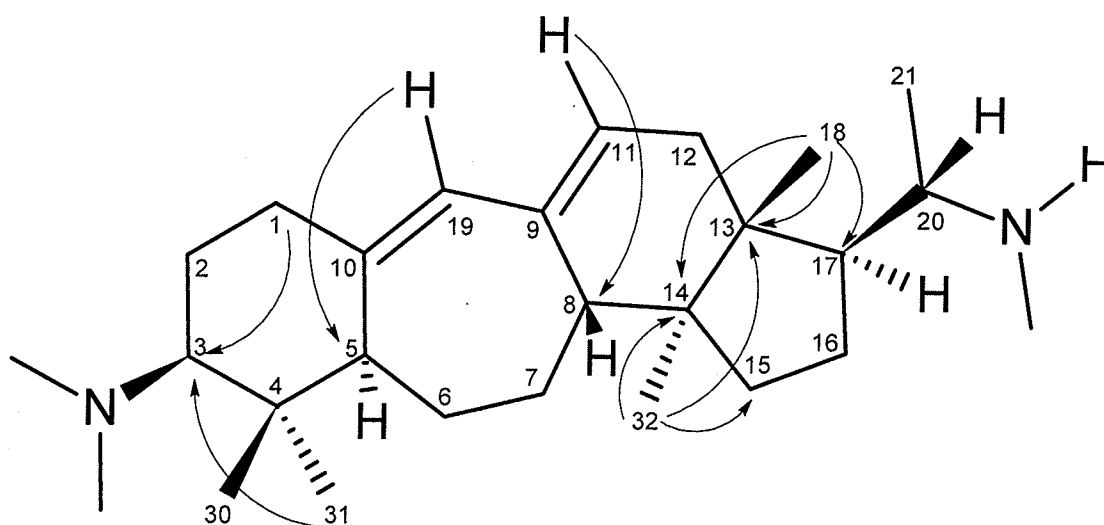
In the HMBC spectrum of **99**, the C-19 olefinic proton ( $\delta$  5.92) showed long-range coupling with C-5 (50.9), while the C-11 olefinic proton (5.51) showed coupling with C-8 (48.6). The C-1 methylene protons ( $\delta$  1.76, 1.73) showed HMBC interaction with C-3 (52.0). The C-31 methyl protons (1.02) showed coupling with C-3 (52.0). The C-18 methyl protons ( $\delta$  0.74) showed interaction with C-13 (43.2), C-14 (49.5), and C-17 (49.2). The C-32 methyl protons ( $\delta$  0.71) showed coupling with C-13 (43.2), C-14 (49.5), and C-15 (33.0). Important HMBC interactions of **99** are displayed in Figure 21.

The stereochemistry of the exchangeable NH ( $\beta$ ); the C-30, C-31 methyl groups ( $\beta$  and  $\alpha$ , respectively); the H-5, H-8, H-17, and H-20 methine protons ( $\alpha$ ,  $\beta$ ,  $\alpha$ , and  $\beta$  respectively); and the C-18 and C-32 methyl groups ( $\beta$  and  $\alpha$ , respectively) were decided based on very close matching with literature values of chemical shifts of similar compounds ( $\leq \delta 0.1$ ). Additionally, other  $^{13}\text{C}$  NMR and  $^1\text{H}/^{13}\text{C}$  one-bond



shift correlations and literature spectra helped conclude the structure as buxamine B

(99).<sup>72, 79, 80, 81</sup>



(99)

**Figure 21: Important HMBC Interactions Observed in Compound 99**

**Table 7:  $^{13}\text{C}$  NMR Chemical Shift Assignments and  $^1\text{H}/^{13}\text{C}$  One-Bond Shift Correlations of 99 as determined from its HSQC Spectra**

Carbon #	99		
	$^1\text{H} \delta$	$J$ (Hz)	$^{13}\text{C} \delta$
1	$\alpha$ 1.76 $\beta$ 1.73		23.0
2	$\beta$ 1.27 $\alpha$ 1.24		25.6
3	$\alpha$ 3.64		52.0
4	-		38.5
5	$\alpha$ 1.20		50.9
6	$\beta$ 1.61 (m) $\alpha$ 1.59 (m)		27.0
7	$\alpha$ 1.42 (m) $\beta$ 1.38 (m)		30.1
8	$\beta$ 2.13 (m)		48.6
9	-		138.6
10	-		136.6
11	5.51 (m)		128.4
12	2.02 1.96		41.2
13	-		43.2
14	-		49.5
15	1.46 1.41		33.0
16	2.31 2.10		42.8
17	$\alpha$ 1.88 (d)	6.8	49.2
18	$\beta$ 0.74 (s)		15.7
19	5.92 (s)		128.8
20	$\beta$ 2.56 (m)		61.5
21	0.89 (d)		9.5
30	$\beta$ 0.72 (s)		15.0
31	$\alpha$ 1.02 (s)		24.9
32	$\alpha$ 0.71 (s)		17.1
NH	5.30 (s)		-
MeHN <sub>b</sub>	2.29 (s)		44.5
Me <sub>2</sub> N <sub>a</sub>	2.11 (s)		39.9

### Minimum Inhibitory Concentration (MIC) Assay

All positive (growth) controls and negative (sterile) controls were satisfactory (not shown). The MIC values for the standards, penicillin G (**5**) and chloramphenicol (**72**) were in agreement with the published values for those agents.<sup>69</sup>

The MIC results indicated that both *N*<sub>1</sub>-dimethylcyclohexoviridine (**85**) and buxamine B (**99**) possessed very weak to no antimicrobial activity as there was no activity detected in the concentration range tested (see Table 8).

**Table 8: MIC Assay for Compounds 85 and 99**

Bacteria	Compounds		Standards	
	<b>85</b>	<b>99</b>	<b>5</b>	<b>72</b>
<i>S. aureus</i>	>128	>128	≤1	≤8
<i>S. agalactiae</i>	>128	>128	≤1	≤2
<i>E. coli</i>	>128	>128	≤32	≤4
<i>P. aeruginosa</i>	>128	>128	>128	≤64

\*Values are expressed as concentration of analyte (µg/mL)

## Chapter 4.0 Biotransformations of Natural Products

Microorganisms are ubiquitous and owe this to their ability to adapt to virtually any ecosystem, even extremely hostile conditions. This adaptation is largely due to evolution in their enzymatic systems which enable them to utilize diverse substrates for their metabolism.<sup>84</sup> Microorganisms perform nearly every conceivable type of oxidative or reductive reaction with suitable substrates.<sup>85</sup> All nutrients such as cellulose, amino acids, peptides, etc. undergo metabolic reactions. The metabolites produced occur by the action of complementary enzyme systems of single and/or mixed microbial populations. Thus, a logical step in the use of microorganisms as a technology would be to harness this colossal enzymatic potential to produce desired intermediates or metabolites.

Biotransformations can be defined as the enzymatic conversions of natural and synthetic products into compounds having specifically modified structures. Most often these enzymatic reactions are accomplished by using whole cell cultures of microorganisms, mostly fungi, and some bacteria. These enzymatic reactions produce new compounds (derivatives) that would be either most taxing or impossible via synthetic techniques. The derivatives that are produced are generally more polar than the original parent compound, so that they can be more readily excreted.<sup>86</sup> An example of this is hydroxylation of a molecule at an inactivated methylene site, which is a very common biotransformation.<sup>87</sup> This is a viable technology because the enzymes associated with oxidative biotransformations appear to be promiscuous; they exhibit a low degree of substrate specificity.<sup>84,88</sup> In general, the biotransformed derivatives produced possess less biological activity / and or toxicity; however

derivatives with enhanced activities or less toxicity have also been documented.<sup>84, 87</sup>  
89, 90

An interesting fact to note is that a very prominent reason why only a few antifungal compounds are available for therapy is that most fungi have an enzymatic system that can hydroxylate most antibiotics<sup>91</sup>, reducing their efficiency. An additional, practical reason for the small number of antifungal agents is perhaps that fungal infections were infrequent and non-life threatening, although both their frequency and seriousness are increasing.

Biotransformations can accomplish a wide variety of organic reactions such as synthesis or hydrolysis of esters (especially lactones), amides anhydrides, epoxides, and nitriles; alkylation and dealkylation; halogenation and dehalogenation; oxidation or reduction of alkanes, alkenes, alcohols, aldehydes, ketones, aromatics, sulphides, and sulphoxides; addition-elimination of water, ammonia, and HCN; isomerization, acylation, aldol condensation and Michael addition.<sup>92</sup>

The first biotransformation was reported by Patterson and co-workers in 1952, using the steroid progesterone (**100**) resulting in the conversion into 11 $\alpha$ -hydroxyprogesterone (**101**), 6 $\beta$ , 11 $\alpha$ -dihydroxyprogesterone (**102**), and 11 $\alpha$ -hydroxyallopregnane-3,20-dione (**103**) from progesterone using the fungi *Rhizopus arrhizus*.<sup>93</sup>

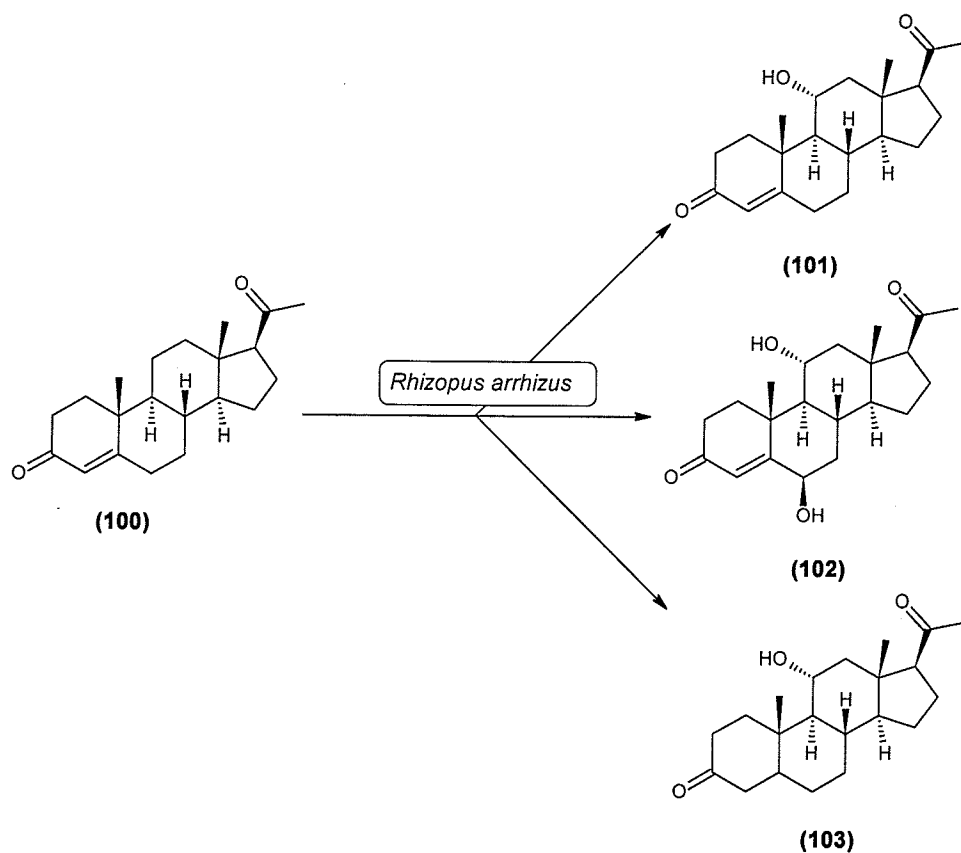


**Figure 22: The first reported biotransformation: transformation of progesterone (100) into 11 $\alpha$ -hydroxyprogesterone (101), 6 $\beta$ , 11 $\alpha$ -dihydroxyprogesterone (102), and 11 $\alpha$ -hydroxyallopregnane-3,20-dione (103) using *Rhizopus arrhizus***

This discovery began an extensive research effort to find more biocatalysts (organisms) to produce a wide variety of steroid derivatives, and today with regard to biotransformations, steroids are the most thoroughly studied class of natural products, followed by the antibiotics.<sup>84, 87</sup> Today, any center in a steroid can be selectively hydroxylated by choosing appropriate microorganisms. It can be easily said that without the new technology of biotransformations, high-yielding steroid hormone syntheses would not be at their current state of development.<sup>89, 91</sup>

Since then, biotransformations have been investigated on a multitude of major natural product classes such as 1) sesquiterpenoids, such as nootkatone **(104)**; 2) diterpenoids, such as taxol [also known as paclitaxel] **(105)**<sup>94</sup>; 3) triterpenoids (and also steroids), such as withaferin-A **(106)**;<sup>88</sup> 4) alkaloids, such as acronycine **(107)**; 5) aromatics, such as chromanone **(108)**,<sup>95</sup> and 6) antibiotics, such as Viridicatumtoxin **(109)**.

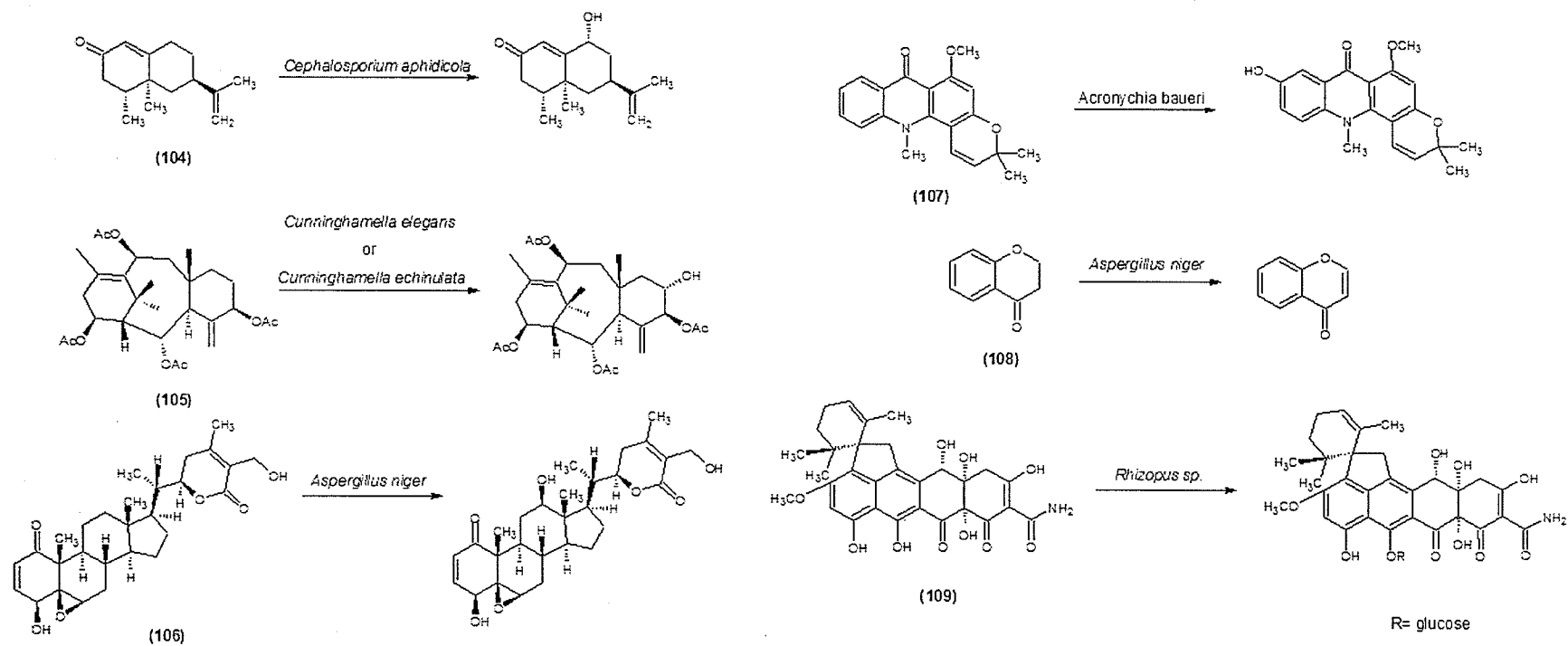


**Figure 23: An Overview of biotransformation reactions on examples of different natural product classes and their corresponding biotransformed derivatives**



Using biotransformations to produce derivatives has the advantages of extremely mild reaction conditions and highly selective reactions (no requirement of protecting groups). The disadvantages of using biotransformations can include unwanted side-products and low yields.<sup>87</sup>

Although low yields can be encountered with biotransformation studies, there has been great interest in this research area to find ways to maximize production, but it should be understood that the initial isolation of a derivative is of key importance as it reveals that it can be produced in the first place. Increases of 1000-fold in yield for metabolites, including xenobiotics is often possible.<sup>4</sup>

There are several ways to maximize yield for biotransformations, as there is great similarity for maximizing a natural metabolite or a xenobiotic. Screening for related higher-yielding species or strains, and developing greater-expressing mutants is an excellent way to accomplish this early in a research program. Additionally, growth conditions such as pH, temperature, medium composition, aeration, and inoculation (of substrate) conditions, etc. can have a profound effect on the yield. Adding limiting precursors that inhibit steps in biosynthesis after the desired metabolite is produced is another option. These steps can not only increase the yield of the desired metabolite, but also work to improve the process by eliminating side-products.

#### **4.1 Biotransformations and their Role in Microbial Metabolite Modeling**

Beginning in 1975, an additional reason for investigating biotransformations began being explored, that of predicting mammalian metabolism (i.e. as a biomimetic model). This was especially significant for drug metabolism,<sup>96</sup> as well as other chemicals such as vitamins, hormones, pollutants,<sup>97</sup> insecticides, amino acids,<sup>87</sup> and other classes of natural products.

Metabolism of xenobiotic chemicals has been and continues to be (with the new research field of Metabolomics) an area of intense interest.<sup>98</sup> This importance is due to the fact that the vast majority of drugs or other foreign chemicals entering the mammalian organism are chemically altered.<sup>87</sup> An example of this is that <10% of administered Taxol is excreted unchanged in urine; the prime metabolite is 6 $\alpha$ -hydroxytaxol.<sup>99</sup> Before a drug is approved, its metabolites must be studied and their structures elucidated, as well as possess sufficient quantity for toxicological testing.

These studies have historically been most taxing to accomplish due to several obstacles: 1) development of suitable analytical methods for dealing with biological media, 2) qualitative and quantitative differences in analytes produced using animal models, 3) extremely low levels of metabolites that are recovered from such systems, enough for complete structure determination and biological testing.<sup>87</sup>

Of principle interest in biotransformations for drug metabolism are the reactions 1) aromatic hydroxylation, 2) *N*-dealkylation, 3) *O*-dealkylation, and 4) *S*-oxidation.<sup>87</sup> The enzymes most often responsible for hydroxylation of a substrate are Cytochrome P<sub>450</sub> Oxidases (CYP), which exist in both microbial and mammalian systems. In mammals they are mainly concentrated in the liver<sup>85</sup> and also to some extent in the kidney, lung, small intestine, spleen, and steroidogenic organs.<sup>100</sup> It is

these enzymes (or very similar enzymes) that are responsible for hydroxylations and are believed to be responsible for reactions 1) – 4) above.

Cytochrome P<sub>450</sub> monooxygenases' mechanism of action can be briefly described as follows: the oxidized cytochrome P<sub>450</sub> (Fe<sup>3+</sup>) first complexes with a substrate, near the iron site of the heme protein. This complex is rapidly reduced via cytochrome P450 reductase to produce the Fe<sup>2+</sup> form. Next a molecular oxygen (O<sub>2</sub>) / cytochrome / substrate complex is formed. The iron atom is then oxidized back to its Fe<sup>3+</sup> form by reducing the oxygen to an oxide. Reduction (from an unknown source) reduces the P<sub>450</sub> enzyme to its Fe<sup>2+</sup> form again. Finally a rearrangement occurs involving the bond between the molecular oxygen bond cleaves resulting in one oxygen being incorporated into the substrate while the other accepts two protons to become water, and cytochrome P<sub>450</sub> is oxidized back to its Fe<sup>3+</sup> form.<sup>87, 97</sup>

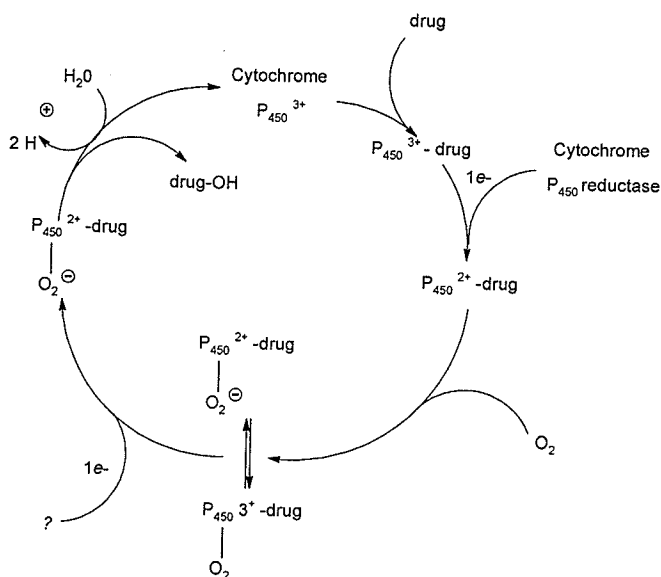


**Figure 24: Cytochrome P<sub>450</sub> monooxygenase mechanism on drugs**

Their fungal P<sub>450</sub> counterparts have been reported to yield parallel transformations.

Fungi are perhaps a better choice than bacteria for studying animal metabolism because of greater similarities in their enzyme systems (since they are both heterotrophic and eukaryotic), not to mention a greater number of enzymes.

Advantages of this approach include better cost efficiency, simple maintenance of subjects, easy scale-up capabilities, and vastly increased yield of metabolites (comparing  $\mu\text{g}$  to  $\text{g}$ ) for detection of analytes.<sup>97, 101, 102</sup>

Additionally, the selectivity of biotransformations can greatly aid in structure-activity relationship (SAR) studies,<sup>84</sup> particularly with complex, polyfunctional compounds. This is another way that biotransformations assist in the drug development process.

Utilization of biotransformation for derivative production is known to work best if the substrate is similar in structure to a known, successfully biotransformed structure. As the scholarly literature on biotransformations becomes more extensive and the certainty of a desired reaction is validated, biotransformations have begun to be more widely used in organic synthesis<sup>89</sup> (and in some cases, total synthesis<sup>103</sup>), much the way that enzymatic reactions have found their way into the synthetic chemist's repertoire.

This new research project was designed to investigate the biotransformations of three natural products: sclareol (**110**), sclareolide (**111**), and colchicine (**112**).

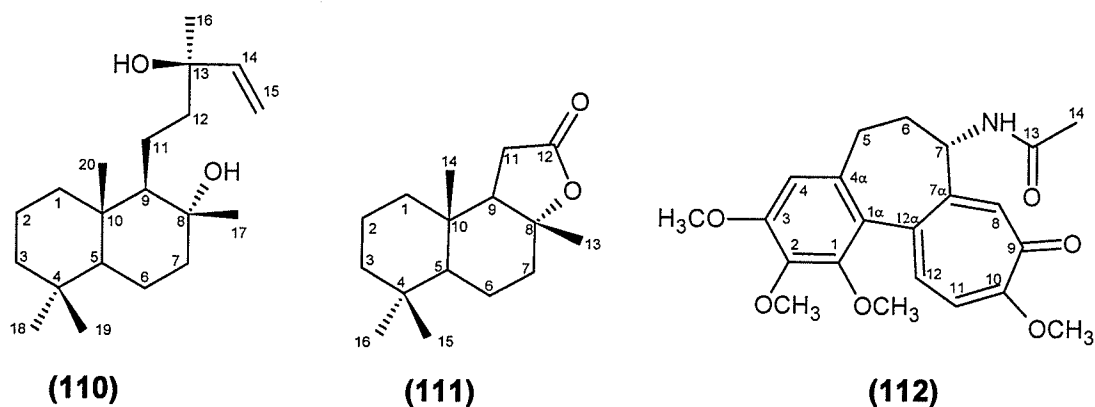


**Figure 25: Structures of the natural products for biotransformation: sclareol (110), sclareolide (111), and colchicine (112)**

These compounds were chosen most importantly due to their availability, but also due to their relevance because they all possess some biological activity, and all three have had (at least) some success having been a substrate for biotransformation studies in the past.

#### 4.2 Sclareol and its Reported Biotransformations

Sclareol [ladb-14-en-13 $\beta$ -ol]<sup>104</sup> (110) is a labdane diterpenoid that is widely distributed in nature<sup>105, 106</sup> but was first isolated as a minor constituent from the leaves of the plant, *Salvia sclarea* Linn (clary sage)<sup>107, 108, 109, 110, 111</sup> in 1931.<sup>112</sup> It is also quite abundant in *Nicotiana Spp.* (tobacco).

It is commercially available<sup>113</sup> and is used in preparation of scented compounds in perfumery,<sup>114</sup> and as a flavoring agent in food, alcoholic, cosmetic, and tobacco products.<sup>105</sup> It is also used in folklore medicine.<sup>115</sup> Its biological activity includes cytotoxicity,<sup>116</sup> herbicidal activity,<sup>117</sup> strong antibacterial activity,<sup>118</sup> and fungal-growth regulation.<sup>119</sup>

Biotransformation experiments have previously been executed on sclareol (**110**), beginning in 1982 (Hieda and co-workers).<sup>103</sup> To summarize, 18 derivatives have been characterized using eight fungi and four bacteria to date. The reported biotransformations of sclareol are summarized below.

Fermentation with the fungi, *Mucor plumbeus* has generated 18-hydroxysclareol (**113**), 3 $\beta$ -hydroxysclareol (**114**), and the 6 $\alpha$ -hydroxysclareol derivative (**115**),<sup>109</sup> while *Cunninghamella Spp.* NRRL 5695<sup>104</sup> and *Rhizopus stolonifer*<sup>106</sup> were only capable of producing the first two (**113**, **114**).

The 18-hydroxysclareol (**113**) and 3 $\beta$ -hydroxysclareol (**114**) derivatives have also been produced by *Cephalosporia aphidicola* [along with the 2 $\alpha$ -hydroxysclareol derivative (**115**) and 18-acetoxysclareol (**116**)],<sup>112</sup> while *Cunninghamella elegans* has also produced the 2 $\alpha$ -hydroxysclareol derivative (**115**) and 19-hydroxysclareol (**117**)<sup>107</sup>

*Bacillus cereus* [which has additionally generated 18-hydroxysclareol (**113**) 3 $\beta$ -hydroxysclareol (**114**), 2 $\alpha$ -hydroxysclareol (**115**)], 2 $\alpha$ , 18-dihydroxysclareol (**118**), the sclareol 18-O-D-glycoside (**119**), the sclareol 2 $\alpha$ -O-D-glycoside (**120**), and the sclareol 3 $\beta$ -O-D-glycoside (**121**),<sup>104</sup> whereas *Bacillus sphaericus* is limited to the 18-hydroxy (**113**) and 3 $\beta$ -hydroxy (**114**) derivatives of sclareol.<sup>107</sup>

3 $\beta$ -hydroxysclareol (**113**), 2 $\alpha$ -hydroxysclareol (**115**), 3-ketosclareol (**122**) are biotransformation products using *Septomyxa affinis*.<sup>120</sup> *Botrytis cinerea* fermentation results in two very unusual derivatives: epoxysclareol (**123**), and 8-deoxy-14, 15-dihydro-15-chloro-14-hydroxy-8,9-dehydrosclareol (**124**).<sup>115</sup>

Finally, the Bacterium JTS – 162 has resulted in transformations into sclareol 18-carboxylic acid (**125**), sclareol 18-carboxylic acid methyl ester (**126**), sclareol 18-aldehyde (**127**), manool (**128**), manoyl oxide (**129**), and the 13-ketosclareol (**130**),<sup>103</sup> whereas Soil Bacterium JTS – 131 was only capable of transforming the first two (**125, 126**).<sup>121</sup>

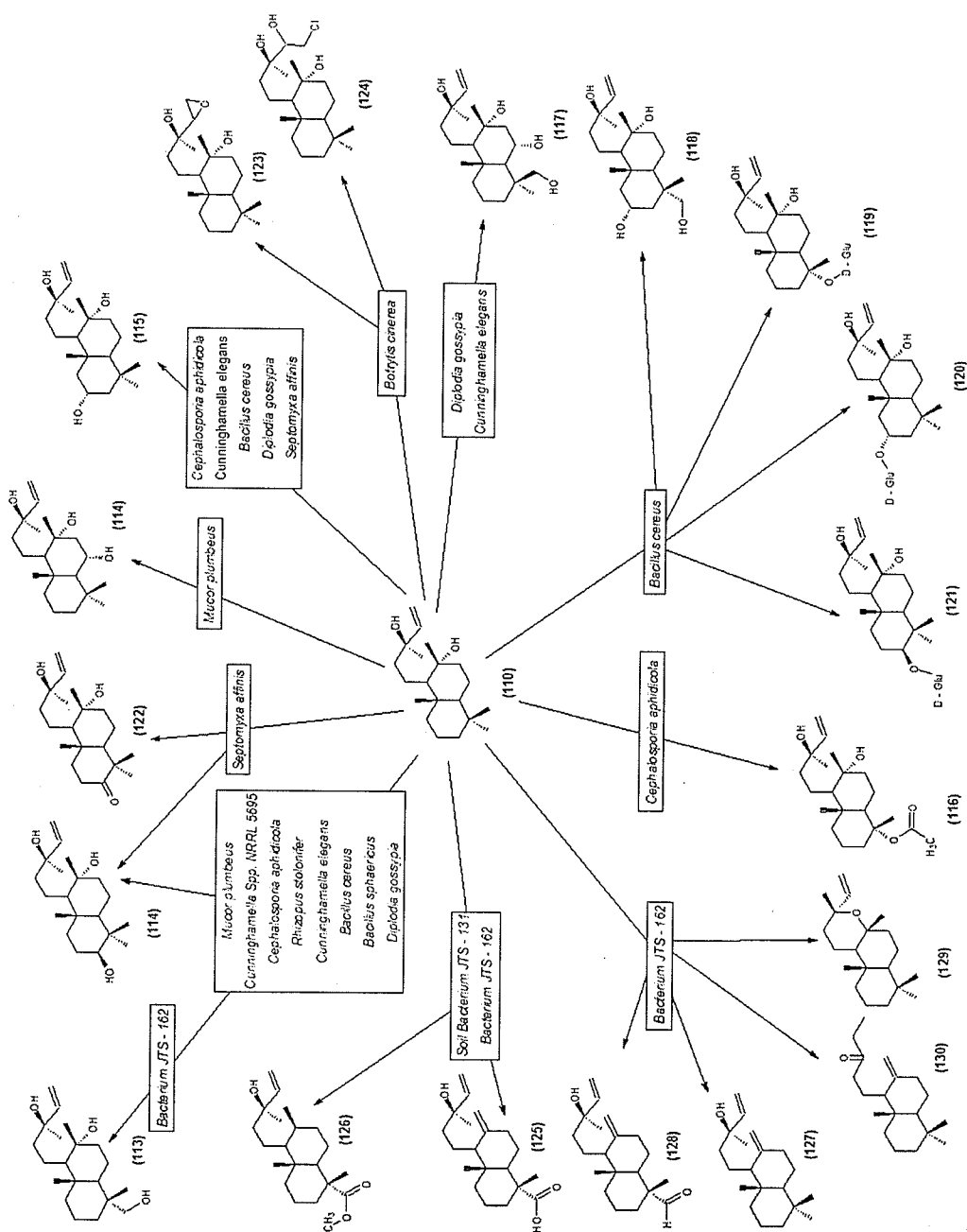


Figure 26: Reported Biotransformations of Sclareol (110)

### 4.3 Sclareolide and its Reported Biotransformations

Sclareolide (**111**) is a sesquiterpenoid lactone isolated from the plant, *Arnica angustifolia*,<sup>122, 123</sup> *Sideritis nutans*,<sup>123, 124</sup> and *Kyllinga erecta*<sup>125</sup>

Its biological activity includes phytotoxicity<sup>126</sup> as well as anticancer activity, specifically it possesses modest cytotoxicity against breast (MCF-7), colon (CKCO-1), lung (H-1299), and skin (HT-144) human cancer cell lines.<sup>127</sup> It is also commercially available.<sup>128</sup>

Several previous biotransformation of sclareolide (**111**) have been reported in the literature, beginning in 1991 (by Aranda and co-workers).<sup>109</sup> As an overview, sixteen derivatives have been characterized using 10 fungi as of the time of this writing. The reported biotransformations are summarized below.

Fermentation with the fungi, *Aspergillus niger* has generated 3-ketosclareolide (**131**), 3 $\beta$ -hydroxysclareolide (**132**), and 1 $\beta$ -hydroxysclareolide (**133**).<sup>123</sup> Incubation with *Mucor plumbeus*<sup>109, 110</sup> and *Curvularia lunata*<sup>123</sup> also results in the three previously mentioned derivatives being produced (**131 - 133**), along with two other dihydroxylated derivatives: 1 $\beta$ , 3 $\beta$ -dihydroxysclareolide (**134**), and 1 $\alpha$ , 3 $\beta$ -dihydroxysclareolide (**135**).

The genus *Cunninghamella* has been studied thoroughly for the ability to transform sclareolide as a substrate.<sup>125, 127</sup> *Cunninghamella blakesleeana* fermentation has produced 3-ketosclareolide (**131**), 3 $\beta$ -hydroxysclareolide (**132**), 1 $\beta$ , 3 $\beta$ -dihydroxysclareolide (**134**), *O*<sup>6</sup>-sclareolide (**136**), 9-hydroxysclareolide (**137**), and 3 $\beta$ , 6 $\alpha$ -dihydroxysclareolide (**138**).<sup>127</sup> *Cunninghamella echimulata* as a biocatalyst has resulted in 3 $\beta$ -hydroxysclareolide (**132**), 5-hydroxysclareolide (**139**) and 7 $\beta$ -



hydroxysclareolide (**140**) being produced.<sup>127</sup> *Cunninghamella elegans* produces the derivatives: 3-ketosclareolide (**131**), 3 $\beta$ -hydroxysclareolide (**132**), 1 $\alpha$ , 3 $\beta$ -dihydroxysclareolide (**135**), 2 $\alpha$ -hydroxysclareolide (**141**), 2 $\alpha$ , 3 $\beta$ -dihydroxysclareolide (**142**), and 3 $\beta$ -hydroxy-8-episclareolide (**143**).<sup>125</sup>

*Cephalosporium aphidicola* fermentation results in 3-ketosclareolide (**131**), 3 $\beta$ -hydroxysclareolide (**132**), and 3 $\beta$ , 6 $\beta$ -dihydroxysclareolide (**144**).<sup>129</sup> 3 $\beta$ -hydroxysclareolide (**132**), 1-ketosclareolide (**145**), 3 $\beta$ ,14-dihydroxysclareolide (**146**) were the fermentation products using the fungi, *Botrytis cinerea*.<sup>130</sup> *Gibberella fujikuroii* fermentation produces 3-ketosclareolide (**131**), 3 $\beta$ -hydroxysclareolide (**132**), 1 $\beta$ -hydroxysclareolide (**133**), and 1 $\alpha$ , 3 $\beta$ -dihydroxysclareolide (**135**).<sup>123</sup> Lastly, *Fusarium lini* biotransformation products include 3 $\beta$ -hydroxysclareolide (**132**) and 1 $\alpha$ , 3 $\beta$ -dihydroxysclareolide (**135**).<sup>123</sup>

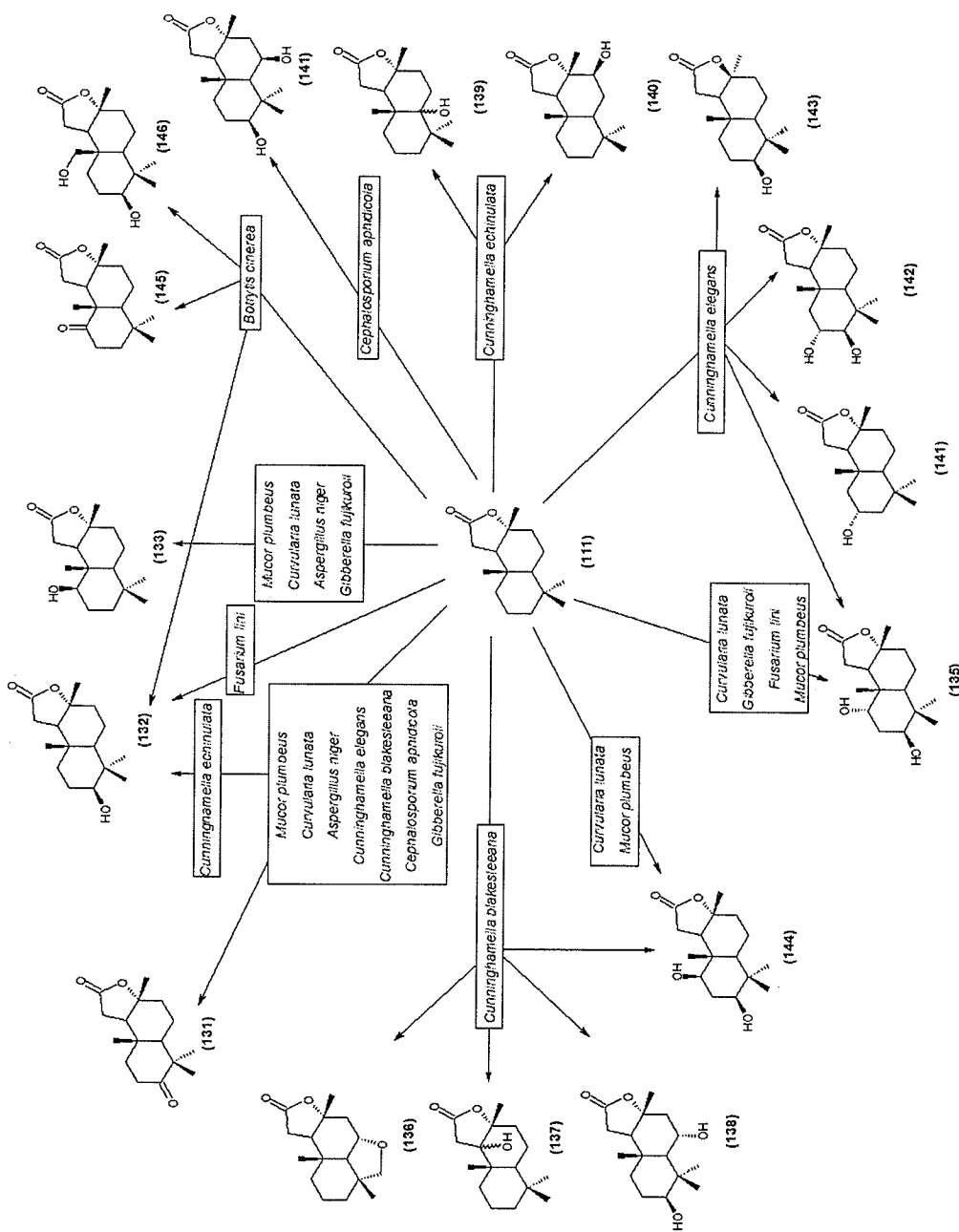


Figure 27: Reported Biotransformations of Sclareolide (111)

#### 4.4 Colchicine and its Reported Biotransformations

Colchicine (112), an alkaloid produced by *Colchicum autumnale* (autumn crocus or meadow saffron) – in addition to others - and has been (and still is) used in treatment of gout (described by the Romans since the first century C.E.), as well as other diseases.<sup>131</sup> It was first isolated in 1820 by Pelletier and Caventon.<sup>132</sup> It acts as an anti-inflammatory agent.<sup>133</sup> Additionally, it has been investigated as an anticancer

agent due to its ability of inhibiting mitosis by binding to tubulin. Cancer cells are more susceptible since the rate of mitosis is significantly greater in cancer cells.

Only a few biotransformed derivatives of colchicine have been reported despite fairly extensive screening of this natural product. Fermentation with the fungi, *Streptomyces griseus* and *Streptomyces spectrabilis* have both generated  $O^2$ -demethylcolchicine (**147**) and  $O^3$ -demethylcolchicine (**148**) as derivatives of colchicine (**112**). The soil bacterium, *Arthobacter colchovorum* has been reported to produce 7-deacetylcolchicine (**149**) and 7-deacetamino-7-ketocolchicine (**150**).

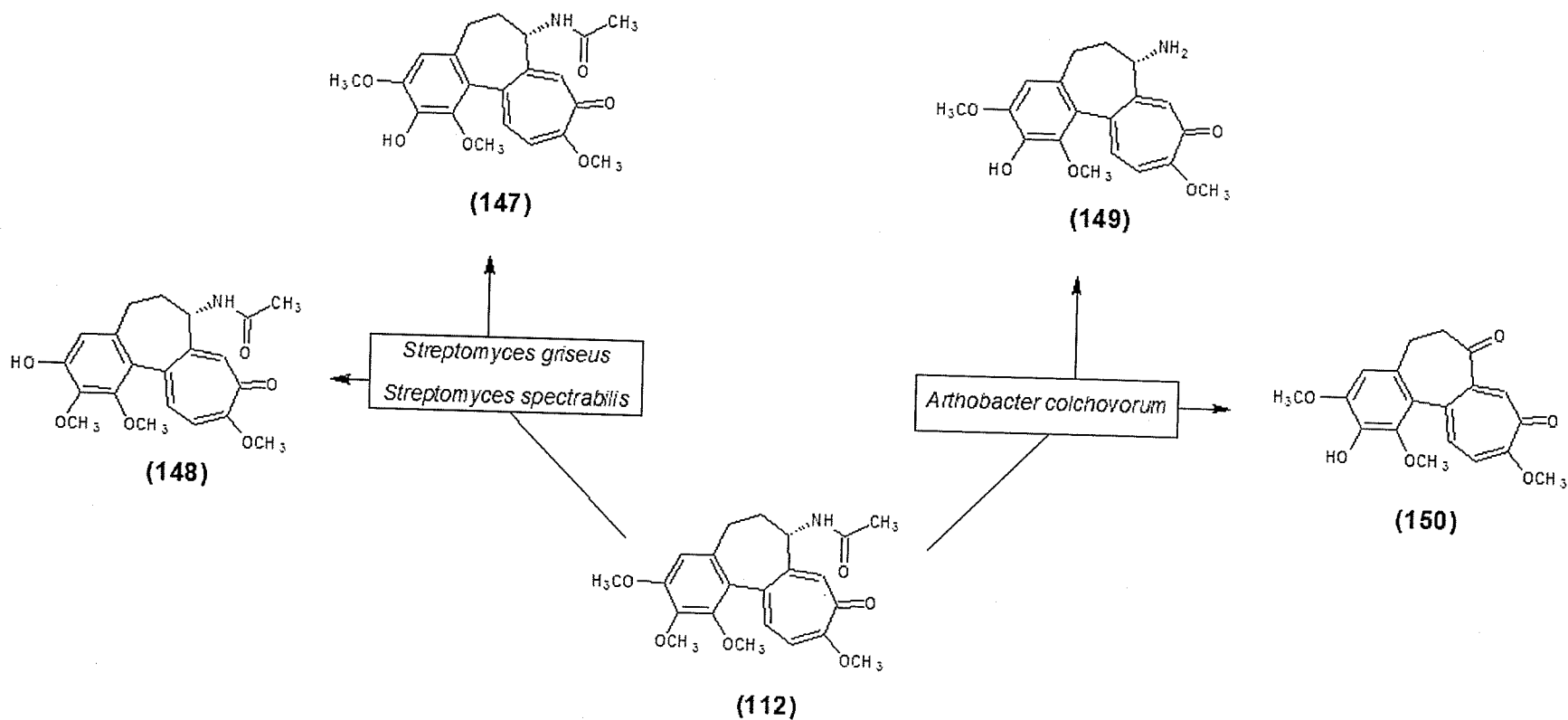


**Figure 28: Reported Biotransformations of Colchicine (112)**

## 4.5 Biotransformation Experimental

### General

Sclareol (95%) and Colchicine were purchased from Aldrich. Sclareolide (97%) was purchased from Fluka. Lo Fat Soy Flour was purchased from Canasoy, DIFCO BACTO™ yeast extract was purchased from Becton Dickinson, NaCl was supplied by BDH, K<sub>2</sub>HPO<sub>4</sub> and dextrose were purchased from EM Science. Potato dextrose agar and Sabouraud dextrose agar (powders) were supplied by Becton Dickinson.

General experimental conditions used in this research were the same as those discussed in section 2.2

### Fungi

The following fungal strains were purchased from the American Type Culture Collection (ATCC): *Aspergillus niger* (ATCC#9142), *Mucor plumbeus* (ATCC#4740), *Penicillium crustosum* (ATCC#90147), and *Candida albicans* (ATCC #14053 & #90028). *A. niger* and *P. crustosum* stock cultures were replated onto potato dextrose agar, while the *C. albicans* stock cultures were replated onto Sabouraud dextrose agar. Replating of these stock cultures was executed once a month and the cultures were maintained at 4°C.

### Broth Media

The ingredients and proportions used in the preparation of the soy broth media were as follows: soybean flour (20 g/L), dextrose (5 g/L), yeast extract (5 g/L), sodium chloride (5g/L), and dipotassium hydrogen phosphate [K<sub>2</sub>HPO<sub>4</sub>] (5 g/L). This was a slight modification of the media suggested by Smith and Rosazza.<sup>134</sup> The broth

was portioned into 50 mL aliquots in 250 mL Erlenmeyer flasks and the pH was adjusted to 7.0 using NaOH before sterilization in a steam autoclave.

### **Screening Experiment – Incubation Procedure**

The initial step in the conducted biotransformation studies was to perform a screening experiment, the objective of which was to perform a fermentation of the natural product substrate on a small scale using several fungi, to efficiently determine the presence of biotransformed products.

Biotransformation experiments were performed in shake culture flasks by a two-stage fermentation procedure to ensure experimental reproducibility and produce sufficient biomass.<sup>84, 128</sup> For the preparation of stage I cultures, a 25 mm<sup>2</sup> (1 inch<sup>2</sup>) square from the fungal stock cultures was transferred to an Erlenmeyer flask containing 50 mL aliquot of sterile soy broth. Incubation of the stage I cultures was carried out on a gyrorotary shaker at room temperature (~25°C) for 72 hours at ~220 rpm.

Stage II cultures were prepared by 5 mL each of the stage I broth being transferred into five new flasks containing sterile broth. Incubation of the stage II cultures was permitted for 24 hours (under similar conditions as mentioned above) before inoculation with the natural product substrate solution. After this time, the natural product substrate (400 mg sclareol **(110)**, sclareolide **(111)**, or colchicine **(112)**, respectively) was then transferred to the five flasks of a stage II culture (95% ethanol solution for sclareol **(110)** and sclareolide **(111)**, or aqueous solution for colchicine **(112)** [100 mg/mL]). Final titer of substrate after addition to the stage II

cultures was 0.4 mg/mL. Incubation was then resumed for 10 days under similar conditions.

Two types of controls were utilized as well to ensure proper interpretation of the data. A positive “growth” control was prepared in which the fungi were subjected to identical conditions but without any substrate. A negative “media” control was prepared in which the substrate was added to the broth media but without any fungi.

After the final incubation, the flasks (both samples and controls) were removed and their contents gravity- filtered using a Whatman #5 filter. The mycelia were vigorously pressed to maximize the filtrate. The filtrates (~250 mL) were extracted with ethyl acetate (3x, equal volume) and dried, which resulted in light brown extracts.

Screening biotransformation experiments were carried out on all three substrates (sclareol **(110)**, sclareolide **(111)**, colchicine **(112)**) using the five fungi listed above.

#### **Screening Experiment – Extract Analysis**

The extracts were dissolved in dichloromethane and tested for evidence of biotransformation on analytical thin layer chromatography, along with the growth and media controls. An optimum mobile phase for separation in each case was determined [100% ethyl acetate for sclareol **(110)**, 70% ethyl acetate/30% hexanes for sclareolide **(111)**, and 100% methanol for colchicine **(112)**]. Visualization was done by the charring treatment for sclareol **(110)** or sclareolide **(111)** analysis or by examination under UV light at 256 nm for colchicine **(112)** analysis. During the TLC analysis, the

pure parent compound (sclareol (**110**), sclareolide (**111**), and colchicine (**112**), respectively) were also spotted on the same TLC plate

Biotransformed derivatives were detected by samples having spots with similar but lower (more polar) retention factors ( $R_f$ ) values than the parent compound on TLC, which are not present in the controls. TLC spots in both samples and the positive (growth) control indicates the presence of natural fungal metabolites, such as tyrosol [(2,4-hydroxyphenyl)-ethanol] (**151**).

### **Scale-Up Experiment –Incubation Procedure**

Following a screening experiment with confirmation that one or several of the fungi that were screened were capable of metabolizing the natural product substrate (usually in miniscule quantity), the next step in the biotransformation study was a scale-up experiment, the purpose of which was to perform a fermentation of the natural product substrate on a larger scale using only one fungus (20 fungal soy broth cultures, instead of 5), which was more suitable for collection and further analysis of the biotransformed products. This is because the detection limit on analytical TLC is lower than the quantity necessary for structure determination.

To this end, the procedure and all other parameters for scale-up biotransformation experiments (media composition, incubation time, etc.) were identical to a screening experiment.

After stage II incubation is complete, the 20 flasks were pooled, vacuum-filtered, and the filtrate (~ 1 L) extracted with ethyl acetate (3x, equal volume) and dried, resulting in a light brown extract.



Scale-up biotransformation experiments were carried out on sclareol (**110**) using *Penicillium crustosum*; on sclareolide (**111**) using *Penicillium crustosum* and *Candida albicans*; and on colchicine (**112**) using *Mucor plumbeus* due to their screening experiment results, indicating possible derivatives. The fungi were chosen based on previous biotransformations in the literature.

### **Scale-Up - Extract Separation**

The dried, light brown scale-up extracts were each dissolved in a minimum amount of dichloromethane and then loaded onto a 30 cm x 100 cm chromatography column (wet addition) containing 30.0 g of silica gel.

Column chromatography was carried out on the extracts, following a stepwise gradient elution using hexanes/ethyl acetate, followed by ethyl acetate/methanol (50 mL fractions) in the following manner: for the mobile phases from 100% hexanes/0% ethyl acetate to 100% ethyl acetate/0% methanol (fractions 1-21), the gradient was 10%; i.e. 100 % hexanes → 90% hexanes/10% ethyl acetate, etc., for the mobile phases from 100% ethyl acetate/0% methanol to 100% methanol (fractions 22-38), the gradient for subsequent mobile phases was 20%.

For each biotransformation scale-up extract, 38 fractions were collected and examined using analytical TLC. The fractions that showed well-isolated species were pooled with others that showed similar Retention Factor ( $R_f$ ) values.

#### **4.6.1 Sclareol – *Penicillium crustosum* Scale-Up Experiment**

Column chromatography of the Scale-Up extract resulted in no biotransformed products that could be isolated in sufficient yield for structure

determination, but elution with the mobile phase, 80% ethyl acetate/20% methanol [fraction 22] afforded the parent compound, sclareol (**110**) (45.0 mg, 11.25% yield).

#### 4.6.2 Sclareolide – *Penicillium crustosum* Scale-Up Experiment

During column chromatography of the Scale-Up extract, elution with 70% ethyl acetate/ 30% hexanes [fractions 15 – 16] afforded the parent compound, sclareolide (**111**) (40.1 mg). Elution with 100% ethyl acetate [fractions 20-21] resulted in elution of 3-ketosclareolide (**131**) (42.6 mg, 10.65% yield). While elution with 60% ethyl acetate/40% methanol [fractions 25 – 29] afforded 3 $\beta$ -hydroxysclarolide (**132**) (23.9 mg, 5.98% yield).

3-ketosclareolide **131**; white powdery solid, 42.6 mg, fraction 20-21; UV  $\lambda_{\max}$  (MeOH) = 256 nm; IR (CCl<sub>4</sub>) = 3370, 2930, 1784, 1704, and 1112 cm<sup>-1</sup>; <sup>1</sup>H NMR (CDCl<sub>3</sub>, 300.13 MHz) = see Table 10; <sup>13</sup>C NMR (CDCl<sub>3</sub>, 75.47 MHz) = see Table 10; EI-MS = m/z 264 (M<sup>+</sup>), 249

3 $\beta$ -hydroxysclarolide **132**; white powdery solid, 23.9 mg, fraction 25 – 29; UV  $\lambda_{\max}$  (MeOH) = terminal; IR (CCl<sub>4</sub>) = 3380 cm<sup>-1</sup>, 2933, 1775, and 1120 cm<sup>-1</sup>; <sup>1</sup>H NMR (CDCl<sub>3</sub>, 300.13 MHz) = see Table 11; <sup>13</sup>C NMR (CDCl<sub>3</sub>, 75.47 MHz) = see Table 11; EI-MS = m/z 266 (M<sup>+</sup>), 251, 233, 207, 55

#### 4.6.3 Sclareolide – *Candida albicans* Scale-Up Experiment

The parent compound, sclareolide (**111**), was not isolated during column chromatography, nor were any fractions upon  $^1\text{H}$  NMR analysis indicating biotransformed derivatives. However, elution with 80% ethyl acetate / 20% hexanes (fraction 18) afforded a slightly impure aromatic compound.

HPLC separation of the 4 predominant compounds in this sample was executed by using the following operating parameters: 80%  $\text{H}_2\text{O}$ /20% acetonitrile isocratic mobile phase, 12 min run time, 50  $\mu\text{L}$  injection volume, 1 mL/min flow rate, and 254 nm detection (scan 210 – 380 nm). The principal compound was isolated by collecting the eluent from  $R_T$  1.56 – 2.06 min in 10 collection runs, a white, crystalline solid was afforded, identified as tyrosol (**151**) (2.7 mg). The other three constituents of this fraction, though isolated, had insufficient quantity for structure determination.

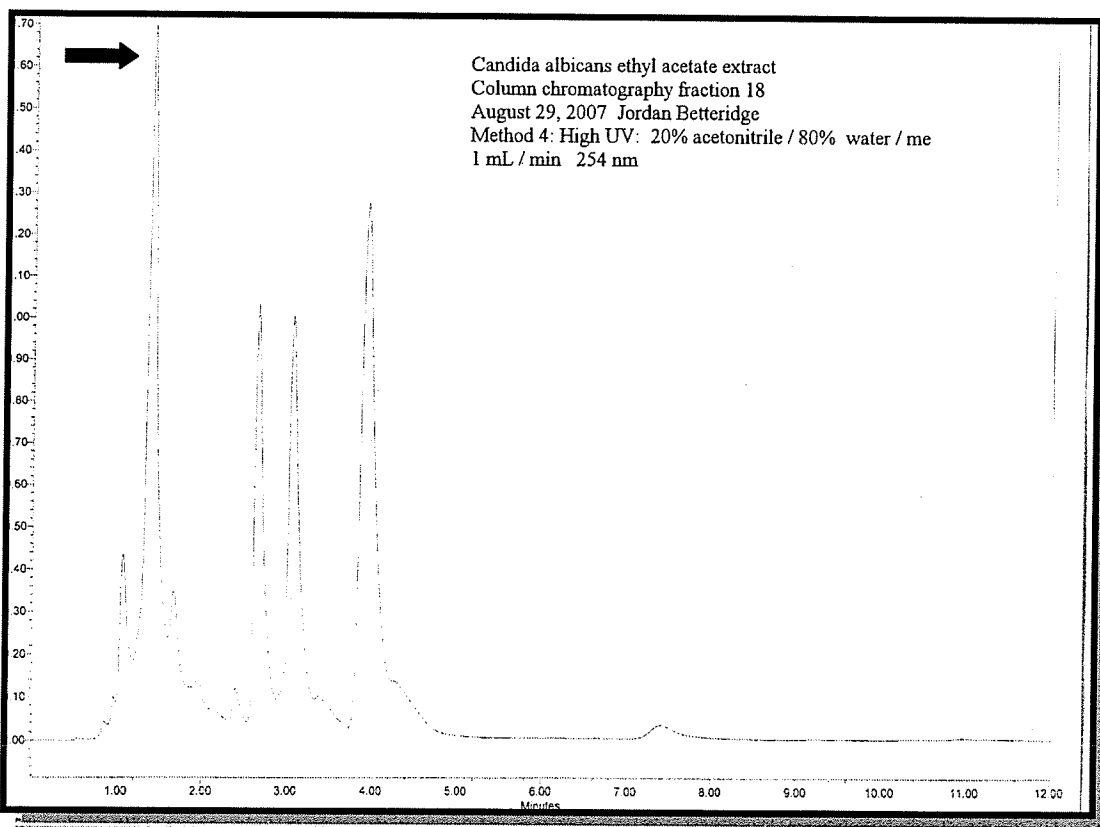


**Figure 29: HPLC Chromatogram of Collection Run for Column Chromatography Fraction #18 of Sclareolide – *Candida albicans* Scale Up extract (with peak of interest selected)**

Tyrosol **151**; white powdery solid, 2.7 mg, fraction 18; UV  $\lambda_{\text{max}}$  (MeOH) = 223 nm;  
IR (CCl<sub>4</sub>) = 2932, 3394.6, 2926, 1655, 1545, 1453, 1246, and 758 cm<sup>-1</sup>; <sup>1</sup>H NMR  
(CDCl<sub>3</sub>, 300.13 MHz) = see Table 12; <sup>13</sup>C NMR (CDCl<sub>3</sub>, 75.47 MHz) = see Table 12;  
EI-MS = m/z 138 (M<sup>+</sup>)

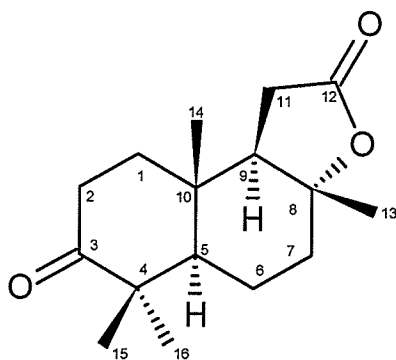
**4.6.4 Colchicine – *Mucor plumbeus* Scale-Up Experiment**

Column chromatography of the Scale-Up extract resulted in no biotransformed products isolated in sufficient yield for structure determination, but elution with the mobile phase, 100% methanol [fraction 35] afforded the parent compound, colchicine (**112**) (30.5 mg, 7.63% yield).

## 4.6 Biotransformation Results and Discussion

### 3-ketosclareolide (**131**)

The UV spectrum of compound **131** showed only terminal absorption with no significant absorbance maximum, indicating the lack of a conjugated  $\pi$  system. It has been previously reported,<sup>109, 110, 123, 125, 127, 129</sup> though not as a derivative of *Penicillium crustosum*. The IR spectrum of **131** displayed strong peaks at 3370 (OH), 2930 (CH), 1784 (ester C=O), 1704 (ketone C=O), and 1112 (CO)  $\text{cm}^{-1}$ .



(**131**)

The  $^1\text{H}$  NMR spectrum of compound **131** was similar to the respective spectra for the parent compound, sclareolide (**111**) with no appreciable differences and some minor downfield chemical shifts.

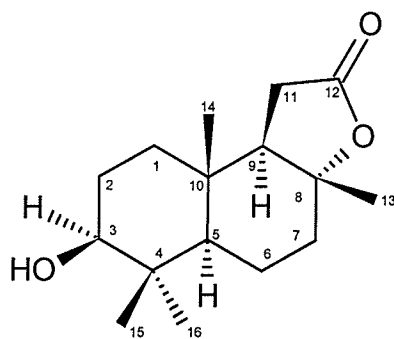
The  $^{13}\text{C}$  NMR spectrum of **131** displayed all 16 carbon signals. A downfield signal at  $\delta$  215.4 confirmed the presence of the C-3 ketonic carbon. Due to only two known keto-derivatives (3-keto or 1-keto) of this compound being reported, the literature values of both were examined and it was found that the chemical shifts were near equivalent ( $\leq \delta 0.1$ ) with the published values for 3-ketosclareolide (**131**)<sup>126, 128</sup> (see Table 10). These spectroscopic conclusions led to the establishment of structure **131** for this derivative.

**Table 9:  $^1\text{H}$  and  $^{13}\text{C}$  NMR Chemical Shift Assignments of **131****

Carbon #	<b>131</b>		$^{13}\text{C}$ $\delta$
	$^1\text{H}$ $\delta$	$J$ (Hz)	
1	$\alpha$ 1.70 (m)		37.7
	$\beta$ 1.58 (m)		
2	$\beta$ 2.52 (m)		33.4
	$\alpha$ 2.49 (m)		
3	-		215.4
4	-		47.3
5	1.62 (dd)		54.3
6	$\alpha$ 1.85 (m)		21.4
	$\beta$ 1.80 (m)		
7	$\beta$ 2.15 (m)		37.7
	$\alpha$ 2.06 (m)		
8	-		85.6
9	$\alpha$ 1.98 (m)		58.1
10	-		35.5
11	$\beta$ 2.44 (dd)	15.1	28.6
	$\alpha$ 2.28 (dd)	6.4	
12	-		175.9
13	$\beta$ 1.35 (s)		21.1
14	$\beta$ 1.00 (s)		14.5
15	$\beta$ 1.03 (s)		20.7
16	$\beta$ 1.10 (s)		26.6

**3 $\beta$ -hydroxysclareolide (132)**

The UV spectrum of compound **132** showed only terminal absorption indicating the lack of a conjugated  $\pi$  system. It has been previously reported,<sup>109, 110, 123, 125, 127, 129, 130</sup> though not as a derivative of *Penicillium crustosum*. The IR spectrum of **132** displayed strong peaks at 3380 (OH), 2933 (CH), 1775 (C=O), and 1120 (CO)  $\text{cm}^{-1}$ .



(132)

The  $^1\text{H}$  NMR spectrum of compound **132** showed the presence of an additional downfield peak at  $\delta$  3.25 (m), indicative of this derivative containing a hydroxyl group. The multiplicity of this signal suggested that the hydroxyl group may be at C-3.

The  $^{13}\text{C}$  NMR spectrum of **132** showed the resonance of all sixteen carbon atoms. A downfield signal at  $\delta$  78.6 confirmed the presence of the C-3 hydroxylated carbon.

The COSY spectrum of **132** showed cross-peaks between the proton signal of C-3 ( $\delta$  3.25), and the C-2 methylene protons (1.69 and 1.62), which showed further coupling with the signals at 1.45 and 1.18, the C-1 methylene protons. This spin system aided to reduce the site of hydroxylation to half the possibilities. Cross-peaks were evident between the proton signal,  $\delta$  1.03, the C-5 methine, and the signals at 1.92 and 1.87, the C-6 methylene protons, which showed further coupling with the signals at 2.08 and 1.68, the C-7 methylene protons. Lastly, the COSY spectrum revealed cross-peaks between the signal at  $\delta$  1.94, the C-9 methine, and the signals at 2.41, 2.22), the C-11 methylene protons.

The HSQC spectrum of **132** was used to find the  $^1\text{H}/^{13}\text{C}$  chemical shift assignments of **132** (see Table 11).

In the HMBC spectrum of **132**, heteronuclear cross-peaks existed between the C-3 methine ( $\delta$  3.25) and C-15 (15.1). Along with the COSY coupling data, this fact unambiguously confirmed the site of hydroxylation as C-3. Cross-peaks were also evident between the C-6 methylene protons ( $\delta$  1.92, 1.87) and C-8 methine (86.1), while the C-7 methylene protons ( $\delta$  2.08, 1.68) showed coupling with C-9 methine (58.8). Also, the C-11 methylene protons ( $\delta$  2.41, 2.22) showed coupling with C-9 methine (58.8) and C-12 (176.5). Long range heteroatomic coupling also existed between the C-13 methyl protons ( $\delta$  1.33) with C-8 (86.1) and C-9 (58.8). The C-14 methyl protons ( $\delta$  0.80) showed cross-peaks with C-5 (55.2). Lastly, The C-15 methyl protons ( $\delta$  0.91) showed cross-peaks with C-5 (55.2), while the C-16 methyl protons (1.00) showed cross-peaks with with C-4 (38.8) and C-5 (55.2). Important HMBC interactions of **132** are displayed in Figure 31.

The NOESY spectrum of **132** was used to establish the stereochemistry at C-3/OH. The C-3 methine proton ( $\delta$  3.25) showed an NOE with the C-16 methyl protons (1.00) indicative of a *cis* relationship between them. H-3 showed an NOE with H-16. H-3 did not show an NOE with H<sub>3</sub>-14, which indicated the  $\alpha$ -orientation of H-3 and thus  $\beta$ -stereochemistry for C-3/OH. These spectroscopic conclusions led to the establishment of structure **132** for this derivative.

Additionally, the <sup>13</sup>C chemical shifts showed impressive correlation ( $\leq \delta 0.1$ ) with the published values for **132**.<sup>126, 128</sup> Accordingly, **132** was assigned as the proposed structure for this compound.



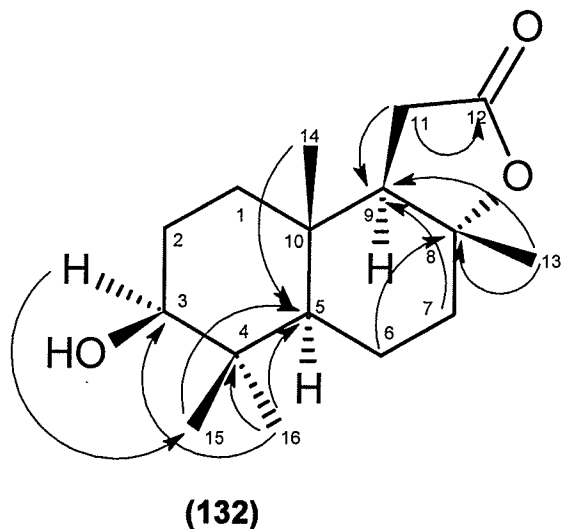


**Figure 30: Important HMBC Interactions Observed in 132**

**Table 10:  $^{13}\text{C}$  NMR Chemical Shift Assignments and  $^1\text{H}/^{13}\text{C}$  One-Bond Shift Correlations of 132 as determined from its HSQC Spectra**

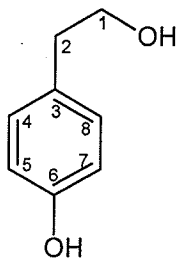
Carbon #	<b>132</b>		
	$^1\text{H}$ $\delta$	$J$ (Hz)	$^{13}\text{C}$ $\delta$
1	$\alpha$ 1.45 (m) $\beta$ 1.18 (m)		37.6
2	$\beta$ 1.69 (m) $\alpha$ 1.62 (m)		26.8
3	$\alpha$ 3.25 (dd)	5.3, 5.4	78.6
4	-		38.8
5	1.42 (m)		55.2
6	$\alpha$ 1.92 (m) $\beta$ 1.87 (m)		20.2
7	$\beta$ 2.08 (m) $\alpha$ 1.68 (m)		38.3
8	-		86.1
9	$\alpha$ 1.94 (m)		58.8
10	-		35.7
11	$\beta$ 2.41 (dd) $\alpha$ 2.22 (dd)	15.1 6.4	28.7
12	-		176.5
13	$\beta$ 1.33 (s)		21.5
14	$\beta$ 0.80 (s)		15.0
15	$\beta$ 0.91 (s)		15.1
16	$\beta$ 1.00 (s)		27.8

### Comment on Sclareolide – *Candida albicans* Scale-Up Experiment

The anomalous result of sclareolide (**111**) not being retrieved from the extract may indicate that sclareolide was utilized as a source of carbon by *C. albicans* – since it is a chemoorganotrophic heterotroph - and completely metabolized.

### Tyrosol (**151**)

The UV spectrum of compound **151** displayed two absorbance maximums ( $\lambda_{\text{max}}$ ) at 223 and 278 nm, indicative of conjugation.<sup>135</sup> It has been previously reported.<sup>136, 137</sup> The IR spectrum of **151** displayed strong peaks at 2932 (CH), 3394.6 (OH); 2926 (CH); 1655, 1545, 1453 (aromatic); 1246 (CO); and 758 (aromatic)  $\text{cm}^{-1}$ .



**(151)**

The  $^1\text{H}$  NMR spectrum of compound **151** showed two aromatic doublet signals centered at  $\delta$  7.09 and 6.78, respectively, which suggested a disubstituted aromatic ring with *para*-positioning, assigned to C-4/8 and C-5/7 methine protons. Two triplets are integrating for 2H each, at  $\delta$  3.82 and 2.80 indicated two methylene groups each coupling to two protons, and were assigned to the protons of C-1 and C-2. C-2 was determined to be vicinal to the hydroxyl-bearing C-1 due to its downfield chemical shift in the appropriate range. The broad singlet at  $\delta$  4.70 indicated a phenolic hydrogen, and was assigned to the phenol group of C-6.

The  $^{13}\text{C}$  NMR spectrum of **151** showed resonances for all 8 carbon atoms, and their multiplicities determined with the aid of APT spectrum. Positive-sign peaks at  $\delta$  63.8 and 38.2 were assigned to  $2^\circ$  methylene carbons C-1 and C-2, respectively. The negative-sign peaks at  $\delta$  130.2 and 115.4 were assigned to the aromatic carbons, C-4/8 and C-5/7, respectively. The quaternary aromatic signals of C-3 and C-6 were not visible in the  $^{13}\text{C}$  spectrum, but their coupling was evident in the HMBC spectrum (see Table 12).

The COSY spectrum of **151** depicted vicinal coupling between the two aromatic doublets at  $\delta$  7.09 and 6.78, corresponding to the C-4/8 and C-5/7 methines, respectively, which confirmed *para*-substitution. Additionally, the triplets at  $\delta$  3.82 and 2.80, also exhibited cross-peaks, further indicative of vicinal coupling between C-1 and C-2 triplets, respectively

The HMBC spectrum of **151** most importantly indicated coupling between the aromatic methine protons of C-4/8 and C-5/7 ( $\delta$  7.09 and 6.78), and the phenolic C-6 ( $\delta$  155.5). Additionally, coupling was evidenced between the  $4^\circ$  C-3 ( $\delta$  130.2) and the methylene protons of C-1 and C-2 ( $\delta$  7.09 and 6.78, respectively). Cross-peaks showed the long-range heteroatomic coupling between C-4/8 ( $\delta$  130.4) and the aromatic methine protons of C-5/7 ( $\delta$  6.78). Additionally, cross-peaks indicated long-range coupling between C-2 ( $\delta$  38.2) and the methylene protons of C-1 ( $\delta$  3.82). The literature values of the NMR chemical shifts for tyrosol were compared to the experimental values and close correlation was found between the two ( $\leq \delta 0.31$  for  $^1\text{H}$  NMR,  $\leq \delta 0.8$  for  $^{13}\text{C}$  NMR) with the published NMR values for tyrosol (**151**), performed in DMSO- $d_6$  and  $\text{D}_2\text{O}$ .<sup>134</sup> Important HMBC interactions of **151** are

displayed in Figure 32. Consequently, the structure **151** was assigned to this compound.

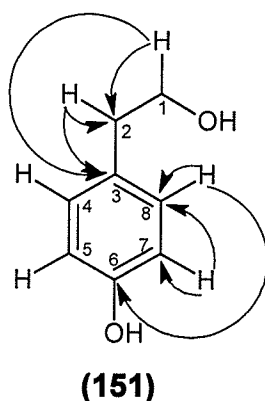


**Figure 31: Important HMBC Interactions Observed in 151**

**Table 11:  $^1\text{H}$  and  $^{13}\text{C}$  NMR Chemical Shift Assignments of 151**

Carbon #	<b>151</b>		
	$^1\text{H } \delta$	$J$ (Hz)	$^{13}\text{C } \delta$
1	3.82 (t)	6.4	63.8
2	2.80 (t)	6.4	38.2
3	-	-	130.2
4, 8	7.09 (d)	8.3	130.4
5, 7	6.78 (d)	8.4	115.4
6	-	-	155.5
OH	4.70 (br.s)	-	-

Tyrosol (**151**), a previously reported compound, is produced when the amino acid tyrosine undergoes hydrolytic decarboxylation.<sup>136</sup> Tyrosol is known for being an important metabolite produced by *Candida albicans*, used as a quorum (threshold population) sensor and is important in biofilm development, a major factor in its virulence.<sup>137</sup> It is also a component of table olives (along with other phenolics) and is significantly responsible for their intrinsic antioxidant activity and antibacterial activity.<sup>138, 139</sup>

#### 4.6.5 Minimum Inhibitory Concentration (MIC) Assay

All positive (growth) controls and negative (sterile) controls were satisfactory (not shown). The MIC values for the standards, penicillin G (**5**) and Chloramphenicol (**72**) were in agreement with the published values for those agents.<sup>69</sup>

The MIC results indicated that sclareolide (**111**) and its biotransformed derivatives possessed very weak to no antimicrobial activity as there was no activity detected in the concentration range tested.

However, tyrosol (**151**), the *Candida albicans* metabolite displayed intermediate activity towards the Gram-positive bacteria, *Staphylococcus aureus* and *Streptococcus agalactiae* (see Table 13). This activity may, in part, explain the virulence of this pathogen, which is the causative agent of Candidiasis, often called Thrush (oral infection). This may greatly aid in annihilating the indigenous skin bacteria (which is mostly Gram-positive *S. epidermidis* and some *S. aureus* and possibly *Lactobacillus spp.*); the competing microbial populations, during infection.

**Table 12: MIC Assay for Compounds 131, 132, and 151**

Bacteria	Compounds				Standards	
	<b>111</b>	<b>131</b>	<b>132</b>	<b>151</b>	<b>5</b>	<b>72</b>
<i>S. aureus</i>	>128	>128	>128	≤64	≤1	≤8
<i>S. agalactiae</i>	>128	>128	>128	≤32	≤1	≤2
<i>E. coli</i>	>128	>128	>128	>128	≤32	≤4
<i>P. aeruginosa</i>	>128	>128	>128	>128	>128	≤64

\*Values are expressed as concentration of analyte (µg/mL)

## Chapter 5.0: Conclusions

In summary, an examination of the constituent compounds from a methanolic *Sphaeranthus indicus* extract resulted in the isolation of dihydrocholesterol (**70**), 7 $\alpha$ -hydroxyfrullanolide (**54**), and 7 $\alpha$ -hydroxyeudesmanolide (**56**). Structural elucidation for these compounds was done using spectroscopic methods. Chemical derivatization of **54** was done for Structure Activity Relationship (SAR) studies, resulting in the semi-synthesis of **71**. Minimum Inhibitory Concentration (MIC) testing was executed to determine/quantify their antibacterial activity. This is the first study to characterize the antibacterial activity of individual constituents of this plant. The SAR results indicated that **54** has strong antibacterial activity against Gram-positive bacteria (*Staphylococcus aureus* and *Streptococcus agalactiae*) but not Gram-negative bacteria (*Escherichia coli* and *Pseudomonas aeruginosa*), while **56** and **71** had progressively decreasing, respectively. Compound **70** possessed no antibacterial activity in the concentration range tested.

Additionally, a methanolic extract of *Buxus hyrcana* resulted in the isolation of N<sub>b</sub>-dimethylcycloxobuxoviricine (**85**) and buxamine B (**99**), and two previously reported steroidal alkaloids. N<sub>b</sub>-dimethylcycloxobuxoviricine (**85**) has been isolated before, but the correct assignment for this compound was done here. Buxamine B (**99**) has not been isolated from this species of *Buxus* before. Structural elucidation for these compounds was also done using spectroscopic methods. MIC testing indicated that they possess no antibacterial activity in the concentration range tested.

Lastly, biotransformation experiments were carried out on three natural products, sclareol (**110**), sclareolide (**111**), and colchicine (**112**) using different fungi. The sclareol – *Penicillium crustosum* (ATCC#90147) and colchicine – *Mucor plumbeus* (ATCC#4740) biotransformation experiments resulted in insufficient quantity of derivatives for structure elucidation. The sclareolide – *Penicillium crustosum* (ATCC#90147) biotransformation experiment resulted in two previously reported derivatives: 3-ketosclareolide (**131**), and 3 $\beta$ -hydroxysclareolide (**132**). The sclareolide - *Candida albicans* (ATCC#90028) biotransformation experiment resulted in the isolation of a non-xenobiotic, important fungal natural product, tyrosol (**151**). Structural elucidation for these compounds was also done using spectroscopic methods. MIC testing on **111**, **131**, and **132** indicated no antibacterial activity in the concentration range tested, whereas **151** possessed intermediate activity for Gram-positive bacteria (*S. aureus*, *S. agalactiae*), possibly relevant to the organism's role as a human pathogen of growing concern.

## Chapter 6.0 References:

- <sup>1</sup> Pichersky, E.; Gang, D.R. Genetics and biochemistry of secondary metabolites in plants: an evolutionary perspective. *Trends in Plant Science*: 5 [10] (2000): 439 – 445
- <sup>2</sup> Rouhi, A.M. Rediscovering Natural Products. *Chemical & Engineering News*: 81 [41] (2003): 77 – 91
- <sup>3</sup> Meinwald, J.; Eisner, T.; Natural products chemistry: new opportunities, uncertain future. *Helvetica Chimica Acta*: 86 [11] (2003): 3633 – 3637
- <sup>4</sup> Demain, A.L. From natural products to commercialization: A success story. *Journal of Industrial Microbiology & Biotechnology*: 33 [7] (2006): 486 – 495
- <sup>5</sup> Souza, N.J.; Ganguli, B.N.; Reden, J. Strategies in the discovery of drugs from natural sources. *Annual Reports in Medicinal Chemistry*: 17 (1982): 301 – 310
- <sup>6</sup> Fleming, A. The antibacterial action of cultures of a penicillium, with special reference to their use in the isolation of *B. influenzae*. *British Journal of Experimental Pathology*: 10 (1929): 226 – 236
- <sup>7</sup> Herrell, W.E. History of the development of antibiotics. *Clinical Medicine*: 77 [7] (1970): 10 – 17
- <sup>8</sup> Anonymous. A brief history of antibiotics. *The John Hopkins Medical Letter Health After 50*: 11 [5] (1999): 7
- <sup>9</sup> Chain, E.; Florey, H.W.; Gardner, A.D.; Heatley, N.G.; Jennings, M.A.; Orr-Wing, J.; Sanders, A.G. Penicillin as a chemotherapeutic agent. *Lancet*: 2 (1940): 226 – 228
- <sup>10</sup> Gootz, T.D. Discovery and Development of New Antimicrobial Agents. *Clinical Microbiology Reviews*: 3 [1] (1990): 13 – 31
- <sup>11</sup> Newman, D.J.; Cragg, G.M.; Snader, K.M. Natural Products as Sources of New Drugs over the Period 1981 – 2002. *Journal of Natural Products*: 66 (2003): 1022 – 1037
- <sup>12</sup> Feher, M.; Schmidt, J. M. Property distributions: differences between drugs, natural products, and molecules from combinatorial chemistry. *Journal of Chemical Information and Computer Sciences*. 43 [1] (2003): 218 -227
- <sup>13</sup> Horton, D.A; Bourne, G.T.; Smythe, M.L. Exploring privileged structures: the combinatorial synthesis of cyclic peptides. *Molecular Diversity* : 5 [4] (2002): 289 – 304



- 
- <sup>14</sup> Finland, M.; Wilcox, C. *In vitro* susceptibility of pathogenic staphylococci to seven antibiotics. *American Journal of Clinical Pathology*: 20 [4] (1950): 335 – 340
- <sup>15</sup> Levy, S.B. The Challenge of Antibiotic Resistance. *Scientific American*: 278 [3] (1998): 46 – 53
- <sup>16</sup> Kapil, A. The challenge of antibiotic resistance: need to contemplate. *The Indian Journal of Medical Research*: 121 [2] (2005): 83 – 91
- <sup>17</sup> Opal, S.M.; Mayer, K.H.; Medecros, A.A. Mechanisms of Bacterial Resistance. (Mandell, G.L.; Bennetl, J.E.; Dolin, R. editors) *Principles and practice of infectious diseases*; 5<sup>th</sup> edition. Volume II. (2000) New York, USA: Churchill Livingstone: 236 – 253
- <sup>18</sup> Kumar, V.P.; Chauhan, N.S.; Padh, H.; Rajani, M. Search for antibacterial and antifungal agents from selected Indian medicinal plants. *Journal of Ethnopharmacology*: 107 (2006): 182 – 188
- <sup>19</sup> Chopra, L.; Hodgson, J.; Metcalf, B.; Poste, G. New approaches to the control of infections caused by antibiotic resistant bacteria. An industrial perspective. *Journal of the American Medical Association*: 275 (1996): 401 – 403
- <sup>20</sup> Baquero, F. Gram-positive resistance: challenges for the development of new antibiotics. *Journal of Antimicrobial Chemotherapy*: 39 (1997): 1 – 6
- <sup>21</sup> Chopra, C.L.; Bhatia, M.C.; Chopra, I.C. *In vitro* antibacterial activity of oils from Indian medicinal plants. *Journal of the American Pharmaceutical Association*: 49 (1960): 780 – 781
- <sup>22</sup> Nisha, M.; Kalyanasundaram, M.; Paily, K.P.; Abidha,; Vanamail, P.; Balaraman, K. *In vitro* screening of medicinal plant extracts for macrofilaricidal activity. *Parasitology research*: 100 [3] (2007): 575 – 579
- <sup>23</sup> Sadaf, F.; Saleem, R.; Ahmed, M.; Ahmad, S.I. Navaid-ul-Zafar. Healing Potential of cream containing extract of *Sphaeranthus indicus* on dermal wounds in Guinea pigs. *Journal of Ethnopharmacology*: 107 [2] (2006): 161 – 163
- <sup>24</sup> Gupta, R.K.; Chandra, S.; Mahadevan, V. Chemical components of *Sphaeranthus indicus*. *Indian Journal of Pharmacy*: 29 [2] (1967): 47 – 48
- <sup>25</sup> Singh, S.K.; Tripathi, V.J.; Singh, R.H.  $\beta$ -D-Glucoside of (24S)-ethylcholesta-5,22-dien- $\beta$ -ol from *Sphaeranthus indicus* L. *Indian Drugs*: 26 [6] (1989): 317 – 318
- <sup>26</sup> Lodha, V. Chemical analysis of the essential oil of *Sphaeranthus indicus* – an Ayurvedic plant of India. *Indian Perfumer*: 47 [1] (2003): 29 – 30

- 
- <sup>27</sup> Dubey, K.S.; Ansari, A.H.; Hardaha, M. Antimicrobial activity of the extract of *Sphaeranthus indicus*. *Fitoterapia*: 70 [2] (1999): 127 – 129
- <sup>28</sup> Bafna, A.R.; Mishra, S.H. Protective effect of bioactive fraction of *Sphaeranthus indicus* Linn. against cyclophosphamide induced suppression of humoral immunity in mice. *Journal of Ethnopharmacology*: 104 [3] (2006): 426 – 429
- <sup>29</sup> Sharma, M.; Tripathi, J. Developmental effect of a bicyclic sesquiterpene lactone from *Sphaeranthus indicus* on the preimaginal stage of *Anopheles stephensi*. *Journal of Ecophysiology & Occupational Health*: 3 [1 & 2] (2003): 79 – 84
- <sup>30</sup> Baslas, K.K. Essential oil from *Sphaeranthus indicus*. *Perfumery and Essential Oil Record*: 50 (1959): 765 – 768
- <sup>31</sup> Yadava, R.N.; Kumar, S. A novel isoflavone glycoside from the leaves of *Sphaeranthus indicus*. *Fitoterapia*: 70 (1999): 127 – 129
- <sup>32</sup> Sohoni, J.S.; Rojatkar, S.R.; Kulkarni, M.M.; Dhaneshwar, N.N.; Tavale, S.S.; Gururaw, T.N.; Nagasampagi, B.A. A new eudesmanolides and 2-hydroxycaustic acid from *Sphaeranthus indicus* Linn. X-ray molecular structure of 4 $\alpha$ , 5 $\alpha$ -epoxy-7 $\alpha$ -hydroxyeudesmanolide. *Journal of the Chemical Society, Perkin Transactions 1: Organic and Bio-organic Chemistry (1972 – 1999)*: [2] (1988): 157 – 160
- <sup>33</sup> Warriar, P.K.; Nambiar, V.P.K.; Raman, K.C. *Indian Medicinal Plants, Vol. 1* Orient Longman, Hyderabad, India (2004): 180
- <sup>34</sup> Rojatkar, S.R.; Nagasampagi, B.A. 7-hydroxyeudesmanolides from *Sphaeranthus indicus*. *Phytochemistry*: 31 [9] (1992): 3270 – 3271
- <sup>35</sup> Rojatkar, S.R.; Sawaikar, D.D.; Nagasampagi, B.A. Photooxidation of 7-hydroxyeudesmanolide, a constituent from *Sphaeranthus indicus* Linn. *Indian Journal of Chemistry, Section B: Organic Chemistry Including Medicinal Chemistry*: 33B [12] (1994): 1203 – 1204
- <sup>36</sup> Kirtikar, K.R.; Basu, B.D. *Indian medicinal plant, II*. Allahabad: Lalit Mohan Basu Publication (1935): 1347
- <sup>37</sup> Chadha, Y.R. *The wealth of India*. Dictionary of raw materials and industrial products, X. New Delhi: CSIR (1982): 4
- <sup>38</sup> Basu, N.K.; Lamsal, P.P. Chemical investigation of *Sphaeranthus indicus* Linn. *Journal of the American Pharmaceutical Association (1912 – 1977)*: 35 (1946): 274 – 275

- 
- <sup>39</sup> Yadava, R.N.; Kumar, S. Chemical examination of the leaves of *Sphaeranthus indicus*. *Asian Journal of Chemistry*: 10 [4] (1998): 764 – 766
- <sup>40</sup> Chopra, R.N.; Nayar, S.L.; Chopra, I.C. *Glossary of Indian medicinal plants*. CSIR, New Delhi, India (1956): 9
- <sup>41</sup> Dhar, L.M. ; Dhar, M.M.; Dhawan, B.N.; Mehrotra, B.N.; Ray, C. Screening of Indian plants for biological activity. Part I. *Indian Journal of Experimental Biology*: 6 (1968): 232 – 247
- <sup>42</sup> Gogtet, M.G.; Anathasubramanian, L.; Nargund, K.S.; Bhattacharyya, S.C. Some interesting sesquiterpenoids from *Sphaeranthus indicus* Linn. (compositae). *Indian Journal of Chemistry*: 25B (1986): 233 – 238
- <sup>43</sup> Nadkarni, K.M. *Indian material medica*. (1954) Bombay, India: K.M. Nadkarni: 1163
- <sup>44</sup> Dahanukar, S.A.; Kulkarni, R.A.; Rege, N.N. Pharmacology of medicinal plants and natural products. *Indian Journal of Pharmacology*: 32 (2000): S81 – S118
- <sup>45</sup> Perumal Samy, R.; Ignacimuthu, S. Screening of 34 Indian medicinal plants for antibacterial properties. *Journal of Ethnopharmacology*: 62 (1998): 173 – 178
- <sup>46</sup> Perumal Samy, R.; Ignacimuthu, S. Antibacterial activity of some folklore medicinal plants by tribals in Western Ghats of India. *Journal of Ethnopharmacology*: 69 (2000): 63 – 71
- <sup>47</sup> Kumar, V.P.; Chauhan, N.S.; Padh, H.; Rajani, M. Search for antibacterial and antifungal agents from selected Indian medicinal plants. *Journal of Ethnopharmacology*: 107 (2006): 182 – 186
- <sup>48</sup> Shekhani, M.S.; Shah, P.M.; Khan, K.M.; Atta-ur-Rahman. New eudesmanolides from *Sphaeranthus indicus*. *Journal of Natural Products*: 54 [3] (1991): 882 – 885
- <sup>49</sup> Kirtikar, K.R.; Basu, B.D. *Indian Medicinal Plants*. (1918) Allahabad, India: Lalit Mohan Basu: 1 – 2
- <sup>50</sup> Chadha, Y.R. *The wealth of India*: 10 (1976) CSIR, New Delhi: 4 – 5
- <sup>51</sup> Pujar, P.P.; Sawaikar, D.D.; Rojatkar, S.R.; Nagasampagi, B.A. Eudesmanolides from *Sphaeranthus indicus*. *Fitoterapia*: 71 [3] (2000): 264 – 268
- <sup>52</sup> Yoganarasimhan, S.N. *Medicinal plants of India – Tamil Nadu*; Vol. 2. (2000) Bangalore, India: Cyber Media: 512

- 
- <sup>53</sup> Nadkarni, A.K. Indian material medica; Vol. 1. (2000) Mumbai, India: Popular Prakashan Ltd.: 113
- <sup>54</sup> Naqvi, B.S.; Hashmi, K.; Sheikh, D.; Mahdi, A. Antibacterial activity in fruits and vegetables. *Pakistan Journal of Pharmacology*: 15 (1998): 7 – 11
- <sup>55</sup> Narasimha Rao, B.G.V.; Nigam, S.S. *In vitro* antimicrobial efficiency of some essential oils. *Flavour Industry*: 1 [10] (1970): 725 – 729
- <sup>56</sup> Shirwaikar, A.; Prabhu, K.S.; Punitha, I.S.R. *In vitro* antioxidant studies of *Sphaeranthus indicus* (Linn). *Indian Journal of Experimental Biology*: 44 (2006): 993 – 996
- <sup>57</sup> Cross, C.E. Oxygen radicals and human disease. *Annals of Internal Medicine*: 107 [4] (1987): 526 – 545
- <sup>58</sup> Kaul, P.R.; Rao, B.R.; Rajeswara, B.; Arun, K.; Singh, K.; Mallavarapu, G.R.; Ramesh, S. Essential oil composition of *Sphaeranthus indicus* L. *Journal of Essential Oil Research*: 17 [4] (2005): 453 – 454
- <sup>59</sup> Jirovetz, L.; Buchbauer, G.; Shahabi, M. Medicinal used plants from India: analysis of the essential oils of *Sphaeranthus indicus* flowers, roots, and stems with leaves. *Scientia Pharmaceutica*: 71 [3] (2003): 251 – 259
- <sup>60</sup> Chughtai, M.I.D.; Khokhar, I.; Ahmad, A. Isolation, purification and structural determination of alkaloids from the flowers of *Sphaeranthus indicus*. *Science International (Lahore)*: 4 [2] (1992): 151 – 154
- <sup>61</sup> Dewick, P. M. *Medicinal natural products: a biosynthetic approach*; 2<sup>nd</sup> edition. (2002) West Sussex, England: John Wiley & Sons: 191 – 193
- <sup>62</sup> Atta-ur-Rahman; Shehhani, M.S.; Perveen, S.; Habib-ur-Rehman, Yasmin, A. Zia- ul-Haque, A.; Shaikh, D. 7-hydroxyfrullanolide, an antimicrobial sesquiterpene lactone from *Sphaeranthus indicus* Linn. *Journal of Chemical Research, Synopses*: [3] (1989): 68
- <sup>63</sup> Shekhani, M.S.; Shah, P.M.; Yasmin, A.; Siddiqui, R.; Perveen, S.; Khan, K.M.; Kazmi, S.U.; Atta-ur-Rahman. An immunostimulant sesquiterpene glycoside from *Sphaeranthus indicus*. *Phytochemistry*: 29 [8] (1990): 2573 – 2576
- <sup>64</sup> Ruangrunsi, N.; Kasiwong, S.; Likhitwitayawuid, K.; Lange, G.L.; Decicco, C.P. Studies on Thai medicinal plants. Part X. Constituents of *Grangea maderaspatana*. A new eudesmanolide. *Journal of Natural Products*: 52 [1] (1989): 130 -134

- <sup>65</sup> Jadhav, R.B.; Sonawane, K.B.; Panse, G.T.; Rojatkar, S.R. A new eudesmanolides from *Sphaeranthus indicus* (Linn). *Indian Journal of Chemistry*: 43B (2004): 217 – 218
- <sup>66</sup> Jadhav, R.B.; Sonawane, K.B.; Deshpande, N.R.; Rojatkar, S.R. *Indian Journal of Chemistry, Section B: Organic Chemistry Including Medicinal Chemistry*: 46B [2] (2007): 379 – 381
- <sup>67</sup> Atta-ur-Rahman; Choudhary, M.I.; Ata, A.; Alam, M.; Farooq, A.; Perveen, S.; Shekhani, M.S. Microbial Transformations of 7 $\alpha$ -hydroxyfrullanolide. *Journal of Natural Products*: 57 [9] (1994): 1251 – 1255
- <sup>68</sup> Dewick, P. M. *Medicinal natural products: a biosynthetic approach*; 2<sup>nd</sup> edition. (2002) West Sussex, England: John Wiley & Sons: 192 – 195
- <sup>69</sup> National Committee for Clinical Laboratory Standards. Methods for Dilution Antimicrobial Susceptibility Tests for Bacteria that Grow Aerobically -3<sup>rd</sup> ed; approved standard. (1993) NCCLS document M7-A3 (ISBN 1-56238-209-8). NCCLS, Villanova, Pennsylvania
- <sup>70</sup> SDBS-<sup>13</sup>C NMR SDBS No. 11141 CDS-07-892 5 $\alpha$ -cholestan-3 $\beta$ -ol. *Spectral Database for Organic Compounds (SDBS), National Institute of Advanced Industrial Science and Technology (AIST)*. (2007, Sept. 10) Retrieved Sept. 12, 2007 from <[http://riodb01.ibase.aist.go.jp/sdbs/cgi-bin/img\\_disp.cgi?disptype=disp3&imgdir=cds&fname=CDS07892&sdbno=11141](http://riodb01.ibase.aist.go.jp/sdbs/cgi-bin/img_disp.cgi?disptype=disp3&imgdir=cds&fname=CDS07892&sdbno=11141)>
- <sup>71</sup> Choudhary, M.I.; Shahnaz, S.; Parveen, S.; Khalid, A.; Mesaik, M.A.; Ayatollahi, S.A.M.; Atta-ur-Rahman. New cholinesterase-inhibiting triterpenoid alkaloids from *Buxus hyrcana*. *Chemistry & Biodiversity*: 3 [9] (2006): 1039 – 1052
- <sup>72</sup> Atta-ur-Rahman; Choudhary, M.I.; Nisa, M.; The isolation and structure of buxaquamarine – a new steroidal alkaloid from *Buxus papilosa*. *Heterocycles*: 23 [8] (1985): 1951 – 1954
- <sup>73</sup> Babar, Z.U.; Ata, A.; Meshkatalasadat, M.H. New bioactive steroidal alkaloids from *Buxus hyrcana*. *Steroids*: 71 (2006): 1045 – 1051
- <sup>74</sup> Cordell, G.A. *Introduction to Alkaloids – A Biogenetic Approach*. (1981) New York, New York: Wiley – Interscience: 907
- <sup>75</sup> Aynehchi, Y.; Sormaghi, M.H.S.; Amin, G.H.; Khoshkhow, M.; Shabani, A. Survey of Iranian plants for saponins, alkaloids, flavonoids and tannins. III. *International Journal of Crude Drug Research*: 23 [1] (1985): 33 – 41

- <sup>76</sup> Heusler, K.; Schlittler, E. The alkaloids from beechwood, *Buxus sempervirens*. II. The structure of alkaloid A. *Helvetica Chimica Acta*: 32 (1949): 2226 – 2240
- <sup>77</sup> Atta-ur-Rahman; Choudhary, M.I. In *The Alkaloids*; Cordell, G.A. Ed.; San Diego, USA: Academic Press: vol. 50, Ch. 2 (1998): 61 – 108
- <sup>78</sup> Kurakina, I.O.; Tolkachev, O.N.; Pakains, D. Alkaloids of *Buxus hyrcana*. *Khimiya Prirodnikh Soedinenii*: [6] (1974): 814 – 815
- <sup>79</sup> Aliev, A.M.; Orazmuradov, G.M. Alkaloid cycloprotobuxine C from *Buxus hyrcana*. II. *Khimiya Prirodnikh Soedinenii*: [6] (1974): 808 – 809
- <sup>80</sup> Atta-ur-Rahman; Parveen, S.; Khalid, A.; Farooq, A.; Ayatollahi, S.A.M.; Choudhary, M.I. Acetylcholinesterase inhibiting triterpenoidal alkaloids from *Buxus hyrcana*. *Heterocycles*: 49 (1998): 481 – 488
- <sup>81</sup> Atta-ur-Rahman; Choudhary, M.I. Recent studies on bioactive natural products. *Pure and Applied Chemistry*: 71 [6] (1999): 1079 – 1081
- <sup>82</sup> Choudhary, M.I.; Shahnaz, S.; Parveen, S.; Khalid, A.; Ayatollahi, S.A.M.; Atta-ur-Rahman; Parvez, M. New triterpenoid alkaloid cholinesterase inhibitors from *Buxus hyrcana*. *Journal of Natural Products*: 66 (2003): 739 – 742
- <sup>83</sup> Vassova, A.; Voticky, Z.; Cernik, J.; Tomko, J. *Buxus* alkaloids. XVIII. Alkaloids of *Buxus harlandii* Hance. *Chemicke Zvesti*: 34 [5] (1980): 706 – 711
- <sup>84</sup> Sariaslani, F. S.; Rosazza, J.P.N. Biocatalysis in natural products chemistry. *Enzyme Microbial Technology*: 6 (1984): 242 – 253
- <sup>85</sup> Rosazza, J.P. Microbial transformations of natural antitumor agents. *Lloydia*: 41 [4] (1978): 297 – 311
- <sup>86</sup> Ferris, J.P.; MacDonald, L.H.; Patrie, M.A.; Martin, M.A. Aryl hydrocarbon hydroxylase activity in the fungus *Cunninghamella bainieri*: evidence for the presence of cytochrome P-450. *Archives of Biochemistry and Biophysics*: 175 [2] (1976): 443 – 452
- <sup>87</sup> Sih, C.J.; Abushanab, E.; Jones, J.B. Biochemical Procedures in Organic Synthesis. *Annual Reports in Medicinal Chemistry*: 12 (1977): 298 – 308
- <sup>88</sup> Smith, R.V.; Rosazza, J.P. Microbial models of mammalian metabolism. *Journal of Pharmaceutical Sciences*: 64 [11] (1975): 1737 – 1759
- <sup>89</sup> Fuska, J.; Proska, B.; Sturdikova, M.; Fuskova, A. Microbial transformation of 2,3-dihydro-3-methoxywithaferin-A by *Cunninghamella elegans*. *Phytochemistry*: 25 [7] (1986): 1613 – 1615

- 
- <sup>90</sup> Kishimoto, S.; Sugino, H.; Tanaka, K.; Kakinuma, A.; Noguchi, S. Potential anti-inflammatory agents. V. Synthesis of metabolites of 6-chloro-5-cyclohexylindan-1-carboxylic acid (TAI-284) using microbial hydroxylation. *Chemical & Pharmaceutical Bulletin*: 24 [4] (1976): 584 – 590
- <sup>91</sup> Prescott, L.M.; Harley, J.P.; Klein, D.A. *Microbiology, 5<sup>th</sup> edition*. (2002) New York, New York: McGraw-Hill: 820
- <sup>92</sup> Rosazza, J.P. Anticancer Agents Based on Natural Product Models. Chapter 13. Microbial transformations as an approach to analogue development. (1980): 437 – 463
- <sup>93</sup> Patterson, D.H.; Murray, H.C.; Eppstein, S.H.; Reineke, L.M. Weintraub, A.; Meister, P.D.; Leigh, H.M. Microbiological transformations of steroids. I. Introduction of oxygen at carbon-11 of progesterone. *Journal of the American Chemical Society*: 74 (1952): 5933 – 5936
- <sup>94</sup> Dewick, P. M. *Medicinal Natural Products: A Biosynthetic Approach*; 2<sup>nd</sup> edition. (2002) West Sussex, England: John Wiley & Sons: 205
- <sup>95</sup> Ibrahim, A.; Abul-Hajj, Y.J. Microbiological transformation of chromone, chromanone, and ring A hydroxyflavones. *Journal of Natural Products*: 53 [6] (1990): 1471 – 1478
- <sup>96</sup> Venisetty, R.K. Ciddi, V. Application of microbial biotransformation for the new drug discovery using natural drugs as substrates. *Current Pharmaceutical Biotechnology*: 4 [3] (2003): 153 – 167
- <sup>97</sup> May, S.W. Enzymatic epoxidation reactions. *Enzyme and Microbial Technology*: 1 [1] (1979): 15 – 22
- <sup>98</sup> Smith, R.V.; Rosazza, J.P. Microbial systems for study of the biotransformations of drugs. *Biotechnology and Bioengineering*: 17 (1975): 785 – 814
- <sup>99</sup> Kumar, G.N.; Oatis Jr., J.E.; Thornberg, K.R.; Heldrich, F.J.; Hazard III, E.S.; Walle, T. 6 $\alpha$ -hydroxytaxol: isolation and identification of the major metabolite of taxol in human liver microsomes. *Drug Metabolism and Disposition*: 22 [1] (1994): 177 – 179
- <sup>100</sup> Orrenius, S.; Ernster, L. *Molecular mechanisms of oxygen activation*, Hayaishi, O., Ed. (1974) New York, USA: Academic Press: 215 – 244
- <sup>101</sup> Venisetty, R.K.; Ciddi, V. Application of microbial biotransformation for the new drug discovery using natural products as substrates. *Current Pharmaceutical Biotechnology*: 4 [3] (2003): 153 - 167

- 
- <sup>102</sup> Clark, A.M.; Hufford, C.D. Use of microorganisms for the study of drug metabolism: an update. *Medicinal Research Reviews*: 11 [5] (1991): 473 - 501
- <sup>103</sup> Yasui, K.; Kawada, K.; Kagawa, K.; Tokura, K.; Kitadokoro, K.; Ikenishi, Y. Synthesis of manool-related labdane diterpenes as platelet aggregation inhibitors. *Chemical & Pharmaceutical Bulletin*: 41 [10] (1993): 1698 - 1707
- <sup>104</sup> Hieda, T.; Mikami, Y.; Obi, Y.; Kisaki, T. Microbial transformation of sclareol. *Agricultural and Biological Chemistry*: 46 [10] (1982): 2477 - 2484
- <sup>105</sup> Kouzi, S.A.; McChesney, J.D. Hydroxylation and glucoside conjugation in the microbial metabolism of the diterpene sclareol. *Xenobiotica*: 21 [10] (1991): 1311 - 1323
- <sup>106</sup> Kouzi, S.A.; McChesney, J.D. Microbial models of mammalian metabolism: fungal metabolism of the diterpene sclareol by *Cunninghamella* species. *Journal of Natural Products*: 54 [2] (1991): 483 - 490
- <sup>107</sup> Diez, D.; Sanchez, J.M.; Rodilla, J.M.; Rocha, P.M.; Mendes, R.S.; Paulino, C.; Marcos, I.S.; Basabe, P.; Urones, J.G. Microbial Hydroxylation of Sclareol by *Rhizopus stonifer*. *Molecules*: 10 (2005): 1005 - 1009
- <sup>108</sup> Abraham, W. Microbial Hydroxylation of Sclareol. *Phytochemistry*: 36 [6] (1994): 1421 - 1424
- <sup>109</sup> Jasinski, M.; Stukkens, Y.; Degand, H.; Purnelle, B.; Marchand-Brynaert, J.; Boutry, M. *The Plant Cell*: 13 (2001): 1095 - 1107
- <sup>110</sup> Aranda, G.; Kortbi, M.S.E.; Lallemand, J. Microbial transformation of diterpenes: hydroxylation of sclareol, manool, and derivatives by *Mucor plumbeus*. *Tetrahedron*: 47 [39] (1991): 8339 - 8350
- <sup>111</sup> Aranda, G.; Lallemand, J. Microbial hydroxylation of sclareol by *Mucor plumbeus*. *Tetrahedron Letters*: 32 [15] (1991): 1783 - 1786
- <sup>112</sup> Ruzicka, L.; Janot, M.M. Higher terpene compounds. L. Sclareol. *Helvetica Chimica Acta*: 14 (1931): 645 - 650
- <sup>113</sup> Hanson, J.R.; Hitchcock, P.B.; Nasir, H.; Truneh, A. The Biotransformation of the Diterpenoid, Sclareol, by *Cephalosporium aphidicola*. *Phytochemistry*: 36 [4] (1994): 903 - 906
- <sup>114</sup> Decorzant, R.; Vial, C.; Näef, F.; Whitesides, G.M. A short synthesis of ambrox from sclareol. *Tetrahedron*: 43 [8] (1987) : 1871 - 1879



- 
- <sup>115</sup> Leung, A.Y. *Encyclopedia of common natural ingredients used in food, drugs and cosmetics*. (1980) New York, New York: John Wiley & Sons: 129 – 130
- <sup>116</sup> Farooq, A.; Tahara, S. Biotransformation of Two Cytotoxic Terpenes,  $\alpha$ -Santonin and Sclareol by *Botrytis cinerea*. *Z. Naturforsch*: 55c (2000): 713 – 717
- <sup>117</sup> Cutler, H.G.; Reid, W.W.; Deletang, J. Plant growth inhibiting properties of diterpenes from tobacco. *Plant and Cell Physiology*: 18 (1977): 711 – 714
- <sup>118</sup> Ulubelen, A.; Miski, M.; Johansson, C.; Lee, E.; Mabry, T.J.; Matlan, S.A. Terpenoids from *Salvia palaestina*. *Phytochemistry*: 24 (1985): 1386 – 1387
- <sup>119</sup> Kennedy, B.S.; Nielsen, M.T.; Severson, R.F.; Sisson, V.A.; Stephenson, M.K. ; Jackson, D.M. Leaf surface chemicals from *Nicotiana* affecting germination of *Peronospora tabacina* (Adam) sporangia. *Journal of Chemical Ecology*: 18 [9] (1992): 1467 – 1479
- <sup>120</sup> Kouzi, S.A.; McChesney, J.D. Microbial metabolism of the diterpene sclareol: oxidation of the A ring by *Septomyxa affinis*. *Helvetica Chimica Acta*: 73 [8] (1990): 2157 – 2164
- <sup>121</sup> Hieda, T.; Mikami, Y.; Obi, Y. Microbial transformation of manool and (12Z)-labda-8(17), 12,14-triene by *Rhodococcus erthropolis* JTS-131. *Agricultural and Biological Chemistry*: 47 [4] (1983): 787 – 794
- <sup>122</sup> Schmidt, T.J.; Passreitter, C.M.; Wendisch, D.; Willuhn, G. Diterpenes from *Arnica angustifolia*. *Phytochemistry*: 40 [4] (1995): 1213 – 1218
- <sup>123</sup> Audier, H.; Bory, S.; Fetizon, M. Formation of a derivative of manoyl oxide by oxidation of sclareol. *Bulletin de la Societe Chimique de France*: [6] (1964): 1381 – 1388
- <sup>124</sup> Atta-ur-Rahman, Farooq, A.; Choudhary, M.I. Microbial transformation of sclareolide. *Journal of Natural Products*: 60 (1997): 1038 – 1040
- <sup>125</sup> Dolmazon, R.; Albrand, M.; Bessiere, J.; Mahmoud, Y.; Wernerowska, D.; Kolodziejczyk, K. Diterpeneoids from *Kyllinga erecta*. *Phytochemistry*: 38 [4] (1995): 917 – 919
- <sup>126</sup> Choudhary, M.I.; Musharraf, S.G.; Sami, A.; Atta-ur-Rahman. Microbial transformations of sesquiterpenes, (-)-ambrox® and (+)-sclareolide. *Helvetica Chimica Acta*: 87 (2004): 2685 – 2694
- <sup>127</sup> Atta-ur-Rahman; Farooq, A.; Choudhary, M.I. Microbial transformation of sclareolide. *Journal of Natural Products*: 60 [10] (1997): 1038 – 1040

- 
- <sup>128</sup> Ata, A.; Conci, L.J.; Betteridge, J.; Orhan, I.; Sener, B. Novel microbial transformations of sclareolide. *Chemical & Pharmaceutical Bulletin*: 55 [1] (2007): 118 – 123
- <sup>129</sup> Hanson, J.R.; Truneh, A. The biotransformation of ambrox® and sclareolide by cephalosporium aphidicola. *Phytochemistry*: 42 [4] (1996): 1021 – 1023
- <sup>130</sup> Farooq, A.; Tahara, S. Oxidative metabolism of ambrox and sclareolide by Botrytis cinerea. *Z. Naturforsch*: 55c (2000): 341 – 346
- <sup>131</sup> Hufford, C.D.; Collins, C.C.; Clark, A.M. Microbial transformations and <sup>13</sup>C-NMR analysis of colchicine. *Journal of Pharmaceutical Sciences*: 68 [10] (1979): 1239 – 1242
- <sup>132</sup> Pelletier P.S., Caventon *J. Ann. Chim. Phys*: 14 (1820): 69
- <sup>133</sup> Dewick, P. M. *Medicinal Natural Products: A Biosynthetic Approach*; 2<sup>nd</sup> edition. (2002) West Sussex, England: John Wiley & Sons: 343
- <sup>134</sup> Smith, R.V.; Rosazza, J.P. Microbial models of mammalian metabolism. Aromatic hydroxylation. *Archives of Biochemistry and Biophysics*: 161 [2] (1974): 551 – 558
- <sup>135</sup> Cremer, J.; Vatou, V.; Braveny, I. 2,4-(Hydroxylphenyl)-ethanol, an antioxidative agent produced by *Candida* spp., impairs neutrophilic yeast killing in vitro. *FEMS Microbiology Letters*: 170 (1999): 319 – 325
- <sup>136</sup> Chen, H.; Fujita, M.; Feng, Q.; Clardy, J.; Fink, G.R. Tyrosol is a quorum-sensing molecule in *Candida albicans*. *Proceedings of the National Academy of Sciences of the United States of America*: 101 [14] (2004): 5048 – 5052
- <sup>137</sup> Alem, M.A.S.; Oteef, M.D.Y.; Flowers, T.H.; Douglas, L.J. Production of tyrosol by *Candida albicans* biofilms and its role in quorum sensing and biofilm development. *Eukaryotic Cell*: 5 [10] (2006): 1770 – 1779
- <sup>138</sup> Medina, E.; de Castro, A.; Romero, C.; Brenes, M. Comparison of the concentrations of phenolic compounds in olive oils and other plant oils: correlation with antimicrobial activity. *Journal of Agricultural and Food Chemistry*: 54 (2006): 4954 - 4961
- <sup>139</sup> Pereira, J.A.; Pereira, A.P.G.; Ferreira, I.C.F.R.; Valentao, P.; Andrade, P.B.; Seabra, R.; Estevinho, L.; Bento, A. Table olives from Portugal: phenolic compounds, antioxidant potential, and antimicrobial activity. *Journal of Agricultural and Food Chemistry*: 54 (2006): 8425 – 8431

## Appendix A: IR Spectra

Figure A-1: UV spectra of dihydrocholesterol (**70**)

Figure A-2: UV spectra of 7 $\alpha$ -hydroxyfrullanolide (**54**)

Figure A-3: UV spectra of 7 $\alpha$ -hydroxyeudesmanolide (**56**)

Figure A-4: UV spectra of 4,5-epoxy-7 $\alpha$ -hydroxyfrullanolide (**71**)

Figure A-5: UV spectra of Buxamine B (**99**)

Figure A-6: UV spectra of N<sub>b</sub>-dimethylcycloxobuxoviricine (**85**)

Figure A-7 UV spectra of 3-ketosclareolide (**131**)

Figure A-8 UV spectra of 3 $\beta$ -hydroxysclareolide (**132**)

Figure A-9 UV spectra of tyrosol (**151**)

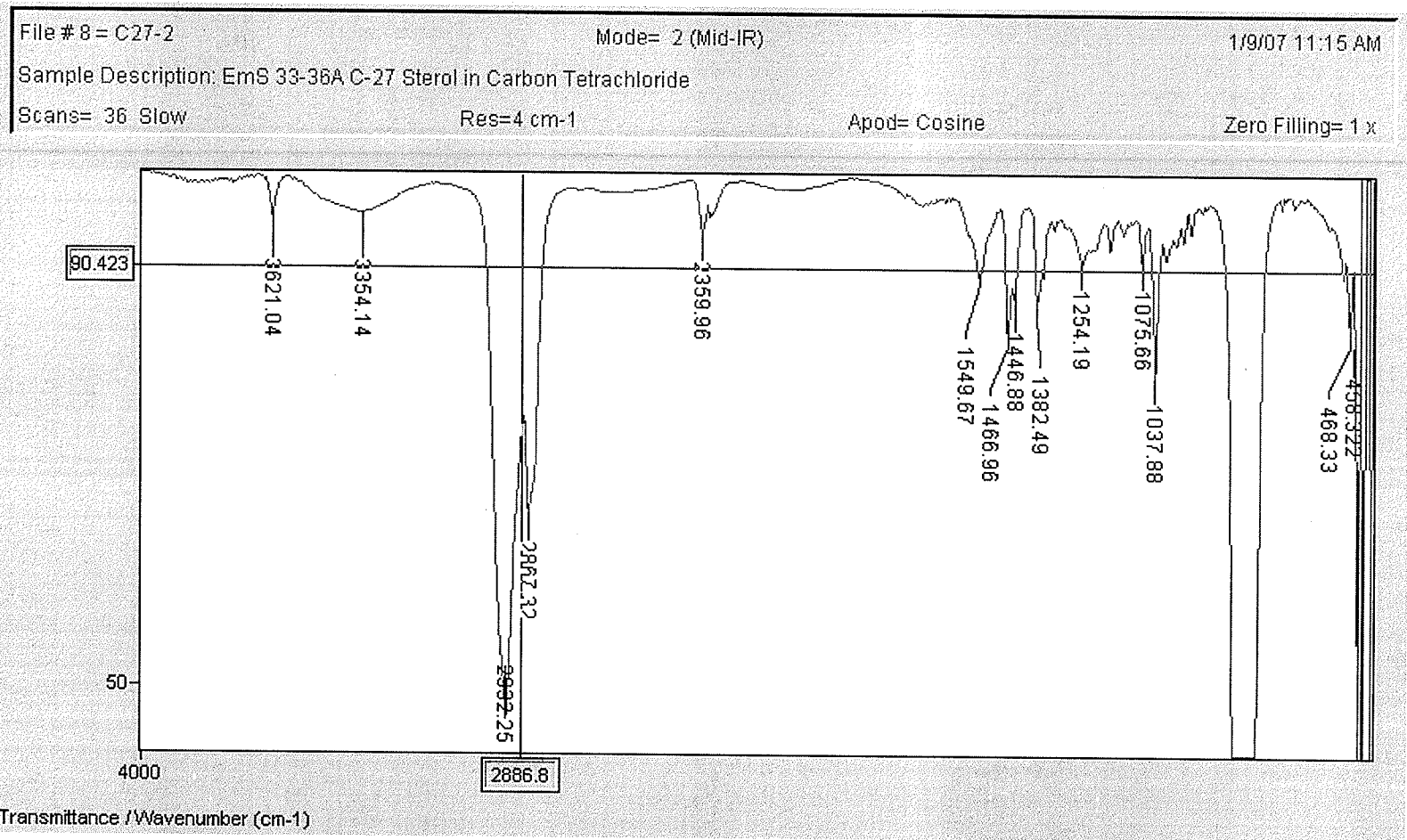


Figure A-1: UV spectra of dihydrocholesterol (70)

File # 9 : 7AOHF

Mode= 2 (Mid-IR)

12/5/06 2:13 PM

Sample Description: 7(a)-hydroxyfrullanolide

Scans= 25 Slow

Res=4 cm-1

Apod= Cosine

Zero Filling= 1 x

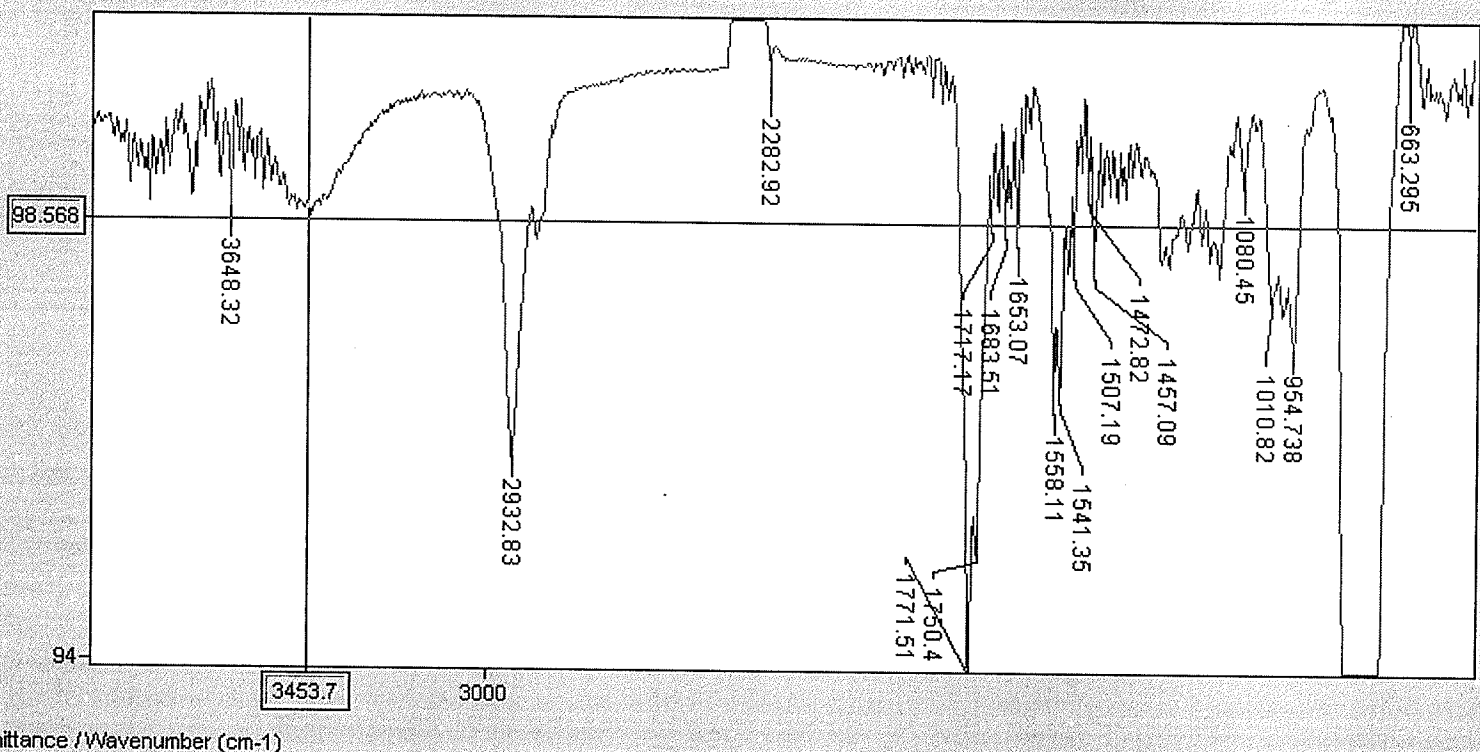


Figure A-2: UV spectra of 7 $\alpha$ -hydroxyfrullanolide (54)

File # 5 : EUDES

Mode= 2 (Mid-IR)

12/5/06 4:57 PM

Sample Description: eudesmanolide

Scans= 25 Slow

Res=4 cm-1

Apod= Cosine

Zero Filling= 1 x

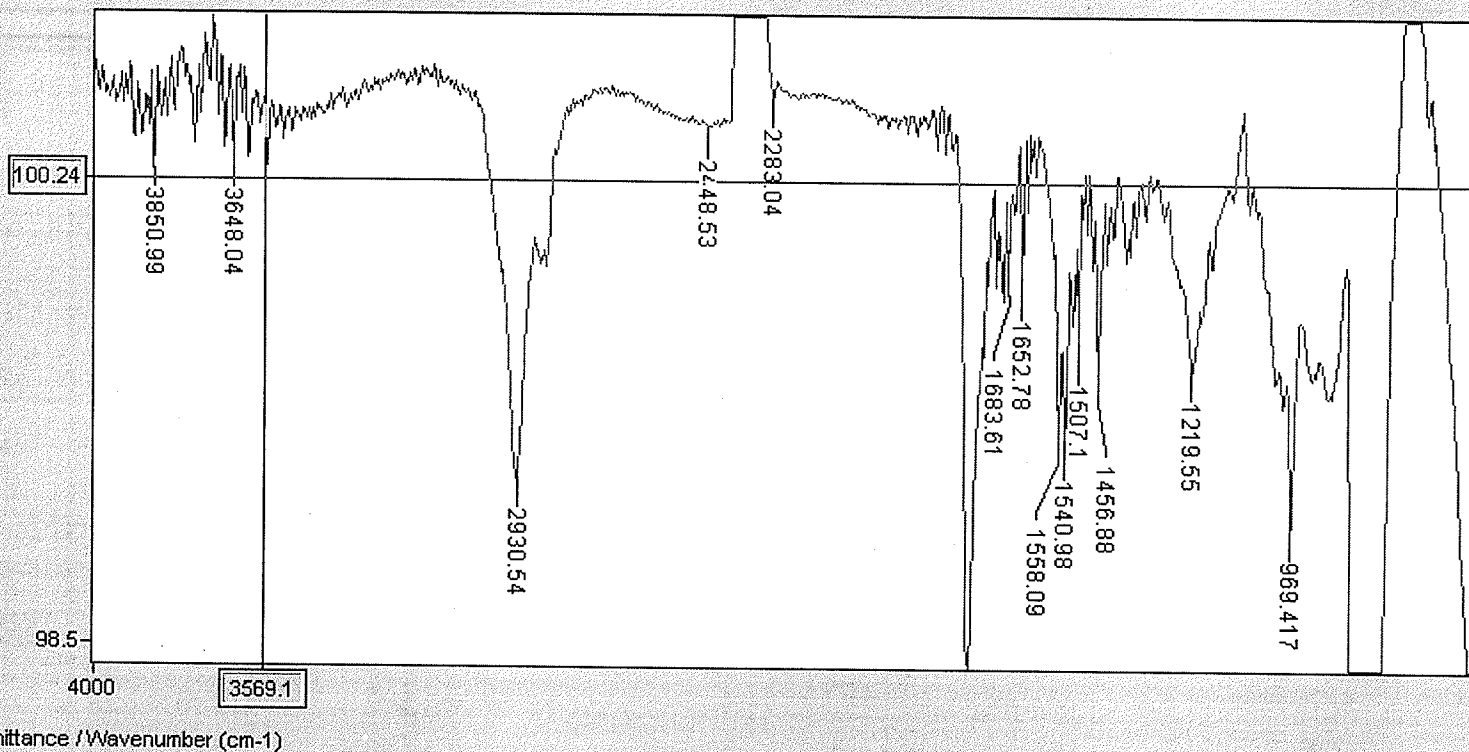


Figure A-3: UV spectra of 7 $\alpha$ -hydroxyeudesmanolide (56)

File #12 : EPOXIDE Mode= 2 (Mid-IR) 1/9/07 12:14 PM  
Sample Description: EmS 33-36A C-27 Sterol in Carbon Tetrachloride  
Scans= 36 Slow Res=4 cm-1 Apod= Cosine Zero Filling= 1 x

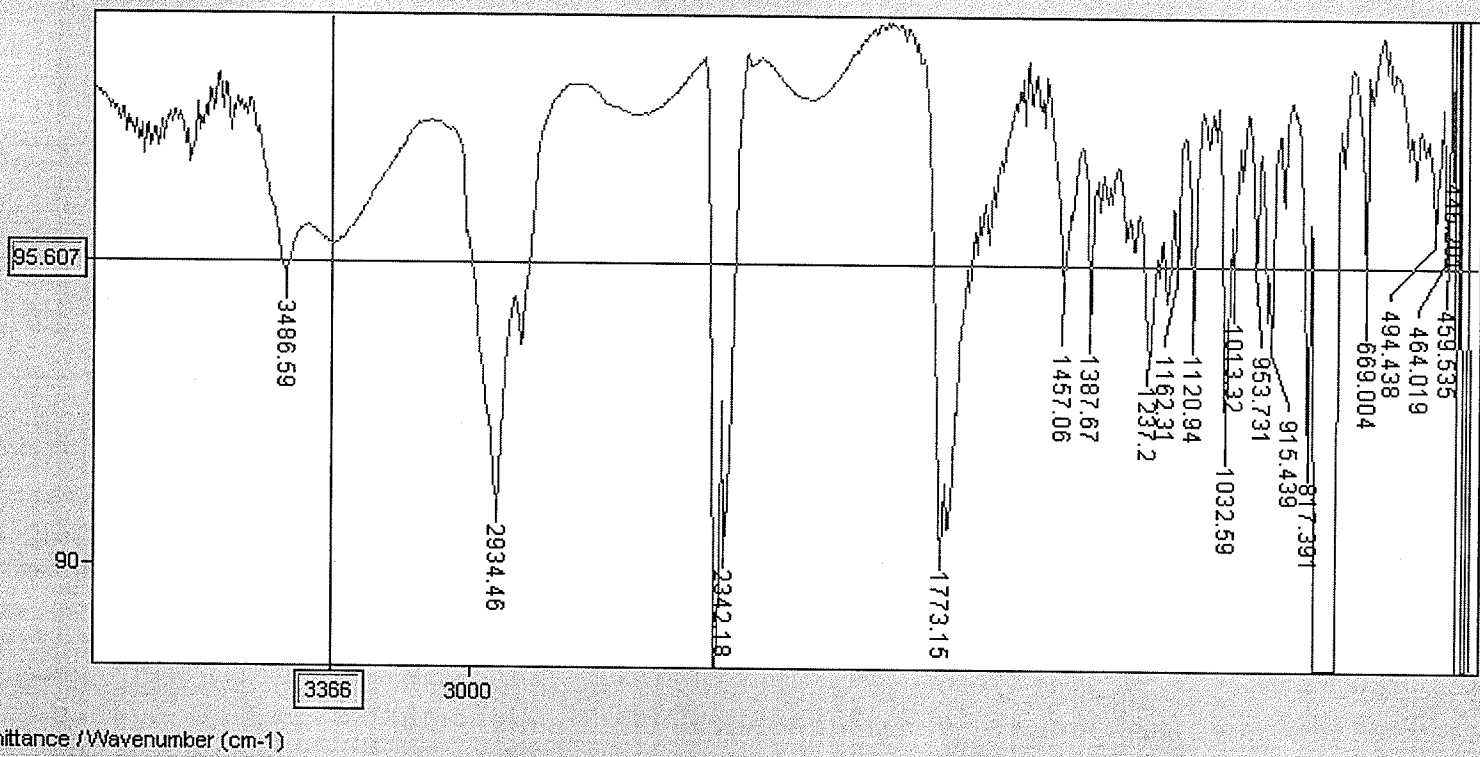


Figure A-4: UV spectra of 4,5-epoxy-7 $\alpha$ -hydroxyfrullanolide (71)

File #13 : 20-1

Mode= 2 (Mid-IR)

1/9/07 3:19 PM

Sample Description:

Scans= 36 Slow

Res=4 cm-1

Apod= Cosine

Zero Filling= 1 x

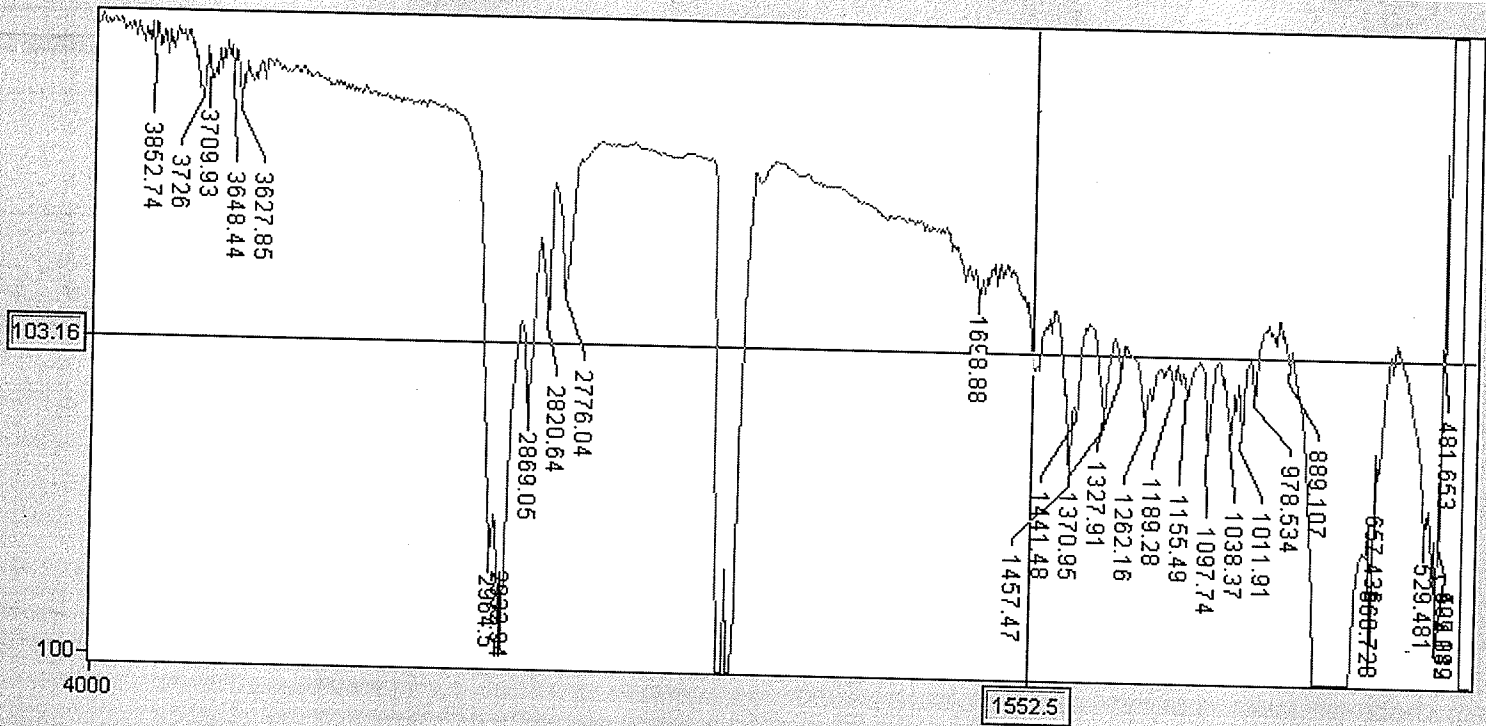


Figure A-5: UV spectra of Buxamine B (99)



File #14 : 31-1

Mode= 2 (Mid-IR)

1/9/07 3:29 PM

Sample Description: 31-1 pTLC in carbon tetrachloride

Scans= 36 Slow

Res=4 cm-1

Apod= Cosine

Zero Filling= 1 x

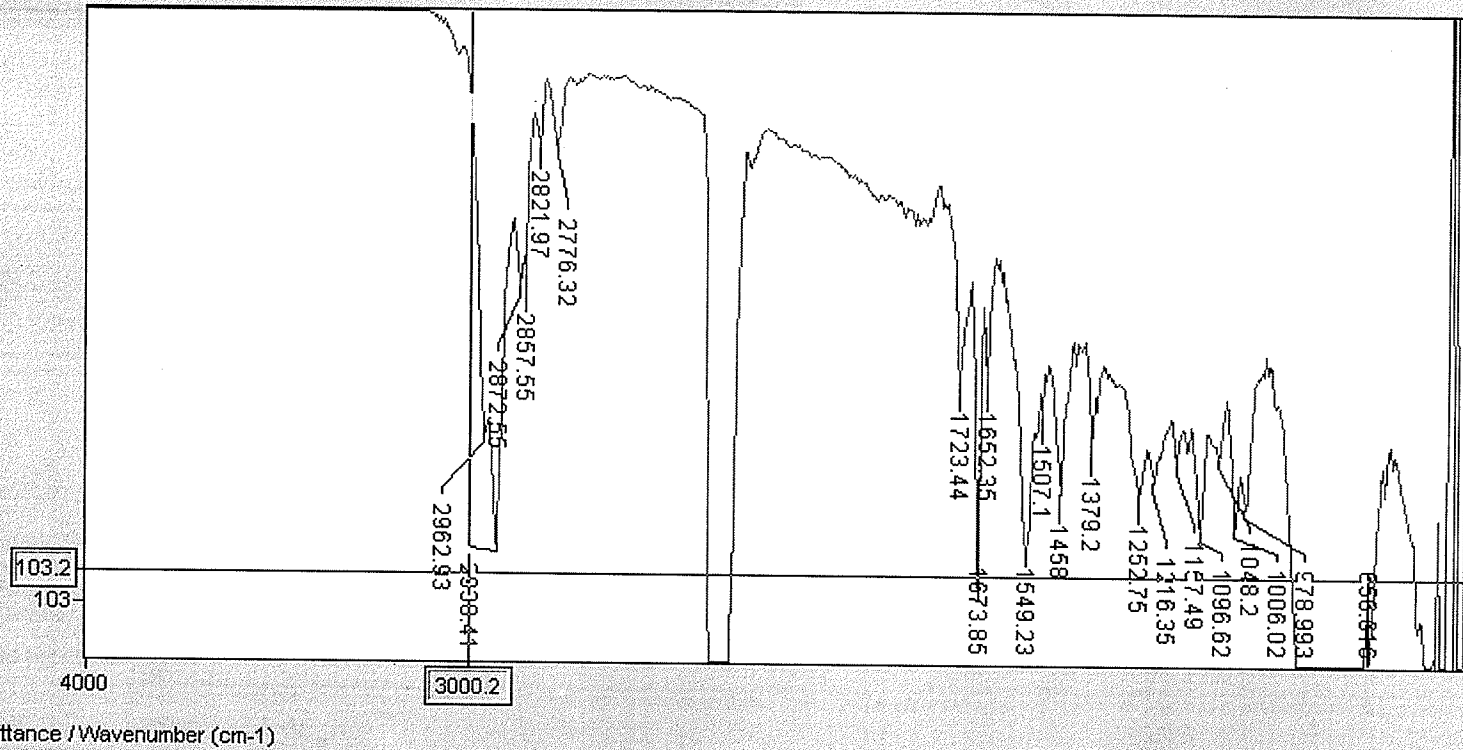


Figure A-6: UV spectra of N<sub>6</sub>-dimethylcyclohexoviricine (85)

File # 3 : 3KETO

Mode= 2 (Mid-IR)

12/5/06 3:57 PM

Sample Description: carbon tetrachloride blank

Scans= 25 Slow

Res=4 cm-1

Apod= Cosine

Zero Filling= 1 x

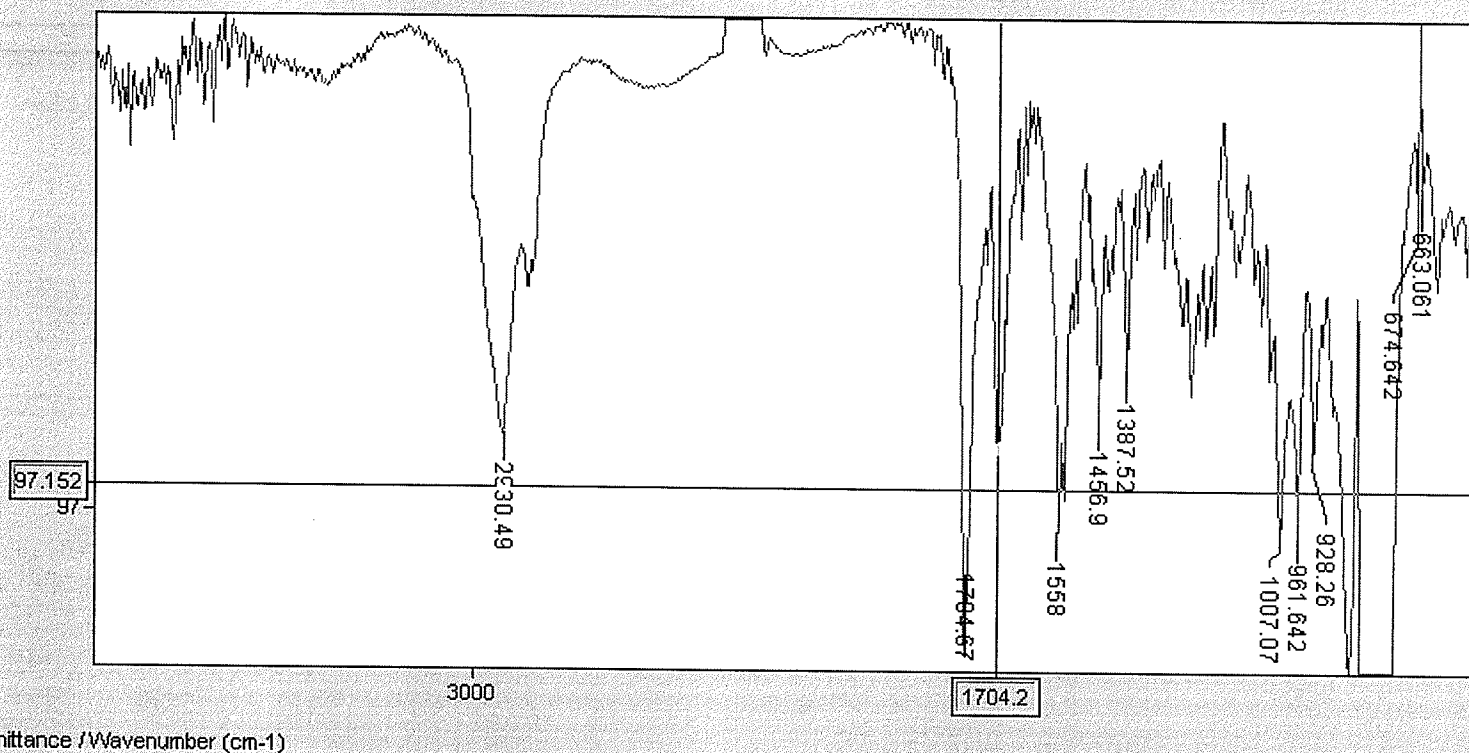


Figure A-7 UV spectra of 3-ketosclareolide (131)

File # 2 = 3BOHSCLD

Mode= 2 (Mid-IR)

1/9/07 11:51 AM

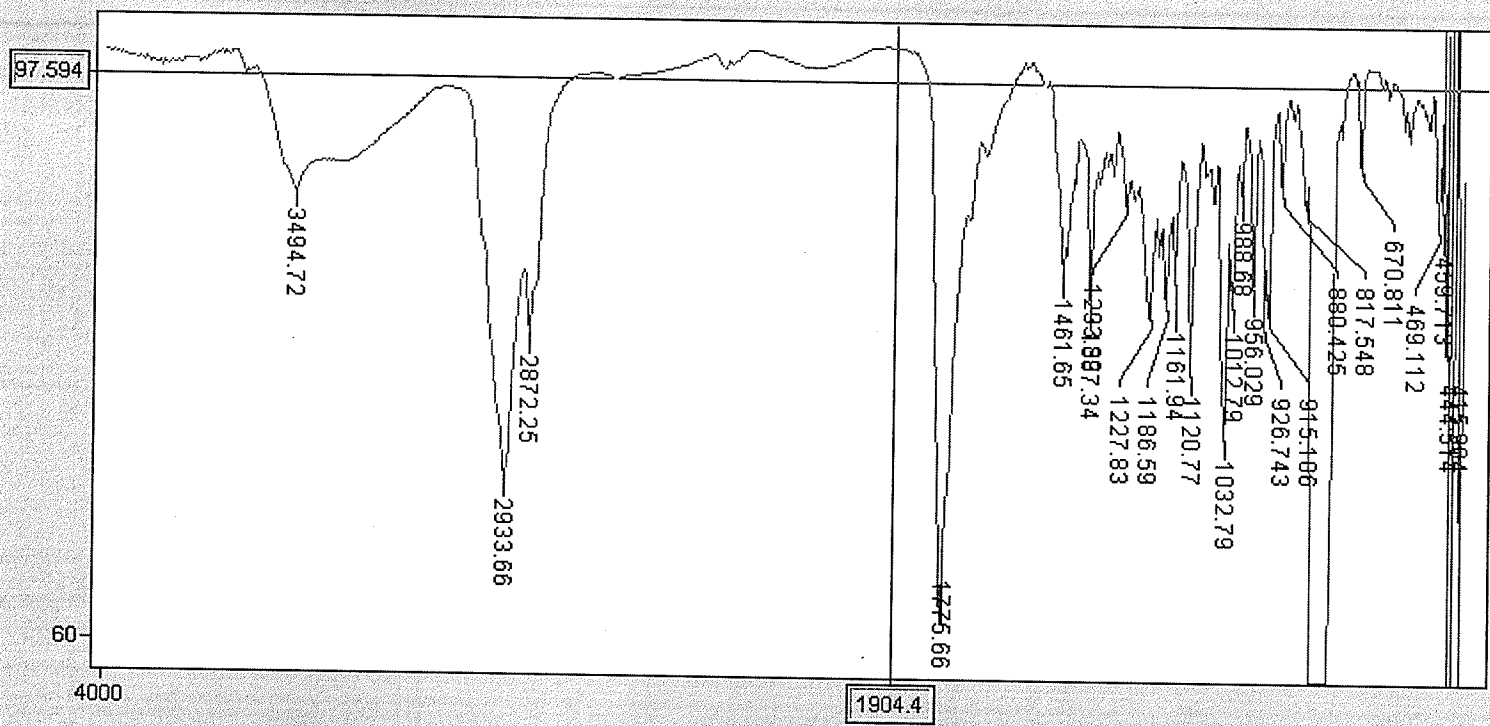
Sample Description: EmS 33-36A C-27 Sterol in Carbon Tetrachloride

Scans= 36 Slow

Res=4 cm-1

Apod= Cosine

Zero Filling= 1 x



Transmittance / Wavenumber (cm-1)

Figure A-8 UV spectra of 3β-hydroxysclareolide (132)

File # 4 = CA18

Mode= 2 (Mid-IR)

12/5/06 12:11 PM

Sample Description: CA 18 collect 1

Scans= 25 Slow

Res=4 cm-1

Apod= Cosine

Zero Filling= 1 x

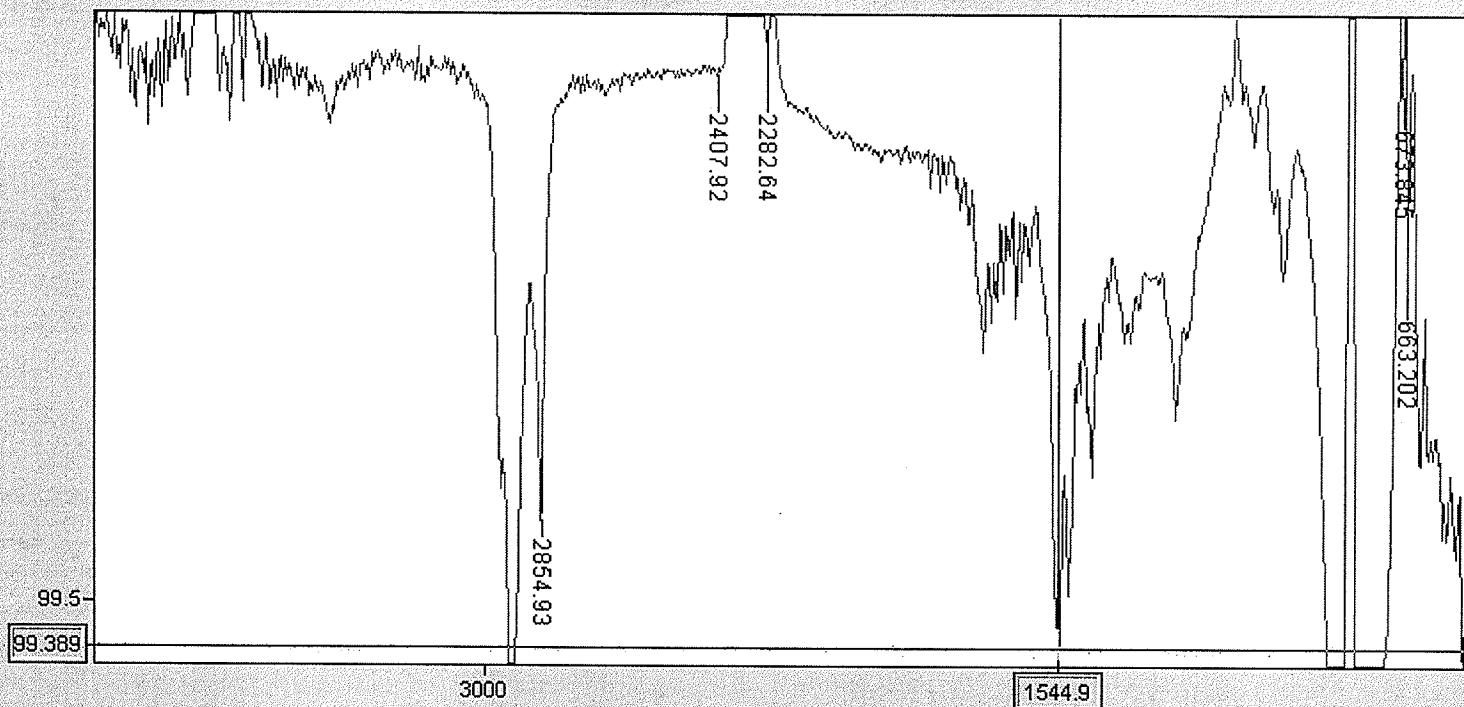


Figure A-9 UV spectra of tyrosol (151)

## Appendix B: NMR spectra of *Sphaeranthus indicus* compounds

Figure B-1:  $^1\text{H}$  NMR of dihydrocholesterol (**70**)

Figure B-2: APT ( $^{13}\text{C}$ ) NMR of dihydrocholesterol (**70**)

Figure B-3: COSY spectrum of dihydrocholesterol (**70**)

Figure B-4: HSQC spectrum of dihydrocholesterol (**70**)

Figure B-5: HMBC spectrum of dihydrocholesterol (**70**)

Figure B-6: NOESY spectrum of dihydrocholesterol (**70**)

Figure B-7:  $^1\text{H}$  NMR of  $7\alpha$ -hydroxyfrullanolide (**54**)

Figure B-8:  $^{13}\text{C}$  NMR of  $7\alpha$ -hydroxyfrullanolide (**54**)

Figure B-9: COSY spectrum of  $7\alpha$ -hydroxyfrullanolide (**54**)

Figure B-10: HSQC spectrum of  $7\alpha$ -hydroxyfrullanolide (**54**)

Figure B-11: HMBC spectrum of  $7\alpha$ -hydroxyfrullanolide (**54**)

Figure B-12:  $^1\text{H}$  NMR of  $7\alpha$ -hydroxyeudesmanolide (**56**)

Figure B-13:  $^{13}\text{C}$  NMR of  $7\alpha$ -hydroxyeudesmanolide (**56**)

Figure B-14: COSY spectrum of  $7\alpha$ -hydroxyeudesmanolide (**56**)

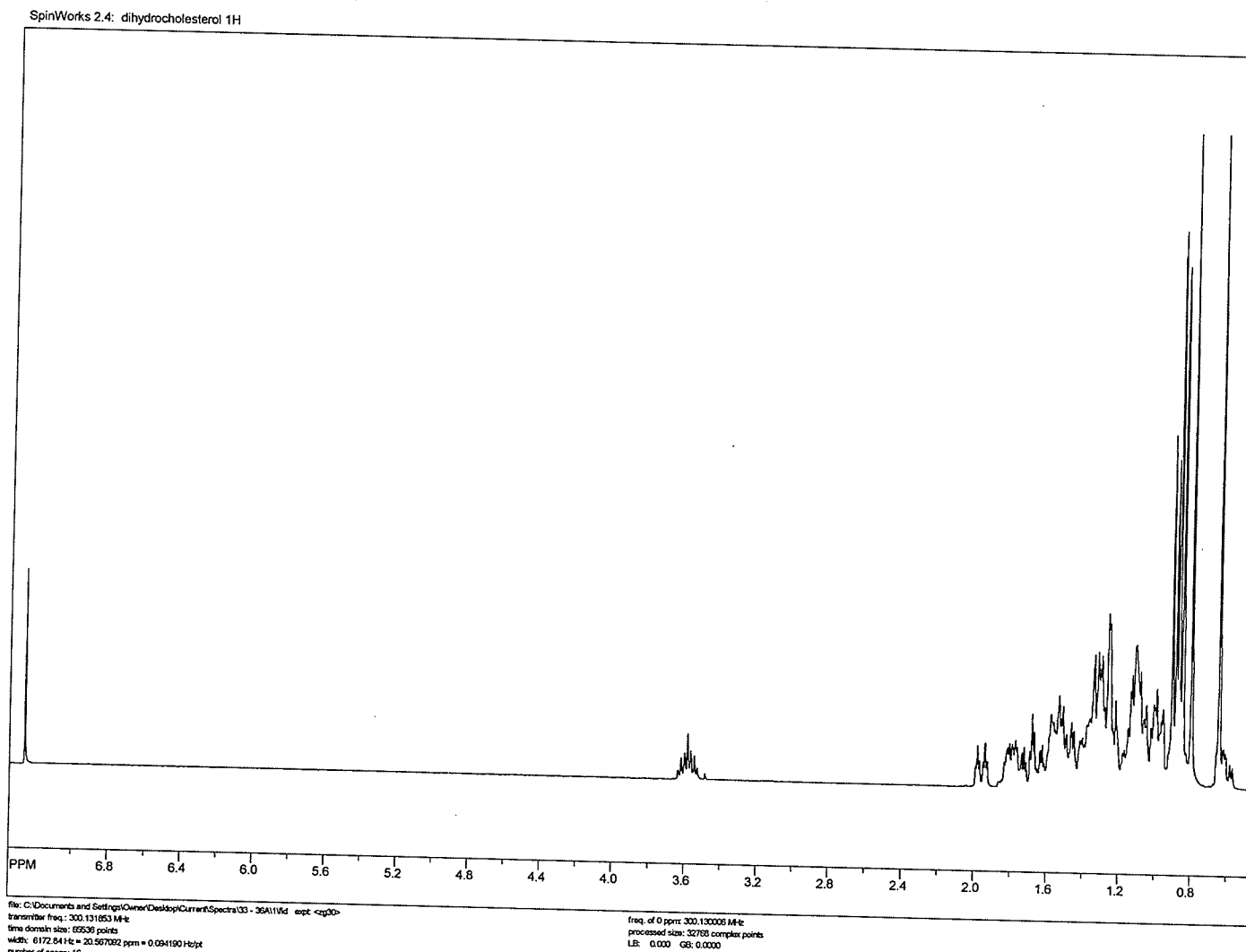
Figure B-15: HSQC spectrum of  $7\alpha$ -hydroxyeudesmanolide (**56**)

Figure B-16: HMBC spectrum of  $7\alpha$ -hydroxyeudesmanolide (**56**)

Figure B-17: NOESY spectrum of  $7\alpha$ -hydroxyeudesmanolide (**56**)

Figure B-18:  $^1\text{H}$  NMR of 4,5-epoxy- $7\alpha$ -hydroxyfrullanolide (**71**)

Figure B-19:  $^{13}\text{C}$  NMR of 4,5-epoxy- $7\alpha$ -hydroxyfrullanolide (**71**)



**Figure B-1:  $^1\text{H}$  NMR of dihydrocholesterol (70)**

SpinWorks 2.4: dihydrocholesterol 13C APT

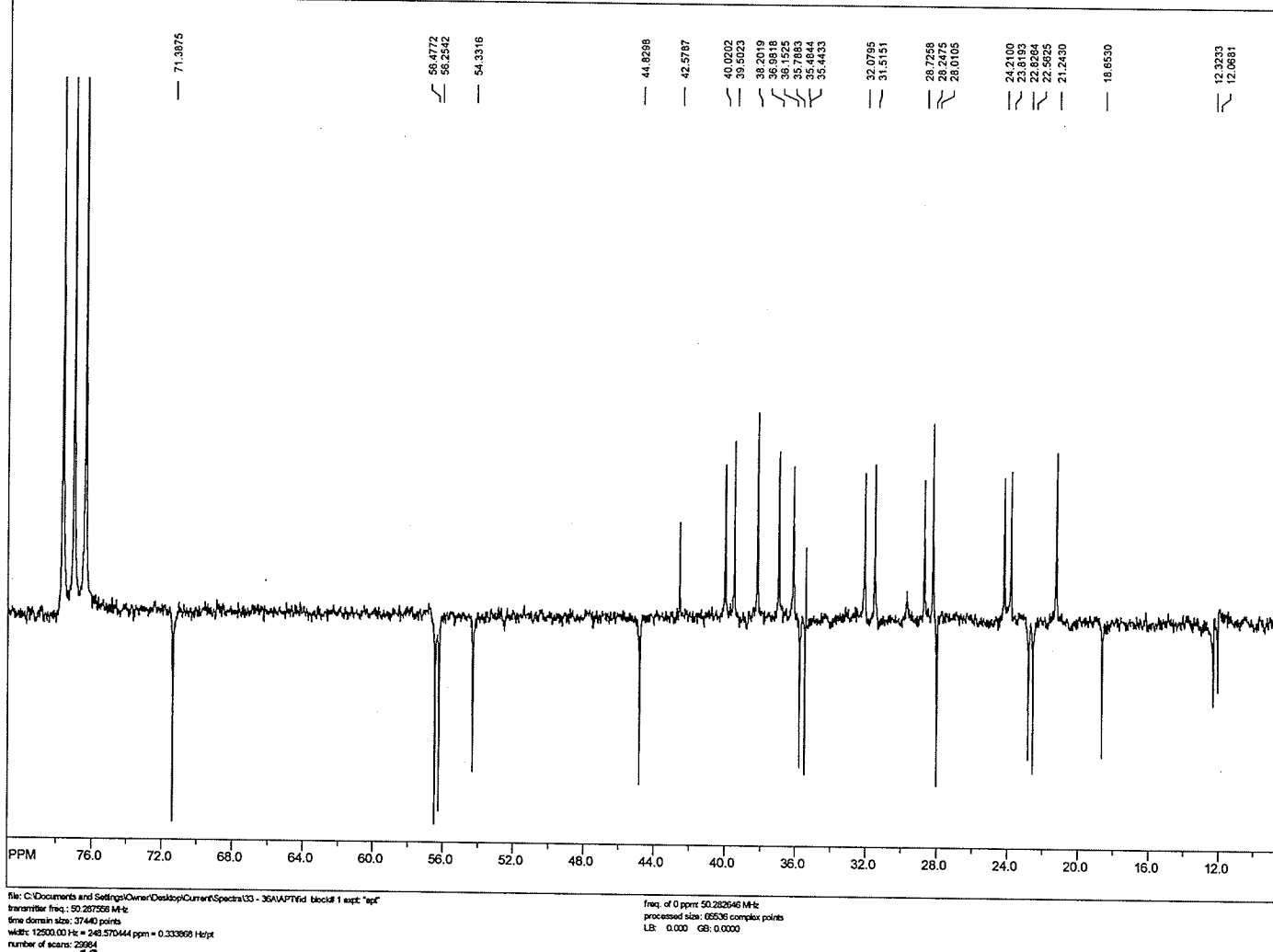
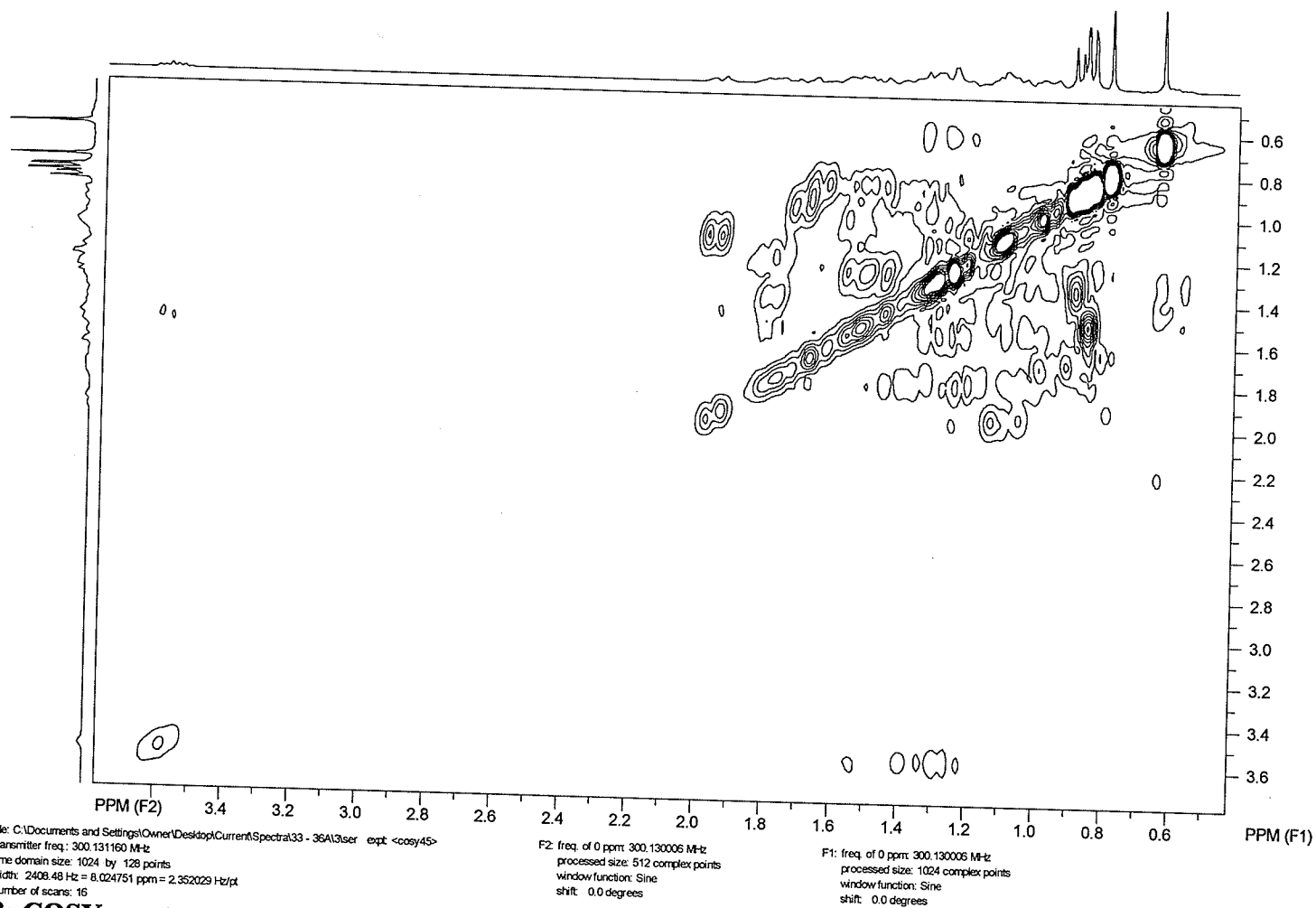
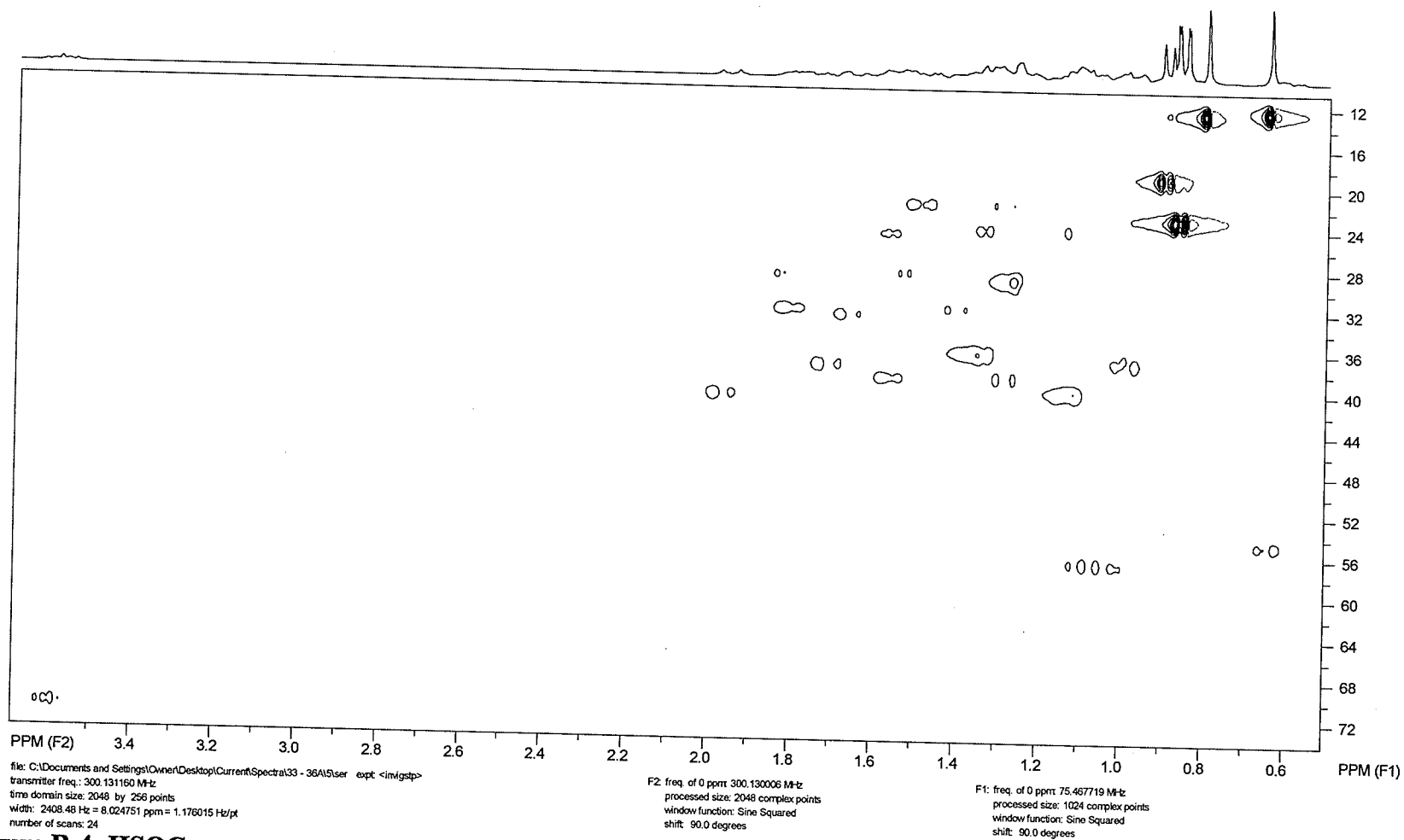


Figure B-2: APT ( $^{13}\text{C}$ ) NMR of dihydrocholesterol (70)



**Figure B-3: COSY spectrum of dihydrocholesterol (70)**





**Figure B-4: HSQC spectrum of dihydrocholesterol (70)**

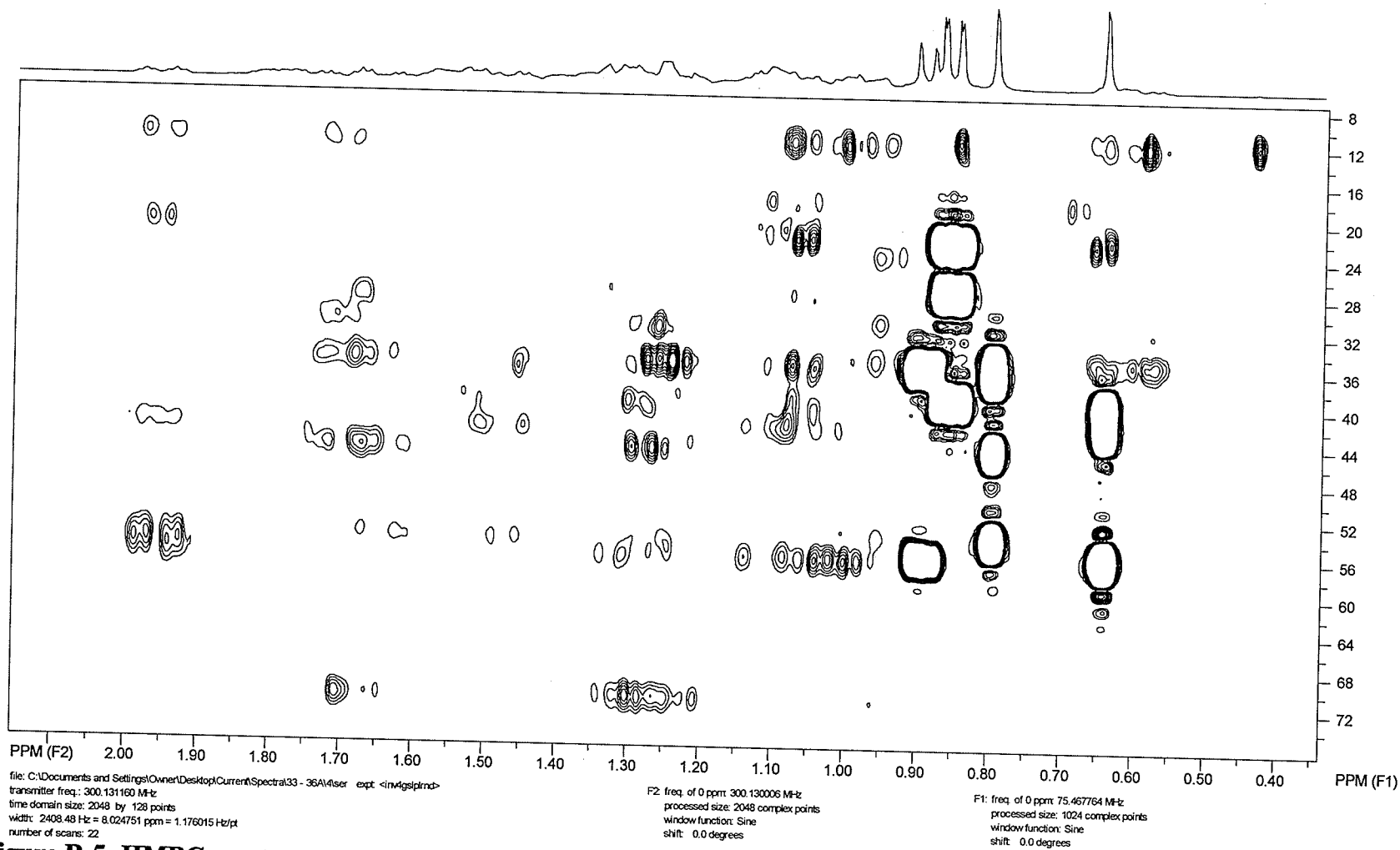


**Figure B-5: HMBC spectrum of dihydrocholesterol (70)**

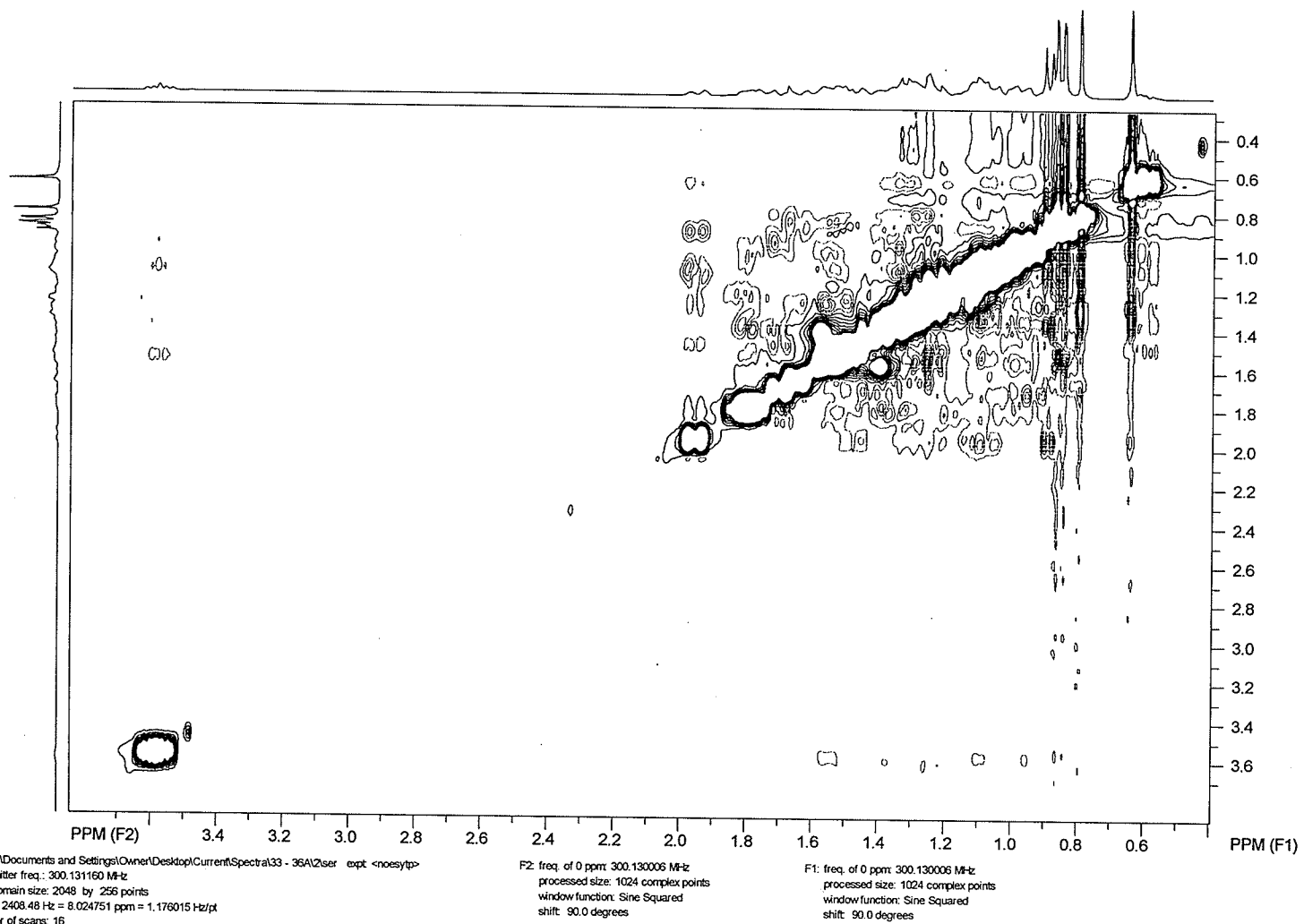


**Figure B-6: NOESY spectrum of dihydrocholesterol (70)**

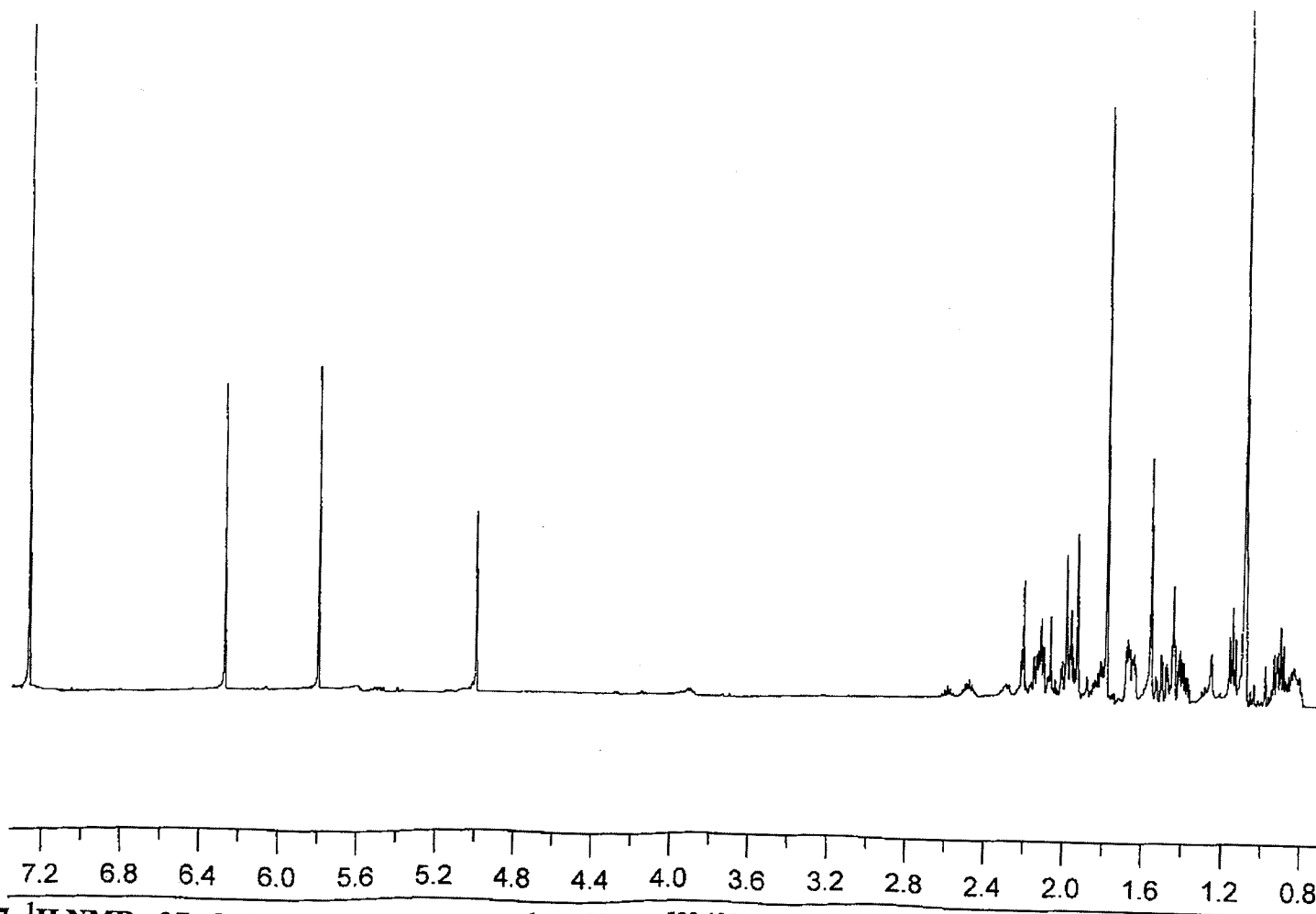


Figure B-7: <sup>1</sup>H NMR of 7α-hydroxyfrullanolide (54)

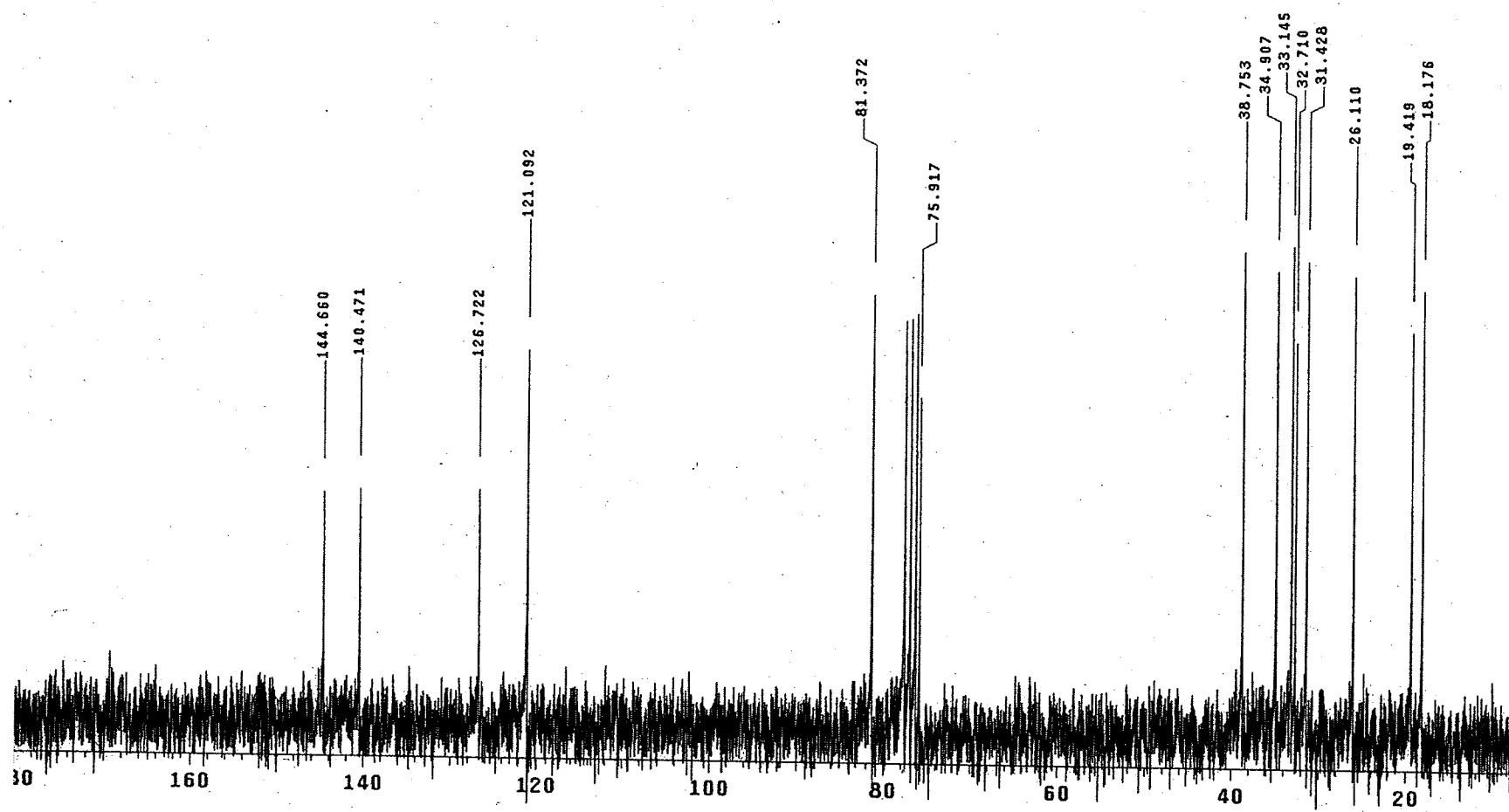
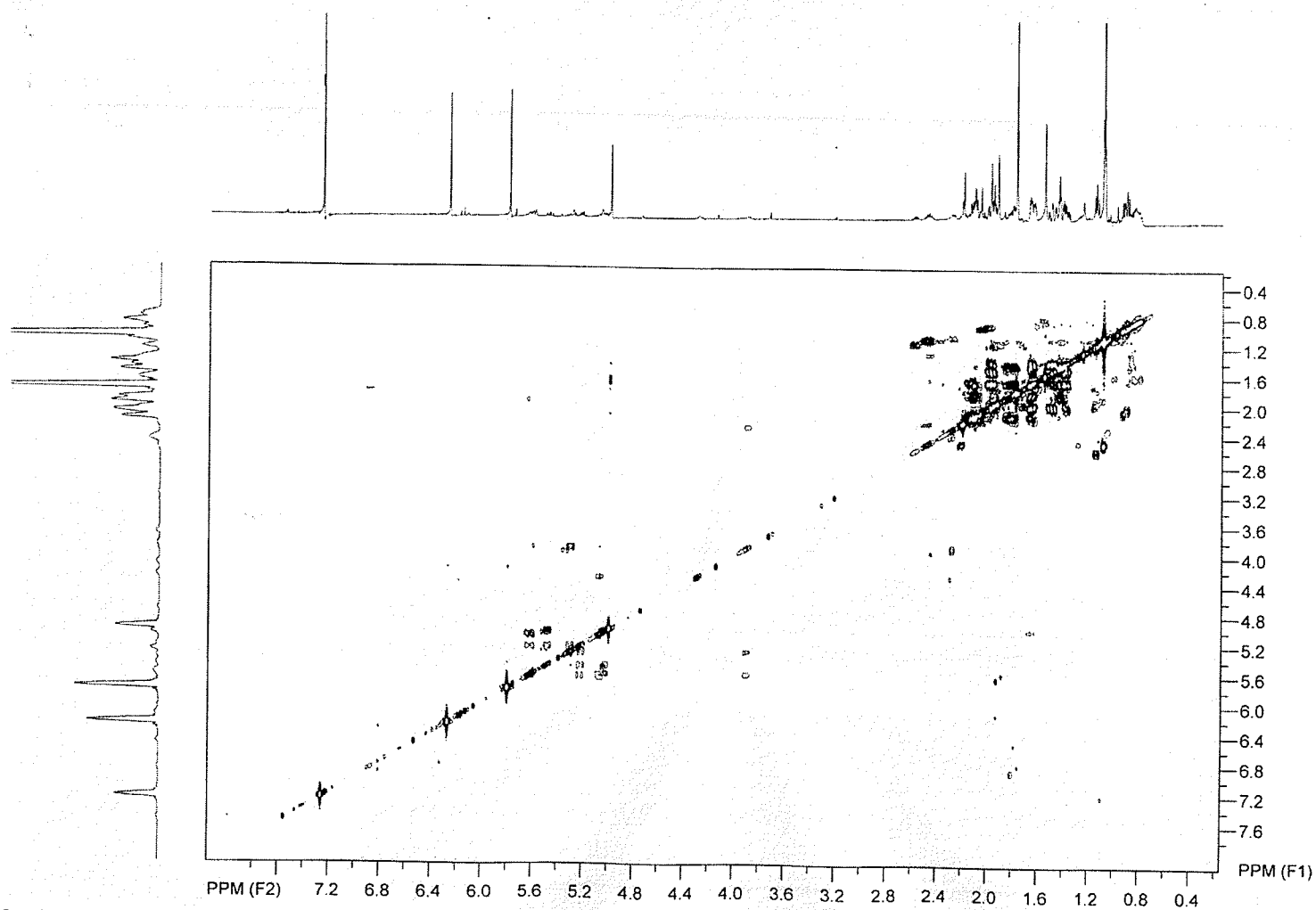
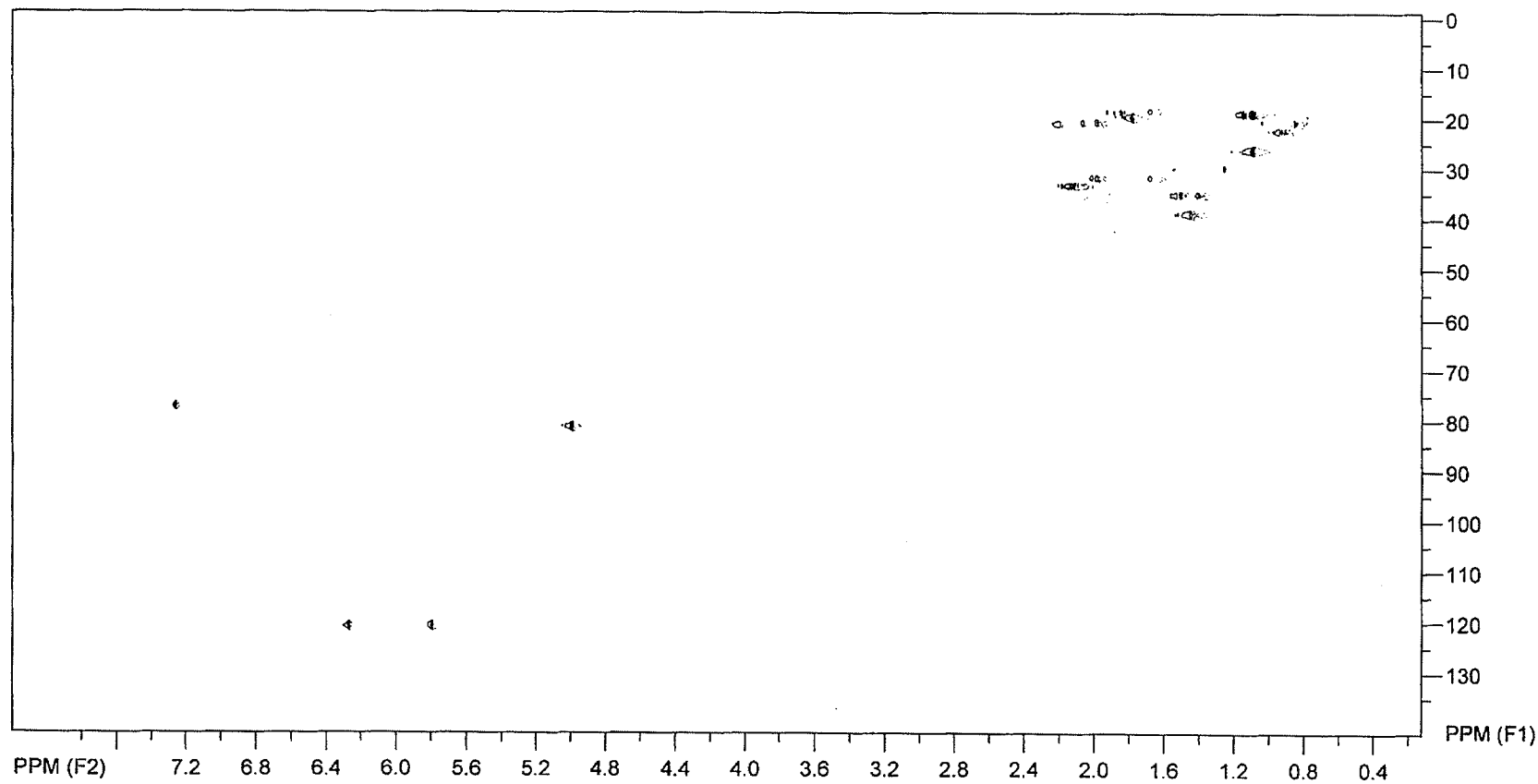
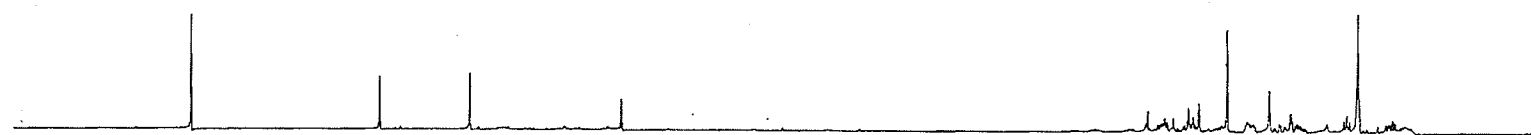


Figure B-8:  $^{13}\text{C}$  NMR of 7 $\alpha$ -hydroxyfrullanolide (54)



**Figure B-9: COSY spectrum of 7 $\alpha$ -hydroxyfrullanolide (54)**



**Figure B-10: HSQC spectrum of 7 $\alpha$ -hydroxyfrullanolide (54)**

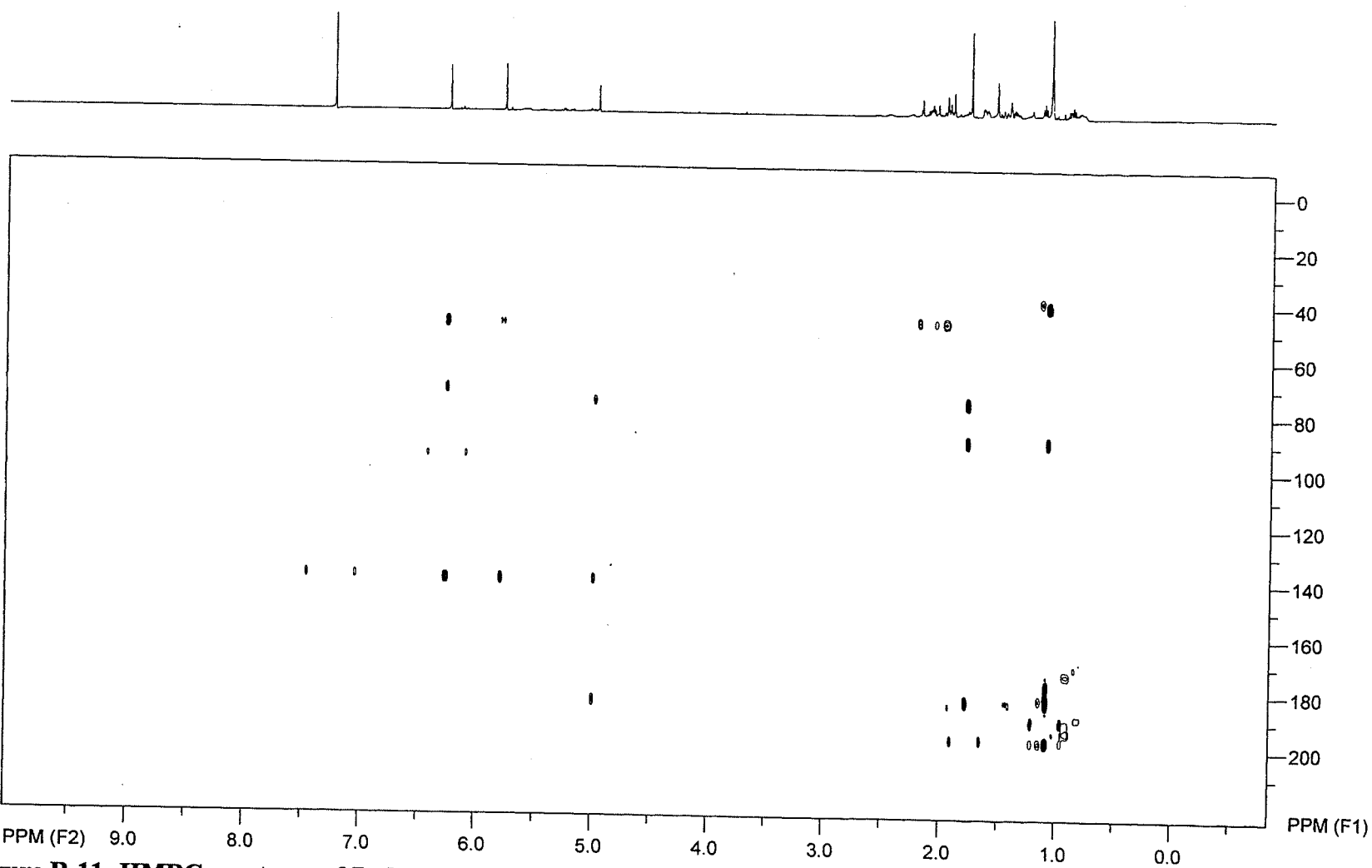


**Figure B-11: HMBC spectrum of 7 $\alpha$ -hydroxyfrullanolide (54)**



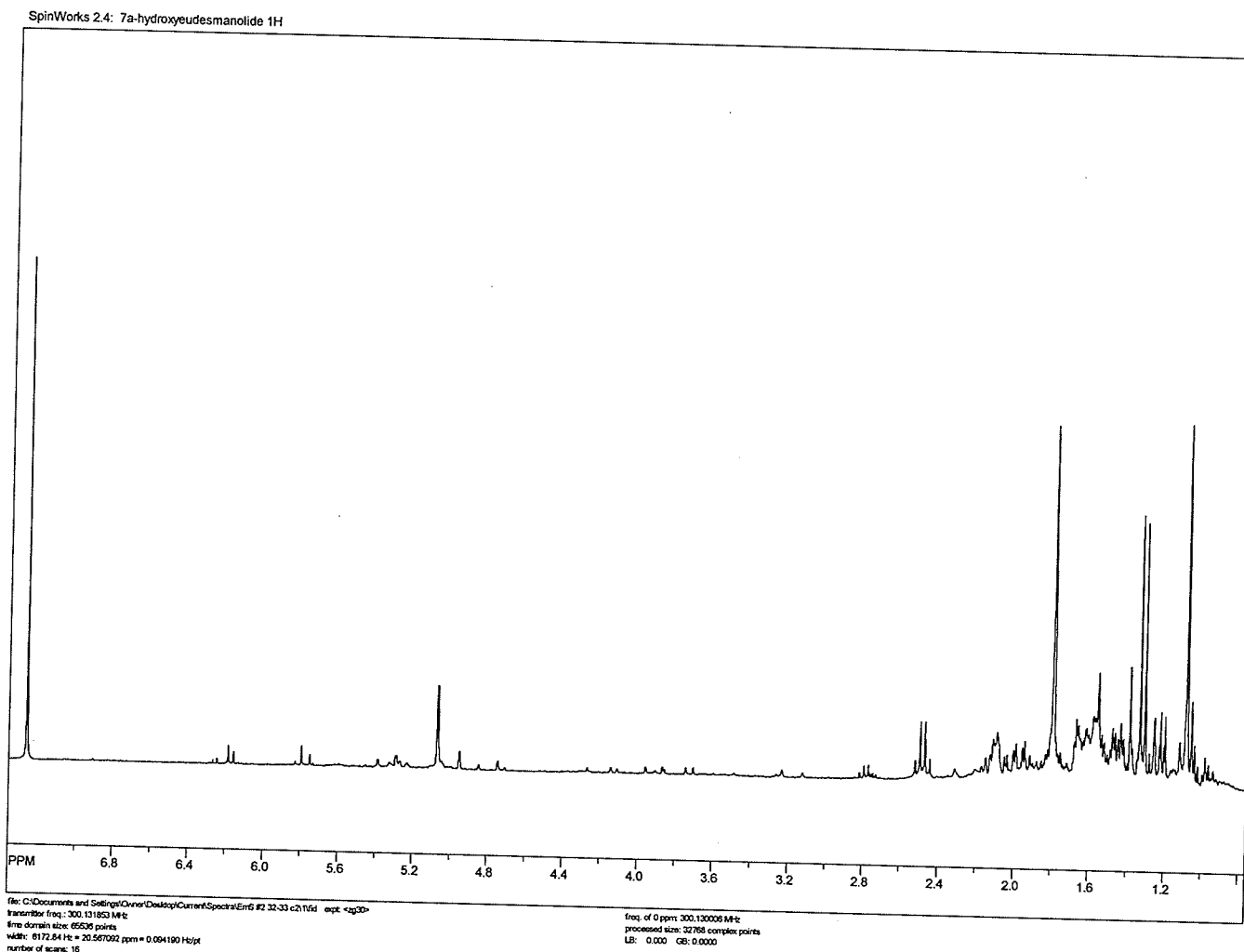


**Figure B-12:  $^1\text{H}$  NMR of 7 $\alpha$ -hydroxyeudesmanolide (56)**

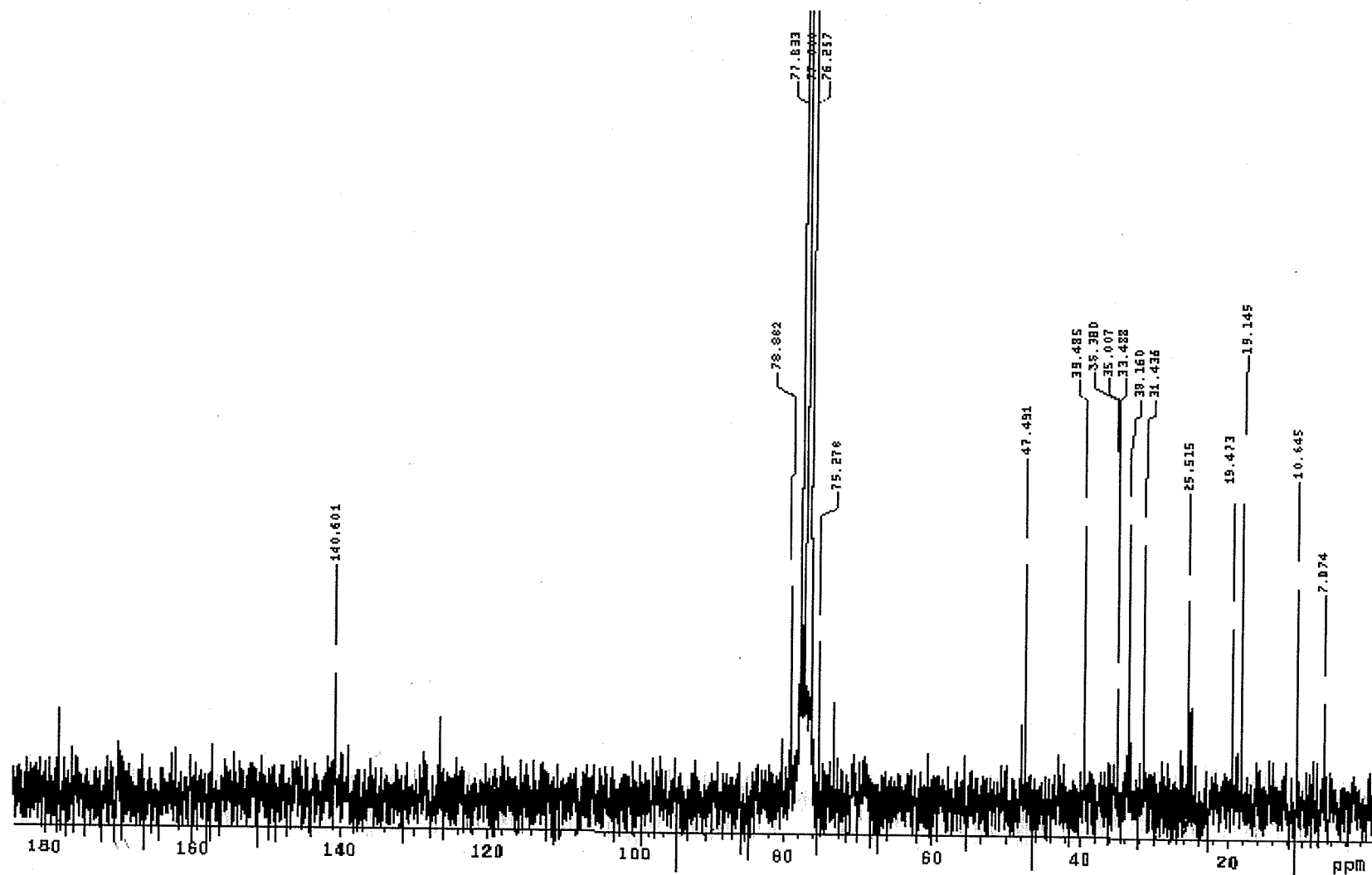
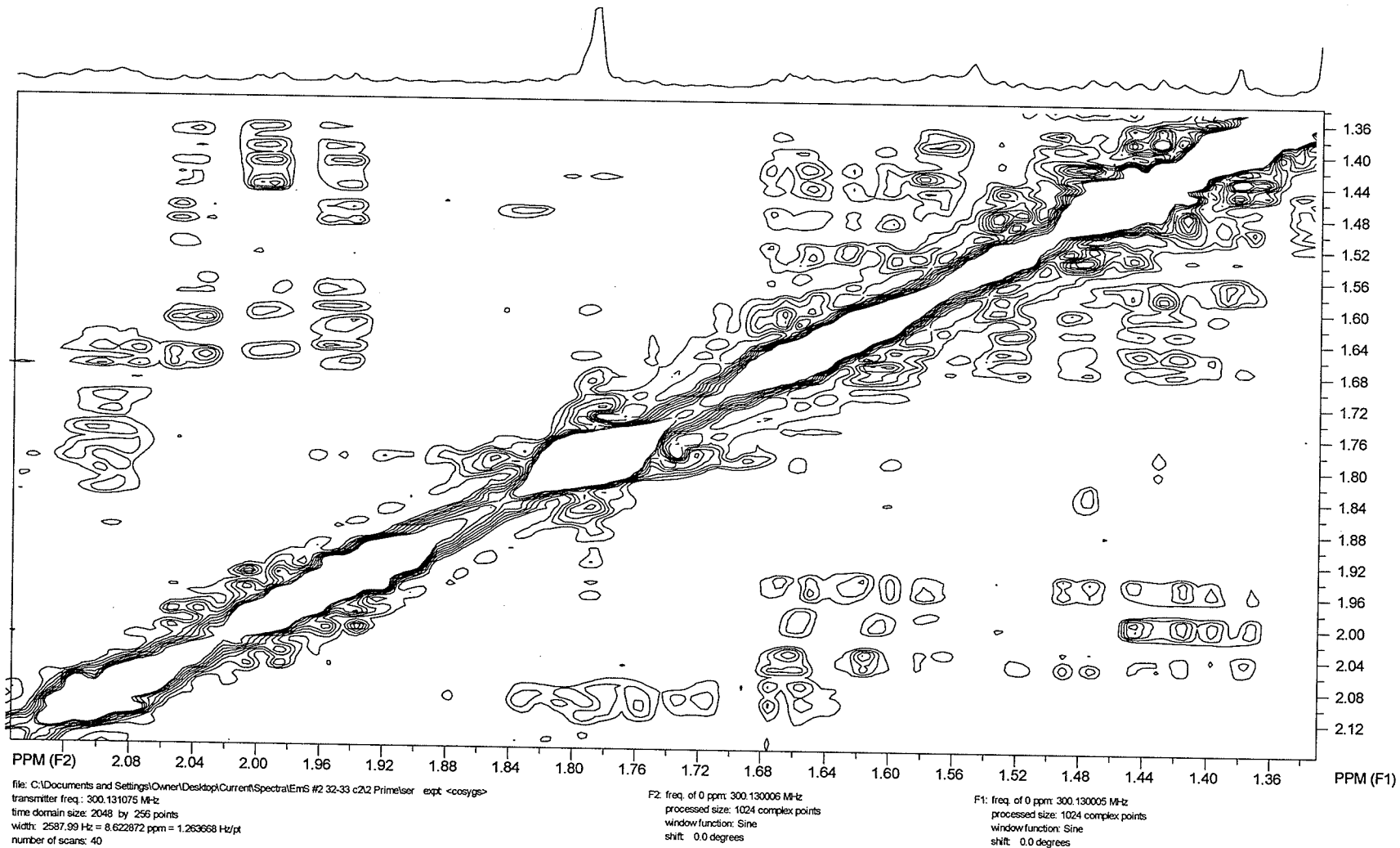
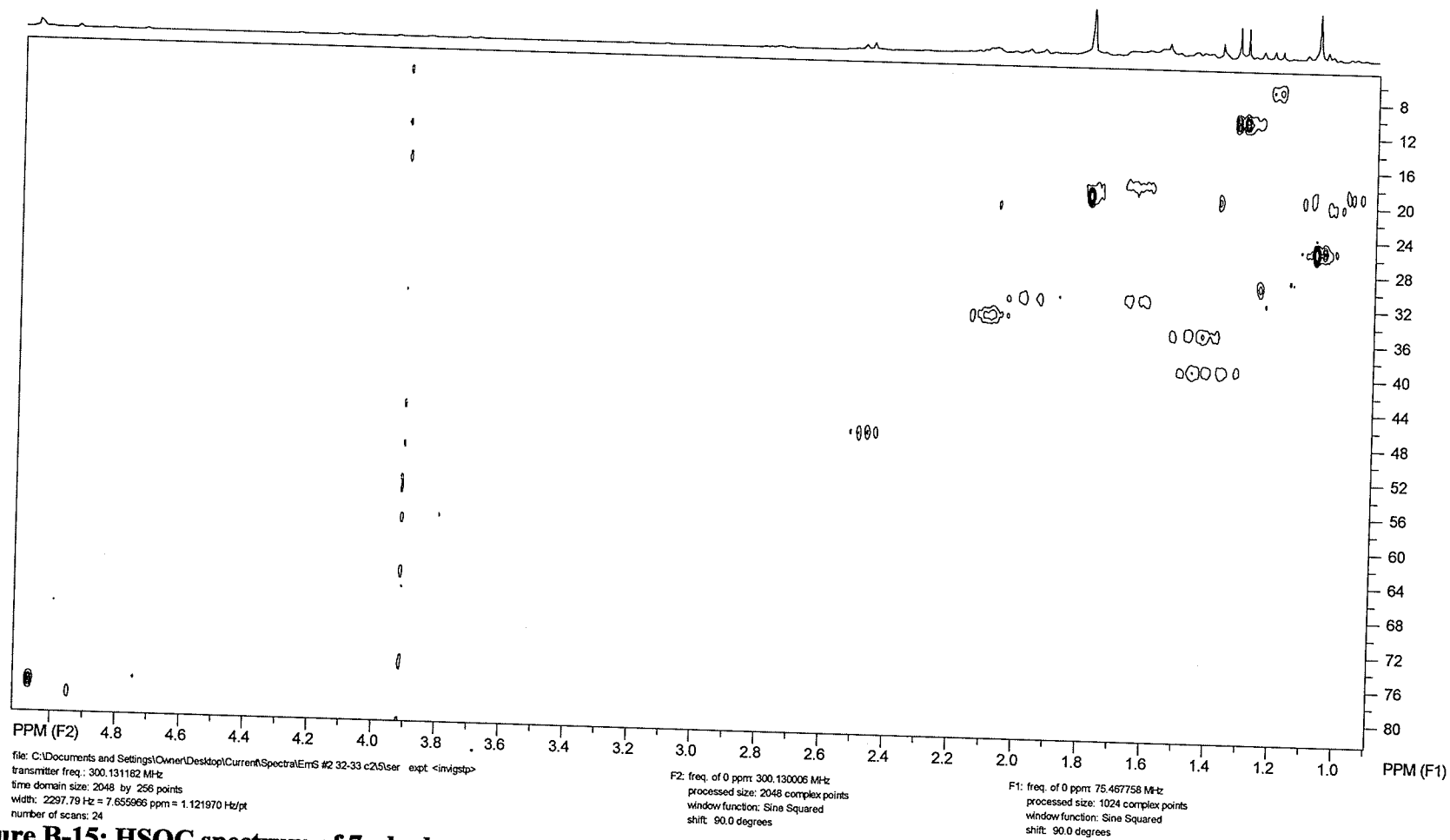


Figure B-13:  $^{13}\text{C}$  NMR of 7 $\alpha$ -hydroxyeudesmanolide (56)



**Figure B-14: COSY spectrum of 7 $\alpha$ -hydroxyudesmanolide (56)**



**Figure B-15: HSQC spectrum of 7 $\alpha$ -hydroxyeudesmanolide (56)**

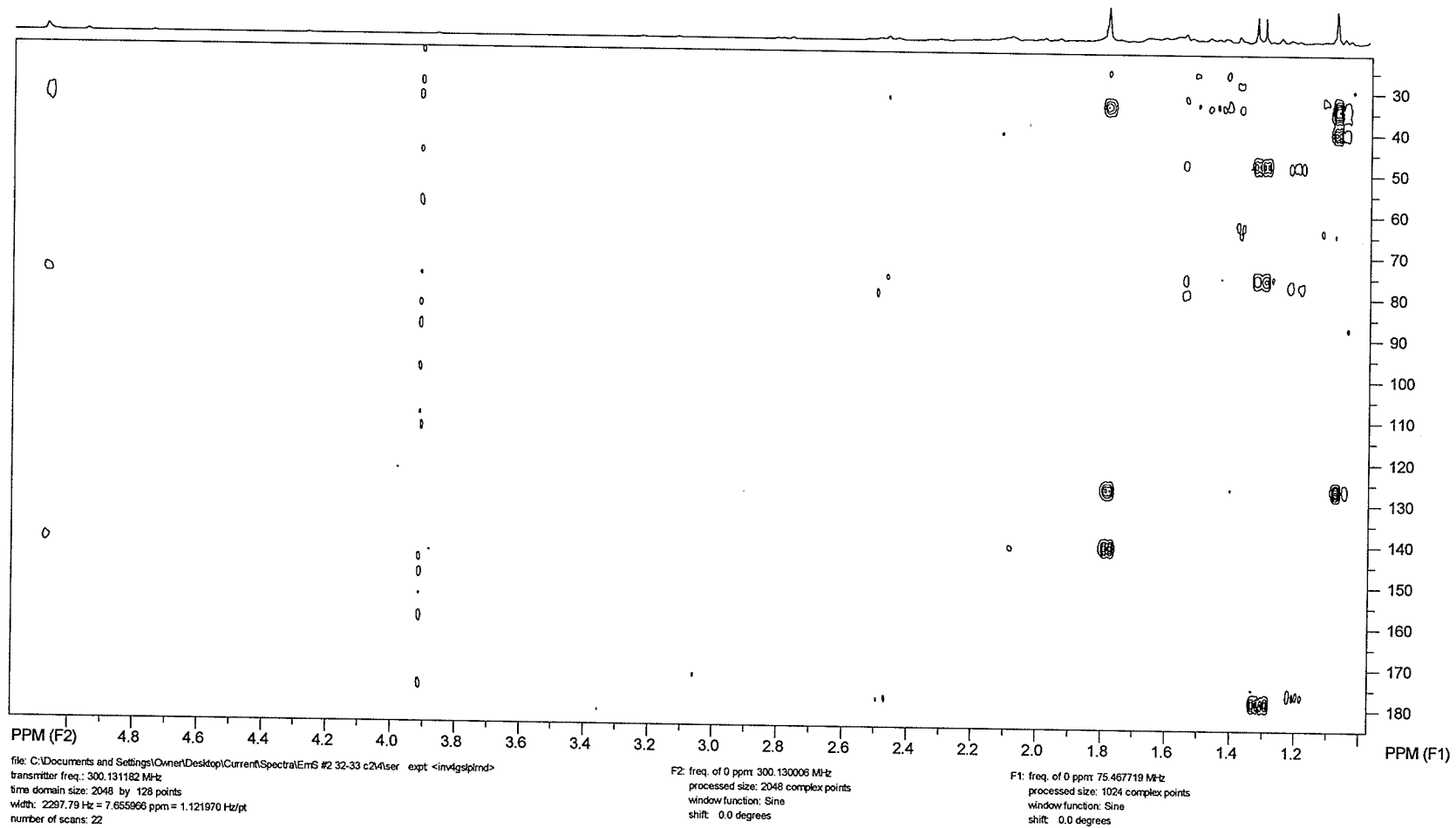


**Figure B-16: HMBC spectrum of 7 $\alpha$ -hydroxyeudesmanolide (56)**

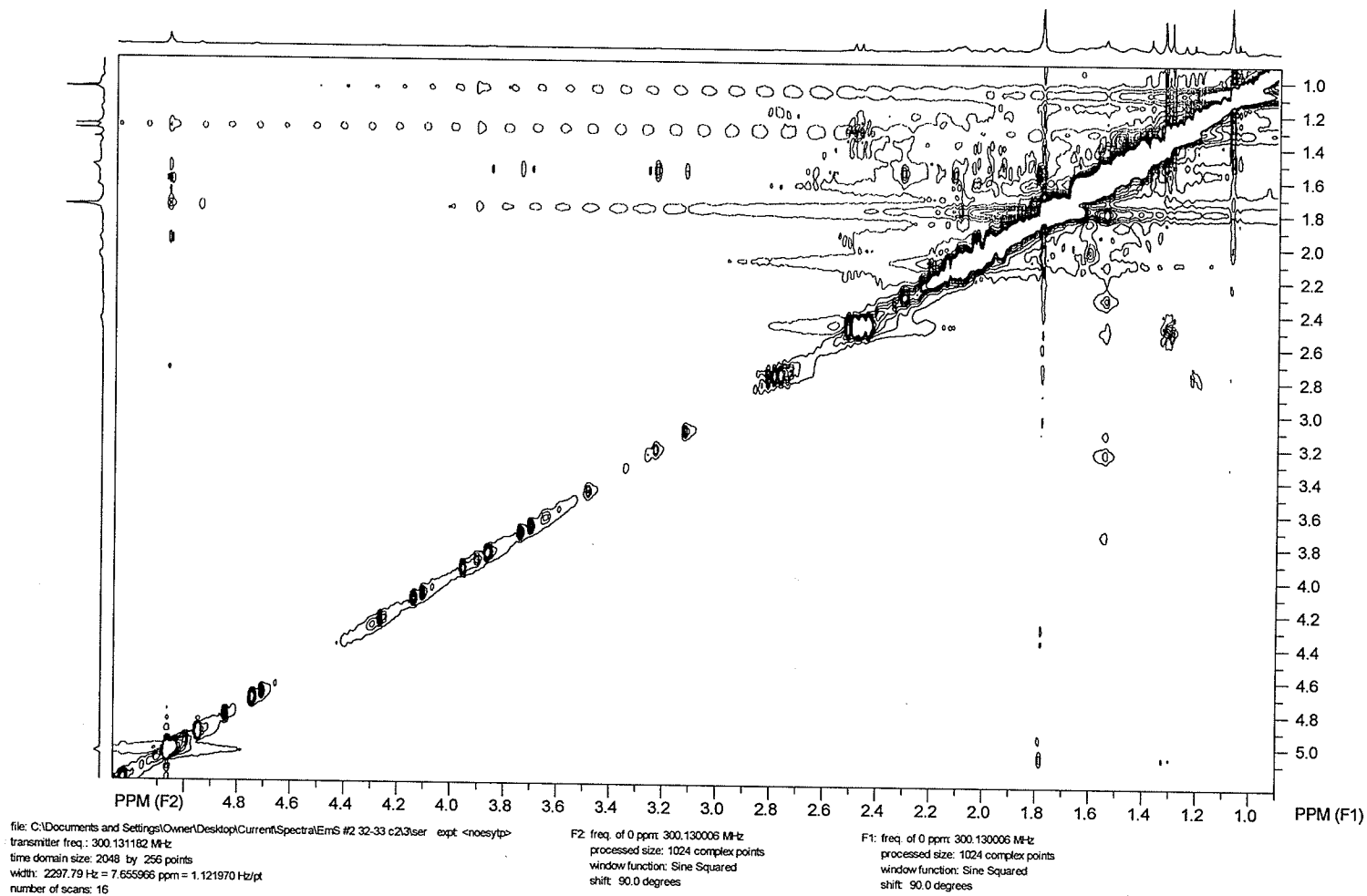


**Figure B-17: NOESY spectrum of 7 $\alpha$ -hydroxyeudesmanolide (56)**

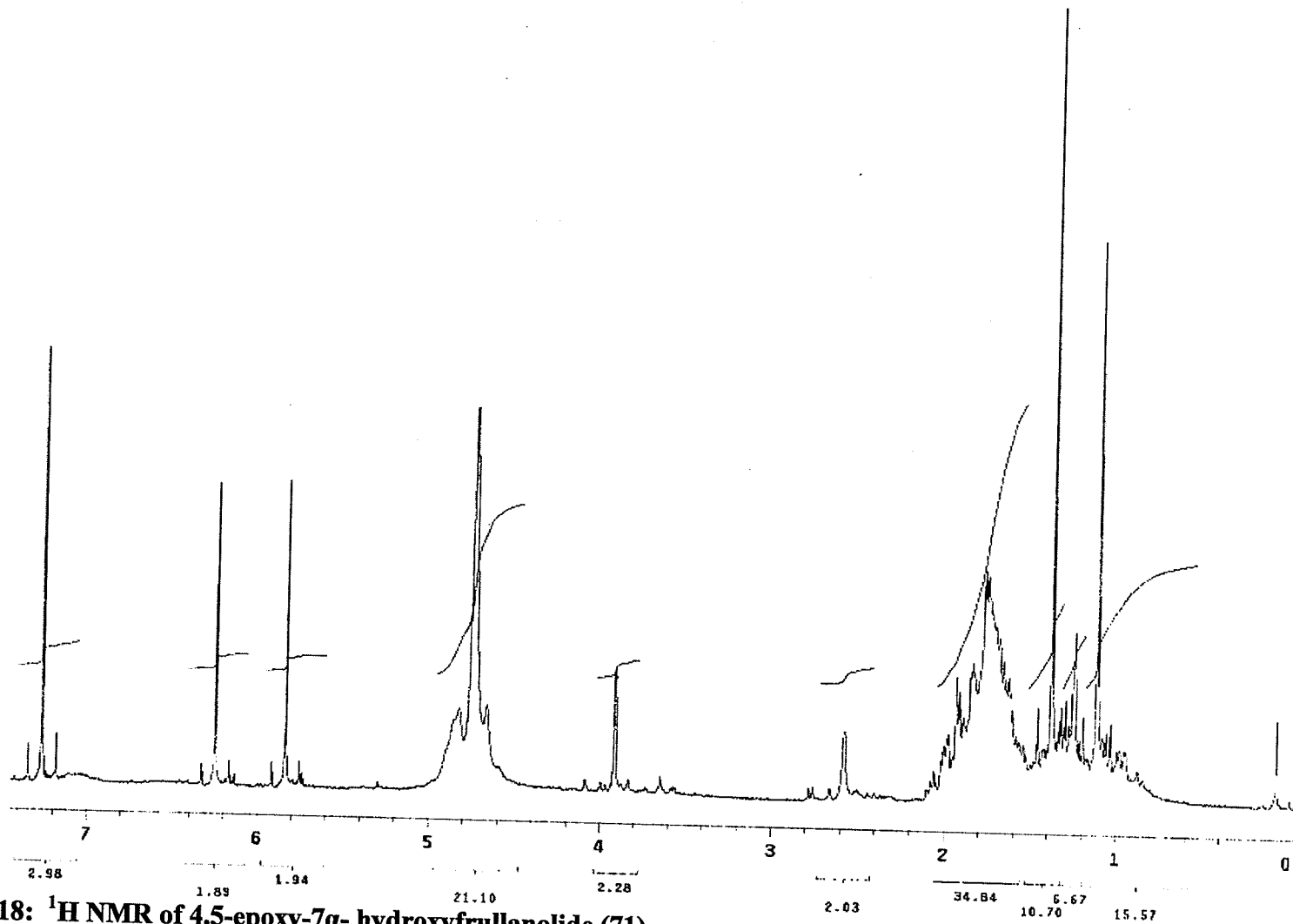


Figure B-18: <sup>1</sup>H NMR of 4,5-epoxy-7α-hydroxyfrullanolide (71)

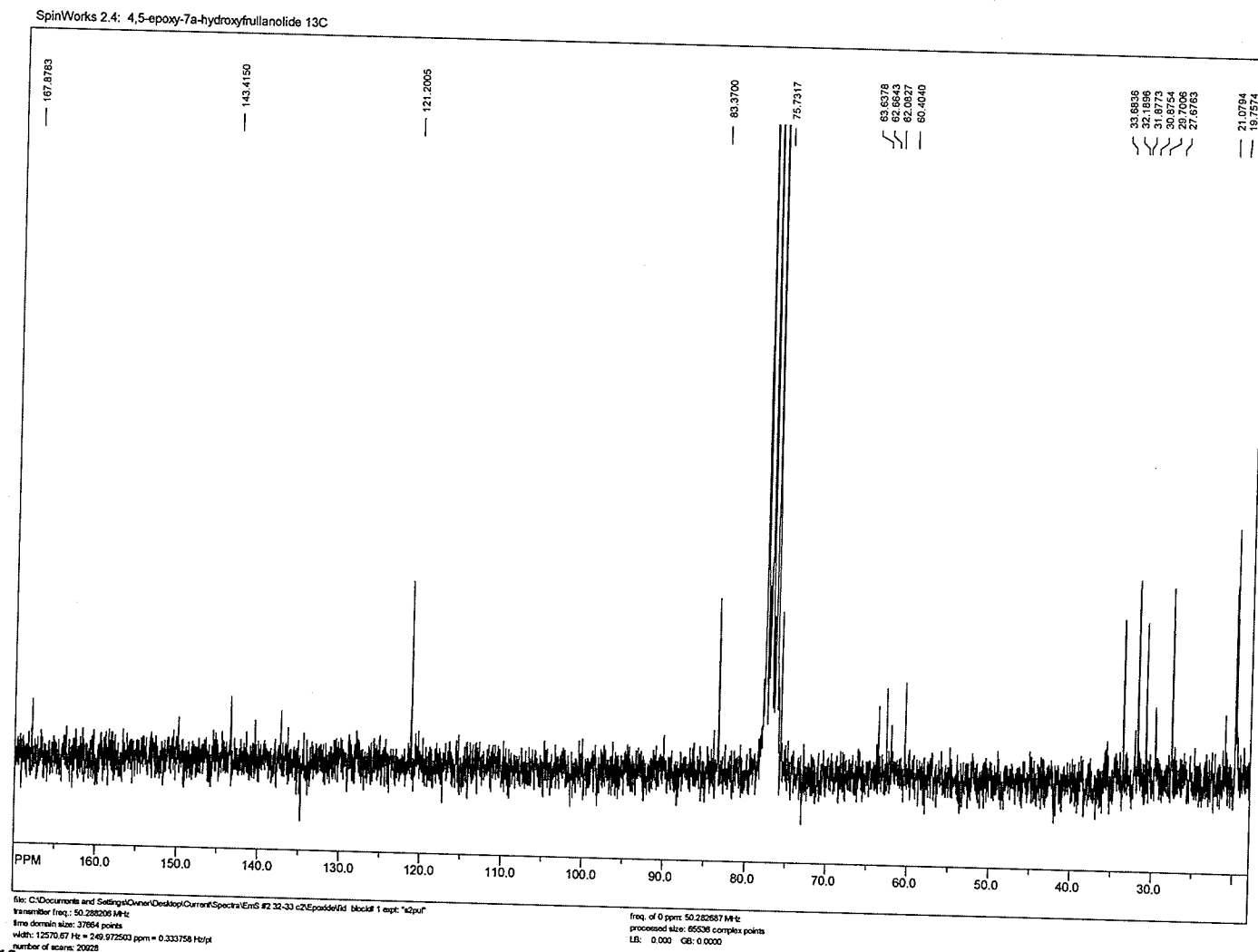


Figure B-19:  $^{13}\text{C}$  NMR of 4,5-epoxy-7 $\alpha$ -hydroxyfrullanolide (71)



## Appendix C: NMR spectra of *Buxus hyrcana* compounds

Figure C-1:  $^1\text{H}$  NMR of buxamine B (99)

Figure C-2:  $^{13}\text{C}$  NMR of buxamine B (99)

Figure C-3: COSY spectrum of buxamine B (99)

Figure C-4: HSQC spectrum of buxamine B (99)

Figure C-5: HMBC spectrum of buxamine B (99)

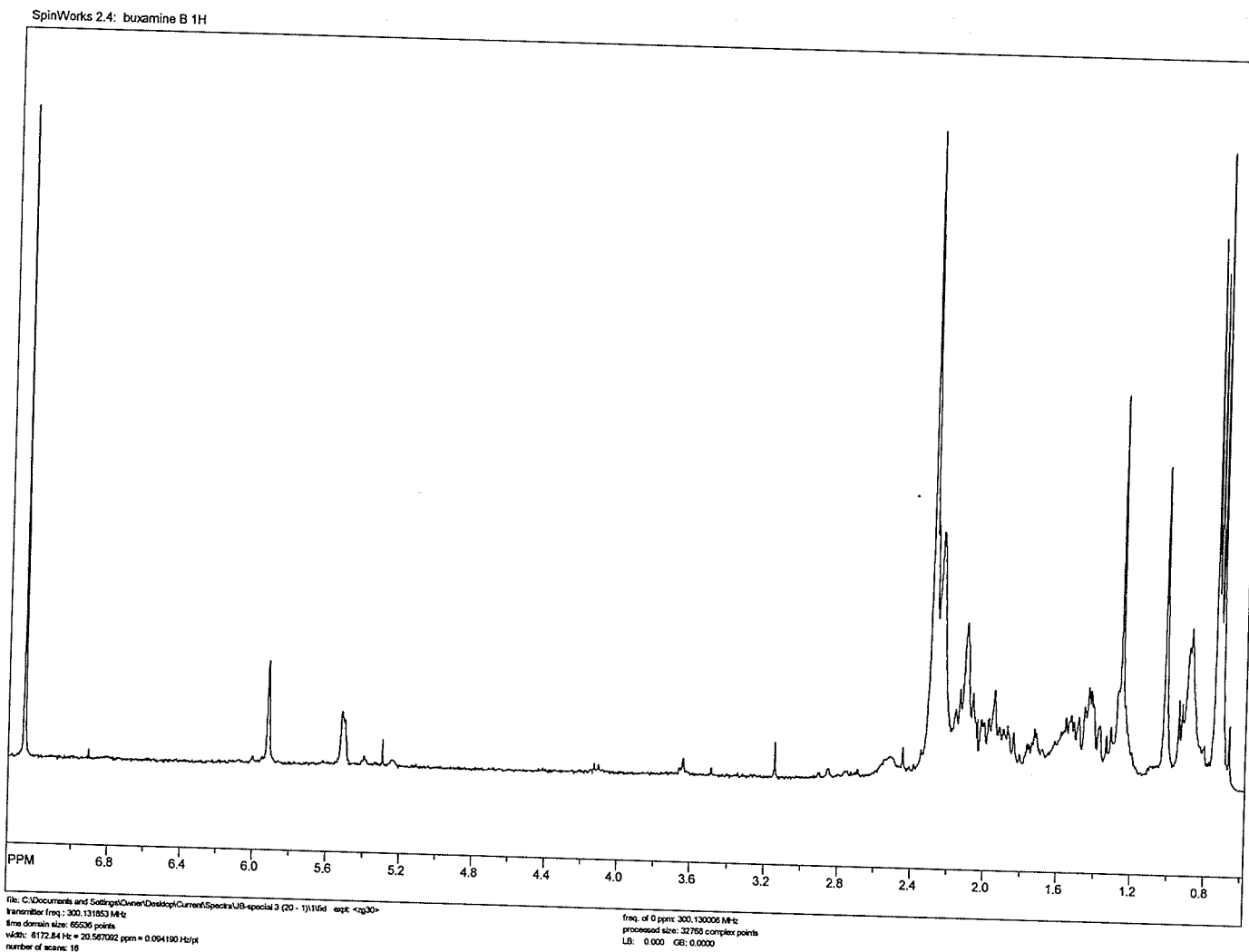
Figure C-6:  $^1\text{H}$  NMR of  $N_b$ -dimethylcycloxobuxoviricine (**85**)

Figure C-7:  $^{13}\text{C}$  NMR of  $N_b$ -dimethylcycloxobuxoviricine (**85**)

Figure C-8: COSY spectrum of  $N_b$ -dimethylcycloxobuxoviricine (**85**)

Figure C-9: HSQC spectrum of  $N_b$ -dimethylcycloxobuxoviricine (**85**)

Figure C-10: HMBC spectrum of  $N_b$ -dimethylcycloxobuxoviricine (**85**)



**Figure C-1:  $^1\text{H}$  NMR of buxamine B (99)**

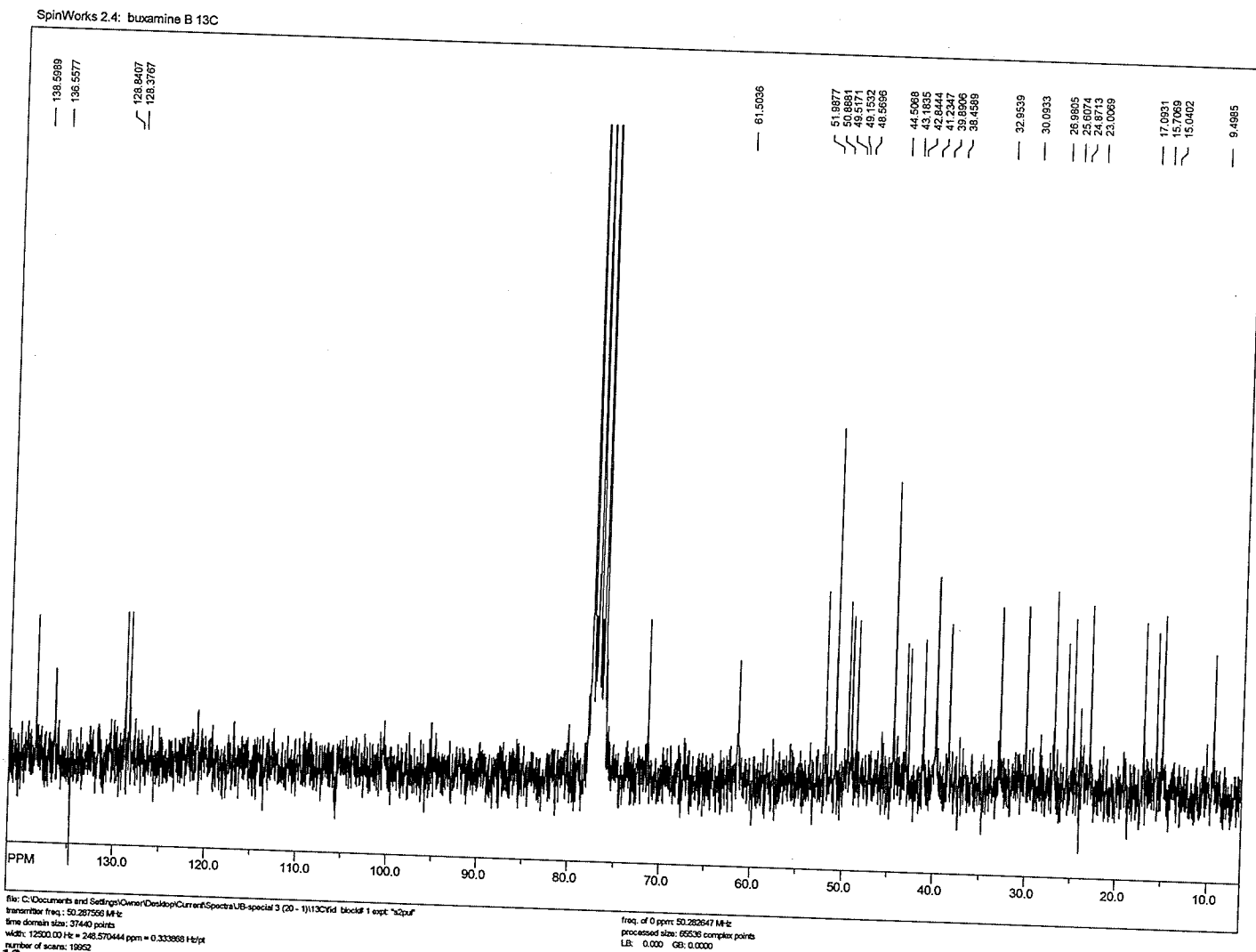
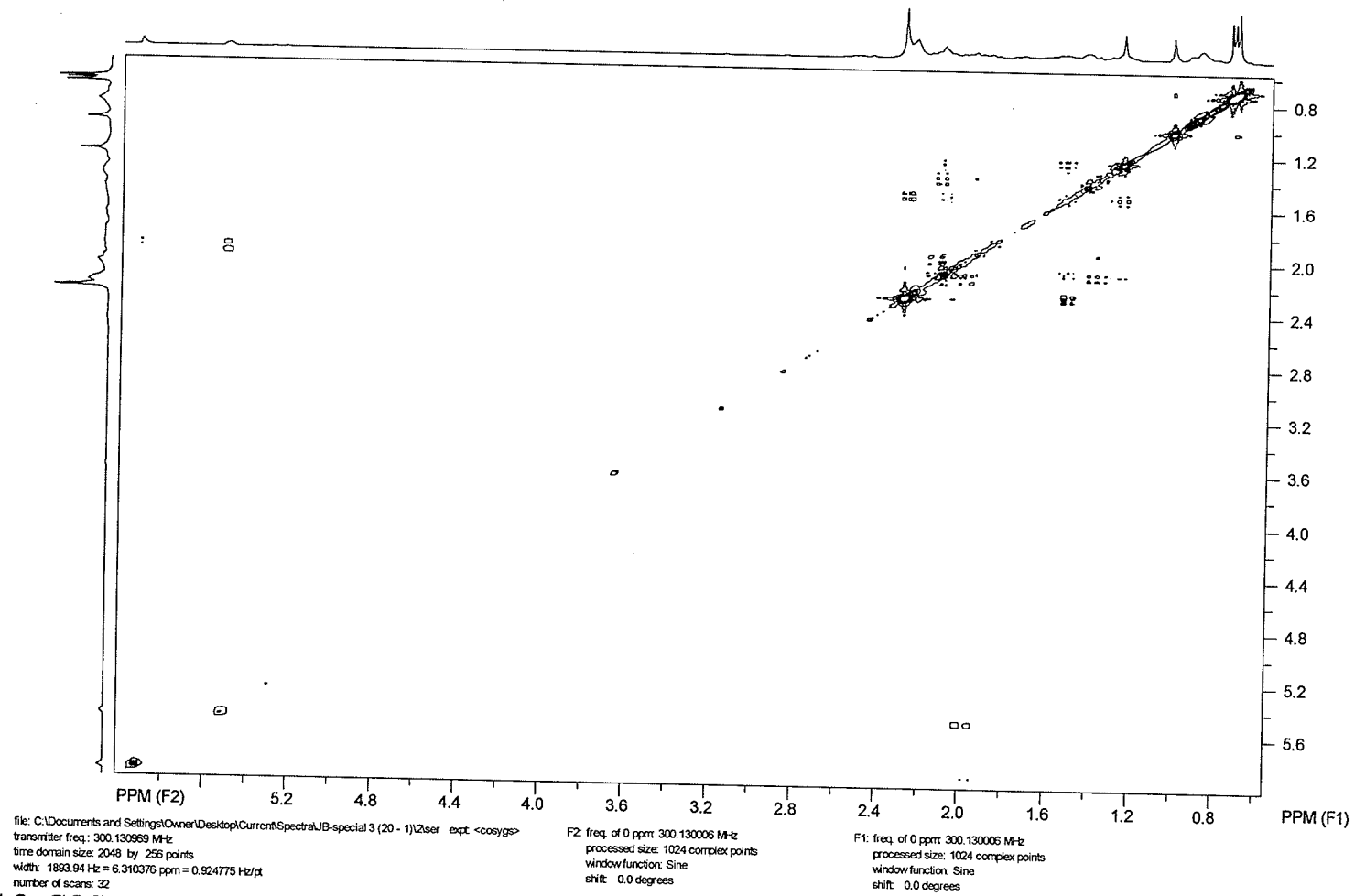
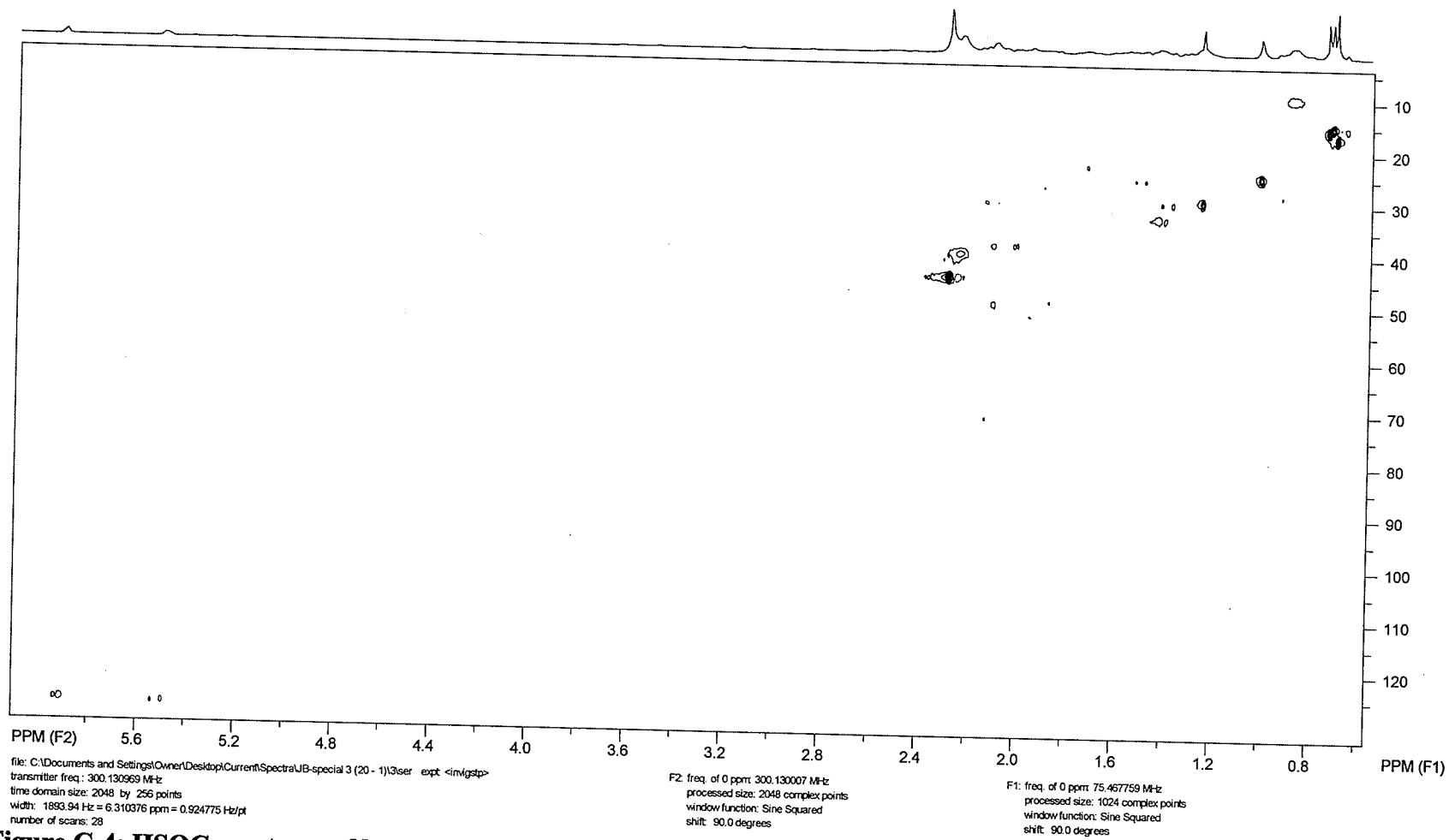


Figure C-2: <sup>13</sup>C NMR of buxamine B (99)



**Figure C-3: COSY spectrum of buxamine B (99)**



**Figure C-4: HSQC spectrum of buxamine B (99)**

SpinWorks 2.5 2D: 20 - 1 pTLC HMBC magnification 1

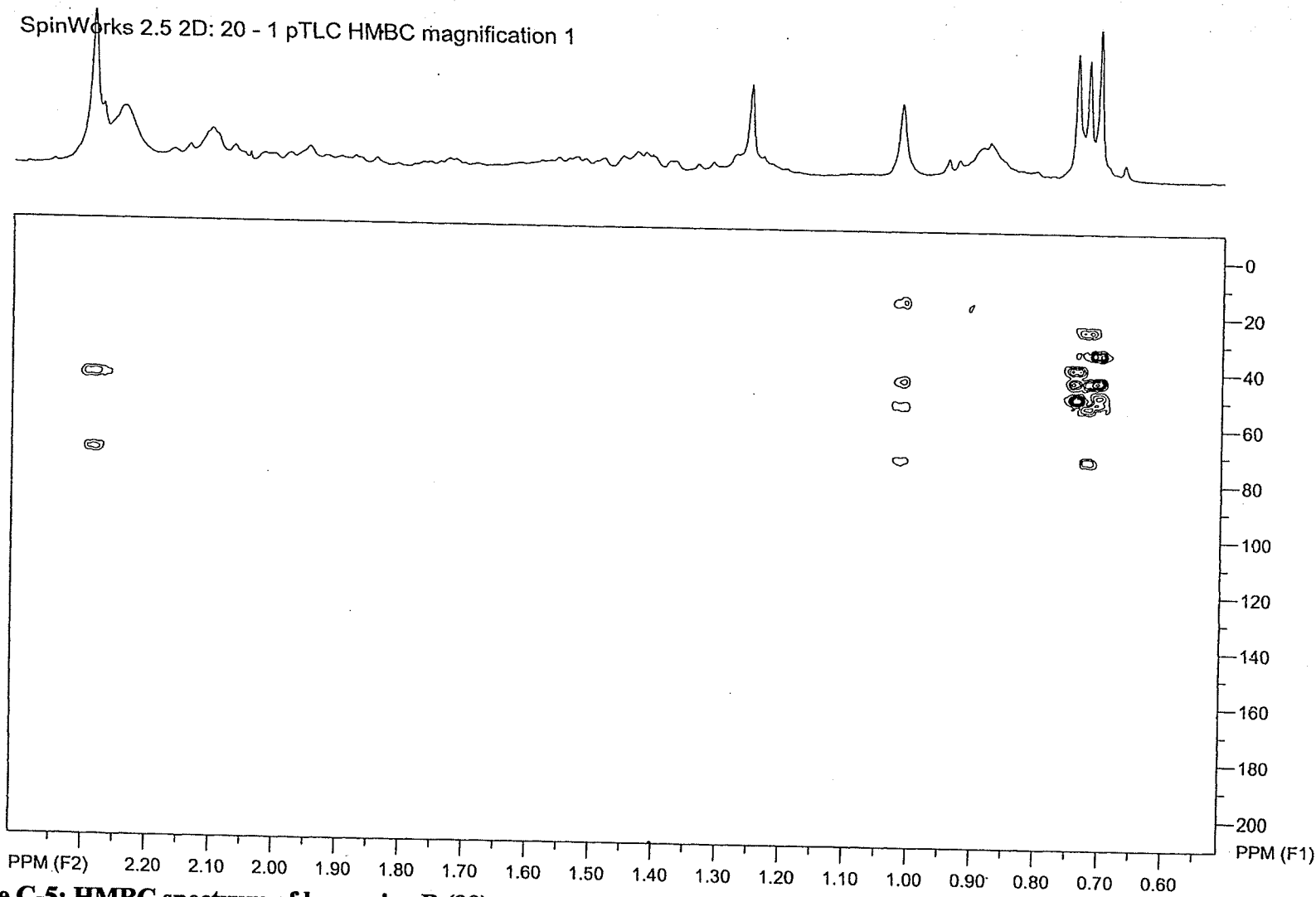


**Figure C-5: HMBC spectrum of buxamine B (99)**

SpinWorks 2.4: Nb-dimethylcyclohexoviricine 1H

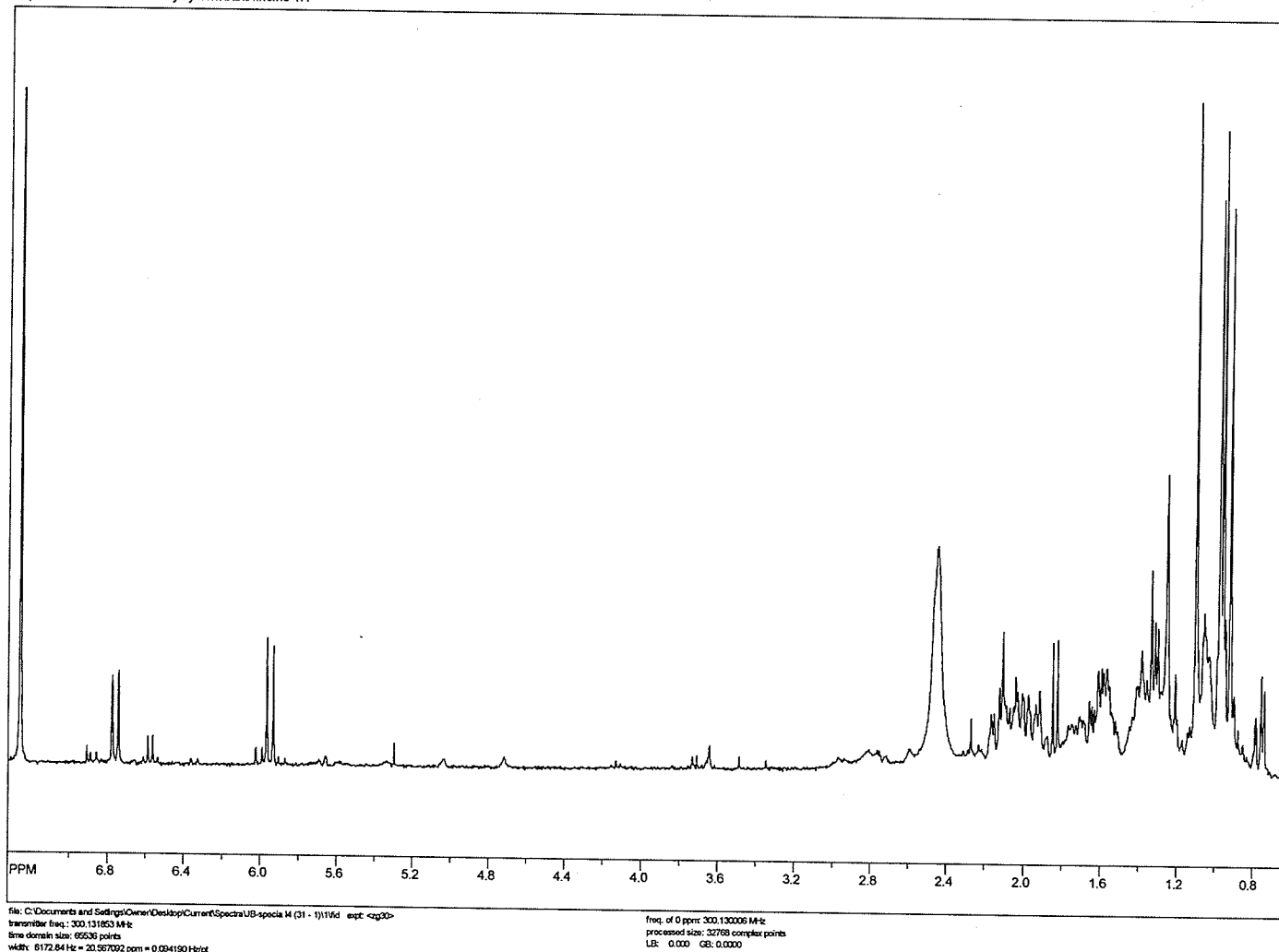


Figure C-6:  $^1\text{H}$  NMR of  $N_b$ -dimethylcyclohexoviricine (85)

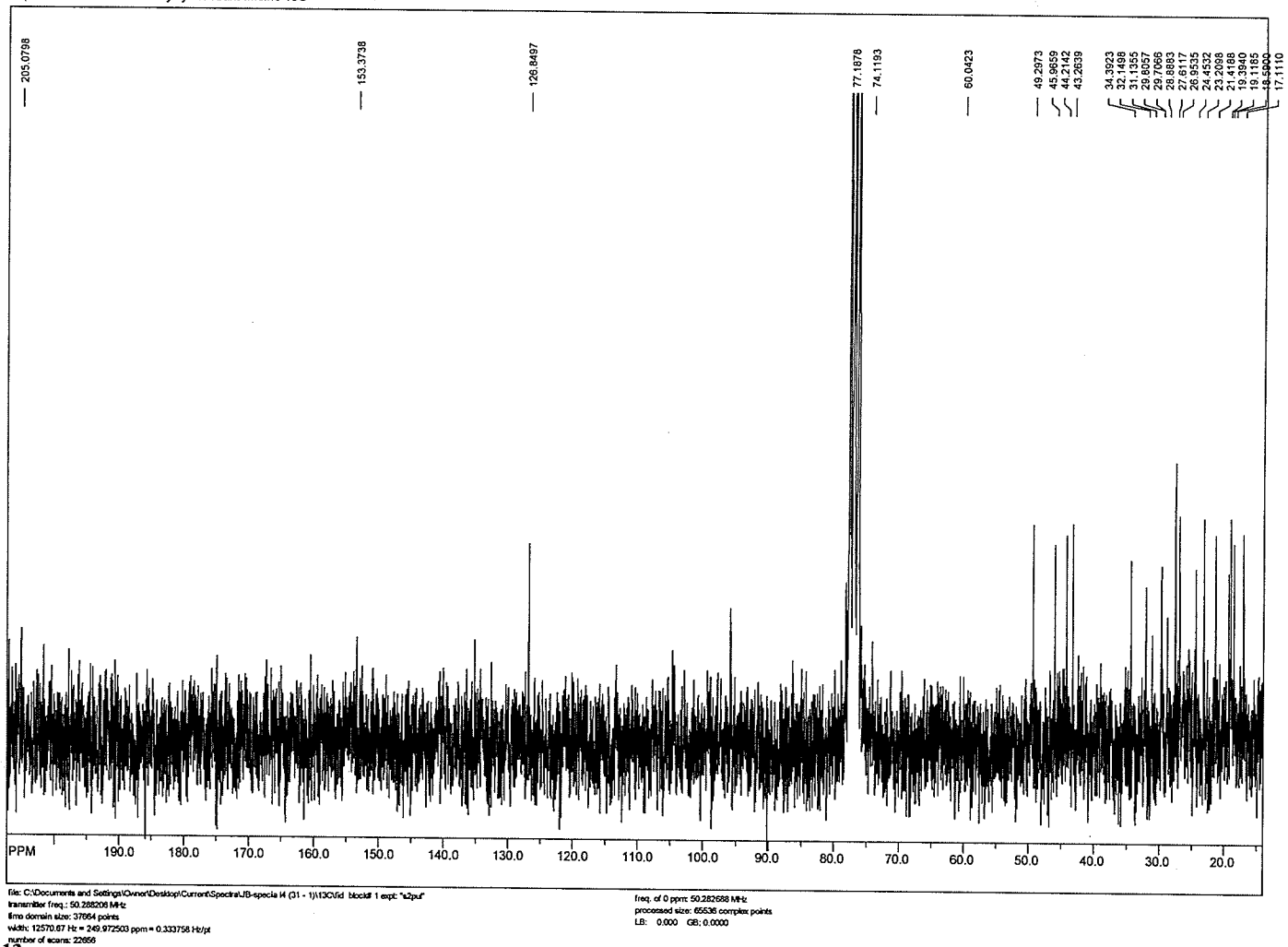
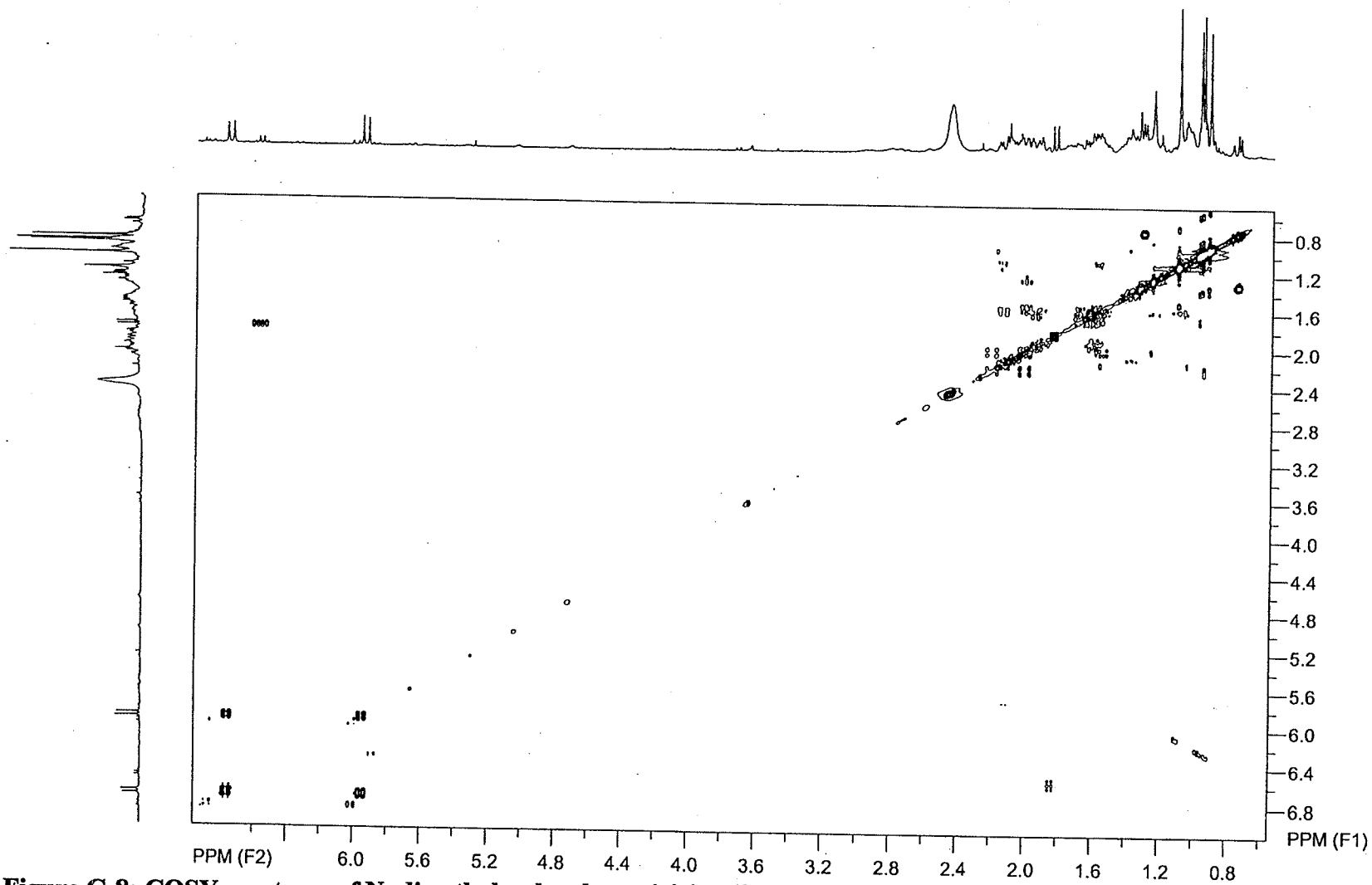
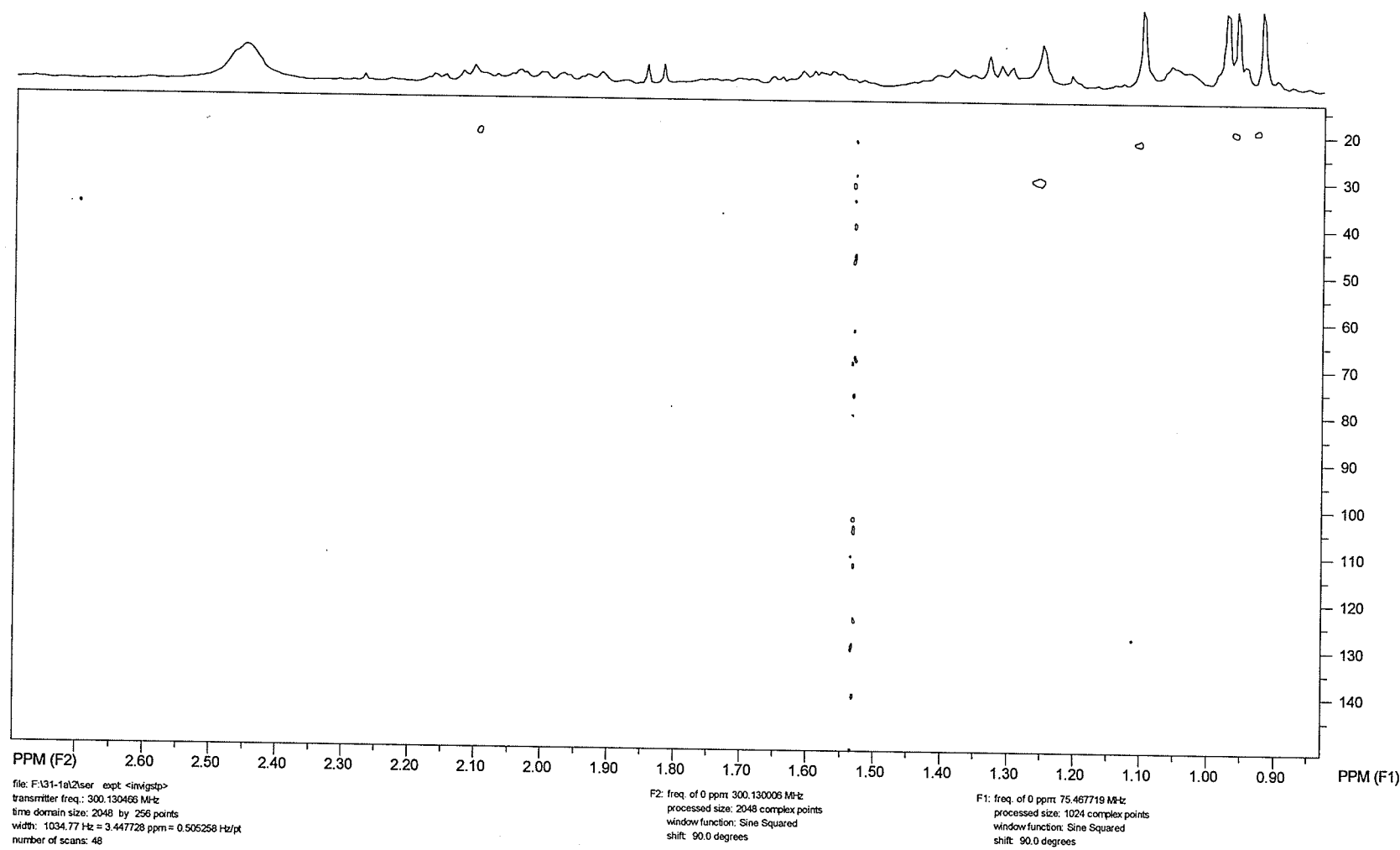


Figure C-7:  $^{13}\text{C}$  NMR of  $N_b$ -dimethylcyclobuxoviricine (85)





**Figure C-8: COSY spectrum of *N*<sub>6</sub>-dimethylcyclohexoviricine (85)**



**Figure C-9: HSQC spectrum of Nb-dimethylcyclohexoviricine (85)**

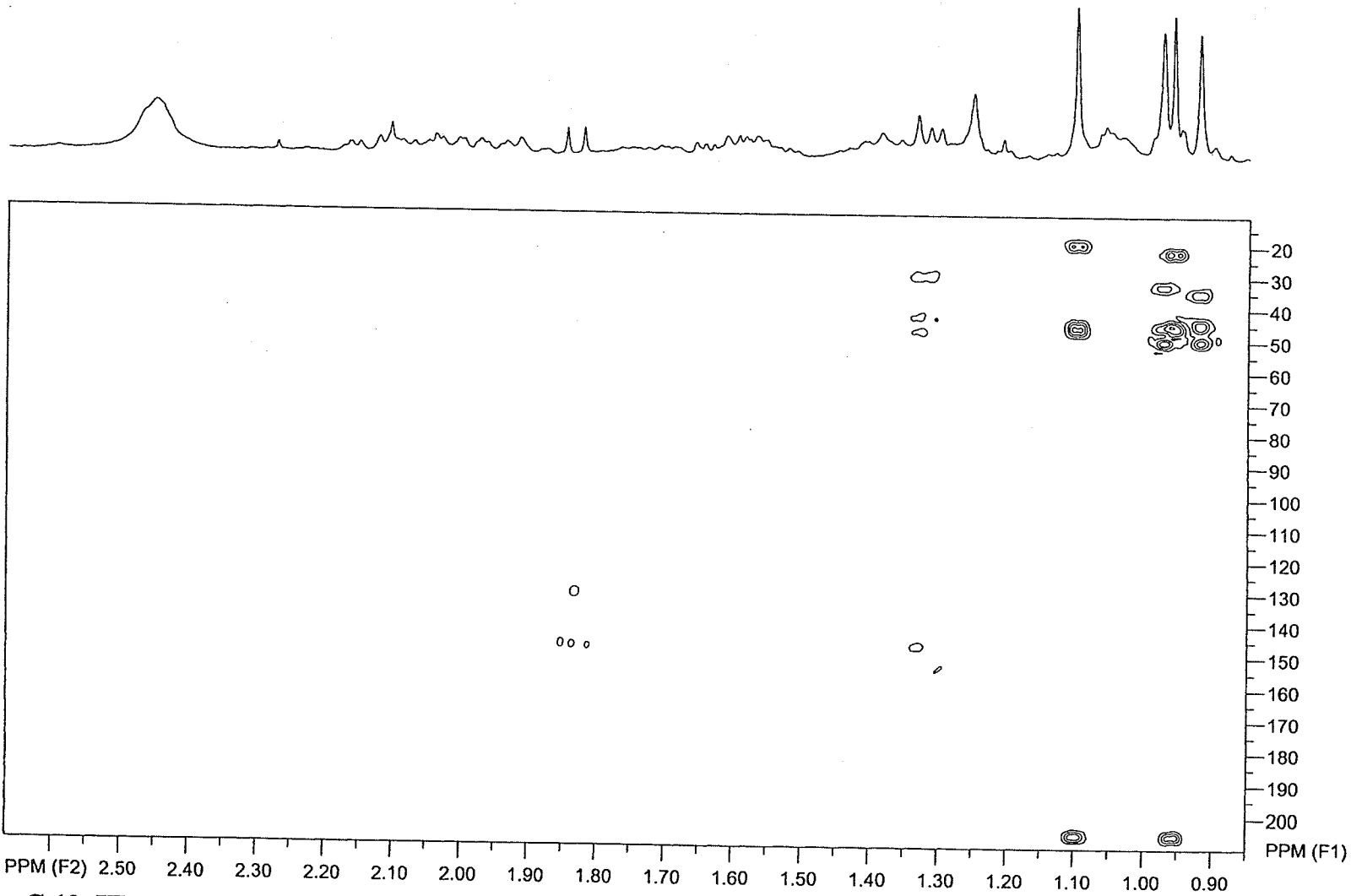


**Figure C-10: HMBC spectrum of *N*<sub>b</sub>-dimethylcyclohexoviricine (85)**

## Appendix D: NMR spectra of Biotransformation compounds

Figure D-1:  $^1\text{H}$  NMR of 3-ketosclareolide (**131**)

Figure D-2:  $^{13}\text{C}$  NMR of 3-ketosclareolide (**131**)

Figure D-3:  $^1\text{H}$  NMR of 3 $\beta$ -hydroxysclareolide (**132**)

Figure D-4:  $^{13}\text{C}$  NMR of 3 $\beta$ -hydroxysclareolide (**132**)

Figure D-5: COSY spectrum of 3 $\beta$ -hydroxysclareolide (**132**)

Figure D-6: HSQC spectrum of 3 $\beta$ -hydroxysclareolide (**132**)

Figure D-7: HMBC spectrum of 3 $\beta$ -hydroxysclareolide (**132**)

Figure D-8: NOESY spectrum of 3 $\beta$ -hydroxysclareolide (**132**)

Figure D-9:  $^1\text{H}$  NMR of tyrosol (**151**)

Figure D-10:  $^{13}\text{C}$  NMR of tyrosol (**151**)

Figure D-11: COSY spectrum of tyrosol (**151**)

Figure D-12: HMBC spectrum of tyrosol (**151**)

PC SCLD(2) CCF#21  
Jordan Bletteridge  
October 27, 2008 CDCl3

Archive directory: /export/home/aata/vnmrsys/data  
Sample directory:

Pulse Sequence: s2pul  
Solvent: CDCl3  
Ambient temperature  
File: PC\_SCLD\_21  
GEMINI-280 "vnmr"

Relax. delay 1.000 sec  
Pulse 45.0 degrees  
Acq. time 1.955 sec  
Width 3199.5 Hz  
64 repetitions  
OBSERVE H1 199.9707248 MHz  
DATA PROCESSING  
FT size 16384  
Total time 3 min, 1

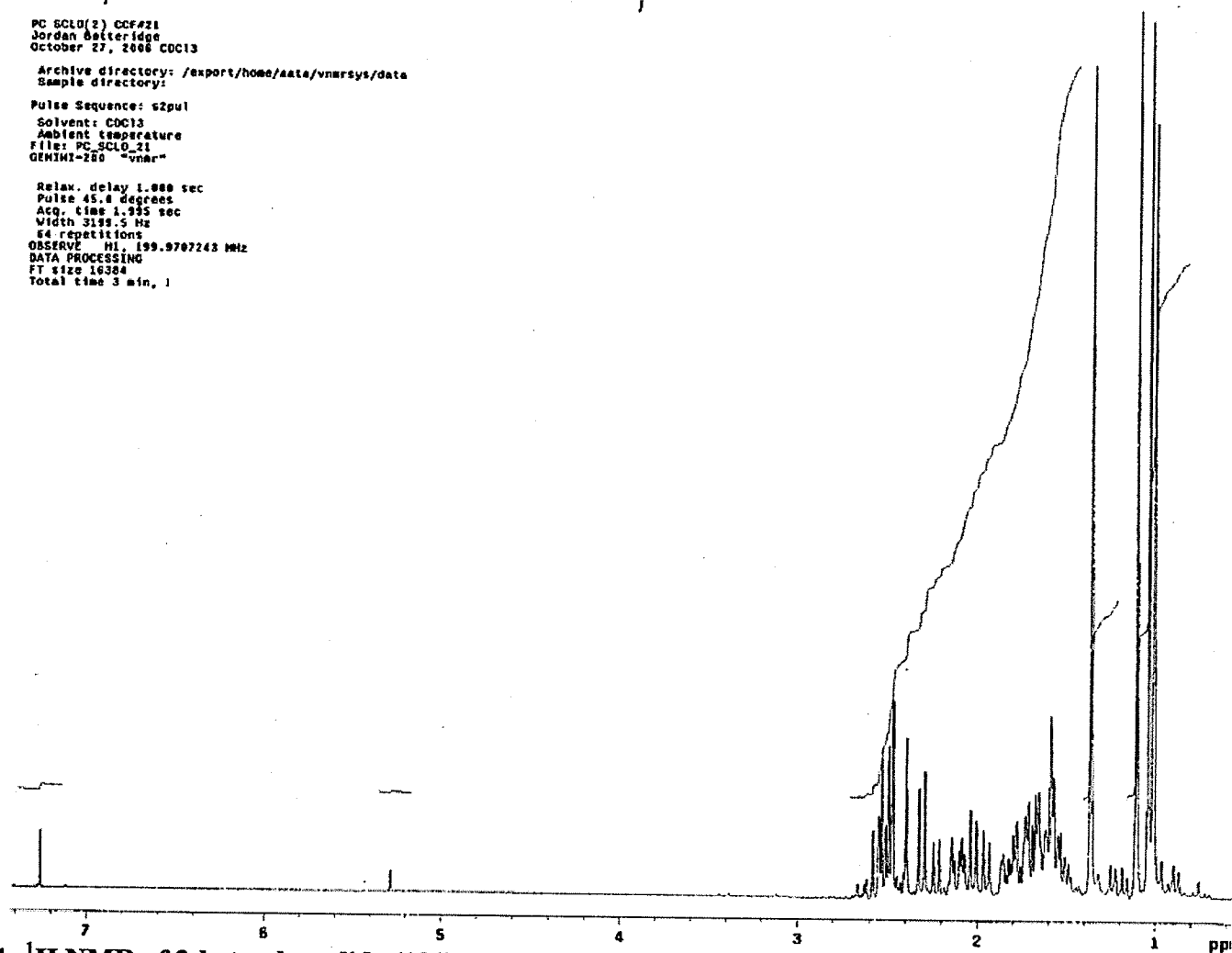


Figure D-1:  $^1\text{H}$  NMR of 3-ketosclareolide (131)

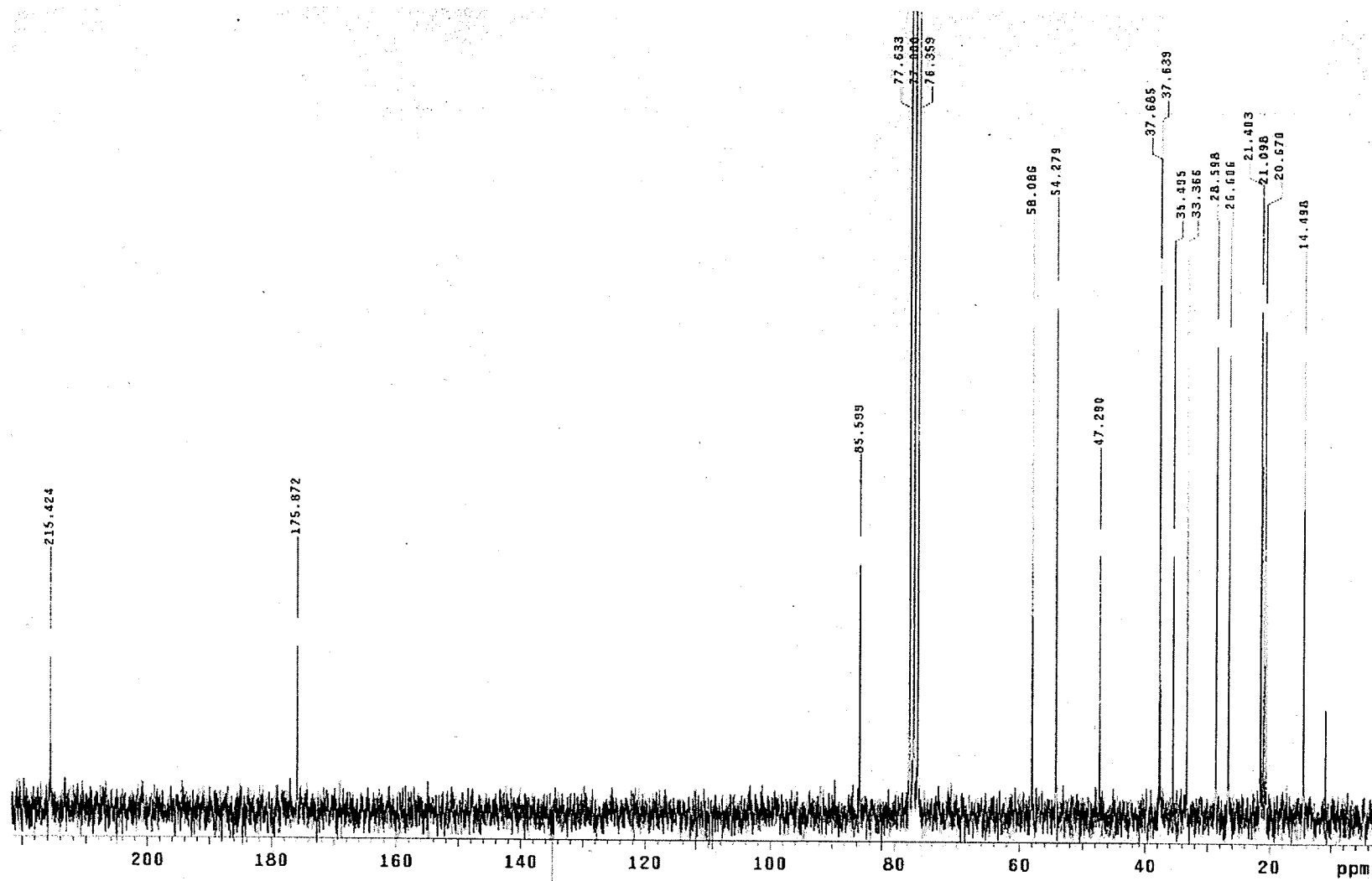
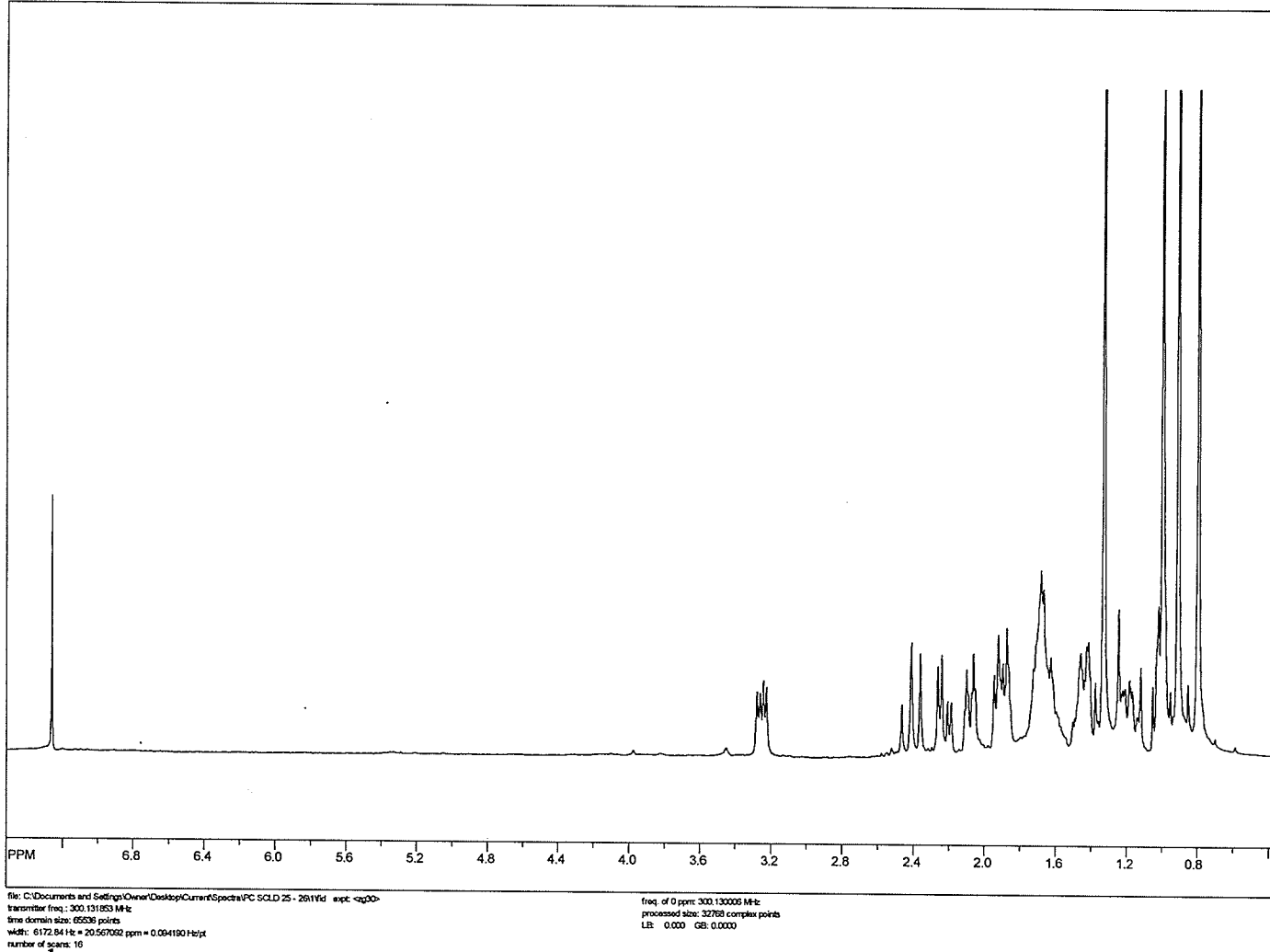


Figure D-2: <sup>13</sup>C NMR of 3-ketosclareolide (131)

SpinWorks 2.4: 3 $\beta$ -hydroxysclareolide 1H



**Figure D-3: <sup>1</sup>H NMR of 3 $\beta$ -hydroxysclareolide (132)**

SpinWorks 2.4: 3 $\beta$ -hydroxysclareolide 13C

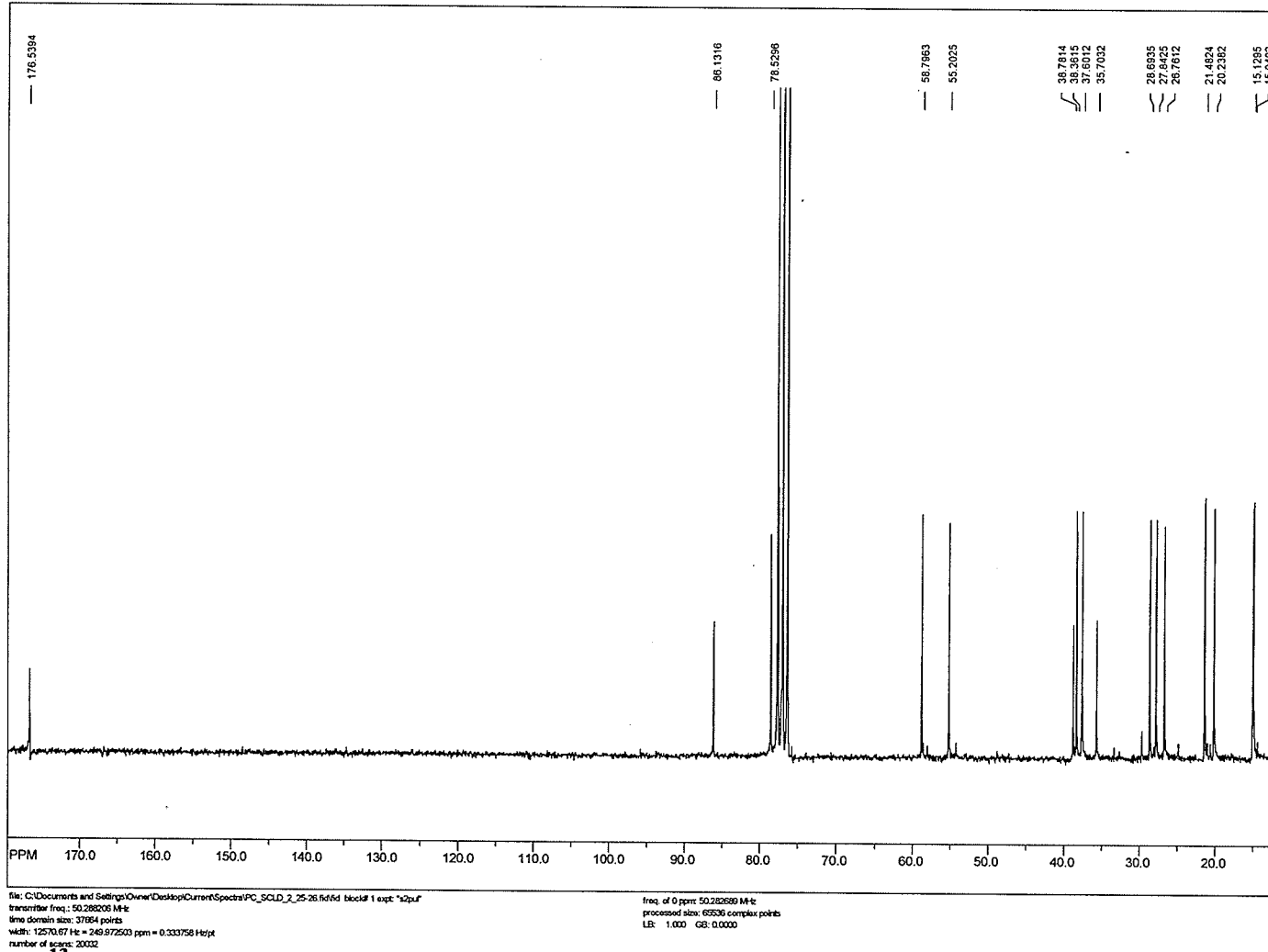


**Figure D-4:**  $^{13}\text{C}$  NMR of 3 $\beta$ -hydroxysclareolide (132)



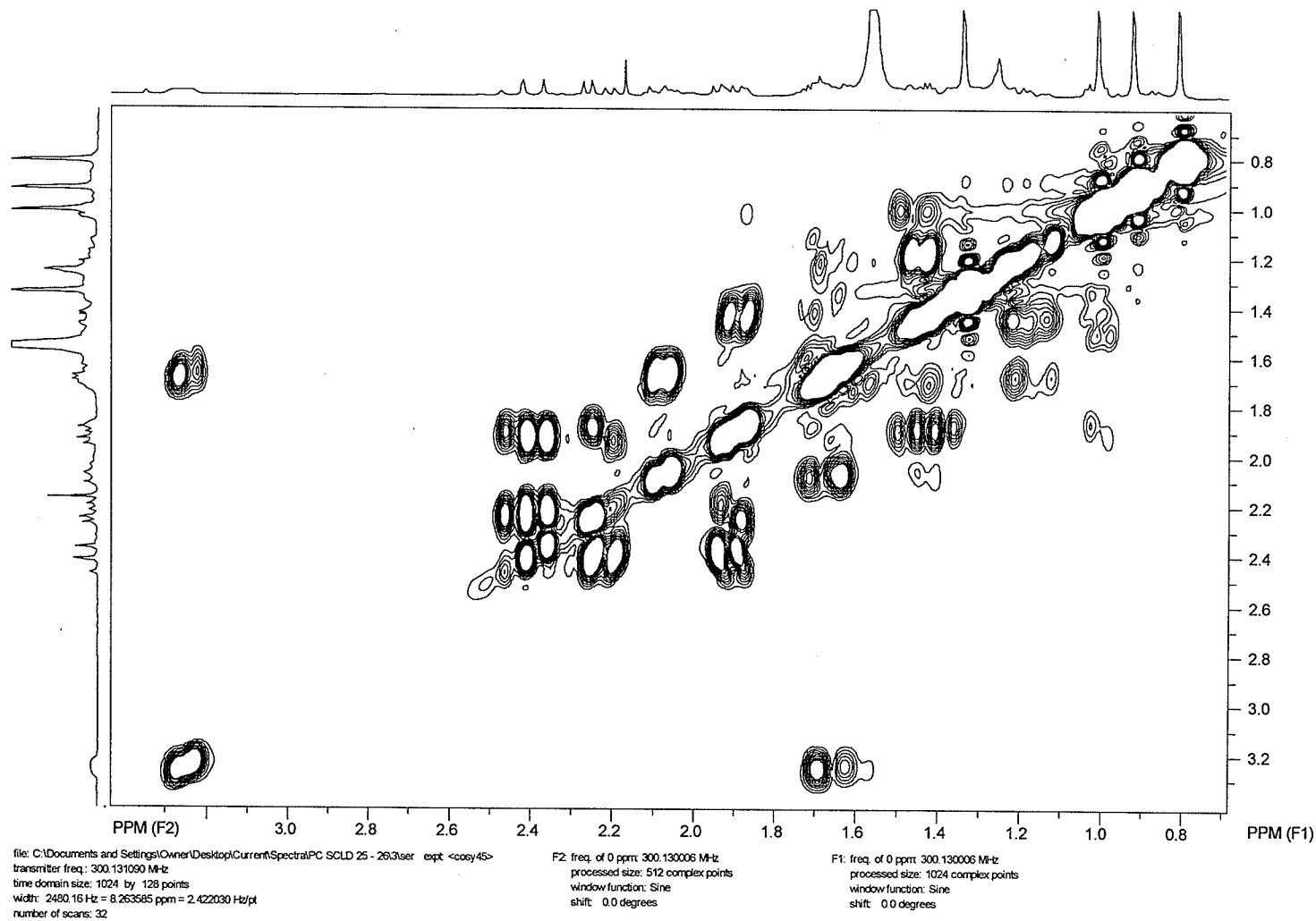


**Figure D-5: COSY spectrum of 3 $\beta$ -hydroxysclareolide (132)**

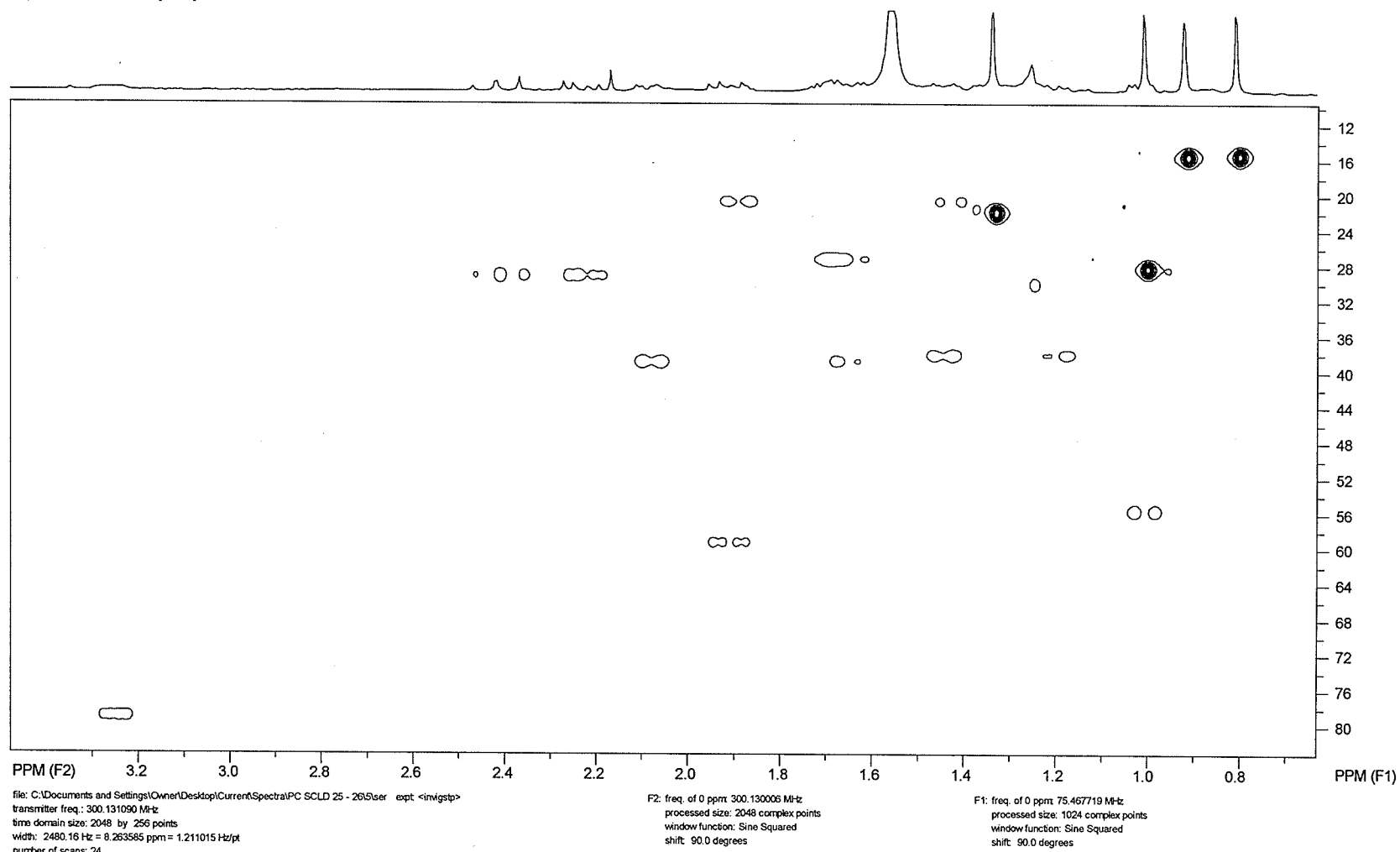


**Figure D-6: HSQC spectrum of 3 $\beta$ -hydroxysclareolide (132)**

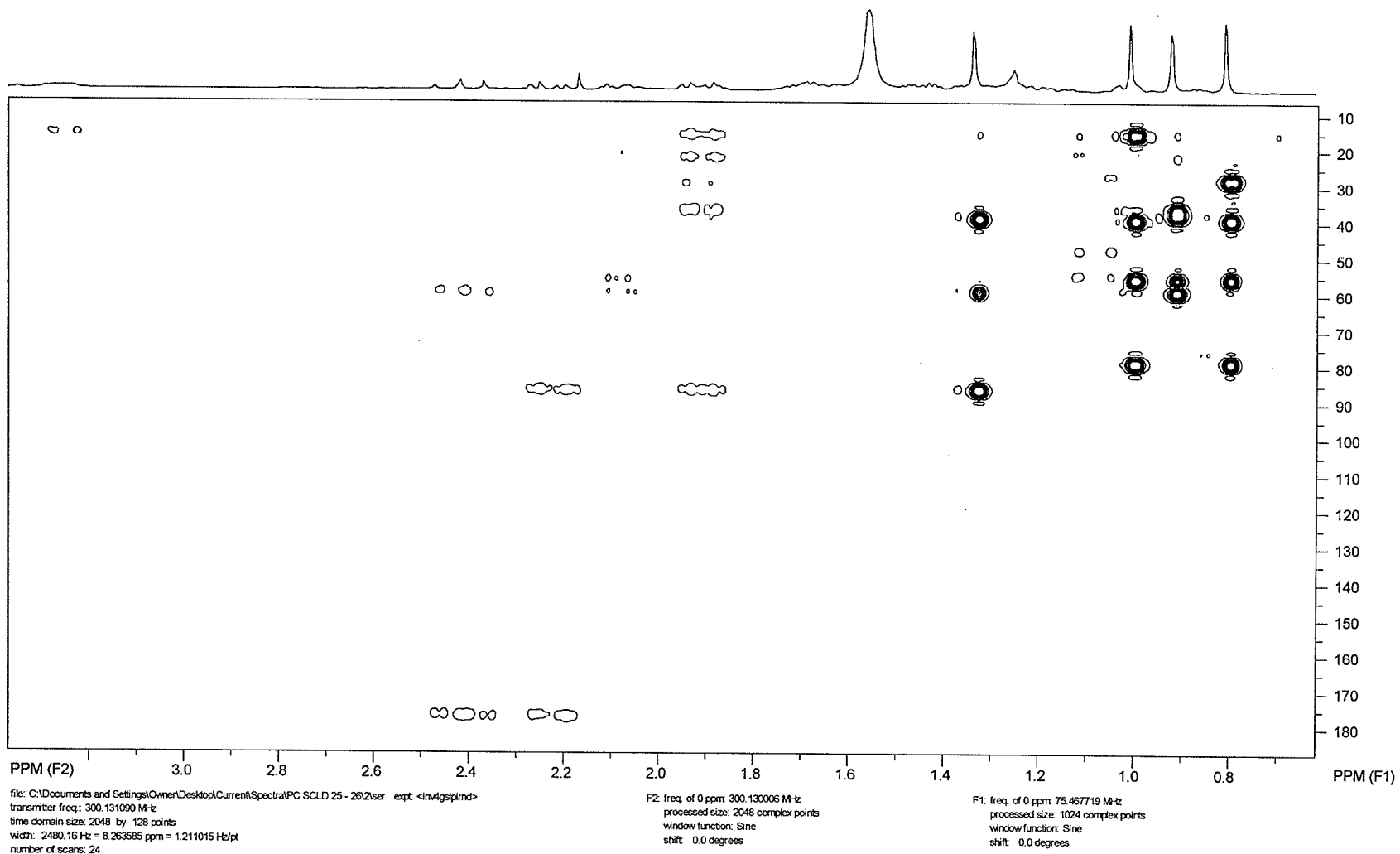


**Figure D-7: HMBC spectrum of 3 $\beta$ -hydroxysclareolide (132)**

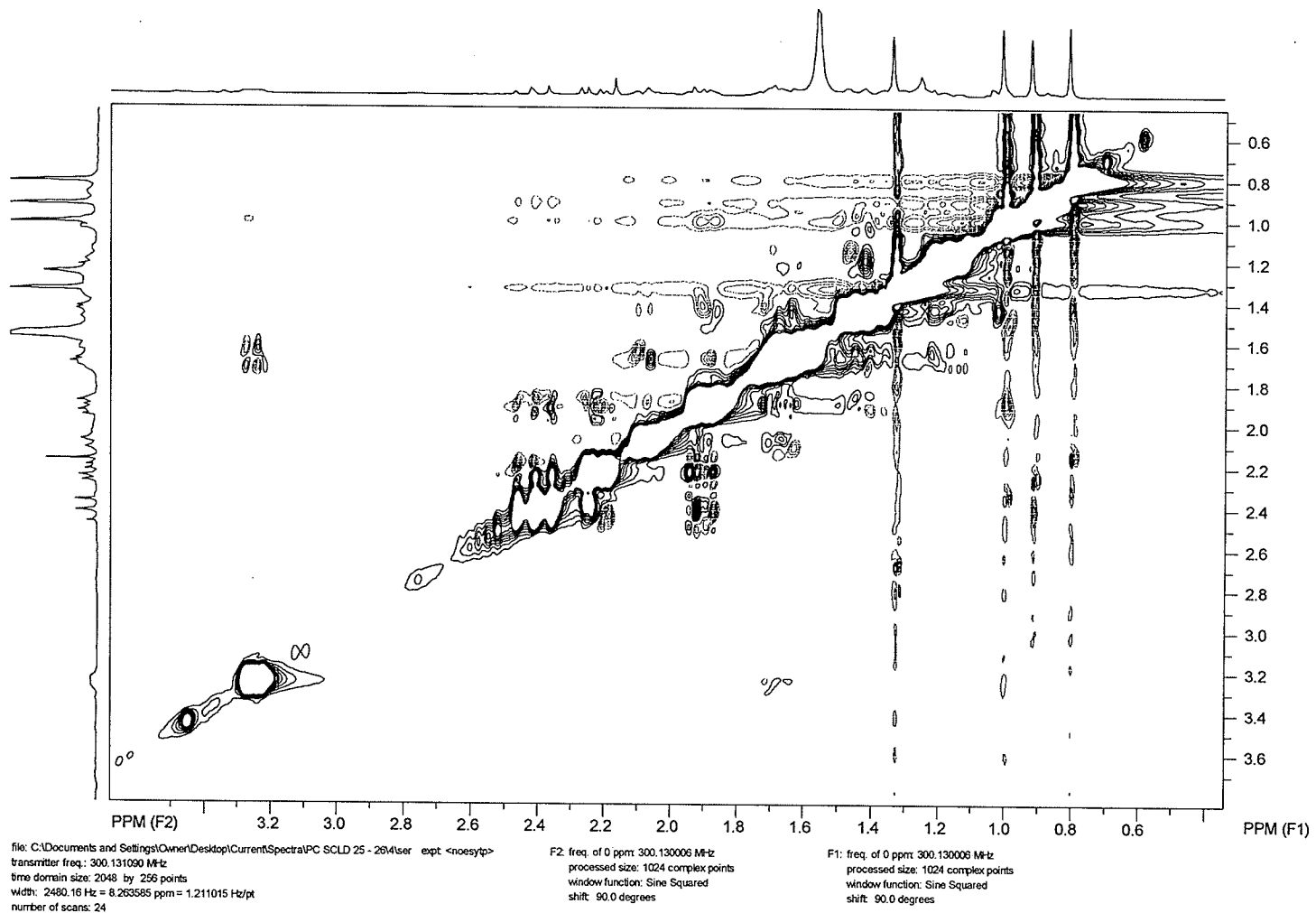
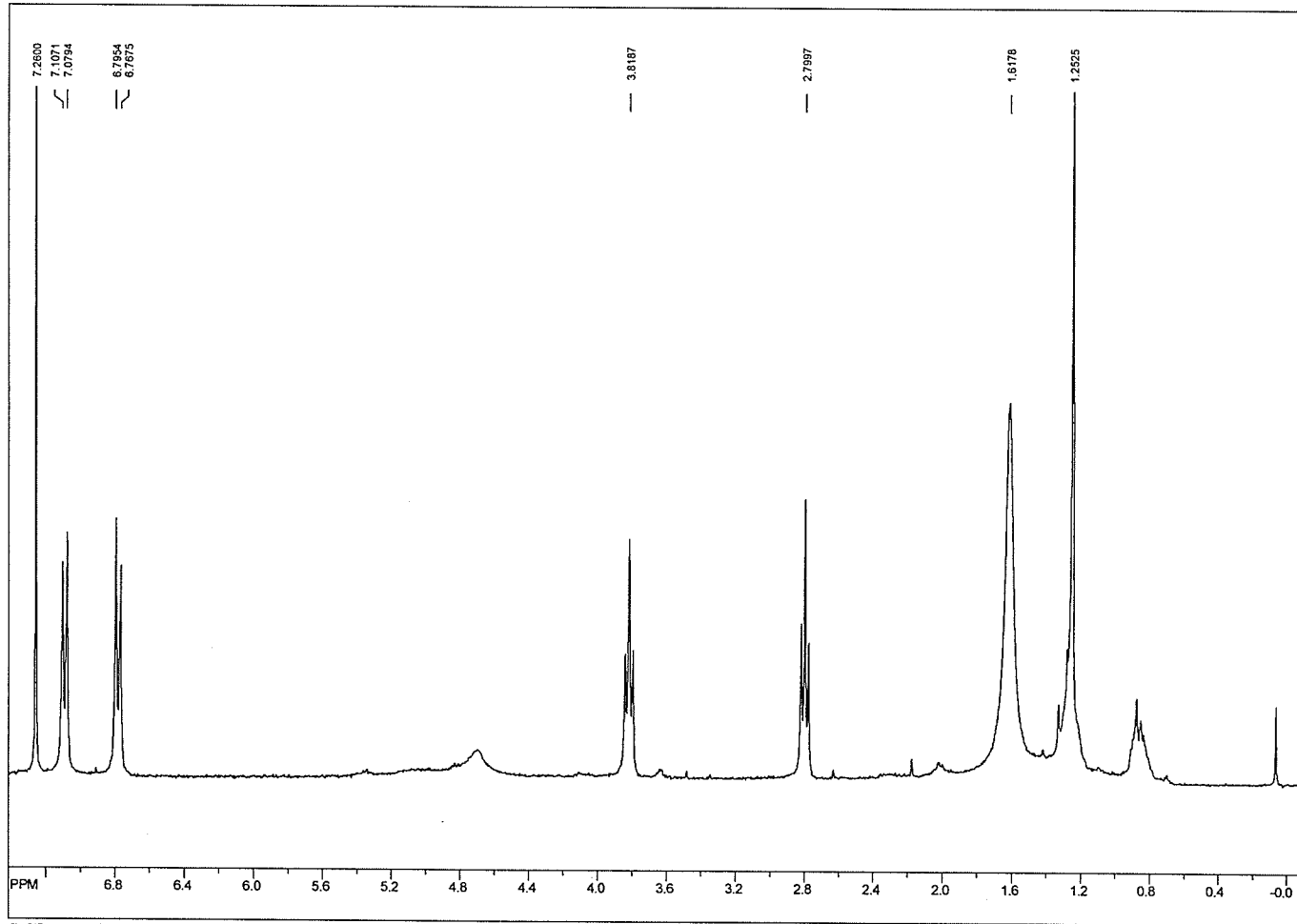


**Figure D-8: NOESY spectrum of 3 $\beta$ -hydroxysclareolide (132)**

SpinWorks 2.4: Tyrosol, proton NMR

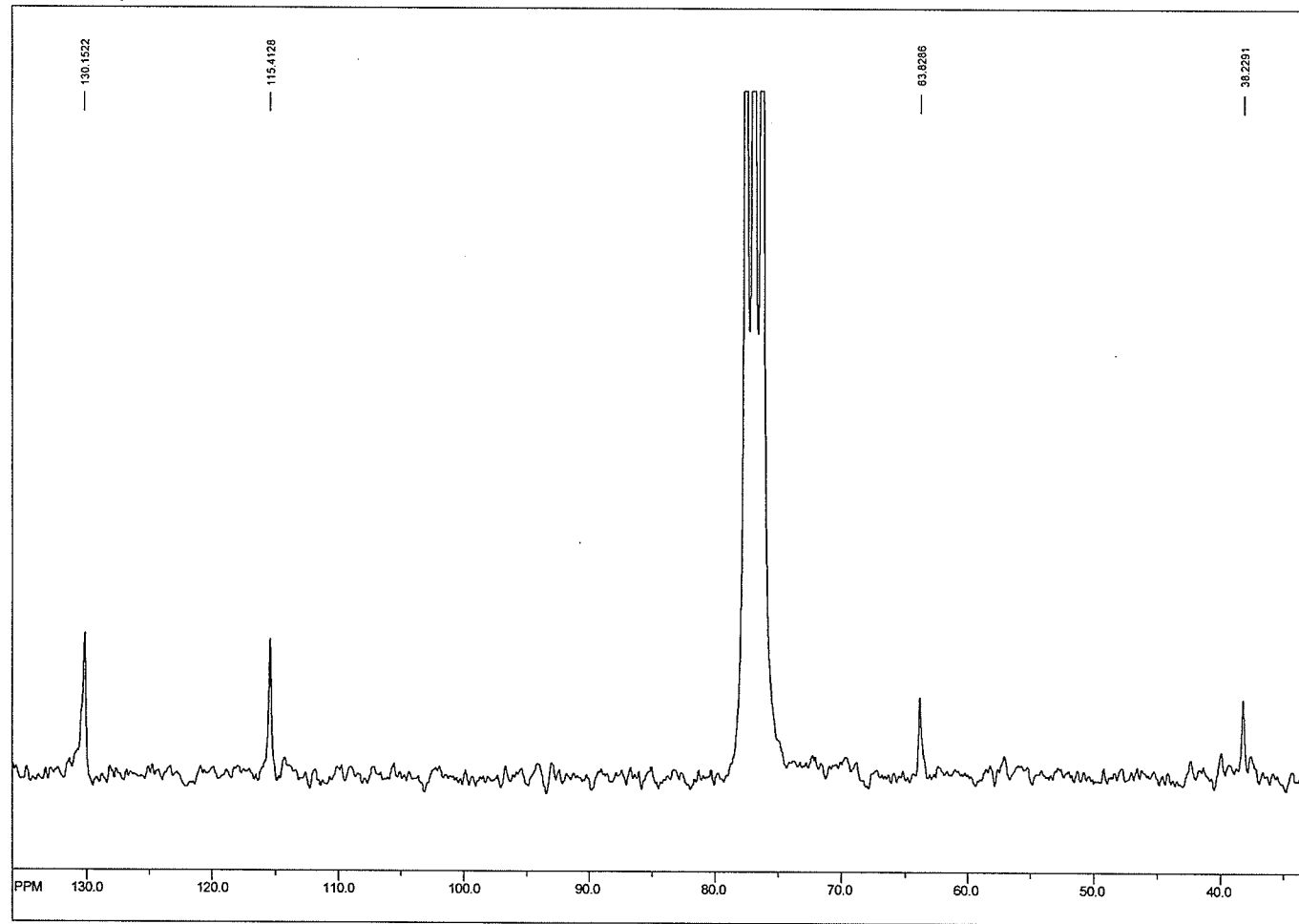


file: C:\Documents and Settings\Owner\Desktop\Current Spectra\CA 18 c11\fid\_ept <ag2>  
transmitter freq.: 300.131863 MHz  
time domain size: 65536 points  
width: 6172.84 Hz = 20.567092 ppm = 0.094190 Hz/pt  
number of scans: 16

freq. of 0 ppm: 300.130008 MHz  
processed size: 32768 complex points  
LS: 0.000 GS: 0.0000

**Figure D-9: <sup>1</sup>H NMR of tyrosol (151)**

SpinWorks 2.4: Tyrosol, 13C

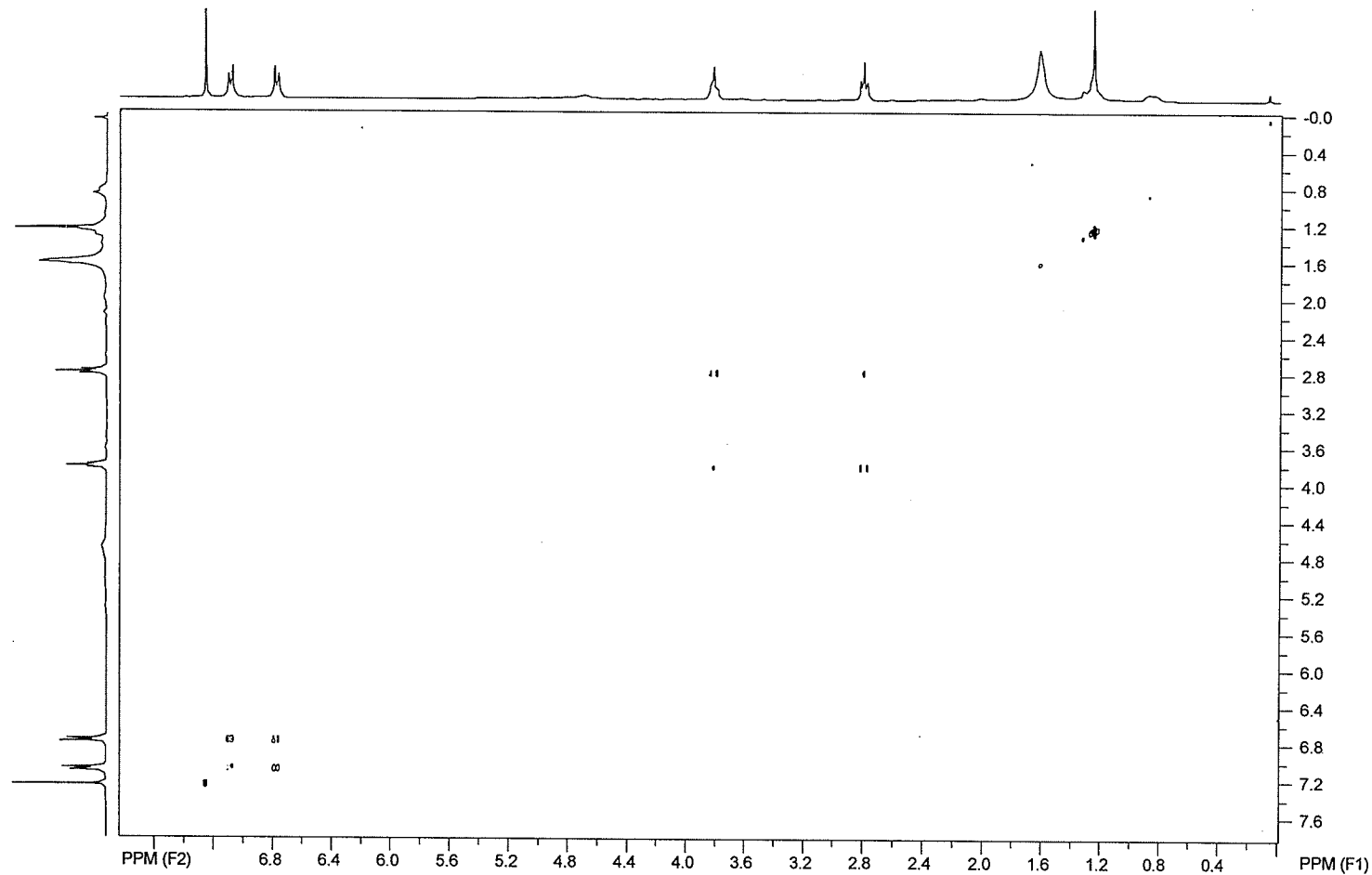


file: C:\Documents and Settings\Owner\Desktop\CurrentSpectra\CA 18 c113C\64f\_block1 1 exp \*sqz.f  
transmitter freq.: 50.26209 MHz  
time domain size: 37664 points  
width: 12570.67 Hz = 249.972500 ppm = 0.333759 Hz/pp  
number of scans: 19968

freq. of 0 ppm: 50.262097 MHz  
processed size: 65536 complex points  
LR: 0.000 GB: 0.0000

**Figure D-10: <sup>13</sup>C NMR of tyrosol (151)**

SpinWorks 2.4: Tyrosol, COSY



file: C:\Documents and Settings\Owner\Desktop\CurrentSpectral\CA 18 c112user expt <cosygs>  
transmitter freq.: 300.131180 MHz  
time domain size: 2048 by 256 points  
width: 2354.05 Hz = 7.843400 ppm = 1.149438 Hz/pt  
number of scans: 32

F2: freq. of 0 ppm: 300.130006 MHz  
processed size: 1024 complex points  
window function: Sine  
shift: 0.0 degrees

F1: freq. of 0 ppm: 300.130006 MHz  
processed size: 1024 complex points  
window function: Sine  
shift: 0.0 degrees

**Figure D-11 COSY spectrum of tyrosol (151)**

SpinWorks 2.4: Tyrosol, HMBC

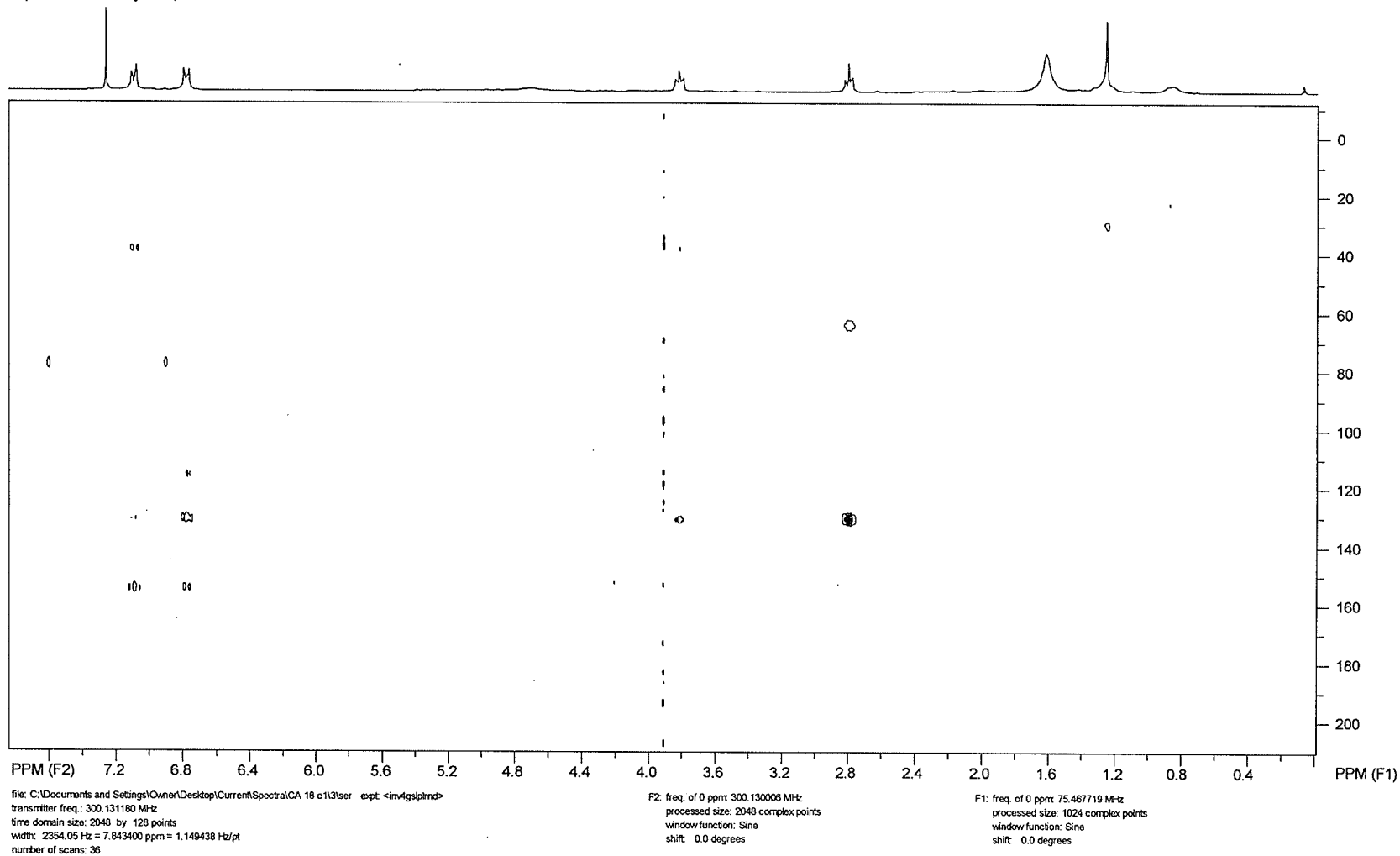


**Figure D-12 HMBC spectrum of tyrosol (151)**